DEVELOPING SILICA BASED NANOCOMPOSITE MATERIALS FOR DENTAL APPLICATIONS USING *BOMBYX MORI* SILK PROTEINS

MUHAMMAD SOHAIL ZAFAR

A thesis submitted in partial fulfilment of requirements of Nottingham Trent University for the degree of Doctor of Philosophy

October 2011

Dedication

To my loving wife Lubna, our kids Ahmed, Khadijah and our families, without whom the completion of this work would not be possible

To my supervisor whose guidance, encouragement, help and
Support made this project possible.

ACKNOWLEDGEMENTS

After thanking God for enabling me to handle this project, my first and foremost thanks go to Professor Carole Perry for offering this opportunity to carry out this research and for her patience and kind supervision throughout the duration of this project. I am very much grateful (special thanks) to Dr. David Belton for his advice at every stage especially helped me in understanding the characterisation techniques.

I am also thankful to my fellow students Graham Hickman and Izhar Wasif for helping me in performing and understanding of gel electrophoresis. I extend my sincere thanks to all my Inorganic research group colleagues especially, Estefania Boix, Simon Thompson, Marion Limo, Tim Green, Valeria Puddu, Marcos DeMurtas, Rajesh Ramasamy, Sara Hasip, Parbharakan Narayanappa and Anna Sola. Thanks to all fellow students and staff at Nottingham Trent University for the friendship and moral support provided. Their suggestions and advice motivated me and made my project interesting, exciting, and enjoyable.

The Nottingham Trent University was a great place to work Indeed, the atmosphere, the friendly environment for learning and developing myself made these years memorable for me. Finally, I would like to thank NIH, for funding this research under the research grant DEO17207.

Preface

This thesis *"developing silica based nanocomposite materials for dental applications using Bombyx mori silk proteins"* is one part of a collaborative research project that has been funded by The National Institutes of Health (NIH grant code DEO17207), USA involving the following research groups.

Professor David Kaplan group – Tufts University, Boston

- Construction, cloning, expression of chimeric (fusion) proteins and *in vitro* cell studies

Professor Carole Perry group – Nottingham Trent University, Nottingham

- Silica chemistry and kinetic control of physical, morphological and mechanical properties of composite materials involving silica and silk based proteins including fusion proteins.

Dr. Bruce Rutherford group - University of Washington, Washington

- *In vivo* testing and clinical application of new dental materials

Currently, the Kaplan and Perry groups are working together with remarkable progress so far (1,2). The remaining group (Rutherford) will contribute more in future work in the development of this material for dental applications.

We (MSZ working under the supervision of Prof. Carole Perry) have contributed to this project by developing a system to understand the reaction kinetics of silica condensation in the presence of different silk proteins and explored the effects of different additives on the mineralising system. Nanocomposite materials were fabricated using electrospinning and gelation techniques followed by their detailed characterisation. The research findings for this part of the project (studies by MSZ) are presented in this thesis.

In addition, Dr D J Belton (The Perry group at NTU) contributed to the project by studying solution properties of natural silk and silk-diatom inspired chimeric proteins. He also studied the effects of natural silk and chimeric proteins on the morphology and rate of silica condensation.

Nanocomposite materials will be available to other collaborative groups for further work in the near future ensuring continued progress in the project towards the development of novel materials for dental applications.

(1) Mieszawska AJ, Fourligas N, Georgakoudi I, Ouhib NM, Belton DJ, Perry CC, et al. Osteoinductive silk–silica composite biomaterials for bone regeneration. Biomaterials 2010 12;31(34):8902-8910.
(2) Mieszawska AJ, Nadkarni LD, Perry CC, Kaplan DL. Nanoscale Control of Silica Particle Formation via Silkâ˜†Silica Fusion Proteins for Bone Regeneration. Chemistry of Materials 2010 10/26;22(20):5780-5785.

Abstract

A significant amount of research is being carried out on natural *Bombyx mori* (BM) silk which has gained remarkable popularity for biomedical applications in recent years. The main objective of this thesis is concerned with the development of a new silk based material with improved properties for dental tissue repair and dentin regeneration.

In the first phase, research was carried out to study the chemistry and kinetics of silica formation and to assess the effects of silk proteins on the mechanical and functional properties of nanocomposite materials. A novel method was developed to separate different silk fractions (heavy chain fibroin and light chain fibroin) from natural silk using formic acid. Silk and its fractions were regenerated for use in gelation studies and fabricating nanocomposites by adding silica. The silica was added using, hydrolysed tetraethoxy silane (TEOS) to condense into gelling silk solutions or by adding pre-condensed silica nanoparticles (14-350 nm), prepared using a modified Stöber method. Silk solutions were characterised using viscometery, dynamic light scattering (DLS) and electrophoresis (SDS-PAGE).

In the second phase, silk based nanocomposites were fabricated using electrospinning and gelation routes. The fabricated nanocomposite materials were characterised using scanning electron microscopy (SEM), elemental analysis (EDX), Fourier transform infra-red spectroscopy (FTIR), Thermogravimetric analysis (TGA) and compressibility testing. Both silk fractions (heavy chain fibroin and light chain fibroin) have entirely different structural, conformational and functional properties and can be regenerated using ionic solutions. Heavy chain silk due to its unique properties such as high hydrophobic amino acid domains (repeats of GAGAGS or GAGAGY) resulted in comparatively more β-sheet content, producing different solution as well as materials properties. Silk fractions were electrospun and the morphology of electrospun fibres was affected by the relative proportion of heavy and light chain silk in the solutions. Similar results were found for materials prepared by the gelation route. Addition of pre-condensed silica particles improved mechanical properties of composite materials compared to silica derived from TEOS.

The development of novel methods of separating silk fractions will improve the availability of these fractions for future research and give a robust base for further studies in areas such as dental materials, biomaterials, biochemistry and biotechnology. Natural silk fractions and inorganic composites have a large potential for future applications in industry and research however a lot more research is required for their detailed characterisation and their interaction studies within the biological environment.

Contents

List of Figures

List of tables

List of Abbreviations

[Silk]	silk concentration
≃	Approximately
°C	Celsius
A	Alanine
A	Absorbance
Ag	Silver
Al	Aluminium
Al_2O_3	Alumina
ATR	Attenuated total reflectance
Au	Gold
BM	*Bombyx mori* silk
BSA	Bovine serum albumin
BT	Bis-tris propane/citric acid buffer
C	carbon
ca.	Circa

$Ca_3(PO_4)_2$	Tri-calcium phosphate
$Ca_3(PO_4)_2.xH_2O$	Amorphous calcium phosphate
$Ca_5(PO_4)_3.F$	Fluorapatite
$CaCl_2$	Calcium chloride
$CaCl_2$:EtOH:H_2O	Ajisawa solvent
$CaCO_3$	Calcium carbonate
$CaHPO_4$	Calcium phosphate anhydrous
$CaHPO_4.2H_2O$	Calcium hydrogen phosphate dihydrate
CRT	Cathode ray tube
D	Aspartic acid
Da	Dalton
dd.water	de-ionised distilled water
DLS	Dynamic light scattering
E	Glutamic acid
F	Phenylalanine
FA	Formic acid
Fe	Iron
FTIR	Fourier transforms infrared
G	Glycine
g	Gram
H	Histidine
H_2O	Water
HA	Hydroxyapatite
HCl	Hydrochloric acid
H-fibroin/Chain	Heavy chain fraction

I	Isoleucine
K	Lysine
kDa	kilo Daltons
L	Leucine
L-fibroin/L-chain	Light chain
LiBR	Lithium bromide
LiSCN	Lithium thiocynate
M	mole
Me-SH	2-Mercaproethanol
ml	millilitre
mM	millimole
Mw	Molecular weight
Na	Sodium
$NaHCO_3$	Sodium bicarbonate
nm	nanometre
O	Oxygen
OB	Odontoblast
P	Proline
P	Phosphorous
P	poise
Pa	Pascal
PAGE	polyacrylamide gel electrophoresis
PDC	Dentin and pulp Complex
PDI	Poly dispersity index
PEG	polyethylene glycol

PTFE	Polytetrafluoroethylene
R	Arginine
R5	Silica condensing peptide from Diatom
RDS	Regenerated soluble silk
rpm	rotations per minute
RTS	Regenerated total silk
RUDS	Regenerated insoluble silk
S	Serine
s	Seconds
SDS	Sodium dodecyl sulphate
SEM	Scanning electron microscope
Si	Silicone
$Si(OH)_4$	Monosilicic acid
SiO_2	Silica
Solvent A	Calcium chloride/ethanol solvent
T	Threonine
T	Transmittance
TEOS	Tetraethoxy silane
TGA	Thermogravimetric analysis
Ti-6Al-4V	Titanium alloy
TiO_2	Titania
UV-Vis	Ultraviolet visible spectroscopy
V	Valine
V	volt
v/v	Volume by volume

v/w	Volume by weight
wt %	weight percent
wt	weight
Y	Tyrosine
ZnO	Zinc oxide
ZOE	Zinc oxide eugenol
µ	micron

Chapter 1
INTRODUCTION

The use of synthetic materials in the body by medical and dental care practitioners has grown outstandingly in the last 30-40 years, though the concept of using such artificial materials is very old. For example, plaster of paris was pioneered as a bone-substitute material towards the end of the nineteenth century, and dental fillings, including amalgam, have been known for more than 150 years (1). The use of engineered structures fabricated from metals and polymers in orthopaedic surgery has a more recent history, beginning with Dr (later Sir) John Charnley's work on the replacement of arthritic hips in the early 1960s (2,3). The major aim of using dental biomaterials is to maintain and improve the quality of dental care to patients which can be achieved by preventing or treating disease or relieving pain, improving the aesthetics or functions such as speech and mastication. Many of these objectives need the use of materials to alter or replace the lost or diseased tooth portion (4). This chapter presents a brief description of natural biomaterials in relation to dentistry and how different biominerals are formed in nature and their

applications as well as significance of using nano-composite materials and silk containing fusion proteins.

1.1- Role of materials science in dentistry

Considering the dental applications of materials, all major types of materials; metals, ceramics, polymers and composites have been widely tried for a variety of applications (4). The concept of using materials in dentistry is very old and has gone through different evolutionary steps at present times. The earliest account of using gold by Greeks and Romans as a dental prosthesis has been recorded up to several centuries before Christianity and from the first century AD, the filling of decayed teeth with lead or lint was used to prevent its fracture before extraction (5). As dentistry developed with time, more and newer materials have been developed (6) . Some important milestones in the development of materials for dental applications (5), are listed below.

- 1746: First book to describe mechanical dentistry by Claude Mouten
- 1770: Jean Darcent introduced low fusing metal alloys
- 1796: Use of dentures in dentistry
- 1806: G Fonzi baked the first ever porcelain tooth and developed different shades using metallic oxides
- 1826: O. Taveau disclosed about amalgam using silver and mercury
- 1851: Discovered vulcanite rubber for denture bases, however it was replaced by acrylic resin in 1937

More recently, the concept of adhesive materials was introduced in 1955, leading to the use of composite resins in dentistry (7). In 1972, Wilson and Kent (at the Laboratory of the Government Chemist, London) published their work about the invention of alumino-silicate glass ionomers that can bind chemically to tooth hydroxyapatite [HA] (8). Mostly materials being used at present in dentistry have been developed in 20^{th} century (5).

Despite a better understanding of the materials chemistry and recent improvements in the physical properties, no material has been found that is ideal for dental applications (9). There is a wide range of applications of materials in all fields of dentistry as are described in the following section.

1.2- Applications of materials in the dentistry

There is a wide range of applications of materials in all disciplines of dentistry. Some of the major applications and materials used are described in the table 1.1.

Table 1.1: Major applications and materials being used in dentistry

Discipline	Applications	Materials used
Restorative Dentistry	•Tooth restoration •Inlay and onlays •Crowns	Amalgams, composite resins, glass silicates, dental cements, porcelain, metal alloys and gold (4,5,10,11)
Endodontics	•Pulp capping •Core build ups •Root filling •Root sealers •disinfectants	Calcium hydroxide, mineral trioxide aggregate (12), amalgams, composite resins, glass silicates (4,5,10,11), Zinc oxide eugenol (ZEO) (6) gutta percha, silver points, sodium hypochlorite (12)
Periodontics	•Guided tissue/bone regeneration •Bone grafts	Polytetrafluoroethylene (PTFE), polylactic acid, collagen (12) Demineralised freeze dried bone, bioglass, calcium phosphate (12)
Orthodontics	•Band and brackets •Wires •Luting agents	Nickel titanium and cobalt chromium alloys, stainless steel, self-reinforcing composites (4,5)
Oral surgery	•Splinting •Sutures	Steel and titanium (12) PTFE, silk, collagen, nylon (13)
Prosthetic dentistry	•Impression material •Teeth •Denture base	Alginate, agar, plaster, ZEO, poly sulphide, poly silicone (14), ceramic, methyl methacrylate(14)
Preventive dentistry	•Fluoride release •Fissure sealants	Glass ionomers(15) , composite resins, compomers, giomers (16)
Dental implants	•Endosseous •subperiosteal	Titanium alloys (Ti-6Al-4V), HA or glass ceramic coatings (4,13,14),
Cosmetic dentistry	•Veneers •Bleaching agents	Porcelain, (11) Carbamide peroxide, hydrogen peroxide (14)
Dental tissue engineering	•Dentin regeneration	Bone morphogenetic proteins (17-19), demineralised dentin (20-22), dentin matrix protein 1 (23)

1.3- Oral environment

It is important to consider the complex oral environment in order to understand the material and oral tissue interactions required for successful applications. The oral environment plays a vital role in certain functions such as keeping it moist with saliva which helps in the swallowing of food, taste and texture of food (24). Detailed description of these processes is beyond the scope of this thesis. The oral environment is different from other parts of the body in structural and functional aspects and may produce different kinds of biological response to biomaterials (4). For example, exposure to body fluids (in the mouth) can result in the degradation or corrosion of material inside the oral cavity, or alternatively, the oral environment may react with material to release cytotoxic or harmful components (25).
In addition, other factors are involved in making the oral environment complex for synthetic materials;

I. Materials undergo high chewing forces and wear (6)
II. Degradation of materials, corrosion from by products and food in the mouth (6)
III. Temperature variations in the mouth (from hot and cold food) resulting in shrinkage and contraction of materials (6,26)
IV. A large number of micro-organisms that can produce acid and different other chemicals to affect biomaterials (27)
V. pH fluctuations (27)
VI. Certain pathological conditions like bruxism, bulimia (27)
VII. Interaction with different food chemicals like nicotine, caffeine, alcohol, medicines that can also affect material longevity

Anatomically, there are mainly two groups of tissue in the oral cavity, soft tissues and hard tissues (28,29). Soft tissues are muscle and fascia lined by a protective lining of mucosa and connective tissue, while hard tissues are teeth and bone (28,29). As this new material has intended application of replacing hard oral tissues (tooth), tooth structure is reviewed in the next section.

1.4- Natural tooth materials

Teeth are required for chewing and incising of food, proper speech and aesthetics (28). The tooth has to survive in a variety of different conditions, bear forces of

mastication (up to ~ 700 N), abrasion, chemical attacks from acidic food or bacterial products (25). Wear and tear is always there when teeth are used in the harsh oral environment however, when affected it is crucial to maintain the health and appearance of teeth using different dental biomaterials.

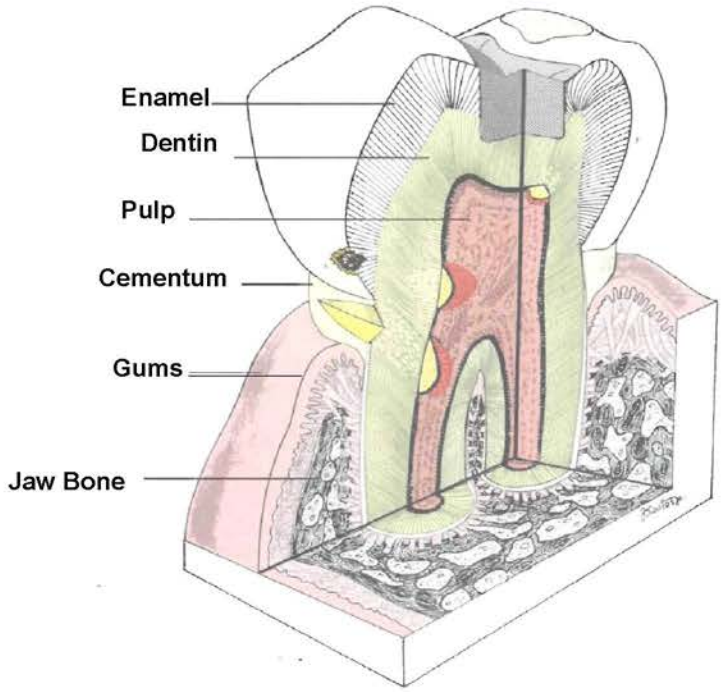

Figure 1.1: Vertical cross section of a tooth showing structural components (11).

Understanding of natural tooth and structural components is vital. Ignoring the properties and parameters of natural tooth material can result in disaster or failure of man-made materials. Natural tooth is composed of mainly hard tissues containing hydroxyapatite and an inner core of soft connective tissue in the form of pulp (30). There are three different types of hard tissues (enamel dentin and cementum) in the tooth with varying proportions of hydroxyapatite and organic matrix. The structural, physical and chemical properties of these natural materials are described below.

1.4.1- Enamel

Enamel is the hardest tissue covering the crown dentin of the tooth (5,11,31). The enamel forming cells (Ameloblasts) are epithelial cells and are lost during the eruption of a tooth, hence enamel is a non-vital tissue and cannot be regenerated or renewed by itself (11,30). Due to the crucial role of enamel tissue in protection of dentin and aesthetic, long life preservation of enamel is desired by the dentist (32).

Enamel is a highly mineralised tissue with 96 wt. % inorganic contents and 4 wt. % organic contents and water, where 75 % is water (5,29) and present in the inter-crystalline spaces and micro-pore network (33,34). The inorganic component is composed of mainly calcium phosphate in the form of crystalline hydroxyapatite. Other ions such as carbonate, magnesium, strontium, lead and fluoride may also be incorporated depending on their availability during the period of enamel formation (30).

The presence of high inorganic content makes enamel a very hard tissue to withstand the heavy forces of mastication. However enamel is always supported by dentin and becomes very brittle when unsupported (5,30). Otherwise it has excellent mechanical properties, as hard as steel with a Knoop hardness of 343 kg/mm^2 compared to 68 kg/mm^2 for dentin (5). A full comparison of different mechanical features of enamel and dentin has been described in the table 1.2. Enamel has a translucent appearance and may reflect difference in colour depending on the underlying dentin and thickness of enamel which can be 0.5 mm – 2.5 mm (11,25,30).

Structurally, the basic unit of enamel is an enamel rod which is a cylinder shaped structure separated by inter-rod material (30). Enamel rods having diameter of 4 to 5 µm with a variable morphology and a population density of 30,000-40,000 rods/mm^2 and have crystals arranged parallel to the long axis (5),(11). If we go further in details of crystal morphology, the crystals in the enamel are closely packed hexagonal structure with a thickness of 25-39 nm and width of 45-90 nm (11,29,30), and are significantly larger than crystals in dentin (11).

The organic matrix in enamel has at least two types of protein amelogenin and enamelin (5,11,28). Amelogenin has molecular weight of 20-30 kDa, is hydrophobic, with amino acids proline, glutamine and histidine forming 90 % of total enamel proteins (35). Amelogenin is considered very important in the organisation and crystal growth of enamel (28). Enamelin has a higher molecular weight of 48-70 kDa and having amino acids mainly serine, glutamic acid and aspartic acid. Enamlin is secreted in the first formed enamel tends to bind to the crystals and considered responsible for hyper-mineralised enamel adjacent to the dentin (28). The process of biomineralisation in enamel is described later in this chapter.

1.4.2- Cementum

Cementum is a bone like tissue that surrounds the root dentin of tooth and provides attachment to the fibres of the periodontal ligament (25,30,31). The thickness of the

cementum layer is 20-50 µm near the coronal dentin and increased up to 200 µm in the apical area of root (28,30). Cementum is a hard and avascular tissue that can be classified in mainly two types (cellular and acellular) depending on the presence or absence of cementum forming cells. Acellular cementum is responsible for the tooth attachment to the bone while cellular cementum responds to tooth movement and wear to adapt accordingly (30).

The biochemical composition of cementum is very similar to bone containing 45-50 % inorganic in the form of hydroxyapatite (28,30) and the rest is collagen and organic matrix. There is little information available about the Cementum proteins while collagen type I constitutes 90 % of total organic contents alongside type III and XII (30). Some of the other organic molecules found in the cementum are fibronectin, osteaocalcin, alkaline phosphatase, osteopontin, osteonectin, proteoglycans, proteolipids and several growth factors (30). The cells associated with the production and maintenance of cementum throughout the tooth life are cementoblasts, cementocytes and cementoclasts (28,30). As for other biomineralised tissues, the organic matrix plays a vital role in cementum formation as growth factors are involved in cell differentiation and cementogenesis; bone proteins enhance mineralisation and regulate the extent of crystal growth while collagen regulates the periodontal tissues (30).

1.4.3- Dentin and pulp Complex (PDC)

It is very important to understand the structure, chemistry and properties of natural dentin as any newly developed material will be in very close proximity with the dentin-pulp complex for the purpose of new dentin formation using dentin tissue engineering and regeneration techniques. Dentin is a unique dental tissue, and is considered a vital tissue even without the presence of a blood supply or innervations and has the ability to respond to stimuli like tactile, thermal or chemical changes (11). Dentin is a hard bonelike connective tissue that forms bulk of the tooth while pulp forms the inner core of soft connective tissue. As both tissues are correlated embryologically and functionally, they are usually considered together as the pulp-dentin complex (28,30). Dentin is an elastic tissue, slightly harder than bone and softer than enamel providing support to overlying enamel as well as a protective covering to the soft and delicate pulp (5,28). Dentin is pale yellow in colour, has 70 wt. % (45 v/v %) inorganic contents, 20 wt. % organic (33 % v/v) and 10 wt. % water (22 v/v) (5,11,28,30,36).

The inorganic part of dentin is composed of mainly hydroxyapatite [HA] (5,28,30) however the dentin HA crystals have dimensions of 20 nm x 20 nm x 3.5 nm, are significantly smaller than enamel HA crystals proving higher surface to volume ratio (11). Dentin HA is also higher in F^- and Mg^{2+} ions (37). The organic phase of dentin is mainly collagen from 85 % of total organic content (5) up to 92 % (29) mainly type I (5,28,29) with lesser amounts of type V (5). The non collageneous organic matrix consists of dentin specific proteins like phosphophoryns, dentin sailoprotein, and dentin matrix protein-1 (5) and other proteins like osteocalcin, and osteopontin (5,28,30,35). Phospholipids are detected in the dentin matrix however their function is not yet known (36).

Structurally, dentin is composed of a basic unit "dentinal tubule" that runs throughout the structure of dentin (5,11,25,28-30,34,38). Dentinal tubules get thinner towards enamel, 0.5 µm near the dentino-enamel junction and up to 2.5 µm (5), 3.0 µm (11) near pulp. The population density of tubules is also variable being as much as 20,000 tubules/mm^2 near the dentino-enamel junction and more than double this near the pulp area (5,39), up to 76,000 tubules/mm^2 (30). Furthermore, tubules show extensive terminal branching producing many canaliculi near the dentino-enamel junction that are connected to each other making a highly interconnected network system (28,40).

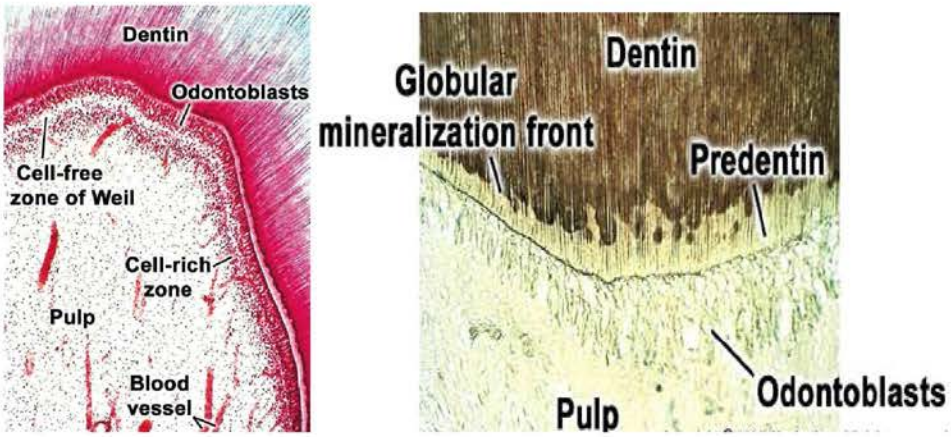

Figure 1.2: Histological picture of the pulp dentin complex (30)

Dentinal tubules are occupied by odontoblastic cellular processes which are extensions from the odontoblastic cells lying in the dentinal lining of the pulp tissue (5,11,25,28-30,38), and supersaturated dentinal fluid (serum like fluid) that drives

the deposition of HA inside the tubules making them narrow with time and sclerosis of dentin is found in old age (5,25).

Table 1.2: A comparison of the properties of enamel and dentin

Properties	**Enamel**	**Dentin**	**References**
Basic Unit	Rod	tubule	(5,29,38)
Population	30-40 K/mm^2	50-90 K/mm^2	(11)
Vitality	Non vital	Vital	(11,28-30,38)
Inorganic (wt. %)	96 %	67 %	(11,29,29,30,38)
Organic (wt. %)	3 %	20 %	(5,11,28,30,36)
Collagen	none	90 % of organic, mainly type I	(28-30)
HA Crystal size	45-90 x 25-39 nm Length= 1-2 mm	20x20x3.5 nm	(11)
Thermal expansion	11.4 M/K	8.3 M/K	(10)
Compressive Strength	384 MPa	297 MPa	(5)
Tensile Strength	10.3 MPa	98.7 MPa	(5)
Shear Strength	90 MPa	138 MPa	(5)
Elastic modulus	84.1 GPa	18.3 GPa	(5)
Nano-indentation	4.48 GPa	0.70 GPa	(5)
Knoop Hardness	343 Kg/mm^2	68 Kg/mm^2	(5)
Dielectric constant	--	8.6	(5)

1.5- The odontoblast (OB)

The new dental nano-composite material will target odontoblast cells to grow on it and start producing the dentin. It is well known that odontoblasts have the ability to form reparative (reactionary) dentin in response to an insult to the dentin-pulp complex (11,28-30,34,38,41) or in response to therapeutic application of pulp capping materials (4,11,41). The process of dentin formation is called dentinogensis (11,28-30,34,38,42), and Odontoblasts (dentinoblast) are much specialised, highly differentiated cells of neural crest origin, responsible for the production of any type of dentin and maintenance throughout the life of a tooth (5,11,28-31,34,36,38,43,44). Odontoblasts are large size plump cells, having a nucleus at the base (towards pulp)

in basophilic cytoplasm and rich in cellular organelles required for production of organic and inorganic matrix (28,30,36). Different morphological types of odontoblast cells have been described depending the activity states (36,45) for example pre-odontoblast, secretary odontoblast and resting odontoblast cells (28,30), furthermore they can differ in shapes depending on the availability of space in pulp canals and chamber e.g. columnar (35 µm x 3-5 µm) in crown, cuboid in mid-portion and turns to flatter and smaller in root dentin (28,30,36).

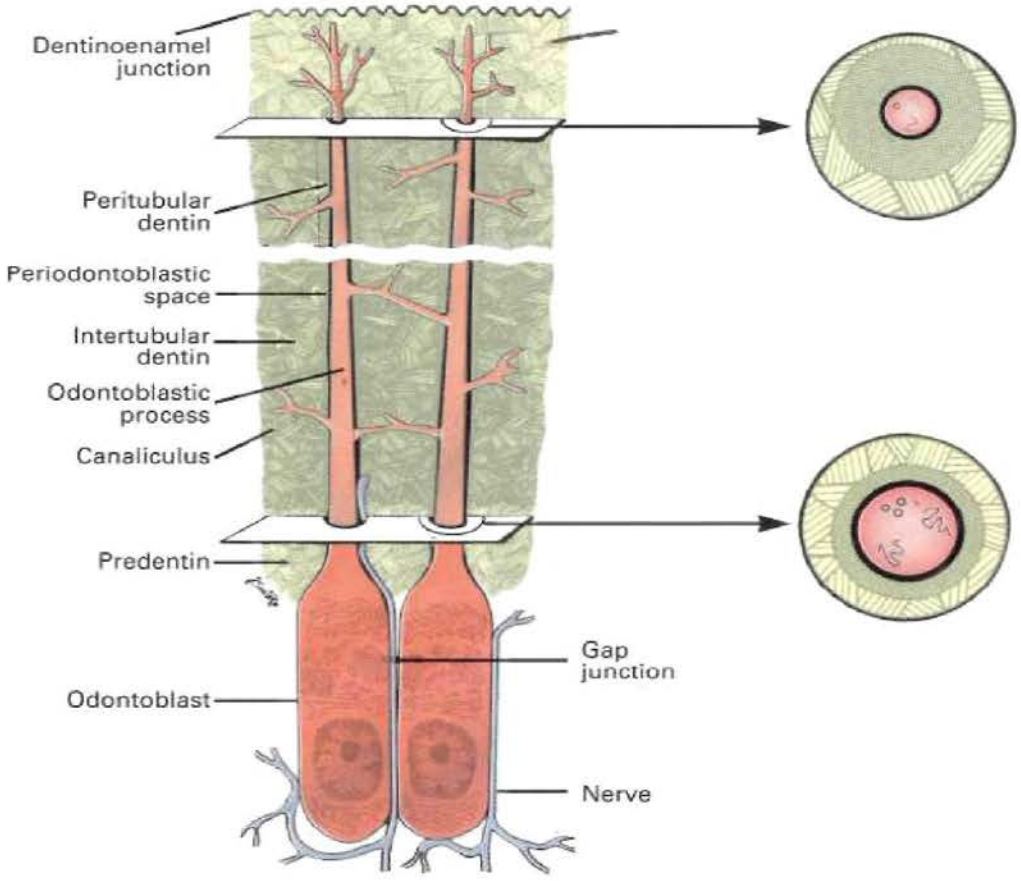

Figure 1.3: Schematic cross sectional presentation of the odontoblast processes progressing through the dentinal tubules and surrounding structures (11).

Another important feature of the odontoblast cells is a cellular extension called odontoblastic process, (5,11,28-30,36,46), that start developing at the neck of cells alongside the formation of dentin and keep occupying the dentinal tubule in mature dentin. These processes (one from each OB) contain secretary organelles and are connected to each other by a cytoskeleton network (11,28,30). However, there is great controversy about the length of these processes either that occupy the full

length of a dentinal tubule or not (5,30,47). There is a lining of the membrane called lamina lamitans that lies between the tubule dentin and cell processes. Tubules also contain collagen, proteoglycans, albumin, tranferrin and sometimes nerves (28,30). Any change in osmotic or hydrostatic pressure or fluid movement in dentinal tubules as a result of any insult is detected by OB or nerve endings (5,11,28,30). A moderate level of damage resulting in the injury or death of OB or even destruction of dentin extra cellular matrix initiate the proliferation of secondary OB that form reparative dentin (5). Little is known about the source of newly formed OB, however it is related to high proliferative activity in the perivascular area of pulp (5).

Pulp is a soft tissue forming the central core of tooth (28-30,34,38,42) containing 75 % water and 25 % organic (34). In addition to OB cells (described above), it contains different types of cells (fibroblasts, undifferentiated mesenchymal cells, macrophages and other defence cells), collagen fibres, nerves and blood vessels (25,28-30,34,38). There are large numbers of fibroblasts in the pulp and they have the ability to produce pulp matrix as well as ingest. Undifferentiated mesenchymal cells present in the pulp can differentiate into OB and fibroblasts depending on the nature of stimuli (28,30). The number of cells in the aging pulp is reduced resulting in a more fibrotic pulp, and it is very crucial to note that decrease in cells will also reduce the dentin regeneration potential (28,30).

The matrix of pulp contains collagen fibres type I and III in a ratio of 55:45 and this ratio is not observed to change with age, however, the ratio of collagen in total to number of cells increases with age (28,30). Ground substance is very similar to other connective tissues and primarily consists of glycoproteins, glycosaminoglycans and water. Pulp is well vascularised and well innervated containing Aβ, Aδ and C fibres from the fifth cranial nerve for pain transmission and sympathetic nerve fibres entering with blood vessels (28,30). It is quite evident from the above discussion that pulp performs certain functions (48); providing the encasement for odontoblast cells for the formation of primary, secondary dentin and tertiary dentin, nourishing dentin from the pulp vessels and maintaining the cells and organic matrix. It also innervates the tooth for pain transmission and plays an important role in the protection of tooth vitality by responding to different stimuli. By using this new composite material and tissue engineering techniques, it could be possible to keep pulp alive so that it can maintain these vital functions throughout the life of the tooth.

Considering the replacement of lost or damaged dentin with this new composite material, it will be beneficial to estimate the quantity of lost tissue and the time required to reproduce the same amount of natural dentin. Many factors can be

involved in calculating the rate of dentin formation. It takes about five days to differentiate new OB after injury of the dentin-pulp complex (5). Rate of primary dentin formation is approximately 4 µm/day (36) but slows down later. For reparative dentin rate of dentin formation may be 1-3.5 µm/day (28,30). The rate of formation may be affected by extent of damage, inflammation of pulp, infection, and presence of diseased dentin or any systemic conditions (5,11). In a previous study (49), 70 µm of reparative dentin was observed to form over a period of fifty days. The rough calculation of time scale would be helpful to estimate how long new nano-composite materials should stay as a tissue engineering scaffold *in situ* to be replaced by natural dentin.

1.6- Inorganic minerals of enamel and dentin

From the discussion above, it is understandable that all calcified tooth materials have a significant amount of inorganic mineral (more than bone) so it is crucial to understand the chemistry of these biominerals. Most biominerals in the human body are based on calcium phosphate compounds (11,25,28-30), however they can exist in a range of phases like dibasic calcium phosphate anhydrous ($CaHPO_4$) or dihydrate ($CaHPO_4.2H_2O$), tri calcium phosphate α or β [$(Ca_3(PO_4)_2$], amorphous calcium phosphate [$(Ca_3(PO_4)_2.xH_2O$], hydroxyapatite (HA) [$(Ca_5(PO_4)_3.(OH)$], and fluorapatite [$(Ca_5(PO_4)_3.F$] (50,51). In terms of teeth and bone structure, HA is the most abundant among all compounds (25). The basic structure of HA has been known for more than 80 years (52) however, it was studied for X-ray and neutron diffraction more recently (53).

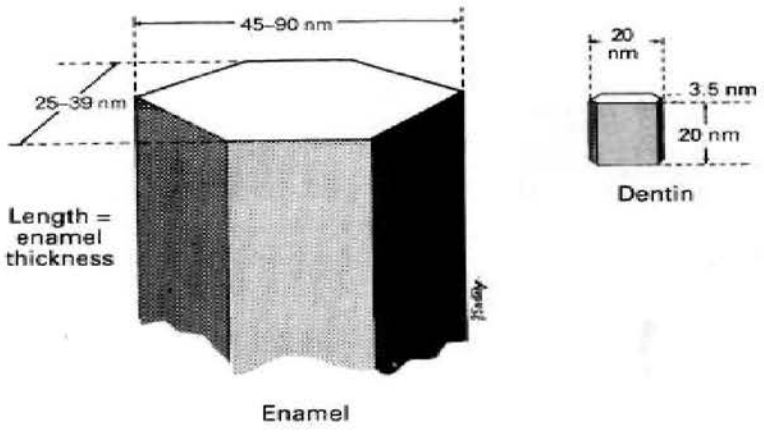

Figure 1.4: Schematic comparison of enamel and dentin HA crystal size showing enamel HA crystals significant size (11).

A crystals exist in an hexagonal shape (25) however their size and morphology varies depending on the tissue and location (11,28,30). Pure HA is very uncommon in the biological system and certain other ions like carbonate, sodium, silicates, and metal cations may be incorporated by replacing calcium, hydroxyl or phosphate ions (25). Such ionic exchange during HA formation may affect the physical and bulk properties of the material (25). For example, in fluorapatite ($Ca_5(PO_4)_3.F$, fluoride ions replace hydroxyl ions of enamel HA crystals (25) and make it more crystalline and less soluble in acid (54-56). Furthermore, the presence of fluoride in teeth tissue has a proven role in re-mineralisation and prevention of tooth decay (27). Topical application of fluoride also results in substitution of it with hydroxyl ions in enamel minerals making it more resistant to acid attack hence dissolution (28).

There is a significant difference in the size and orientation of HA crystals in enamel and dentin (11) as is shown schematically in Figure 1.4. In enamel, crystals are oriented in at least two directions and may be 1-2 mm long (no collagen at all), while in dentin HA crystals are small and uniform around collagen fibres (30).

1.7- How biominerals are made in nature and biomimetic approaches

Natural biological materials show many levels of hierarchical structures from the macroscopic to the microscopic length scale with the smallest building blocks being designed with nano-meter sized hard insertions implanted into a soft protein matrix (57). Teeth like other natural biomaterials are primarily an inorganic/organic composite material with desirable strength and damage-resistant properties (58). Like other biominerals (bone, exoskeleton, shells), the organic matrix of tooth is formed first followed by the introduction of minerals thereby reinforcing the physical properties up to the required level (57). Biomimetics is the science of understanding, how nature has designed and processed and assembled these high performance materials and then applying those principals to make synthetic materials (57). In the natural world nanoscale fabrication can be achieved without use of high temperature or extremes of pH or pressure (59). For example, in the laboratory, conversion of enamel HA to fluorapatite is a very slow reaction and requires the presence of CaF_2 at harsh conditions of 900 ℃ (56), in contrast in nature, this reaction takes place by a simple dissolution-precipitation method (50).

The biomineralisation of enamel takes place in two distinct stages and differs from dentin and other tissues. In the first stage (secretory stage), the ameloblasts (enamel forming cells) produce partially mineralised (30 %) matrix. In the second stage (maturation stage), organic matrix and water is taken out by ameloblasts

adding more minerals up to 96 %. During the maturation stage, the pre-existing HA crystals also grow in all dimensions (30).

In biomineralisation of dentin, organic matrix (mainly collagen as described earlier) is secreted in incremental stages by odontoblast cells. This non-mineralised dentin matrix is called pre-dentin, and is subsequently mineralised. Odontoblasts move towards the pulp leaving a layer of pre-dentin (15-20 µm) between cell bodies and mineralised dentin (30,36). Mineralisation starts with the appearance of vesicles, believed to have single crystal under the influence of phospholipids present in the vesicle membrane. These vesicles are ruptured by rapid crystal growth in them spreading clusters of crystals that fuse with each other forming a continuous mineralised matrix (30).

1.8- How dentin differs from bone? Regenerative potential of dentin

This section explores unique physical land biological properties of dentin and their effects on dentin regeneration. As it has already been described dentin shares many similarities with bone; however it is a distinct tissue and differs from bone in many aspects.

Chemically, dentin has more mineral (67% -70%) than bone (50 %) and is slightly harder than bone (28,30). There are special cells called osteocytes enclosed in bone that are connected through canaliculi to form a network for bone maintenance, whereas there are no cells present in dentin (cell body remains in pulp), only cellular processes extend through to certain depths of dentin (25,28-30). The combination of bone cells (osteoblasts, osteooclast and osteocytes) carry on remodelling the bone throughout life, while no such remodelling is observed in dentin under physiological conditions (25,28-30,36).

It is obvious from these facts that dentin is acellular and less vascular than bone that can make regeneration of dentin quite difficult. In spite of all these factors, dentin regeneration has been observed successfully in previous studies (17-23,41,60-63). The new material will support the damaged dentin tissue to use the master plan of inducing dentin regeneration *in vivo.*

1.9- Why there is need of a new material for dental applications?

The main aim for making this material is to use biomimetic techniques to form natural dentin tissue and maintain the pulp vitality, because no material can be better than natural tissues. Furthermore it is obvious from the discussion above that

dental pulp plays an important role for teeth and keeping the pulp vital as long as possible is desired by dental professionals. Loss of pulp tissue (tooth vitality) results in change in the physical properties of dentin, and it may behave differently compared to a vital tooth (11). There is a decrease in the water content (up to 9 %) of dentin (64,65) the adhesive ability of tooth and tooth colour may change due to the presence of blood break down products that may not be acceptable aesthetically (11). If the tooth is treated for endodontics (treatment for non-vital teeth); the use of chemicals in the preparation method make teeth very weak mechanically and prone to fracture (66,67). Hence, maintaining the pulp vitality will enhance the life of a physiological tooth *in situ.* There are a few more solid arguments described below to emphasise the fact that development of this new material can benefit dentistry and humanity.

I. The need to maintain tooth vitality

Described above

II. No available material is ideal

Despite better understanding of the materials chemistry and recent improvements in the physical properties, no material has been found that is ideal for any dental application (4). For example, there has been a major concern about mercury toxicity from the amalgam restorations for many years (68-72). Another major issue is the colour of amalgam for aesthetic considerations and alternative materials are being sought to replace this (73-75). The composite restorative materials have promising aesthetics but they are not as good mechanically as amalgams and also are very technique sensitive (76). Nature has arranged complex biominerals in the best way from the micro to the nano scale and no one can yet combine biological and physical properties to get ideal structures. In addition, no synthetic material can be intelligent enough to respond to external stimuli and react like nature made tissues (57). The best possible option is to replace lost dentin tissue with regenerated dentin that can have a very close resemblance to the natural dentin and can respond to stimuli accordingly.

III. Large global market

There is a huge demand and global market for modern dental materials, the dental composite resins developed more recently and gained a huge market of €550 million a year in 2005 all over the world (76). According to estimates (13), there is a rapid increase in the use of dental implants; more than 300,000 implanted every year with some patient having more than twelve. There was a market of US$ 910,000 for dental implant in 2000 in the United States alone (13).

There are many other factors that can increase the demand of all biomaterials generally, like more awareness of patients about the biomaterials, better life style, increasing population and life expectancy (average age). For instance, the average life span has increased up to 30 year in USA during the 20th century (77), and is expected to rise up to hundred years by 2050 (78). Furthermore, number of centenarians (100 years old) is increasing every year, with an 8.5 % rise per year being observed in Australia (79). Similarly, there were only 2835 centenarians in Mexico in 1930. This had gone up to 19,000 in 2000 and is expected to increase up to more than 137,000 in 2050 (78). So on the basis of these facts; it can be assumed that there will be very high demand of all biomaterial including dental material to maintain the quality of life in older populations.

1.10- Desired properties for the new material for dentin regeneration

Dentists, materials scientists and toxicologists have described certain required properties for a dental material to be declared 'perfect' for dental applications. Similar to other biomaterial applications, it is desired to be non-toxic, non-irritant and non-corrosive (4). For dental applications, the material should provide a good seal with the natural tooth to prevent any ingress of fluid or secondary decay and should be easy to use (25), conserve tooth structures, with wear resistance equal to tooth enamel, having radiopacity greater than enamel and have long term stability (11). From a tissue engineering point of view, it needs to form a three dimensional structure for cell differentiation and proliferation, can deliver cells, growth factors and be capable of initiating repair and regeneration of lost or diseased dental tissues (12), and be biodegradable over time (80). For this purpose, it must also be a bioactive material having physical properties comparable to dentin as described earlier.

Interestingly, at the present time none of the available materials is perfect for dental applications and this has resulted in the continuation of dental materials research all over the world which is now focusing on nanoparticle containing nanocomposites (4,81,82). Most natural tissues (hard as well as soft) are composite materials made with variable combinations of organic and inorganic components (57), hence, it make sense to consider developing an organic-inorganic composite material at the nano scale. For this purpose, a natural biopolymer (natural silk) and silk containing chimeric proteins have been used with silica as inorganic component. Some of the key properties required for developing materials for dental regeneration are described here

1.10.1- Biocompatibility

Biocompatibility can be defined as the ability of a material to perform with an appropriate host response in a specific application (83). Biocompatibility assessment of biomaterials is a complex process and may comprise *in vitro* and *in vivo* testing. The biocompatibility of any material is not an absolute property and a material biocompatibility can be changed depending on application. Hence, no materials can be declared biocompatible without the mention of the location and practical application of the material (84). For example, for tissue engineering applications, scaffold material which perform in *in vitro* and *in vivo* pathophysiological processes are controlled by careful selection of cells and biomechanical conditions to regenerate new tissues (13).

A variety of methods can be used for testing a material's biological interaction depending on the duration of the application. Different national and international organisations suggest guidelines about what methods are appropriate for any particular application (13). For the development of new materials, the American Dental Association (ADA) and the International Standards Organisation (ISO) have developed guidelines (13). These tests help to evaluate and understand the biological response of any material, however, no material can be declared biocompatible with 100 % certainty (84). These guidelines can be used to prepare submissions for approval of a new material or device to regulatory agencies such as the U.S Food and Drug Administration (FDA).

For short-term *in vivo* testing for example, ASTM Standard F1983 - 99(2008) can be used for assessment of compatibility of absorbable/resorbable biomaterials for implant applications. Application of standard methods for material's testing facilitates

the reproducibility of results and verification by other researchers (13). Prior to clinical evaluation, ISO standard 10993 is followed for biocompatibility screening. For biocompatibility evaluation of dental materials, There are three major types of testing methods used (85).

I. *In vitro* tests
II. Animal tests
III. Usage tests

I. *In vitro* tests

These are laboratory based tests performed using test tubes and cell culture facilities (84). A typical example is the Ames test (86,87), where a biomaterial or its products are exposed to a strain of bacteria or fibroblasts to assess biological interactions. The assessment of these experiments is performed using criteria such as cellular count, growth and functional abilities. The main advantages of *in vitro* testing are that there is no involvement of animals avoiding any ethical and legal issues. Additionally, these experiments are simple, inexpensive, fast to perform and can be repeated in a controllable manner (84). The disadvantages of *in vitro* tests is they do not represent a true picture of biological interactions and results may be misleading (84).

II. Animal tests

The material under investigation is embedded into an experimental animal to study the complex biological interactions in the dynamic environment. Commonly used animals are rat, dog, cat, sheep or monkey. Animal tests provide a lot more information on the material's behaviour compared to *in vitro* tests. Animal testing is expensive, time consuming, has difficult to control variables and may also involve ethical or legal concerns (84).

III. Usage tests

Usage tests are clinical trials performed on a volunteer human in its final intended application. These experiments give most relevant biocompatibility

data for the particular application. Clinical trials may be time consuming, difficult to control due to individual variations and further complicated by the involvement of ethical and legal issues (84).

For the development of new dental materials, it is crucial to test the biocompatibility of a new material so that benefits and risk assessments of any new material can be documented prior to practical applications.

1.10.2- Biodegradation

Biodegradation is a cascade of complex processes involving the breakdown of biomaterials into smaller compounds (88). Biodegradation is one of the vital properties required for certain applications of biomaterials (88). Some important properties of biodegradable biomaterials are mentioned here (89),

- The material should not induce any inflammatory or toxic response upon implantation in body.
- The material should have an adequate shelf life.
- The degradation products should be non-toxic, metabolised and cleared from the body.
- The degradation rate should match the rate of healing and regeneration of tissue.
- The materials should have acceptable mechanical properties for the intended application and any changes in the mechanical properties should be well-matched with healing and regeneration of tissues.
- The materials should have suitable permeability and processability for the intended application.

Both synthetic (poly lactic acid, poly glycolic acid) and natural polymers (starch, alginate, fibrin, chitin,(90) alginate and silk) have been widely used as biodegradable materials (90-93). Depending on the mechanism, degradable biomaterials may be subdivided into hydrolytically and enzymatically degradable materials (94). Most natural polymers including silk fibroin fall into the category of enzymatically degradable materials. Upon *in vivo* implantation, the rate of degradation is determined by multiple factors such as concentration or/and availability of enzymes and chemical modifications of polymers (94).

1.10.2.1- Biodegradation of silk biomaterials

To develop silk based biomaterials, it is vital to understand the degradation behaviours of silk fibroin. In previous studies, *In vivo* implanted silk fibroin (FDA approved biomaterial) for 60 days, retained more than 50 % of its tensile strength (95) hence was declared non-degradable by United States Pharmacopeia. However, silk is degradable over longer periods of time (up to 1 year) and absorbed slowly (88,96). Silk is susceptible to biodegradation by certain proteolytic enzymes such as chymotrypsin, actinase and carboxylase (94). Generally, enzymatic degradation of silk takes place in two stages, firstly, adsorption of the enzymes on the surface using surface binding domains followed by hydrolysis in the second stage (94). Silk degradation products are absorbed easily *in vivo* (88) and this is another significant benefit of using silk biomaterials. Additionally, the degradation rate of silk fibroin can be controlled by altering the enzyme concentration/availability (94), crystallinity (97), pore size, porosity and molecular weight distribution (88). This slow degradation rate of silk fibroin may be very beneficial to support cells and regenerating tissues for prolonged times to cope with the slow rate of dentin regeneration for the proposed application of new material.

1.10.3- Bioactivity

Bioactivity is a property of biomaterials to induce the biological interaction of living tissues by surface mineralisation of calcium and phosphate with specific compositions and structures (98). This process is facilitated by the formation of a thin layer of calcium phosphate at the interface between the host and host hard tissues (98). Bioactive ceramic materials are already in clinical use for orthopaedic and dental application however bioactivity may be required for tissue engineering applications. Some examples of bioactive materials are bioglass, hydroxyapatite and calcium phosphate (99).

The surface of bioactive ceramic materials undergoes kinetic modification upon implantation by forming a layer of hydroxy carbonate apatite providing bonding interfaces with tissues (91). A similar apatite layer can be imitated on the surface of bioactive ceramics in a protein and cell free simulated body fluid (SBF) that has ion concentrations similar to that of blood plasma (91). This approach is commonly used for the *in vitro* evaluation of the bioactivity of biomaterials (100). Bioactivity is an important property required for tissue engineering scaffolds as formation of such

biological interfaces prevents scaffold loosening, supports enzyme activity (101,102), vascularisation (103,104), cell adhesion, growth and differentiation (105,106).

1.11- Natural silk as a biomaterial

Silks are protein polymers that are spun into fibres by silkworms and spiders at ambient conditions (13). Considering the natural sources of silk, there are many silk producing animal organisms but most of natural silk is usually obtained from silk worms (107). Silk proteins are usually produced within specialized glands cells, followed by secretion into the lumen of these glands where the proteins are stored prior to being spun into fibres (96). Silk was discovered in China around 2700 B.C. Silk is cultivated in Asia and Europe, although the main sources remain Japan, China, and India (108). Silk is known to have excellent properties required for biomaterial applications, for example, biocompatibility for a range of applications, non-toxic, non-irritant (109-111) and has excellent mechanical properties (112). Silk has an ability to perform under a wide range of conditions of humidity and temperature (113). Additionally, silk can be manipulated to form a variety of materials to tailor the final properties depending on the application, e.g., films, fibres, hydrogels, foams and coatings on other materials (114,115). Silk has a very long history in biomaterial applications as it has been used as a surgical suture material successfully for decades (116). More recently, silk has also been introduced into other biomaterials applications such as tissue engineering scaffolds (117-121) and drug delivery (122,123).

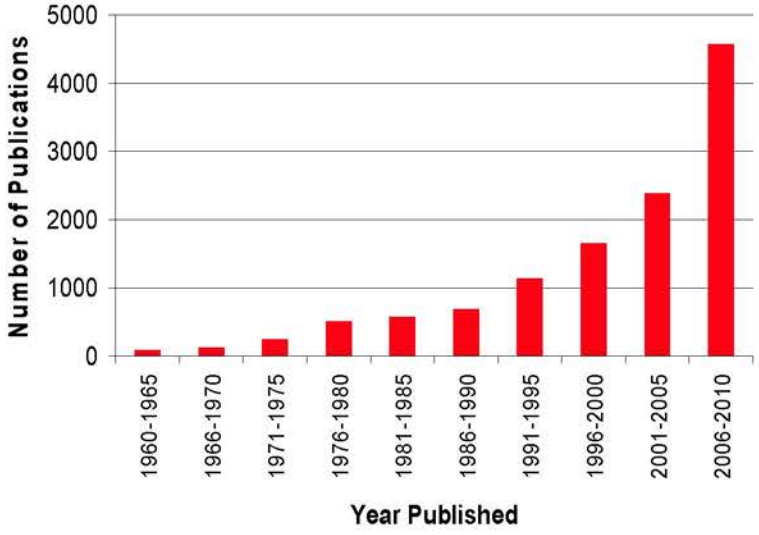

Figure 1.5: Number of scientific publications on silk (Data taken from ISI web of knowledge using keyword "silk").

Due to the unique properties of silk, there is an increasing interest in silk for biological applications (124) as well as in the scientific publications in the recent years (Figure 1.5). In terms of tissue engineering scaffolds, regenerated *Bombyx mori* (*B.mori*) silk is compatible with human mesenchymal stem cells *in vitro*, and is comparable to collagen scaffolds. *In vivo*, the tissue inflammatory reaction is similar to or less than found for collagen (125,126). Silk proteins degrade slowly in the biological environment (127) and which could be an advantage for dentin tissue regeneration.

It is evident from the above discussion that silk can be suggested as a successful material for a variety of biological applications due to its unique properties. Better understanding of silk structure at all levels is likely to expand its application in biomaterials.

1.12- Silica and biosilica

Silica also known as silicon dioxide is the most abundant mineral in the earth's crust (128,129). Silica can be found in nature in different forms like sand, clay, quartz and minerals and has been used for a wide range of applications (129). Chemically, silica is an oxide of silicon (129). Silicon (Si^{14}) is a non-metal and second most abundant element in the earth's crust (129-131). It has great affinity with oxygen, forming silica and silicates and is rarely found in pure form (129,131), Silicon is present as one of the abundant trace elements in the human body (1-2 g), and is required for proper growth and maintenance of bones and connective tissues (131), although its function in the human body at a molecular level is unclear.

Biosilica is produced on a large scale by different unicellular organisms however, In the biological world, the organic matrix plays an important role in the construction and control of morphology of inorganic silica (132,133). For example, proteins (Silaffins) play a crucial role in the formation of complex silica structures in marine organisms such as diatoms (132,133). A short polypeptide called R5 (19 amino acids) is a vital component of silaffin protein (Sil.1) of diatom *Cylindrotheca fusiformis* for controlling the formation and morphology of silica. In addition, R5 peptide has the ability to control the morphology of silica formation *in vitro* when added to silicic acid at neutral pH and ambient temperature (134). It has been demonstrated previously that the RRIL motif at the C-terminus of the R5 peptide encourages *in vitro* silica precipitation, absence of the RRIL motif resulted in no or minimal silica formation (135). More recently, R5 has been used to functionalise silk proteins to fabricate silk and silica nanocomposite materials using biomimetic

techniques (136). Similarly, R5 can be modified in different ways to produce silica containing materials using ambient conditions and biomimetic techniques.

For the application point of view, silica has already been used widely for a range of biomedical and dental applications, and is well known for fabricating composite materials (137), mainly for bone and joint replacement devices e.g., bioglass containing biomaterials (137)(138). Furthermore, silica has been widely used component of many existing dental materials for a range of applications. For example as a filler particle in dental restorative composites in the form of micro to nano size particle (4,5,81,139,140), as silicates in silicate and glass ionomers cements (4,5,8,15), giomers (16), dental porcelains (4,5), as hydrated silica in whitening toothpastes (141-143), tooth polishing (144) and bioactive coating of dental implants (5).

1.12.1- Why use silica as the inorganic component?

Silica has been selected for the fabrication of this novel material considering a number of factors. For instance, like other ceramic materials, silica is bioinert, biocompatible and has good compressive strength (145) needed for the intended application. Silica containing materials (bioglass) has proven bioactivity (99,138,145) that is desired for the new material and can help in dentin regeneration. Aqueous Si in the form of orthosilicic acid helps in the precipitation of calcium phosphate and directs the mineralisation process to stimulate tissue regeneration (146,147) . Formation of biologically active HA like layers has been observed to form spontaneously on silica materials previously (99). Alongside these positive aspects of silica there are also a few drawbacks for in spite of good hardness and stiffness, silica materials are brittle and have high density (137,145). In the next section, how these problems can be overcome by making composite materials is described.

1.13- Why making composite materials?

Composite materials are made by combining two or more materials on a macroscopic level to have better control of mechanical and physical properties than for the individual materials (148,149). It can be suggested that properties of composite materials can be tailored at the fabrication stage accordingly for a range of biomedical applications. For example, almost all tissues in the human body are composites however they vary one to the other in composition and properties depending on their role in the body (137). For dental applications, polymer

composites can provide some additional benefits to obtain desired properties in the materials. For example, to improve mechanical properties (tuneable density, stiffness and hardness), an absence of corrosion, galvanism (like in metal and alloys), and adjustable radiopacity. Furthermore, because of their non-magnetic property, polymer composite materials are very unlikely to interfere with conventional diagnostic tools (radiography) as well as modern techniques like computed tomography and magnetic resonance imaging (137). Briefly, a wide range of properties like stiffness, biodegradability and bioactivity can be obtained by varying combinations of materials. Even better composite biomaterials for certain applications can be fabricated using nano technology as described in the following section.

1.14- Conventionally used dental composite materials

Composite materials (resin composites) are widely used in dentistry (11,76,150). Conventionally used dental composites are highly cross-linked polymeric materials reinforced by inorganic filler particles (glass or crystalline) and/or fibres bound by coupling agents, typically having three structural components (4),

I. Polymer matrix
   Such as tri-ethylene glycol dimethacrylate and urethane dimethacrylate
II. Inorganic fillers
   Ground or milled quartz or glass particles in the size range of 0.1 to 100 μm (microfillers), resulting in improvement of hardness, strength, wettability, radiopacity and reduce water sorption and staining.
III. Coupling agents
   To promote adhesion between fillers and matrix promoting transfer of stresses from flexible polymer to more rigid and stiffer particles. Appropriate coupling using organosilanes is particularly essential for the clinical performance of dental composite restorative materials.

There are a few other components added to dental composites such as pigments to adjust colour and hue to improve aesthetic, initiator/accelerator chemicals to induce light activation, ultraviolet absorbers and inhibitors to improve the shelf life (4).
There are a number of short comings of micro-filled dental composites such as (4,5),

- Volumetric shrinkage upon polymerisation, and developing areas of internal stress concentration compromising the strength due to the fact that the inorganic particles do not shrink.
- Cannot be used in high stress bearing areas
- Marginal leakage
- Low wear resistance
- Susceptible to staining
- Light can penetrate up to 2-2.5 mm so needs manipulation in increments
- Technique sensitive; need isolation, acid etching and materials polymerisation in place

Dynamic research (151-155) is in progress in the community to improve the performance of dental composites. Tissue engineering techniques can provide better options for the replacement of lost dental tissues.

1.15- Nanotechnology and benefits of using nano-composites

The science of nanotechnology has become the most popular area of research currently covering a broad range of applications (59,156-158). Nanotechnology is defined as purposeful engineering on a scale of less than 100 nm to achieve desired properties, functions and performance characteristics (158). Nanocomposites can be defined as special types of materials made with combination of two or more nano-sized objects using suitable techniques resulting in unique physical properties (159). The examples of unique properties are very large surface area to volume ratio, flexibility in surface functionalities, improved mechanical properties, making these materials suitable for a wide range of applications (160). Nanocomposites have also shown significantly better biodegradability (161,162).

Nature has used nano-materials widely in natural biomaterials like bone, teeth, shells, and wood (163) and there is lot more to learn from nature. In 1998, an article published by Chemistry in Britain (164) admiring nature *"Nature is a master chemist with incredible talent"*. Surprisingly, all natural nano-materials are fabricated under ambient conditions without any need of high temperature, pressure or extremes of pH (59). Biomimetic techniques are the way to unlock nature's methodology to optimize nano level materials fabrication (156).

Considering organic/inorganic nano-composite materials, a number of different materials have been used to make nano-particles to blend with polymers. Examples of inorganic nano-particles are metals (Al, Fe, Ag, Au etc), ceramics (ZnO, TiO_2,

$CaCO_3$, Al_2O_3) (163) and silica (165-174). The selection of nano particle depends on the desired properties in the new material for any particular application, for example, metal nano particles can result in higher conductivity or ceramic nano-particles can produce better mechanical properties (163). Moreover, the properties of nano-composites can also be varied by changing proportions of parent materials, morphology (particle, fibres, tubes, wired etc) and interfacial features (164).

Because of excellent physical and biological properties, silica nano-particles have been widely used with different natural and synthetic polymers for making nano-composites for a range of applications (165-174). Silica/silk hybrid materials have been fabricated widely (157,175-177) and are considered to have significant potential for biomaterial applications (157). In a recent study (136), silk containing chimeric proteins functionalised with silica condensing peptide (R5) were used to make nano-composite materials. The significance of such a kind of chimeric protein is described below.

1.16- What are fusion (chimeric) proteins and why to use them?

The national institute of Cancer has defined a fusion protein as a protein made from a fusion gene that is created by joining parts of two different genes (178). Fusion proteins may exist naturally as a result of DNA transfer between chromosomes or can be produced by combining genes from the same or different species in the laboratory using genetic engineering techniques (178). Fusion proteins have been used in a wide range of applications in areas such as cancer research (179-190), immunology studies (191-193), drug delivery (194-197), biosensors (198,199), material synthesis (200), inorganic material synthesis (201,202), and biomimetic synthesis (202).

In a recent study (136), novel nanocomposites were prepared using spider silk-silica fusion proteins and biomimetic techniques. These fusion proteins prepared using genetic engineering techniques consisted of two components. One component of this fusion protein is the self-assembling domain based on the repeat consensus of spider dragline silk, responsible for the formation of highly stable β-sheet formation and excellent mechanical properties. The second part of the fusion protein is the R5 peptide (136) isolated from the silaffin protein of diatom (Cylindrotheca fusiformis), as a 19 amino acid unit (SSKKSGSYSGSKGSKRRIL) that has been shown to induce and regulate silica precipitation under ambient conditions (203). This fusion protein has been used in the production of nanocomposite materials containing silica particles with a narrow distribution range (0.5-2 μm); while mineralization

reactions in the presence of only the R5 peptide produced silica particles of wider size range 0.5-10 μm in diameter. Moreover, the spider drag line silk is a natural fibrous biomaterial which has impressive mechanical and complex self-assembling properties (136).

1.17- Criteria for future dental materials

Restoration of lost dental and oral tissues represent a major problem costing 5-10 % of healthcare budgets in developed countries (204). None of the biomaterials available are ideal for dental applications and there is need of new materials with improved properties. "Why new dental materials" has been explained in detail in section 1.9. There is a long history of using synthetic materials (metals, alloys and ceramics) for dental applications (Section 1.1). There are certain discrepancies in dental restorative materials in use currently, such as silver amalgams have certain toxicity issues and their clinical use in many countries has declined in recent years (205). Shortcomings of dental resin composites are described in section 1.14.

Tissue engineering technologies represent an attractive option to replace existing dental materials and can fulfil many problems found with the present dental materials. Development of biocompatible, biodegradable, bioactive and composite scaffold materials can induce dentin regeneration leading to physiological replacement of lost/damaged dentin that can serve for a longer duration than any synthetic dental material. Over the last few decades, a significant amount of money has been spent on research to develop and improve dental materials (204). Significant progress has been achieved in tissue regenerative techniques by understanding tissue structure-function relationship and tissue engineered products are commercially available for wound, burn and ulcer repair, arterial grafting (206), and articular cartilage (207). However, dental tissue engineering research is challenging, involving multiple disciplines and remarkable progress is expected by designing biomimetic and bioactive scaffolds.

1.18- Aims and objectives

The major goal of this research project is to develop a new silk-silica based bioactive, biodegradable and biocompatible scaffold material with improved properties that will have intend application dental tissue repair and regeneration upon application in the tooth.

The main aims for this research are;

I. To study the chemistry and kinetics of silica formation and to assess the effects of silk proteins on them.
II. To evaluate the effects of silk proteins on structure, morphology and mechanical properties of nanocomposite materials produced.
III. To study the effect of silk containing proteins on the mechanical and functional properties of nanocomposite materials.
IV. Use the results to assess which organic-inorganic combination will provide potential nanocomposite materials for dental applications.

1.19- Hypothesis

The hypothesis for this study is that alteration in silk proteins can affect the structure, morphology and strength of silica based nanocomposite materials for the intended application of dentin tissue engineering.

The outcome of this project will be the production of an entirely new family of nanocomposite biomaterials for dental applications, created from novel self-assembling proteins and silica and providing nanoscale control of morphology and structure. This control will be at the molecular level for interaction of organic and inorganic components which is a hallmark of nature to attain strength and toughness in biological structures. The proposed nanoscale biomimetic approach is also versatile in the sense that protein domains involved can be transformed with other mineral content such as hydroxyapatite or titanium oxide to expand the range of composite materials to be generated. It can be hoped from the on-going research that new materials with improved properties will be available for dental applications in the near future.

1.20- References

(1) Nicholson JW. The chemistry of medical and dental materials. Cambridge: Royal Society of Chemistry; 2002.

(2) Charnley J. Surgical treatment of un-united fractures. J Bone Joint Surg 1960;42 (1):3-4.

(3) Charnley J. Arthroplasty of the hip : A new operation. The Lancet 1961; 277(7187):1129-1132.

(4) Phillips' science of dental materials. 11th ed. St. Louis, Mo. ; Great Britain: Saunders; 2003.

(5) Restorative dental materials. 11th ed. St. Louis, Mo. ; London: Mosby; 2002.

(6) Gladwin MA. Clinical aspects of dental materials : theory, practice, and cases. 3rd ed. Philadelphia, Pa. ; London: Lippincott Williams & Wilkins; 2009.

(7) Buonocore MG. A simple method of increasing the adhesion of acrylic filling materials to enamel surfaces. Journal of Dental Research 1955;34(6):849-853.

(8) Wilson AD, Kent BE. The glass-ionomer cement, a new translucent dental filling material. Journal of Applied Chemistry and Biotechnology 1971;21(11):313.

(9) Phillips DM, Drummy LF, Conrady DG, Fox DM, Naik RR, Stone MO, et al. Dissolution and regeneration of Bombyx mori silk fibroin using ionic liquids. J Am Chem Soc 2004;126(44):14350-14351.

(10) Darvell BW. Materials science for dentistry. 9th ed. Oxford: Woodhead Publishing; 2009.

(11) Fundamentals of operative dentistry : a contemporary approach. 2nd ed. Chicago, Ill. ; London: Quintessence Publishing; 2000.

(12) Hargreaves KM. Cohen's pathways of the pulp. 10th ed. Edinburgh: Mosby; 2010.

(13) Biomaterials science : an introduction to materials in medicine. 2nd ed. Amsterdam ; London: Elsevier Academic Press; 2004.

(14) Dental materials and their selection. 3rd ed. Chicago, Ill. ; London: Quintessence; 2002.

(15) Mount GJ. An atlas of glass-ionomer cements : a clinician's guide. 3rd ed. London: Martin Dunitz; 2002.

(16) Itota T, Carrick TE, Yoshiyama M, McCabe JF. Fluoride release and recharge in giomer, compomer and resin composite. Dental Materials 2004 11;20(9):789-795.

(17) Chen S, Gluhak-Heinrich J, Martinez M, Li T, Wu Y, Chuang HH, et al. Bone morphogenetic protein 2 mediates dentin sialophosphoprotein expression and odontoblast differentiation via NF-Y signaling. J Biol Chem 2008;283(28):19359-19370.

(18) Sloan AJ, Rutherford RB, Smith AJ. Stimulation of the rat dentine-pulp complex by bone morphogenetic protein-7 in vitro. Arch Oral Biol 2000;45(2):173-177.

(19) Saito T, Ogawa M, Hata Y, Bessho K. Acceleration effect of human recombinant bone morphogenetic protein-2 on differentiation of human pulp cells into odontoblasts. J Endod 2004;30(4):205-208.

(20) Smith AJ, Tobias RS, Murray PE. Transdentinal stimulation of reactionary dentinogenesis in ferrets by dentine matrix components. J Dent 2001 7;29(5):341-346.

(21) Smith AJ, Tobias RS, Plant CG, Browne RM, Lesot H, Ruch JV. In vivo Morphogenetic activity of dentin matrix proteins. J Biol Buccale 1990;18(2):123-129.

(22) Tziafas D. The future role of a molecular approach to pulp-dentinal regeneration. Caries Res 2004;38(3):314-320.

(23) Almushayt A, Narayanan K, Zaki AE, George A. Dentin matrix protein 1 induces cytodifferentiation of dental pulp stem cells into odontoblasts. Gene Ther 2006;13(7):611-620.

(24) van der Bilt A, Engelen L, Pereira LJ, van der Glas HW, Abbink JH. Oral physiology and mastication. Physiol Behav 2006;89(1):22-27.

(25) Jones FH. Teeth and bones: applications of surface science to dental materials and related biomaterials. Surface Science Reports 2001;42(3-5):75-205.

(26) Silver FH. Biomaterials, medical devices and tissue engineering : an integrated approach. : Chapman and Hall; 1994.

(27) Cawson RA. Cawson's essentials of oral pathology and oral medicine. 7th ed. Edinburgh: Churchill Livingstone; 2002.

(28) Ten Cate AR. Oral histology : development, structure, and function. 4th ed. St. Louis ; London: Mosby; 1994.

(29) Oral development and histology. 2nd ed. New York: Thieme Medical; 1994.

(30) Nanci A. Ten Cate's oral histology : development, structure, and function. 7th ed. St. Louis, Mo. ; London: Mosby; 2008.

(31) Fairpo JEH. Heinemann dental dictionary. 4th ed. Oxford: Butterworth-Heinemann; 1997.

(32) Bath-Balogh M. Illustrated dental embryology, histology, and anatomy. Philadelphia, Pa. ; London: W.B. Saunders; 1997.

(33) Gwinnett AJ. Structure and composition of enamel. Oper Dent 1992;Suppl 5:10-17.

(34) Human oral histology and embryology. : Munksgaard; 1986.

(35) Krishnaraju RK, Hart TC, Schleyer TK. Comparative genomics and structure prediction of dental matrix proteins. Advances in Dental Research 2003;17(1):100-103.

(36) Linde A, Goldberg M. Dentinogenesis. Critical Reviews in Oral Biology & Medicine 1993;4(5):679-728.

(37) Lodding A. Quantitative ion probe microanalysis of biological mineralized tissues. Scanning Electron Microscopy 1983 Part 3:1229-1242.

(38) Orban's oral histology and embryology. 11th ed.: Mosby-Year Book; 1991.

(39) Garberoglio R, Brännström M. Scanning electron microscopic investigation of human dentinal tubules. Arch Oral Biol 1976;21(6):355-362.

(40) United States. Public Health Service. National Institutes of Health. National Institute of Dental Research. An electron microscopic study of the early stages of dentinogenesis. : pp. iv. 55. Washington; 1958.

(41) Tziafas D, Belibasakis G, Veis A, Papadimitriou S. Dentin regeneration in vital pulp therapy: design principals. Advances in Dental Research 2001;15(1):96-100.

(42) Dorland WAN. Dorland's pocket medical dictionary. 24th ed: W. B. Saunders; 1989.

(43) Butler W. Dentin matrix proteins. European Journal Of Oral Sciences1998;106(Suppl. 1):204-210.

(44) Tziafas D, Smith AJ, Lesot H. Designing new treatment strategies in vital pulp therapy. J Dent 2000 2;28(2):77-92.

(45) Couve E. Ultrastructural-changes during the life-cycle of human odontoblasts. Archives of Oral Biology 1986;31(10):643-651.

(46) Kawasaki K, Tanaka S, Ishikawa T. Incremental lines in human dentin as revealed by tetracycline labeling. J Anat 1977;123(APR):427-436.

(47) Brannstr.M, Garberog.R. Dentinal tubules and odontoblast processes - scanning electron-microscopic study. Acta Odontologica Scandinavica1972;30(3):291.

(48) Provenza DV. Oral histology : inheritance and development. 2nd ed. Philadelphia: Lea & Febiger; 1986.

(49) Stanley HR, White CL, McCray L. The rate of tertiary (reparative) dentine formation in the human tooth. Oral Surg Oral Med Oral Pathol 1966;21(2):180-189.

(50) LeGeros RZ. Calcium phosphates in oral biology and medicine. Basel: Karger; 1991.

(51) Vallet-Regí M. Ceramics for medical applications. Journal of the Chemical Society, Dalton Transactions 2001;2001(2):97-108.

(52) Naray-Szabo S. Structure of apatite $(CaF)Ca_4(PO_4)_3$. Z Kristallogr 1930;75:387-398.

(53) Kay MI, Young RA, Posner AS. Crystal Structure of Hydroxyapatite. Nature 1964;204(496):1050.

(54) Mitchell L. Oxford handbook of clinical dentistry. 3rd ed. Oxford ; New York: Oxford University Press; 1999.

(55) Fluoride in dentistry. Copenhagen: Munksgaard; 1988.

(56) Emsley J. The chemistry of phosphorus : environmental, organic, inorganic, biochemical and spectroscopic aspects. London: Harper & Row; 1976.

(57) Mano JF, Reis RL. Some trends on how one can learn from and mimic nature in order to design better biomaterials. Materials Science and Engineering: C 2005;25(2):93-95.

(58) Low IM, Duraman N, Mahmood U. Mapping the structure, composition and mechanical properties of human teeth. Materials Science and Engineering: C, 2008;28(2):243-247.

(59) Broderick M, Neville F, Gibson T, Millner P. Practical nanobiotechnology: Functional nanoparticle production using silaffin R5 peptide. Journal of Biotechnology, 2007 9;131(2, Supplement 1):S11-S11.

(60) Goldberg M, Six N, Decup F, Buch D, Soheili Majd E, Lasfargues J-, et al. Application of bioactive molecules in pulp-capping situations. Advances in Dental Research 2001;15(1):91-95.

(61) Rutherford RB, Gu KN. Treatment of inflamed ferret dental pulps with recombinant bone morphogenetic protein-7. Eur J Oral Sci 2000;108(3):202-206.

(62) Rutherford RB, Spangberg L, Tucker M, Rueger D, Charette M. The time-course of the induction of reparative dentin formation in monkeys by recombinant human osteogenic protein-1. Arch Oral Biol 1994;39(10):833-838.

(63) Rutherford RB, Wahle J, Tucker M, Rueger D, Charette M. Induction of reparative dentin formation in monkeys by recombinant human osteogenic protein-1. Arch Oral Biol 1993;38(7):571-576.

(64) Gutmann JL. The dentin-root complex - anatomic and biologic considerations in restoring endodontically treated teeth. J Prosthet Dent 1992;67(4):458-467.

(65) Helfer AR, Schilder H, Melnick S. Determination of moisture-content of vital and pulpless teeth. Oral Surgery Oral Medicine Oral Pathology Oral Radiology and Endodontics 1972;34(4):661.

(66) Grigoratos D, Knowles J, Ng YL, Gulabivala K. Effect of exposing dentine to sodium hypochlorite and calcium hydroxide on its flexural strength and elastic modulus. Int Endod J 2001;34(2):113-119.

(67) Sim TPC, Knowles JC, Ng YL, Shelton J, Gulabivala K. Effect of sodium hypochlorite on mechanical propel-ties of dentine and tooth surface strain. Int Endod J 2001;34(2):120-132.

(68) Eley BM. The future of dental amalgam: A review of the literature .2. Mercury exposure in dental practice. Br Dent J 1997;182(8):293-297.

(69) Eley BM. The future of dental amalgam: A review of the literature .4. Mercury exposure hazards and risk assessment. Br Dent J 1997;182(10):373-381.

(70) Jones DW. A Canadian perspective on the dental amalgam issue. Br Dent J 1998;184(12):581-586.

(71) Warfvinge K. Mercury exposure of a female dentist before pregnancy. Br Dent J 1995;178(4):149-152.

(72) Smart ER, Macleod RI, Lawrence CM. Resolution of lichen-planus following removal of amalgam restorations in patients with proven allergy to mercury salts - a pilot-study. Br Dent J 1995;178(3):108-112.

(73) Eley BM. The future of dental amalgam: a review of the literature .7. Possible alternative materials to amalgam For the restoration of posterior teeth. Br Dent J 1997;183(1):11-14.

(74) Mclean JW. Alternatives to amalgam alloys .1. Br Dent J 1984;157(12):432-433.

(75) Yardley RM. Alternatives to amalgam alloys .2. Br Dent J 1984;157(12):434-435.

(76) Moszner N, Salz U. Recent developments of new components for dental adhesives and composites. Macromolecular Materials and Engineering 2007;292(3):245-271.

(77) Centers For Disease Control. Ten great public health achievements - United States, 1900-1999. Morb Mortal Weekly Rep 1999;48(12):241-243.

(78) Ham-Chande R, Orlando F. Shapes and limits of longevity in mexico. 2005.

(79) Richmond RL. The changing face of the Australian population: growth in centenarians. Med J Aust 2008 JUN 16;188(12):720-723.

(80) Young C, Terada S, Vacanti J, Honda M, Bartlett J, Yelick P. Tissue engineering of complex tooth structures on biodegradable polymer scaffolds. J Dent Res 2002;81(10):695.

(81) Hickel R, Dasch W, Janda R, Tyas M, Anusavice K. New direct restorative materials. Int Dent J 1998;48(1):3-16.

(82) Lambrechts P, Goovaerts K, Bharadwaj D, De Munck J, Bergmans L, Peumans M, et al. Degradation of tooth structure and restorative materials: A review. Wear 2006;261(9):980-986.

(83) W. The Williams dictionary of biomaterials. Liverpool: Liverpool University Press; 1999.

(84) John C. W. Principles of biocompatibility for dental practitioners. J Prosthet Dent 2001 8;86(2):203-209.

(85) Hanks C.T., Wataha J.C., Sun Z. In vitro models of biocompatibility: A review. Dental Materials May;12(3):186-193.

(86) Stea S, Savarino L, Ciapetti G, Cenni E, Stea S, Trotta F, et al. Mutagenic potential of root canal sealers: Evaluation through Ames testing. J Biomed Mater Res 1994;28(3):319-328.

(87) Schweikl H, Schmalz G, Federlin M. Mutagenicity of the root canal sealer AHPlus in the Ames test. Clin Oral Investig 1998;2(3):125-129.

(88) Cao Y, Wang B. Biodegradation of Silk Biomaterials. International Journal of Molecular Sciences 2009;10(4):1514-1524.

(89) Lloyd AW. Interfacial Bioengineering to Enhance Surface Biocompatibility. Med Device Technol 2002 Jan;13(1):18.

(90) Lee SB, Kim YH, Chong MS, Hong SH, Lee YM. Study of gelatin-containing artificial skin V: fabrication of gelatin scaffolds using a salt-leaching method. Biomaterials 2005 5;26(14):1961-1968.

(91) Rezwan K, Chen QZ, Blaker JJ, Boccaccini AR. Biodegradable and bioactive porous polymer/inorganic composite scaffolds for bone tissue engineering. Biomaterials 2006 6;27(18):3413-3431.

(92) Seal BL, Otero TC, Panitch A. Polymeric biomaterials for tissue and organ regeneration. Materials Science and Engineering: R: Reports 2001 10/10;34(4-5):147-230.

(93) Di Martino A, Sittinger M, Risbud MV. Chitosan: A versatile biopolymer for orthopaedic tissue-engineering. Biomaterials 2005 10;26(30):5983-5990.

(94) Nair LS, Laurencin CT. Biodegradable polymers as biomaterials. Progress in Polymer Science 2007 9;32(8-9):762-798.

(95) Altman GH, Diaz F, Jakuba C, Calabro T, Horan RL, Chen J, et al. Silk-based biomaterials. Biomaterials 2003;24(3):401-416.

(96) Altman GH, Horan RL, Lu HH, Moreau J, Martin I, Richmond JC, et al. Silk matrix for tissue engineered anterior cruciate ligaments. Biomaterials 2002;23(20):4131-4141.

(97) Minoura N. Physico-chemical properties of silk fibroin membrane as a biomaterial. Biomaterials 1990;11(6):430.

(98) Lee KY. Ceramic bioactivity: progresses, challenges and perspectives. Biomedical Materials 2006;1(2):31.

(99) Hench LL, Xynos ID, Polak JM. Bioactive glasses for in situ tissue regeneration. Journal of Biomaterials Science, Polymer Edition 2004;15(4):543-562.

(100) Chen QZ, Boccaccini AR. Poly(D,L-lactic acid) coated 45S5 Bioglass®-based scaffolds: Processing and characterization. Journal of Biomedical Materials Research Part A 2006;77A(3):445-457.

(101) Aksay IA, Weiner S. Biomaterials is this really a field of research? Current Opinion in Solid State and Materials Science 1998 6;3(3):219-220.

(102) Ohgushi H, Dohi Y, Yoshikawa T, Tamai S, Tabata S, Okunaga K, et al. Osteogenic differentiation of cultured marrow stromal stem cells on the surface of bioactive glass ceramics. J Biomed Mater Res 1996;32(3):341-348.

(103) Day RM, Boccaccini AR, Shurey S, Roether JA, Forbes A, Hench LL, et al. Assessment of polyglycolic acid mesh and bioactive glass for soft-tissue engineering scaffolds. Biomaterials 2004 12;25(27):5857-5866.

(104) Keshaw H, Forbes A, Day RM. Release of angiogenic growth factors from cells encapsulated in alginate beads with bioactive glass. Biomaterials 2005 7;26(19):4171-4179.

(105) Roether JA, Gough JE, Boccaccini AR, Hench LL, Maquet V, Jérôme R. Novel bioresorbable and bioactive composites based on bioactive glass and polylactide foams for bone tissue engineering. J Mater Sci Mater Med 2002;13(12):1207-1214.

(106) Lu HH, Tang A, Oh SC, Spalazzi JP, Dionisio K. Compositional effects on the formation of a calcium phosphate layer and the response of osteoblast-like cells on polymer-bioactive glass composites. Biomaterials 2005 11;26(32):6323-6334.

(107) Zarkoob S, Eby RK, Reneker DH, Hudson SD, Ertley D, Adams WW. Structure and morphology of electrospun silk nanofibers. Polymer 2004 5;45(11):3973-3977.

(108) Gandhi M, Yang HJ, Shor L, Ko F. Regeneration of bombyx mori silk by electrospinning: A comparative study of the biocompatibility of natural and synthetic polymers for tissue engineering applications. Journal of Biobased Materials and Bioenergy 2007;1(2):274-281.

(109) Zuo B, Dai L, Wu Z. Analysis of structure and properties of biodegradable regenerated silk fibroin fibers. J Mater Sci 2006 06/01;41(11):3357-3361.

(110) Xu Y, Shao H, Zhang Y, Hu X. Studies on spinning and rheological behaviors of regenerated silk fibroin/N-methylmorpholine-N-oxideÂ·H2O solutions. J Mater Sci 2005;40(20):5355-5358.

(111) Kim K, Jeong L, Park H, Shin S, Park W, Lee S, et al. Biological efficacy of silk fibroin nanofiber membranes for guided bone regeneration. Journal of Biotechnology, 2005;120(3):327-339.

(112) Gosline J, Guerette P, Ortlepp C, Savage K. The mechanical design of spider silks: from fibroin sequence to mechanical function. J Exp Biol 1999;202(23):3295-3303.

(113) Sheu H, Phyu KW, Jean Y, Chiang Y, Tso I, Wu H, et al. Lattice deformation and thermal stability of crystals in spider silk. International Journal of Biological Macromolecules 2004;34(5):267-273.

(114) Hardy JG, Römer LM, Scheibel TR. Polymeric materials based on silk proteins. Polymer, 2008;49(20):4309-4327.

(115) Tamada Y. Modification of fibroin film with a chimera fibroin fragment for improvement of cell adhesion. Biomaterials Regulating Cell Function and Tissue Development 1998;530:27-32.

(116) Furuzono T, Ishihara K, Nakabayashi N, Tamada Y. Chemical modification of silk fibroin with 2-methacryloyloxyethyl phosphorylcholine. II. Graft-polymerization onto fabric through 2-methacryloyloxyethyl isocyanate and interaction between fabric and platelets. Biomaterials 2000 2;21(4):327-333.

(117) Gellynck K, Verdonk PCM, Van Nimmen E, Almqvist KF, Gheysens T, Schoukens G, et al. Silkworm and spider silk scaffolds for chondrocyte support. Journal of Materials Science-Materials in Medicine 2008;19(11):3399-3409.

(118) Kim HJ, Kim U, Kim HS, Li C, Wada M, Leisk GG, et al. Bone tissue engineering with premineralized silk scaffolds. Bone 2008 6;42(6):1226-1234.

(119) Peh RF, Suthikum V, Goh CH, Toh SL. Novel Electrospun-Knitted Silk Scaffolds for Ligament Tissue Engineering. World Congress on Medical Physics and Biomedical Engineering 2007;14:3287-3290.

(120) Nair LS, Bhattacharyya S, Laurencin CT. Development of novel tissue engineering scaffolds via electrospinning. Expert Opin Biol Ther 2004;4(5):659-668.

(121) Damrongrungruang T, Siritapetawee M, Kamanarong K, Limmonthon S, Rattanathongkom A, Maensiri S, et al. Fabrication of electrospun thai silk fibroin nanofiber and its effect on human gingival fibroblast: a preliminary study. Journal of Oral Tissue Engineering 2007;5(1):1-6.

(122) Wenk E, Wandrey AJ, Merkle HP, Meinel L. Silk fibroin spheres as a platform for controlled drug delivery. Journal of Controlled Release 2008;132(1):26-34.

(123) Li W, Mauck RL, Tuan RS. Electrospun nanofibrous scaffolds: production, characterization, and applications for tissue engineering and drug delivery. Journal of Biomedical Nanotechnology 2005;1(17):259-275.

(124) Bogush V, Sokolova O, Davydova L, Klinov D, Sidoruk K, Esipova N, et al. A novel model system for design of biomaterials based on recombinant analogs of spider silk proteins. Journal of Neuroimmune Pharmacology 2009;4(1):17-27.

(125) Meinel L, Hofmann S, Karageorgiou V, Kirker-Head C, McCool J, Gronowicz G, et al. The inflammatory responses to silk films in vitro and in vivo. Biomaterials 2005 1;26(2):147-155.

(126) Meinel L, Karageorgiou V, Fajardo R, Snyder B, Shinde-Patil V, Zichner L, et al. Bone tissue engineering using human mesenchymal stem cells: Effects of scaffold material and medium flow. Ann Biomed Eng 2004;32(1):112-122.

(127) Hakimi O, Knight DP, Vollrath F, Vadgama P. Spider and mulberry silkworm silks as compatible biomaterials. Composites Part B-Engineering 2007;38(3):324-337.

(128) Iler RK. The chemistry of silica : solubility, polymerization, colloid and surface properties, and biochemistry. New York ; Chichester: Wiley; 1979.

(129) Martin KR. The chemistry of silica and its potential health benefits. Journal of Nutrition Health & Aging 2007;11(2):94-98.

(130) Chumlea WMC. Silica, a mineral of unknown but emerging health importance. Journal of Nutrition Health & Aging 2007;11(2):93-93.

(131) Jugdaohsingh R. Silicon and bone health. Journal of Nutrition Health & Aging 2007;11(2):99-110.

(132) Kroeger N, Poulsen N, Sumper M, Deutzmann R. Biochemistry of silica nanofabrication in diatoms. Abstracts of Papers of the American Chemical Society 2004;227:143.

(133) Tomczak MM, Glawe DD, Drummy LF, Lawrence CG, Stone MO, Perry CC, et al. Polypeptide-templated synthesis of hexagonal silica platelets. J Am Chem Soc 2005;127(36):12577-12582.

(134) Kröger N, Deutzmann R, Sumper M. Polycationic peptides from diatom biosilica that direct silica nanosphere formation. Science 1999;286(5442):1129-1132.

(135) Knecht MR, Wright DW. Functional analysis of the biomimetic silica precipitating activity of the R5 peptide from Cylindrotheca fusiformis. Chem.Commun. 2003(24):3038-3039.

(136) Foo CWP, Patwardhan SV, Belton DJ, Brandon Kitchel, Anastasiades D, Huang J, et al. Novel Nanocomposites from Spider Silk-Silica Fusion (Chimeric) Proteins. Proc Natl Acad Sci 2006 20;103(25):pp. 9428-9433.

(137) Ramakrishna S, Mayer J, Wintermantel E, Leong KW. Biomedical applications of polymer-composite materials: a review. Composites Sci Technol 2001 7;61(9):1189-1224.

(138) Hench LL. The story of Bioglass®. J Mater Sci Mater Med 2006;17(11):967-978.

(139) Xu HHK, Quinn JB, Smith DT, Antonucci JM, Schumacher GE, Eichmiller FC. Dental resin composites containing silica-fused whiskers—effects of whisker-to-silica ratio on fracture toughness and indentation properties. Biomaterials 2002 2;23(3):735-742.

(140) Kim JW, Kim LU, Kim CK. Size control of silica nanoparticles and their surface treatment for fabrication of dental nanocomposites. Biomacromolecules 2007 01/01;8(1):215-222.

(141) Ashcroft AT, Cox TF, Joiner A, Laucello M, Philpotts CJ, Spradbery PS, et al. Evaluation of a new silica whitening toothpaste containing blue covarine on the colour of anterior restoration materials in vitro. J Dent 2008;36(Supplement 1):26-31.

(142) Joiner A, Philpotts CJ, Ashcroft AT, Laucello M, Salvaderi A. In vitro cleaning, abrasion and fluoride efficacy of a new silica based whitening toothpaste containing blue covarine. J Dent 2008;36(Supplement 1):32-37.

(143) Collins LZ, Naeeni M, Platten SM. Instant tooth whitening from a silica toothpaste containing blue covarine. J Dent 2008;36(Supplement 1):21-25.

(144) Silica nanoparticles for polishing teeth. Dental Abstracts 2009 4;54(2):92-93.

(145) Binyamin G, Shafi BM, Mery CM. Biomaterials: A primer for surgeons. Semin Pediatr Surg 2006;15(4):276-283.

(146) Pietak AM, Reid JW, Stott MJ, Sayer M. Silicon substitution in the calcium phosphate bioceramics. Biomaterials 2007 10;28(28):4023-4032.

(147) Damen JJM, Ten Cate JM. Silica-induced precipitation of calcium phosphate in the presence of inhibitors of hydroxyapatite formation. Journal of Dental Research March 01;71(3):453-457.

(148) Biomaterials fabrication and processing handbook. Boca Raton, Fla.; London: CRC; Taylor & Francis distributor; 2008.

(149) Biomaterials : principles and applications. Boca Raton: CRC Press; 2002.

(150) Bentley C, Drake C. Longevity of restorations in a dental school clinic. J Dent Educ 1986;50(10):594-600.

(151) Abdulmajeed AA, Närhi TO, Vallittu PK, Lassila LV. The effect of high fiber fraction on some mechanical properties of unidirectional glass fiber-reinforced composite. Dental Materials 2011 4;27(4):313-321.

(152) David B. Chewing over dental structure: Composites. Materials Today 2011 3;14(3):66.

(153) Karabela MM, Sideridou ID. Synthesis and study of properties of dental resin composites with different nanosilica particles size. Dental Materials 2011 8;27(8):825-835.

(154) Chen M. Update on dental nanocomposites. Journal of Dental Research 2010;89(6):549-560.

(155) Sun J, Forster AM, Johnson PM, Eidelman N, Quinn G, Schumacher G, et al. Improving performance of dental resins by adding titanium dioxide nanoparticles. Dental Materials 2011 10;27(10):972-982.

(156) Paul DR, Robeson LM. Polymer nanotechnology: Nanocomposites. Polymer 2008;49(15):3187-3204.

(157) Hou A, Chen H. Preparation and characterization of silk/silica hybrid biomaterials by sol–gel crosslinking process. Materials Science and Engineering: B 2010;167(2):124-128.

(158) Zhang Y, Lim CT, Ramakrishna S, Huang ZM. Recent development of polymer nanofibers for biomedical and biotechnological applications. J Mater Sci Mater Med 2005;16(10):933-946.

(159) Gangopadhyay R, De A. Conducting polymer nanocomposites: a brief overview. Chem.Mater 2000;12(3):608-622.

(160) Huang Z, Zhang Y-, Kotaki M, Ramakrishna S. A review on polymer nanofibers by electrospinning and their applications in nanocomposites. Composites Science and Technology 2003 11;63(15):2223-2253.

(161) Ray SS, Okamoto M. Biodegradable Polylactide and Its Nanocomposites: Opening a New Dimension for Plastics and Composites. Macromolecular Rapid Communications 2003;24(14):815-840.

(162) Mohanty A, Drzal L, Misra M. Nano reinforcements of bio-based polymers - The hope and the reality. ABSTRACTS OF PAPERS OF THE AMERICAN CHEMICAL SOCIETY 2003;225(Part 2):33.

(163) Hussain F, Hojjati M, Okamoto M, Gorga RE. Review article: polymer-matrix nanocomposites, processing, manufacturing, and application: an overview. J Composite Mater 2006;40(17):1511.

(164) Oriakhi C. Nano sandwiches. Chem Br 1998;34(11):59-62.

(165) Zheng Y, Zheng Y, Ning R. Effects of nanoparticles SiO2 on the performance of nanocomposites. Mater Lett 2003;57(19):2940-2944.

(166) Al-Sagheer F, Ali AAM, Muslim S, Ahmad Z. Thermal and mechanical properties of chemically bonded aramid–silica nano-composites. Science and Technology of Advanced Materials 2006 1;7(1):111-118.

(167) Babooram K, Francis B, Bissessur R, Narain R. Synthesis and characterization of novel (amide–imide)-silica composites by the sol–gel process. Composites Sci Technol 2008 3;68(3-4):617-624.

(168) Lai YH, Kuo MC, Huang JC, Chen M. On the PEEK composites reinforced by surface-modified nano-silica. Materials Science and Engineering: A 2007 6/15;458(1-2):158-169.

(169) Lue SJ, Shieh S. Modeling water states in polyvinyl alcohol-fumed silica nano-composites. Polymer 2009;50(2):654-661.

(170) Mizutani T, Arai K, Miyamoto M, Kimura Y. Application of silica-containing nano-composite emulsion to wall paint: A new environmentally safe paint of high performance. Progress in Organic Coatings 2006 3/1;55(3):276-283.

(171) Mori Y, Saito R. Synthesis of a poly(methyl methacrylate)/silica nano-composite by soaking of a microphase separated polymer film into a perhydropolysilazane solution. Polymer 2004;45(1):95-100.

(172) Tsai J, Kuo J, Chen C. Synthesis and properties of novel HMS-based sulfonated poly(arylene ether sulfone)/silica nano-composite membranes for DMFC applications. J Power Sources 2007 11/22;174(1):103-113.

(173) Wang K, McDermid S, Li J, Kremliakova N, Kozak P, Song C, et al. Preparation and performance of nano silica/Nafion composite membrane for proton exchange membrane fuel cells. J Power Sources 2008;184(1):99-103.

(174) Xu HHK, Smith DT, Simon CGCG. Strong and bioactive composites containing nano-silica-fused whiskers for bone repair. Biomaterials 2004 8;25(19):4615-4626.

(175) Mieszawska AJ, Kaplan D, Perry CC. Silk/silica nanocomposites as novel biomaterials for tissue engineering. Biophys J 2009 2;96(3, Supplement 1):635.

(176) Myung S, Choi I, Lee S, Park J, Kim I, Lee K. Separation of silk proteins and silk oligopeptides by thin film composite ultrafiltration membrane. Desalination 2008;234(1-3):158-165.

(177) Xu Q, Li J, Peng Q, Wu L, Li S. Novel and simple synthesis of hollow porous silica fibers with hierarchical structure using silk as template. Materials Science and Engineering: B, 2006;127(2-3):212-217.

(178) http://www.cancer.gov/dictionary/?CdrID=44591.

(179) Barnard GF, Mori M, Staniunas RJ, Begum NA, Bao S, Puder M, et al. Ubiquitin fusion proteins are overexpressed in colon cancer but not in gastric cancer. Biochimica et Biophysica Acta (BBA) - Molecular Basis of Disease 1995;1272(3):147-153.

(180) Bhattacharya R, Bukkapatnam R, Prawoko I, Soto J, Morgan M, Salup RR. Efficacy of vaccination with plasmid DNA encoding for HER2/neu or HER2/neu-EGFP fusion protein against prostate cancer in rats. Int Immunopharmacol 2002 5;2(6):783-796.

(181) Boormans JL, Hermans KG, Made ACJZd, van Leenders GJHL, Wildhagen MF, Collette L, et al. Expression of the androgen-regulated fusion gene tmprss2-erg does not predict response to endocrine treatment in hormone-naïve, node-positive prostate cancer. Eur Urol 2010;57(5):830-835.

(182) Lo-Coco F, Breccia M, Noguera N, Miller Jr WH. Diagnostic value of detecting fusion proteins derived from chromosome translocations in acute leukaemia. Best Practice & Research Clinical Haematology 2003;16(4):653-670.

(183) Lu J, Peng Y, Zheng ZJ, Pan JH, Zhang Y, Bai Y. EGF-IL-18 fusion protein as a potential anti-tumor reagent by induction of immune response and apoptosis in cancer cells. Cancer Lett 2008;260(1-2):187-197.

(184) Morrissey JJ, Raney S, Cleary ML. The FEL (AF-4) protein donates transcriptional activation sequences to Hrx-Fel fusion proteins in leukemias containing T(4;11)(Q21;Q23) chromosomal translocations. Leuk Res 1997;21(10):911-917.

(185) Penichet ML, Morrison SL. Antibody–cytokine fusion proteins for the therapy of cancer. J Immunol Methods 2001;248(1-2):91-101.

(186) Saito Y, Furukawa T, Arano Y, Fujibayashi Y, Saga T. Fusion protein based on Grb2-SH2 domain for cancer therapy. Biochem Biophys Res Commun ;In Press.

(187) Schwöppe C, Kessler T, Persigehl T, Liersch R, Hintelmann H, Dreischalück J, et al. Tissue-factor fusion proteins induce occlusion of tumor vessels. Thromb Res 2010;125(Supplement 2):S143-S150.

(188) Wang WW, Das D, McQuarrie SA, Suresh MR. Design of a bifunctional fusion protein for ovarian cancer drug delivery: Single-chain anti-CA125 core-streptavidin fusion protein. European Journal of Pharmaceutics and Biopharmaceutics 2007;65(3):398-405.

(189) Yan L, Xiangwei M, Xiao L, Peng G, Chang L, Mingyao T, et al. Construction, expression and characterization of a dual cancer-specific fusion protein targeting carcinoembryonic antigen in intestinal carcinomas. Protein Expr Purif 2010;69(1):120-125.

(190) Zhen Y. Antibody-based conjugates and fusion proteins for cancer. J Biotechnol 2008;136(Supplement 1):S171-S172.

(191) Huang Q, Chen C, Chen Y, Gong C, Cao L, Wang J, et al. Application to immunoassays of the fusion protein between protein ZZ and enhanced green fluorescent protein. J Immunol Methods 2006;309(1-2):130-138.

(192) Peipp M, Saul D, Barbin K, Bruenke J, Zunino SJ, Niederweis M, et al. Efficient eukaryotic expression of fluorescent scFv fusion proteins directed against CD antigens for FACS applications. J Immunol Methods 2004;285(2):265-280.

(193) Weiner RS, Srinivas NR, Calore JD, Fadrowski CG, Wen Chyi Shyu, Tay LK. A sensitive enzyme immunoassay for the quantitation of human CTLA4Ig fusion protein in mouse serum: pharmacokinetic application to optimizing cell line selection. J Pharm Biomed Anal 1997;15(5):571-579.

(194) Koland JG, O'Brien KM, Cerione RA. Expression of epidermal growth factor receptor sequences as E. coli fusion proteins: Applications in the study of tyrosine kinase function. Biochem Biophys Res Commun 1990;166(1):90-100.

(195) Icke C, Schlott B, Ohlenschläger O, Hartmann M, Gührs KH, Glusa E. Fusion proteins with anticoagulant and fibrinolytic properties: Functional studies and structural considerations. Mol Pharmacol 2002;62(2):203.

(196) Asai T, Trinh R, Ng PP, Penichet ML, Wims LA, Morrison SL. A human biotin acceptor domain allows site-specific conjugation of an enzyme to an antibody-avidin fusion protein for targeted drug delivery. Biomol Eng 2005;21(6):145-155.

(197) Park E, Starzyk R, McGrath J, Lee T, George J, Schutz A, et al. Production and characterization of fusion proteins containing transferrin and nerve growth factor. J Drug Target 1998;6(1):53-64.

(198) Medintz IL, Uyeda HT, Goldman ER, Mattoussi H. Quantum dot bioconjugates for imaging, labelling and sensing. Nature Materials 2005;4(6):435-446.

(199) Paternolli C, Antonini M, Ghisellini P, Nicolini C. Recombinant cytochrome P450 immobilization for biosensor applications. Langmuir 2004;20(26):11706-11712.

(200) Frey W, Meyer DE, Chilkoti A. Dynamic addressing of a surface pattern by a stimuli-responsive fusion protein. Adv Mater 2003;15(3):248-251.

(201) Slocik JM, Naik RR, Stone MO, Wright DW. Viral templates for gold nanoparticle synthesis. Journal of Materials Chemistry 2005;15(7):749-753.

(202) Sleyter U, Schuster B, Pum D. Nanotechnology and biomimetics with 2-D protein crystals. IEEE Engineering in Medicine and Biology Magazine 2003;22(3):140-150.

(203) Brott LL, Naik RR, Pikas DJ, Kirkpatrick SM, Tomlin DW, Whitlock PW, et al. Ultrafast holographic nanopatterning of biocatalytically formed silica. Nature 2001;413(6853):291.

(204) Galler KM, D'Souza RN, Hartgerink JD. Biomaterials and their potential applications for dental tissue engineering. J Mater Chem 2010;20(40):8730-8746.

(205) Schmalz G. Biocompatibility of dental materials. Berlin ; London: Springer; 2009.

(206) L'Heureux N. Tissue-engineered blood vessel for adult arterial revascularization. N Engl J Med 2007;357(14):1451.

(207) Nettles DL. Photocrosslinkable hyaluronan as a scaffold for articular cartilage repair. Ann Biomed Eng 2004;32(3):391.

Chapter 2
MATERIALS AND METHODS

This chapter describes all experimental processing methods and materials used for this research. For ease of understanding, it has been divided into the following sections.

1) Processing of *Bombyx mori* (BM) silk
2) Silica
3) Materials fabrication
    - Gelation route
    - Electrospinning and fabrication of nano-fibres
    - Study of electrospinning parameters to improve properties
4) Analytical techniques

2.1- Processing of *Bombyx mori* (BM) silk

Humans have been domesticating *Bombys mori* (BM) silkworms for thousands of years for a range of applications in the textile industry and more recently in biomedical research (1,2).

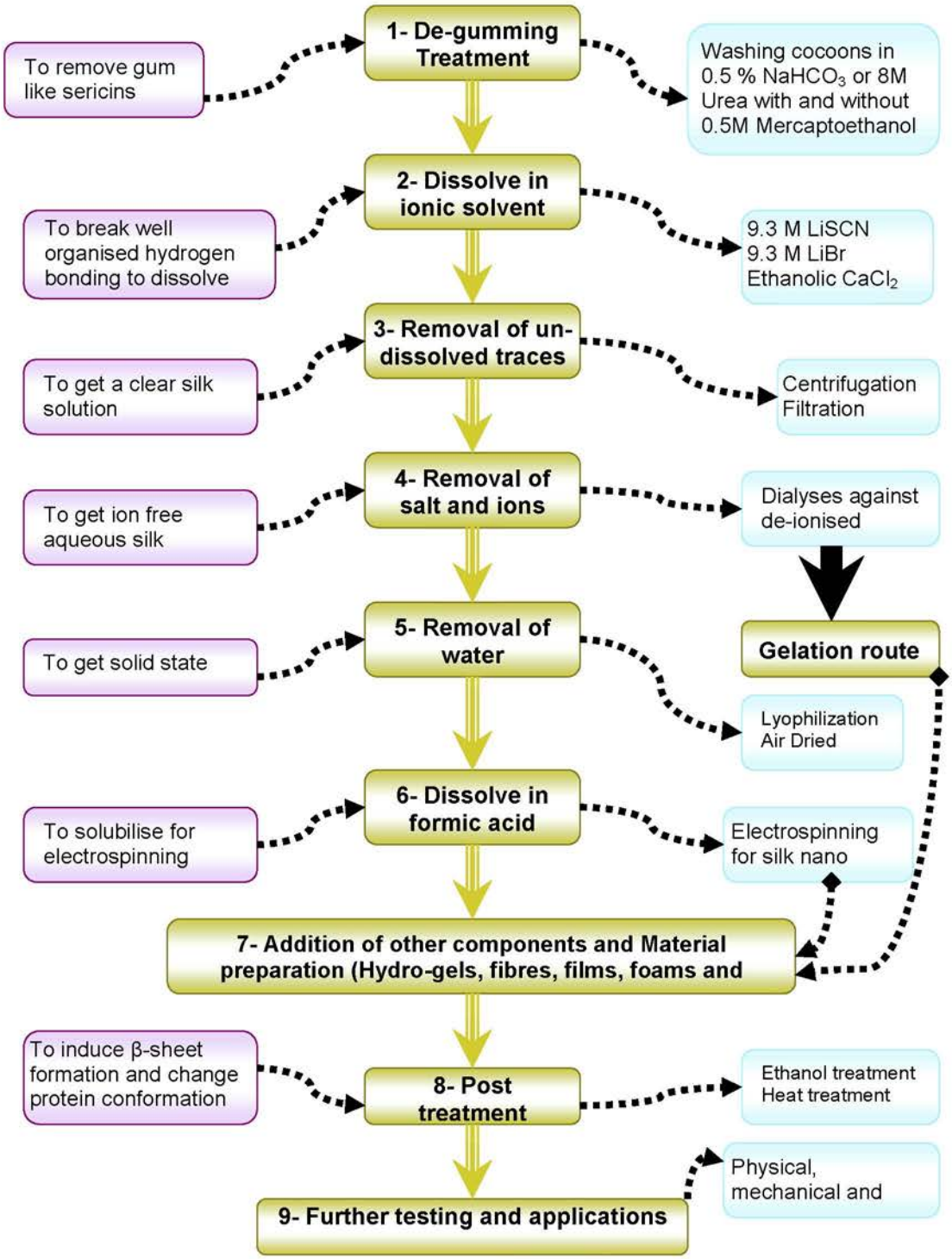

Figure 2.1: Different stages in the processing of BM silk, methods used in the thesis are listed on the right side

For textile applications, very little processing (e.g. dying or spinning) of natural silk fibre is needed (3,4). However for successful biomedical applications, different materials morphologies such as films, foams, and hydrogels on the micron or nano scale are desired to get certain benefits. Natural silk fibres cannot be directly transformed into such material forms and need to be dissolved in a solvent. Due to the complex structural nature of natural silk and the presence of very strong hydrogen bonding, it has a tough nature is hard to dissolve even in harsh solvents and needs long processing (1,5,6). Once silk has been dissolved, it can be used in different ways to produce a variety of materials of different morphologies and properties such as films, gels, granules, foams and electrospun mats (1,7). The main stages in the processing of BM silk for biomedical applications are removal of glue like protein sericins, dissolving in aqueous ionic solutions, dialysis to remove inorganic salts from the silk solutions and then regeneration of various forms of silk. Different stages in the processing of natural *Bombyx mori* (BM) silk are summarized schematically in Figure 2.1 and are below.

2.1.1- De-gumming of silk cocoons

This is the first stage in the processing of BM silk and different expressions such as "de-gumming"(2), "pre-treatment" and "desericinisation" (8) have been used in the literature to describe it. Structurally, BM silk is composed of two distinct proteins called silk fibroin and sericin as shown schematically in Figure 2.2. The purpose of this process is to remove gum like sericin from silk cocoons without degrading silk fibroin (1,2,7).

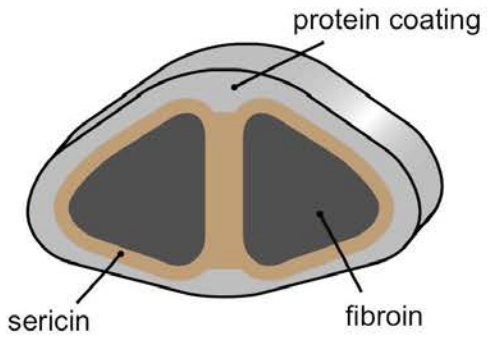

Figure 2.2: Schematic illustration of *Bombyx Mori* silk cross section (7).

Sercin is an amorphous glycoprotein and accounts for 25 wt. % of BM silk (9). Sericin plays a functional role in coating cocoons to adhere the twin filaments and cocoons (10) and protects silk from microbial degradation, animal digestion and environmental damage (11). It also has some surprising properties such as UV resistance, oxidation resistance and an ability to absorb and release moisture easily (12). Due to the proven role of sericin in inducing allergic and immunological reactions (13,14), it is crucial to remove all sericin prior to use for any biological application. A variety of methods have been tried for this purpose over the past 150 years (8,15).

There is some controversy concerning silk de-gumming techniques, as some researchers believe that it has no effect on silk protein conformation (16) while others (2,8), have provided evidence of molecular degradation. After a detailed review of previous literature (2,8,17-19) about de-gumming techniques, the following method and modification were used in the studies described in this thesis.

2.1.1.1 – De-gumming Methods

1) Sodium bicarbonate ($NaHCO_3$) solution

Silk cocoons were boiled at 100 ℃ in 0.5 wt. % aqu eous solution of $NaHCO_3$ (100 v/w) of solution for 30 minutes. A second wash was given in exactly as above; followed by thorough rinsing with warm de-ionized distilled (dd) water and air dried at room temperature.

2) Sodium bicarbonate ($NaHCO_3$) and mercaptoethanol solution

Exactly the same method as described above, the only exception being the addition of 0.5 M of mercatoethanol in the de-gumming $NaHCO_3$ solution.

3) Urea solution

Silk cocoons were heated at 80 ℃ in 8 M aqueous ur ea solution (30 v/w) for 10 minutes (2). Second wash was given in exactly the same way; followed by a thorough rinsing with warm de-ionized distilled (dd) water and air dried at room temperature.

4) Urea and mercaptoethanol

Exactly the same method as for urea (8M) was used, the only exception being the addition of 0.5 M of mercatoethanol in the de-gumming solution. All methods and relevant conditions are summarized in table 2.1

Table 2.1: Comparison of de-gumming conditions used		
	$NaHCO_3$ ± Mercaptoethanol	**Urea ± Mercaptoethanol**
Heating temperature	100℃	80 ℃
Heating time/cycle	30 minutes	10 minutes
Heating cycles	2	2
Total heating time	60 minutes	20 minutes
Solvent volume	100 time v/w	30 times v/w

Once silk was dried completely, it was weighed to explore the effectiveness of each method in removing sercin, considering total sericin contents in BM silk are 25 wt. % (9), and the results are shown in table 2.2

Table 2.2: Effectiveness of different modification in removing sericin					
	Cut Cocoon	**De-gummed silk**	**Sericin removed**		**Efficient**
$NaHCO_3$ - Mercaptoethanol	10 g	7.95 g	2.05 g	20 %	82 %
$NaHCO_3$ + Mercaptoethanol	10 g	7.72 g	2.28 g	23 %	91.2 %
Urea - Mercaptoethanol	10 g	8.4 g	1.6 g	16 %	64 %
Urea + Mercaptoethanol	10 g	7.52	2.48 g	25 %	99.2 %

In the case of 8M urea alone, the silk cocoons were not even opened properly, suggesting incomplete removal of sericin and were sticky upon washing with warm water afterward. This also suggests the importance of using mercatoethanol in the de-gumming solution. The most effective method was 8M urea with mercaptoethanol.

2.1.2- Dissolving silk fibroin in aqueous ionic solutions

The aim of this process is to dissolve de-gummed BM silk fibroin to get clear solutions with the least molecular damage of silk proteins. The presence of very strong intermolecular hydrogen bonding and highly organized clusters of β-sheets in silk has made dissolution a tough challenge (1,20) A variety of methods using different high concentration ionic solutions (5,7,21,22) have been utilized in the past.

A high concentration of ions helps to break the strong hydrogen bonding in silk fibroin (23) and both cations and anions can affect the solubility however the ratio of anions has been found to have much greater impact on the solubility of silk fibroin (7). A few examples of commonly used ionic solutions for dissolving silk are lithium bromide, lithium thiocyanide and calcium chloride.

In this study, mainly three solvents (listed below) were used to get clear silk solutions for different experiments and were compared for their benefits and limitations.

A. Calcium chloride/ethanol/water solvent
B. Lithium Bromide (LiBr)
C. Lithium thiocyanate (LiSCN)

2.1.2.1-Calcium chloride/ethanol/water solvent

The calcium chloride/ethanol solvent also known as "Ajisawa reagent" after the work of Ajisawa (2,24) and has been used widely in different studies to dissolve BM silk (25-31). The calcium chloride/ethanol/water ratio used in these studies was at a molar ratio of (1/2/8) respectively. However, Ajisawa (24) explored calcium chloride solvent with and without ethanol ($CaCl_2$:H_2O in the molar ratio of 1:8) and found that silk could only be dissolved in a solvent with ethanol and heating increases the solubility. Furthermore, ethanol in the solvent was found to help silk fibroin to swell and solution permeability and maximum solubility was observed when 2 moles of ethanol were added. Considering this point, the ternary solvents were made with different molar ratios of ethanol to find out the effect of ethanol on silk solubility and viscosities.

Table 2.3: The effects of ethanol content in the ternary solvent

	Solvent A	**Solvent A_1**	**Solvent $A_{0.5}$**
dd. water	8 moles (144 g)	8 moles (144 g)	8 moles (144 g)
Ethanol	2 moles (92 g)	1 moles (46 g)	0.5 moles (23 g)
Calcium Chloride	1 mole (111 g)	1 mole (111 g)	1 mole (111 g)
Viscosity (cP)	15.25	14.19	12.25
Density (g/ml)	1.2	1.29	1.33

Calcium chloride (1mole/111 g) was dissolved in de-ionized water (8 moles/144 g) followed by addition of ethanol to each solvent. All solutions were left stirring until turned clear by dissolving all calcium chloride. The density of each solvent was calculated using a specific gravity glass bottle and viscosity was measured using an AND SV-10 viscometer. For each experiment, de-gummed silk was weighed and soaked completely in the solvent heated at 85 ° C ± 0.3 ° C in a water bath for 30 minutes to get clear, fully soluble silk solutions. Before viscosity calculations, all solutions were spun at 4000 rpm for half an hour to remove insoluble traces and impurities.

Solvent A produced the most homogeneous and clear solutions for any concentration compared to solvent A_1 and $A_{0.5}$. Additionally, a decrease in ethanol content resulted in an increase in density and more turbidity of the silk solutions. Silk solutions in all three variants showed similar solubility and viscosity (Figure 2.3), the only exception was 8 wt. % solutions where a decrease in ethanol was observed to produce more viscous solutions.

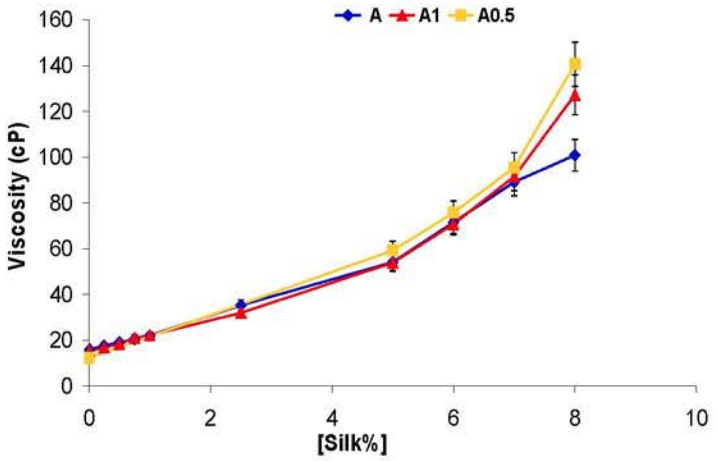

Figure 2.3: The effect of ethanol contents on silk solutions viscosity

Altering the ethanol content did not show any remarkable improvement in the solubility or viscosity behaviour of silk solutions so it was decided to carry on with solvent A (Ajisawa reagent) only for further studies.

2.1.2.2- Lithium Bromide (LiBr)

Lithium bromide (LiBr) is an ionic solvent that has been used frequently in different studies (21,32) typically at a concentration of 9-9.5 M. Solvent A (calcium

chloride/ethanol/water) has been described to dissolve silk fibroin but proved to cause the degradation of fibroin due to heating requirement (2) and cannot be used where sensitive biochemical characterization of silk is desired. Another important limitation of the calcium chloride/ethanol/water solvent was the low solubility (up to 15 wt.%) and cannot be used in certain experiments where higher silk concentrations were desired.

LiBr has the ability to dissolve silk fibroin under comparatively mild conditions, as it can dissolve up to 2 wt. % of fibroin at room temperature (slow process takes about 24 hours) and up to 20 wt. % can be dissolved by heating for 3 hours at 65 º C. considering these features, LiBr was used to dissolve silk for biochemical studies and for gelation studies where the highest silk concentrations were desired to get stronger materials. All solutions were centrifuged at 4000 rpm for half an hour to remove insoluble traces and impurities before proceeding to further experiments.

2.1.2.3- Lithium thiocyanate (LiSCN)

Lithium thiocyanate is another strong ionic solvent that can break the hydrogen bonding to dissolve the silk fibroin. It has been used to at room temperature up to 3 wt. % (2). This solvent is the best to use for biochemical analysis as no heat treatment is required, causing minimum/no damage to the silk structure.

For biochemical analysis, de-gummed silk of each type was soaked in ~ 9.3 M aqueous LiSCN solutions and left overnight to get 3 wt. % clear silk solutions. These LiSCN-silk solutions were dialyzed to obtain aqueous silk solutions for biochemical analysis.

2.1.3- Dialysis of silk solutions

2.1.3.1- Method

The ionic silk solutions were dialyzed against de-ionized distilled water using 12,000-14,000 Da molecular weight cut off cellulose cassettes. The dialyzing water was typically changed after 1 hour, 3 hour, evening-morning-evening for three days. Only in case of silk biochemical analysis, a quick dialysis (dialysis water was replaced after every half an hour and at least 4 changes to make sure of complete dialysis) was used to get quick recovery and avoid denaturation of proteins.

This process resulted in removal of inorganic ions and production of regenerated silk proteins soluble in water. The aqueous silk solutions exhibited entirely different

solution properties from ionic silk solutions because of replacement of ions with water molecules and interaction of water with proteins. Solution properties such as concentration and viscosity are important parameters especially for electrospinning, with very low viscosity solutions generating beads (33). The viscosity of silk solutions is directly proportional to concentration, and is the most critical factor controlling the structural morphology of the nano-fibrous structure (29,34) with both parameters being changed as a result of water ingress inside the cellulose cassette (see below). The aqueous silk solutions were lyophilized to get solid powder like silk and were used for nano-composite fabrication using electrospinning route.

In order to increase the concentration above 3%, aqueous silk solution was injected into a cellulose cassette and was dialyzed against 10-15 wt. % polyethylene glycol (PEG) overnight. That resulted in pulling water out of silk solutions due to difference in osmotic stress and concentrated up the silk solution. The silk concentration was determined by weighing the remaining solid contents after drying. Concentrated silk solutions were recovered from cellulose cassettes before gelation and were used for further experiments.

2.1.3.2- Viscosity measurements

Viscosity of all silk solutions was measured using an AND viscometer model SV-10 (Figure 2.4). The equipment is composed of a main unit containing a pair of gold plated vibrating paddles with a temperature sensor between them and a LCD control display. It can measure viscosity over a wide range 0.3-10,000 mPa.S (1 mPa.S=1 cP). It is supplied with a 10 ml sample cup at the base of main unit. Silk solution (10 ml) was placed in the sample cup and the sample table adjusted so that sensor plates were dipped in the solution up to the marked spot to measure the viscosity reproducibly.

Gold plated paddle sensors once dipped in the solution vibrate at a constant frequency (30 Hz), and these vibratory movements are resisted by the sample and the current required maintaining the set frequency is measured. This process takes about 15-30 second to perform. In this study all measurements were performed at room temperature (20 ° C $\pm$ 0.3 ° C) and were recorded manually.

The major significance of using this equipment was that it can measure a variety of samples quickly over a wide range of temperature (if wished) and can be used to measure time dependent changes in the viscosity. There are limited studies reported on the rheology of silk aqueous solutions (35). As dialysis resulted in the

change of solution properties, so viscosities of dialysed silk solutions were observed over a period of time to explore their stability.

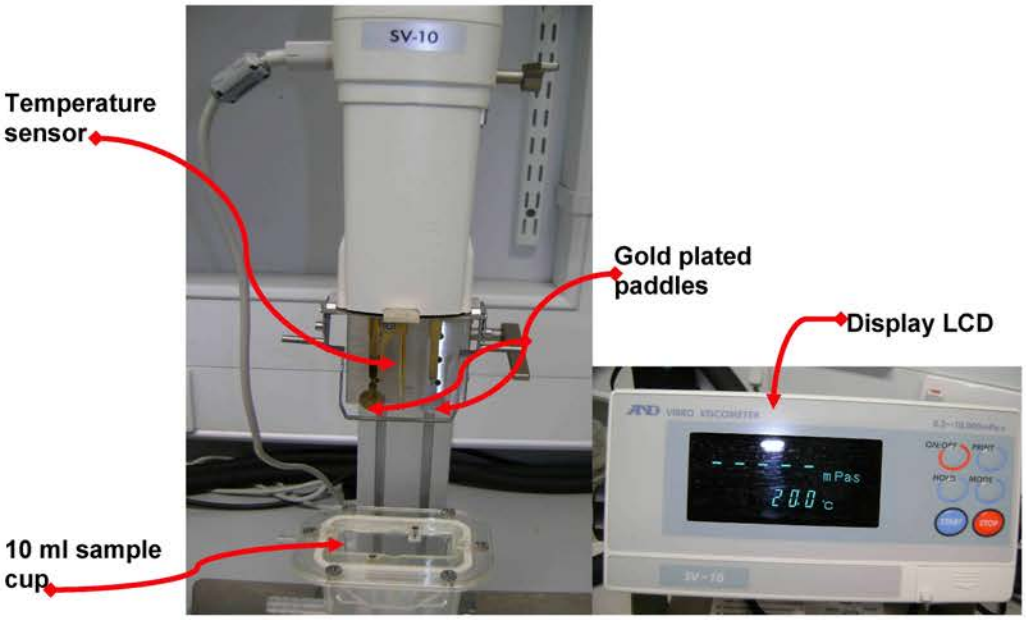

Figure 2.4: AND (SV-10) viscometer and display LCD

Like any other polymer, viscosity of silk solutions were observed to increase with an increase in concentration (Figure 2.5); the lowest being for 0.003 wt. % aqueous silk solution (0.971 cP) immediately after dialysis, which is even slightly less than water at the same temperature and the highest viscosity for a 1.04 wt. % silk solution (1.142 cP).

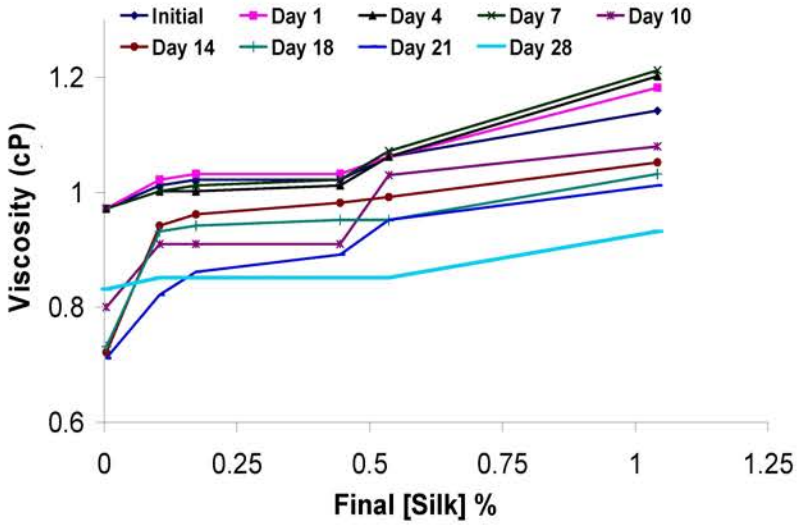

Figure 2.5: Changes in viscosity of aqueous silk solutions of different concentrations over 28 days

Viscosities of all our solutions continued to decrease with time and went down to 0.831 cP and 0.931 cP for 0.003 % and 1.04 % silk solutions respectively by the end of 28 days and were therefore slightly less viscous than water for any concentration of silk. Zainuddin *et* al; (35) observed similar behaviour of aqueous silk solutions; followed by a drastic increase in the viscosity near the gelation point of the silk solutions. The viscosity of the silk solutions in the aqueous ionic solvent before dialysis also increased with increase in silk concentration however, this was much higher (up to 42.4 cP for 2.5 % and 22.033 cP for a 1 % silk solution) than observed with the aqueous solutions. The low viscosity of aqueous silk solutions can affect material fabrication for example in electrospinning as higher viscosity is desired to electrospin polymer fibres without bead formation (33).

2.1.3.3- Particle size measurements

Dynamic light scattering (DLS) also known as photon correlation spectroscopy is a technique used to determine particle sizes in solutions. DLS is a very cost effective technique that can be used for a wide range of particle sizes (as small as a couple of nm up to many microns). DLS works on the principal of diffusion of particles through a liquid medium and is dependent on temperature, viscosity and particle size (36). The particles in the solution shift by three dimension Brownian movement (37). Light passing through the solution is scattered at an angle by particles and recorded by a photomultiplier (detector) and this data is used for further analysis.

For all particle size measurements in this study, a Malvern Zetasizer (Figure 2.6) was used. Samples were filtered using 0.45 µ syringe filters to remove any aggregates and impurities and diluted to get appropriate numbers (amount) of particles. All measurements were performed at room temperature (25 º C controlled automatically by the machine), using disposable plastic cuvettes. Ten measurements were performed at right angle for each sample to calculate average particle size using the DLS data.

Particle sizes in aqueous silk solutions tend to decrease over time for any solution. Particle sizes were in the range of 220-300 nm after one day of dialysis and were observed to reduce to 74-190 nm range on day 28 (Figure 2.7).

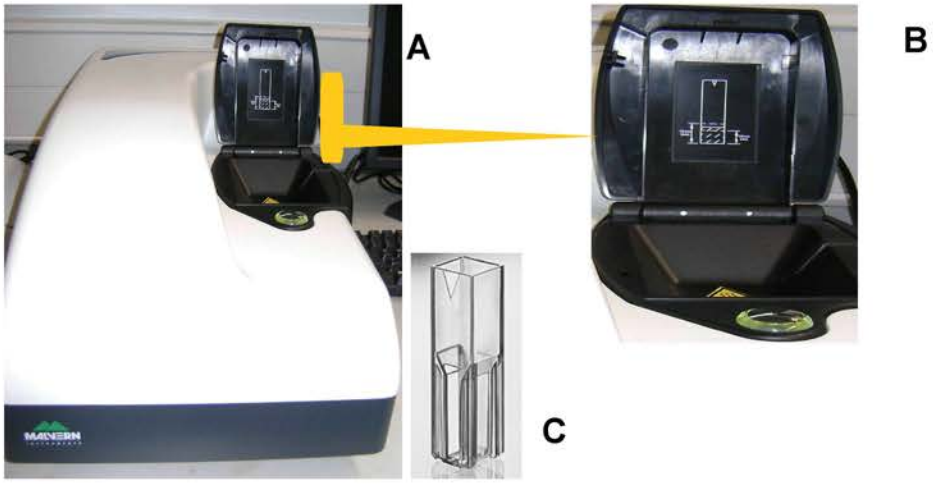

Figure 2.6: Dynamic light scattering (DLS) equipment A)-Machine, B)- Cell area C)- Cuvette

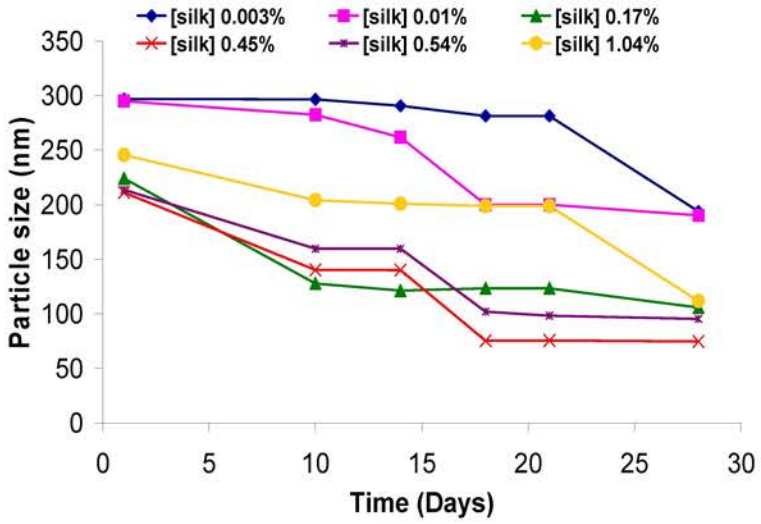

Figure 2.7: Change in particle sizes of aqueous silk over a period of time (28 days)

The decreases in the particle size over time alongside the decrease in viscosity seem related to each other and explain the situation to some extent. It can be suggested that silk proteins in aqueous solutions are not stable for a long time (35) and freshly dialyzed solutions should be used for all experiments.

2.1.4- Segregation of *Bombyx mori* silk fibroin components

Silk proteins have a very complex structure and it is well documented in the literature that silk fibroin can be subdivided into different components, heavy chains (~350 kDa) and light chains (~25 kDa) silks connected by a disulphide bond (2,7,38-

42). Formic acid (FA) is an organic solvent and has been used to dissolve silk. Due to the presence of highly organized hydrogen bonding natural silk is not fully soluble in formic acid (43). However, formic acid has the ability to breakdown BM silk into two components and solubilises one part only. Considering this fact, a novel method has been developed to separate natural silk into two different fractions very easily using formic acid.

2.1.4.1- Methods

In order to develop a method, de-gummed silk was weighed and dispersed in 98-100 % formic acid (FA) at a range of concentrations (0.01-8 wt.%) and centrifuged at 4000 rpm for an hour so that the un-dissolved portion of silk can settle down. The supernatant was removed and filtered using glass filters to remove any impurities.

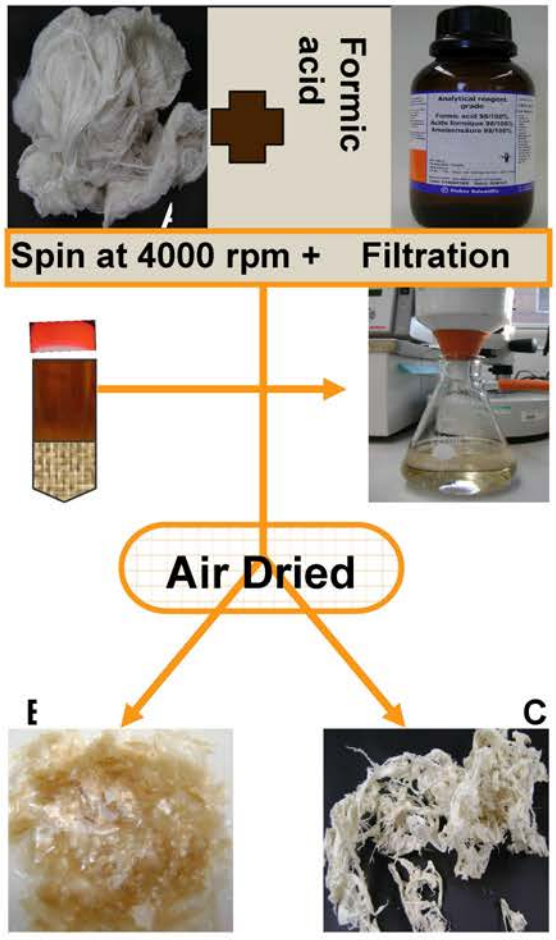

Figure 2.8: Process of separating silk fractions using formic acid A) - De-gummed natural silk, B) - Dried soluble fraction, C) - Dried insoluble fraction

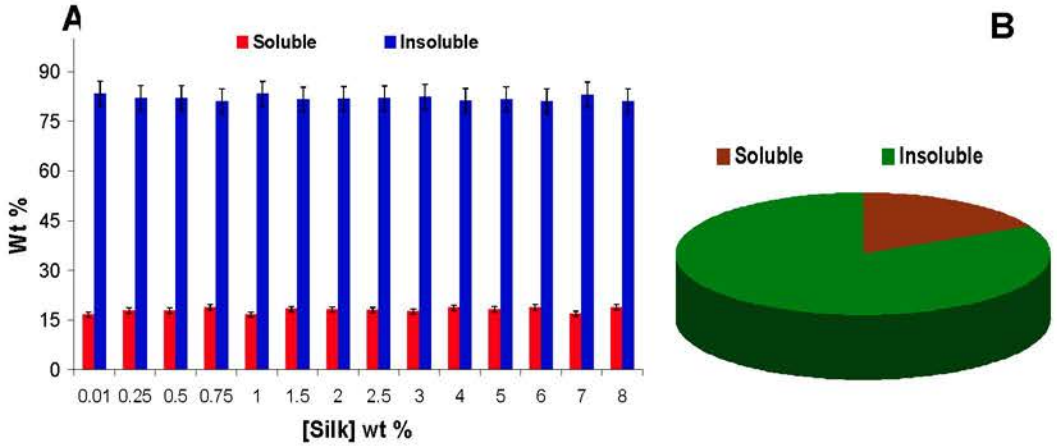

Figure 2.9: Proportion of formic acid soluble and insoluble fractions A) - ratios at different initial silk concentrations, B) - Average weight proportion

The insoluble fraction from each sample was treated twice with formic acid to make sure all soluble components have been removed and the supernatants all combined. The insoluble fractions were washed thoroughly using de-ionized distilled water to remove all residual formic acid and air dried. The soluble fractions were left in a fume hood to evaporate all formic acid leaving solid material. Once both fractions had dried completely, they were weighed to calculate their relevant proportions. The physical appearance of both fractions and the whole process is shown schematically (Figure 2.8).

Once the method has been developed and evidence obtained that the ratio of both fractions constant (17 wt.% soluble) regardless of initial silk concentration (Figure 2.9), typically 1 wt. % silk solutions were made up in 98- 100 % formic acid the silk fractions were separated for further use. Formic acid separated silk fractions were studied for further solution properties.

The effect of different de-gumming methods (as in section 2.1.1.1) on silk-FA treatment was also explored. For this purpose 1 % silk-FA solutions from each de-gumming method were prepared and treated exactly as above to separate both fractions and were later used for biochemical analysis. It was observed that the weight ratios of silk fractions changed according to the de-gumming method used and suggests that the residual sercins present may interfere with this process (Figure 2.10).

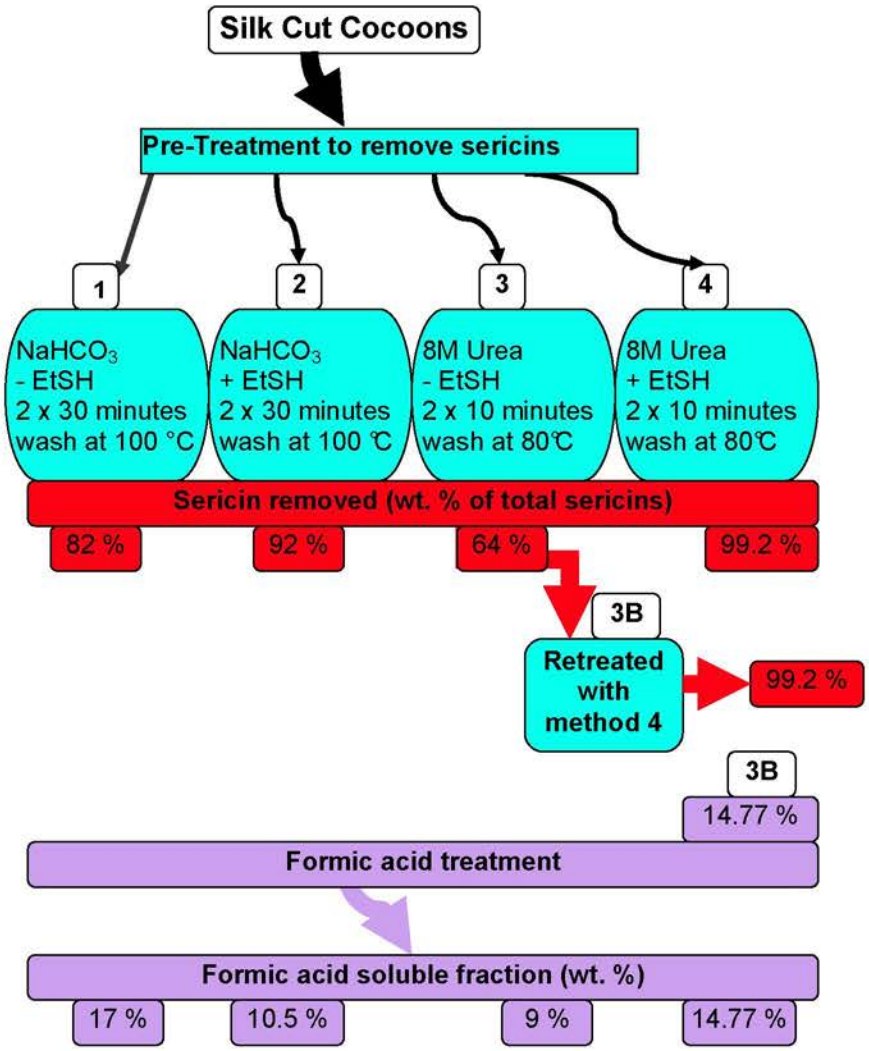

Figure 2.10: The effect of de-gumming methods on removal of sericins and separation of silk fractions

2.1.4.2- FA Soluble fraction

Soluble fractions were re-dissolved in formic acid to get transparent silk solutions of a range of concentrations for viscosity measurement using the method described above (section 2.1.3.2). As for any other polymer solution, there was a general trend of increasing viscosity with increase in concentration (Figure 2.11). The silk solutions in formic acid remained stable for longer time (up to many days) and their properties did not change with time, having maximum solubility limit of about 34 wt. % at room temperature that is comparable to *in vivo* silk solubility in insects and spiders used to produce solid fibres with excellent properties (44).

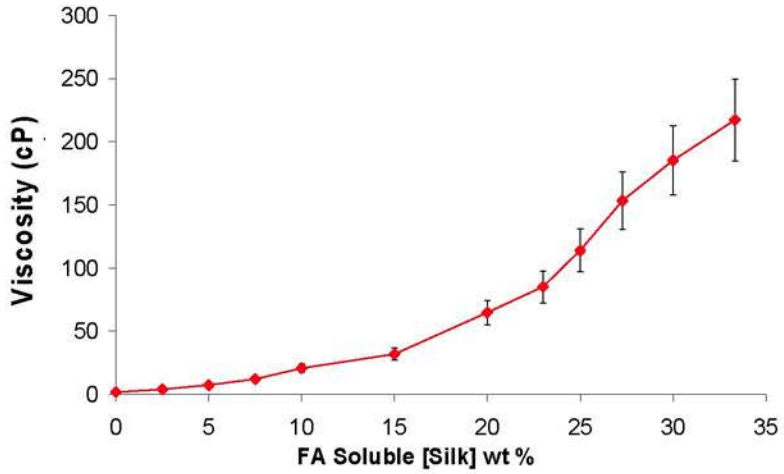

Figure 2.11: Viscosity of FA soluble silk re-dissolved in formic acid at different concentrations

The viscosity of 33.33 wt.. % FA soluble silk solution was as high as 217.2 cP and could be lowered to 1.8 cP depending on the concentration and can be adjusted as required for different electrospinning experiments.

2.1.4.3- FA Insoluble fraction

The FA insoluble fraction was not soluble in formic acid so needed to be treated with ionic aqueous solvents to solubilise using the method described (2.1.2). It was crucial that formic acid had been removed completely by washing otherwise it was found to interfere in solution and reduced sample solubility in ionic solvents.

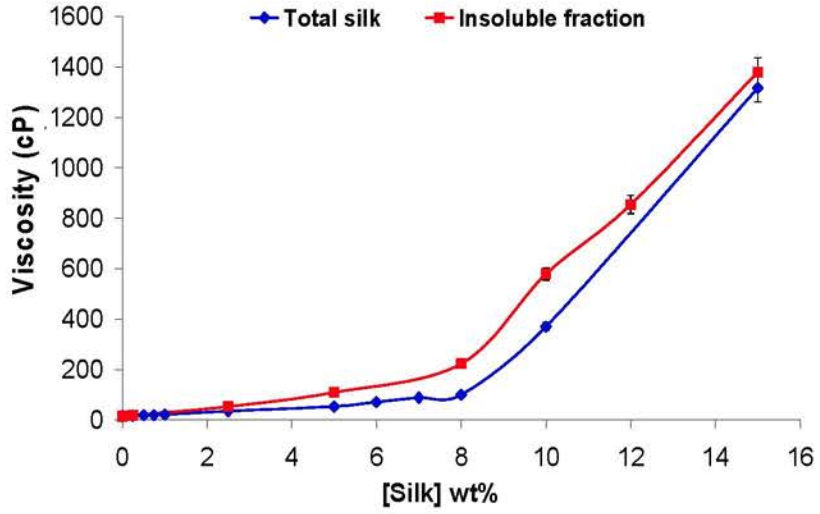

Figure 2.12: Viscosities of total silk and FA insoluble silk fraction compared at different concentrations in solvent A ($CaCl_2$:EtOH:H_2O)

The insoluble fraction could be dissolved in any of the ionic solvent up to reasonable concentration (up to 10 wt. %). The viscosity of FA insoluble silk in ternary solvents remained higher than for total silk at any concentration of silk under similar conditions (Figure 2.12).

2.1.5- Regeneration of total silk and silk fractions

After the detailed exploration of solution behaviour of silk as described above, each type of silk was regenerated using a set protocol. Silk cut cocoons (*Bombyx mori)* were de-gummed using a method (1 of 2.1.1.1) and air dried. Silk fractions and total silk was dissolved in aqueous ionic solvent (2.1.2.1) to get 6 wt. % clear solutions. For certain experiments, higher concentrations of silk solutions (up to 20 wt. %) were prepared. All solutions were dialyzed using protocol (2.1.3) to get regenerated silk in water. After dialysis regenerated silk was mainly used in three ways.

I) Aqueous solutions for silk gelation studies

II) Concentrated up using PEG to make nano-composites through the gelation route

III) Lyophilisation to get solid powdery silk to dissolve in solvent (FA) for electrospinning

2.1.6- Regenerated silk solutions in formic acid

Formic acid (98-100 %) is frequently described in the literature to dissolve and manipulate regenerated *Bombyx mori* silk (30,35,43,45-48) Regarding regenerated silk, Formic acid is known to produce a stable silk solution and is often used in fibre formation from silk polymers, additionally it has also been proven to increase crystallization in the solid state (22). Formic acid-silk solutions remain remarkably stable compared to aqueous silk solutions (43). Regenerated silk of all types (total silk, FA soluble FA insoluble) and natural FA soluble were dissolved in formic acid. For ease of understanding, nomenclature and abbreviation of these silk samples is shown (Figure 2.13).

2.1.6.1- Solubility and viscosities of regenerated silks in formic acid

The maximum solubility of regenerated silks in formic acid at room temperature was measured by dissolving 4 g of silk in 8 ml of formic acid. In order to find out the solubility limit of each type, formic acid was added in increments of 1 ml after 30

minute period until regenerated silk was fully dissolved. The viscosity of each silk solution at its maximum solubility was measured using the method described (2.1.3.2). Regenerated silk-formic acid solutions were diluted with incremental addition of solvent so that viscosities could be measured over a range of concentration of solutions. There was a wide variation of solution properties depending on the type of silk.

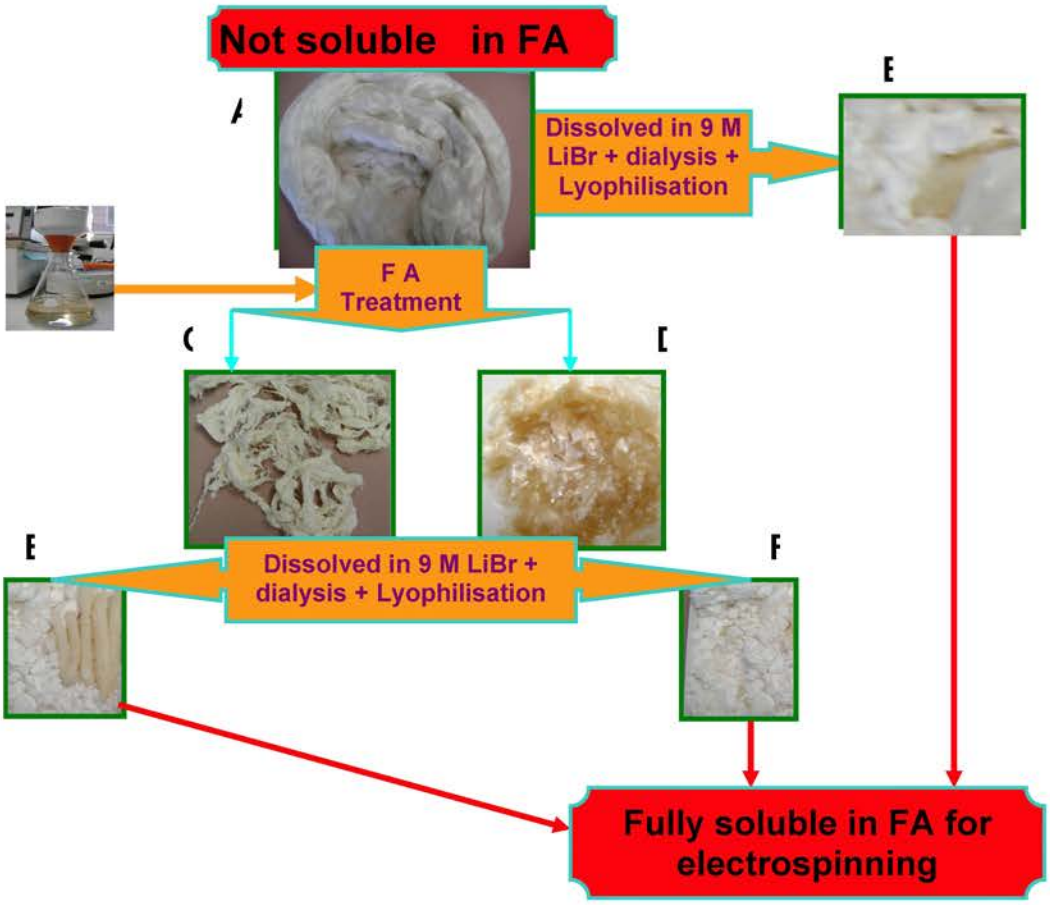

Figure 2.13: Regeneration of natural BM silk and its fractions and their physical appearance. A)- Total silk, B)- Regenerated total silk (RTS), C)- FA insoluble fraction, D)- FA soluble fraction, E)- Regeneration FA insoluble fraction (RUDS), F)- Regenerated FA soluble fraction (RDS). Only A and C could not be dissolved in FA

For example, the maximum solubility was observed in the case of regenerated total silk (RTS), was up to 40 wt. % (Figure 2.14), followed by natural FA soluble and regenerated dissolved silk (RDS) up to 33.33 wt. %.

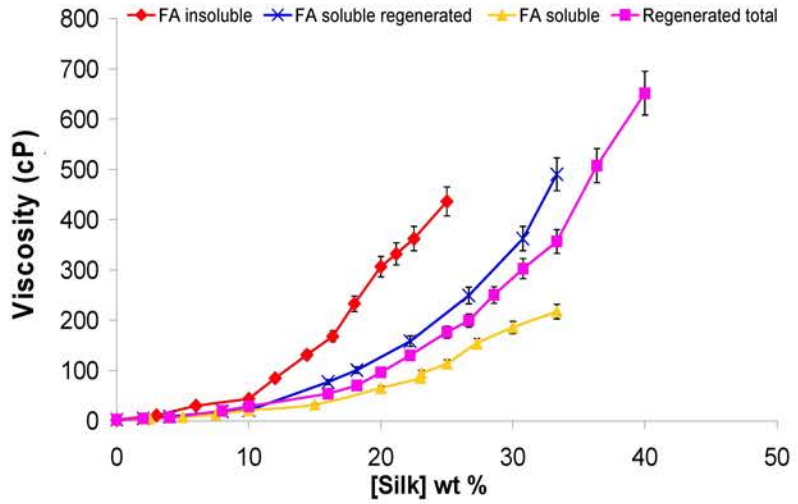

Figure 2.14: Viscosities and solubility limits of regenerated silk solutions in formic acid

The solubility of RUDS was lower (25 wt. %) than other silks however; it produced significantly more viscous solutions than other silks at comparable concentrations.

2.1.6.2- Time dependent changes in regenerated silk solutions

These experiments were performed to observe the change in RTS-formic acid solutions over time to assess their stability.

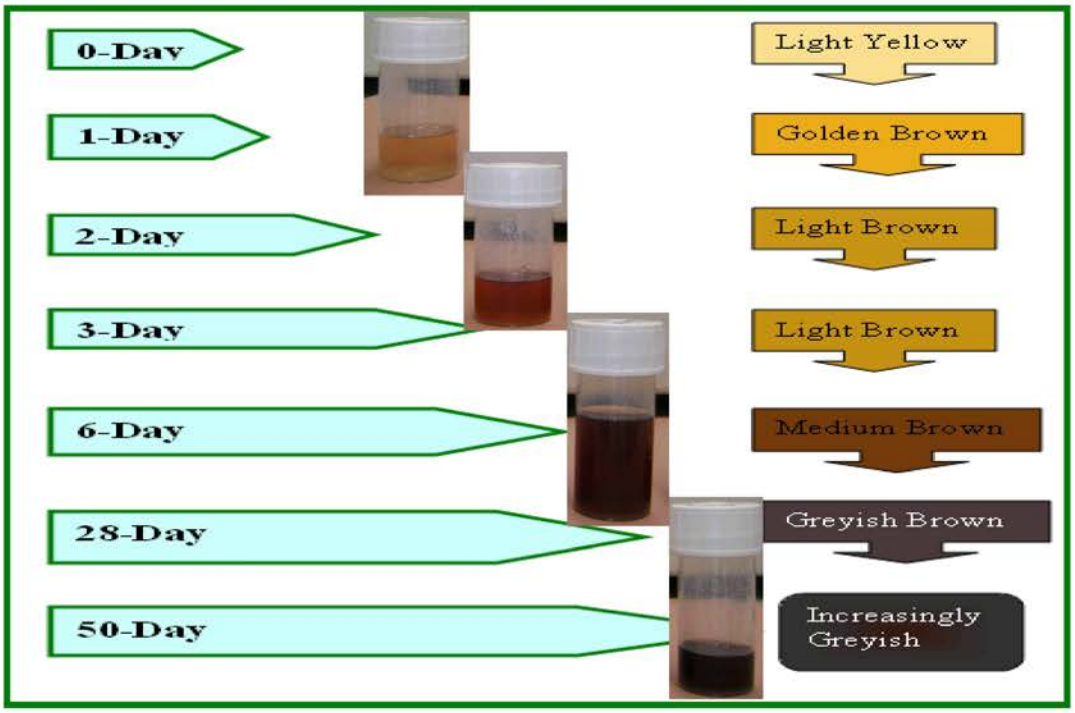

Figure 2.15: Colour changes with time observed in aging regenerated silk-formic acid solutions

Regenerated total silk (RTS) was dissolved in 98-100 % formic acid to make 10 wt. % solutions. After an hour, the RTS dissolved fully to give a clear solution and the initial colour, viscosity and absorbance were recorded. Solutions were stored at ambient conditions and colour changes (visual observation, photographs in Figure 2.15), viscosity (3.1.3.2) and absorbance (UV/Vis spectrometer in range of 390 nm-900 nm) were measured periodically up to 50 days. Absorbance was measured using a UV/Vis spectrometer (390 nm-900 nm with band width of 2.0 nm) and presented (Figure 2.16-B). Formic acid 98-100% (solvent) was stored under similar conditions and was used as a blank each time followed by sample measurements using single use plastic cuvettes.

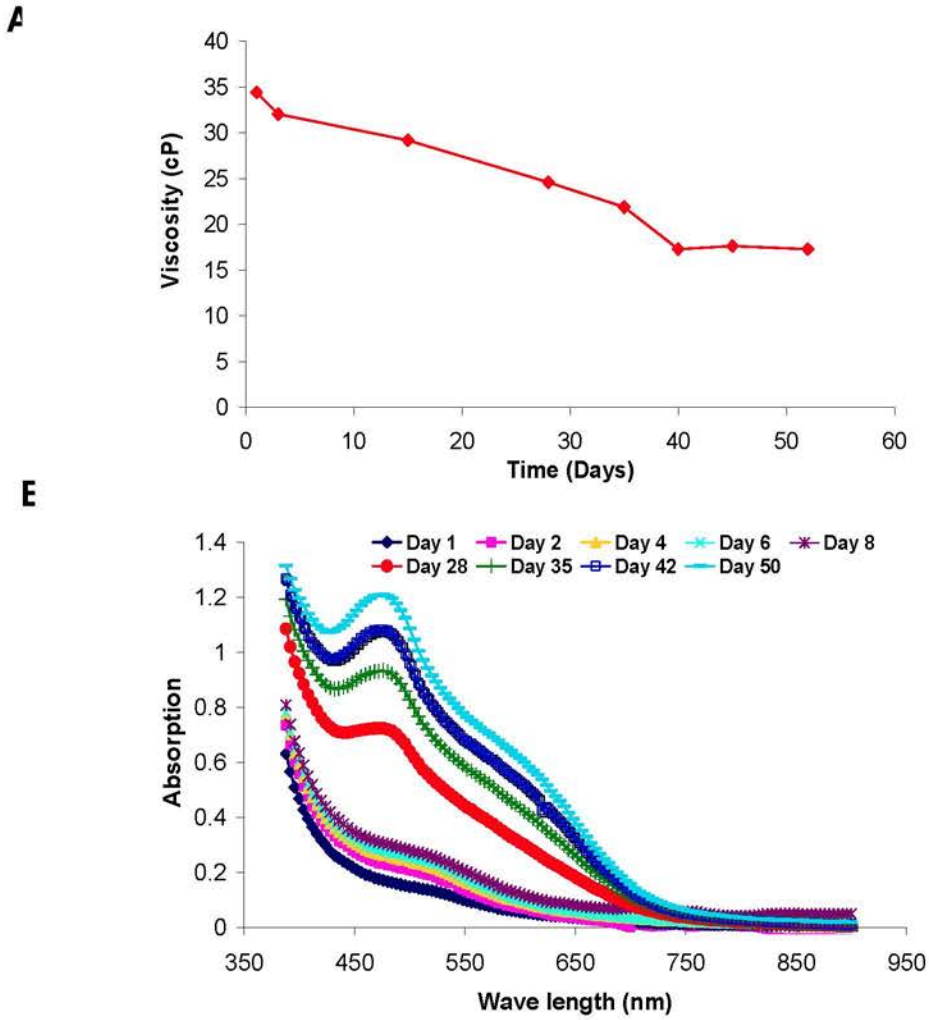

Figure 2.16: Changes in aging regenerated silk-formic acid solutions A)- viscosity B)- Absorbance

The decrease in the silk solution viscosity (Figure 2.16-A) with time is related to silk protein degradation (49). These findings suggested that regenerated silks in FA showed desired properties in terms of solubility and viscosity, however they are not stable for more than few hours and must be used within few hours of preparation.

2.1.6.3- Combination solutions of RUDS and RDS in different ratios

Considering the wide variation in solution behaviour of regenerated total silk and its fractions, different combinations of the silk fractions were studied so that properties could be adjusted as desired for specific outcomes.

Table 2.4 : Composition of different solutions with variable proportions of different silks

Sample	RUDS (wt. %)	RDS (wt. %)	RTS (wt. %)
H90	90	10	0
H75	75	25	0
H50	50	50	0
H25	25	75	0
H10	10	90	0
RUDS (H100)	100	0	0
RDS	0	100	0
RTS	0	0	100

For this purpose, RUDS and RDS were mixed in different weight ratios (table 2.4), and dissolved in FA to get the desired concentration as described above (2.1.6). The final properties of these solutions were studied in further experiments that are described in next chapters.

2.1.7- Sodium dodecyl sulphate polyacrylamide gel electrophoresis (SDS-PAGE)

SDS-PAGE has been used for many years for separation and molecular weight determination of proteins (2,50-58) including silk proteins (2,8,38,39,59). This technique involves the use of a detergent sodium dodecyl sulphate (SDS),

polyacrylamide gel having different size pores and electrophoresis (60). Electrophoresis is a phenomenon of movement of charged molecules in an electric field and can be used for separating proteins and macromolecules (60). Such movements of molecules in the electric field is affected by other parameters such as strength of electric field (*E*), net charge on protein molecule (z), and frictional coefficient (*f*) and can be expressed as (60)

$$\text{Migration velocity } (v) = \frac{E\,z}{f} \qquad \text{(Eq 2.1)}$$

The frictional coefficient (*f*) is dependent on the viscosity of the medium (η) and size and shape of the moving molecule. For a molecule of radius (r), frictional coefficient (*f*) can be calculated by the following equation (60).

$$f = 6\pi\eta r \qquad \text{(Eq 2.2)}$$

On the basis of these equations, the movement of a charged protein can be analysed, for example smaller molecular size proteins or higher charge will move faster in electrophoresis (61) and stack at different levels in a gel. Polyacrylamide gels are used most commonly to separate different size proteins as it has benefits such as to act as a sieve and enhances the separation (Figure 2.17). It is inert and pore size can be controlled easily during polymerisation (60).

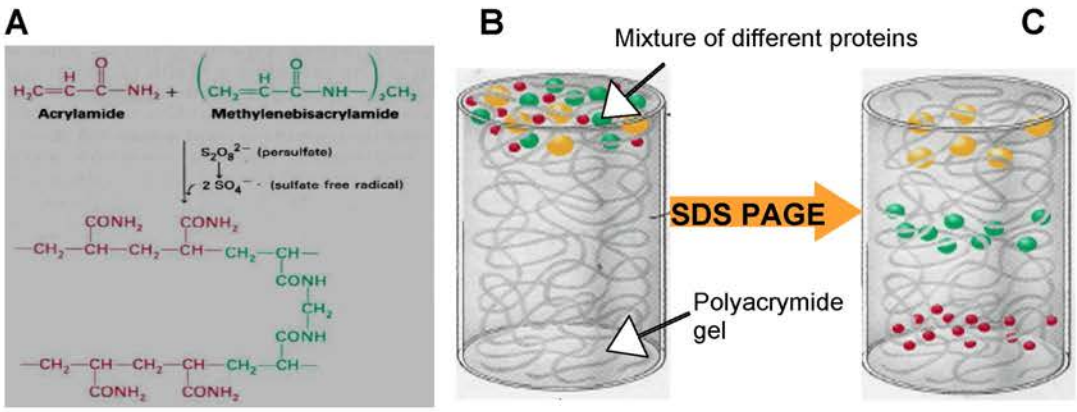

Figure 2.17: A schematic presentation of the structure and role of polyacrylamide gel, A)- Acrylamide (red) monomer and methylenebisacrylamide (green) cross linker; pore size can be controlled during polymerisation, B)- mixture of proteins loaded in gel, C)- proteins of different sizes separated in gel (derived from Biochemistry (62)).

SDS also plays a vital role in the reliability of this method (50,60), so proteins are treated with sample buffer containing SDS and some reducing agents to break sulphide bonds (60). SDS acts to dissociate proteins by completely unfolding each polypeptide to form linear SDS-polypeptide complexes (62) giving denatured protein a large negative charge that is roughly proportional to the protein mass and migrate through the polyacrylamide gels. In the case of most proteins, their mobility is linearly proportional to the logarithm of their mass (60).

Urea and mercaptoethanol are commonly used in sample preparation and help in denaturing and unfolding of proteins (63) as required for SDS PAGE. Urea works by forming hydrogen bonds with protein side chains (Figure 2.18) that are even stronger than hydrogen bonds in proteins themselves and is also able to disrupt the hydrophobic interactions in proteins. It also enhances the accessibility of disulphide to reducing agent (63).

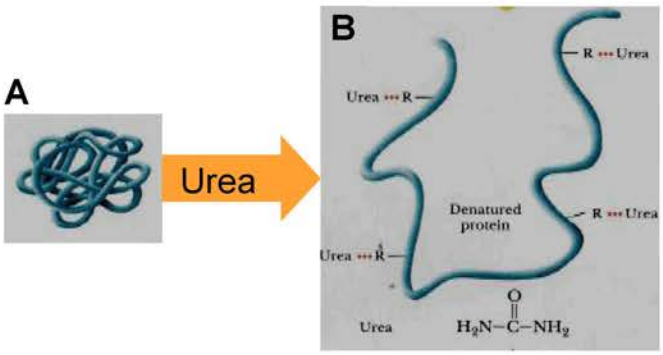

Figure 2.18: A scheme to show the effect of urea on portions A)- Native protein, B)- Denatured protein after urea treatment (65).

Mercaptoethanol is frequently used as a reducing agent (60,63) and works by converting disulphide bonds to sulfhydryl groups (Figure 2.19).

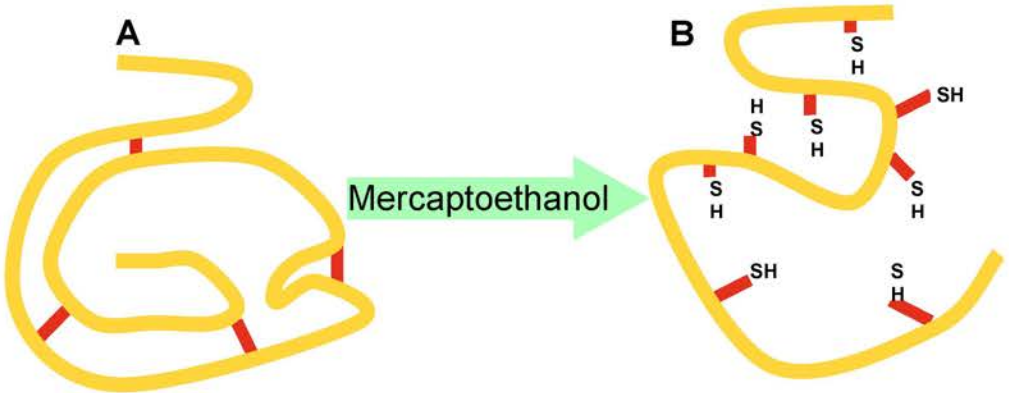

Figure 2.19: A schematic presentation of effect of mercaproethanol, A)- Native protein with disulphide bonds (red lines), B)- Mercaptoethanol treated protein showing replacement of disulphide bonds with sulfhydryl group (65).

In order to match and identify sample proteins, a protein marker (set of known molecular weight standard proteins) is also run under identical conditions. Once electrophoresis is completed, the gel can be removed for protein staining giving stained bands in the area of protein in each well (detailed in 2.1.7.3).

2.1.7.1- Method for SDS-PAGE

De-gummed silk of each type was dissolved in ionic solvents using methods (2.1.2) to get 3 wt. % solutions. Each solution was dialysed against de-ionised distilled water (2.1.3) to get aqueous solutions. Final protein concentration after dialysis was calculated using the Bradford protein assay (2.1.7.2). Sample buffer (Laemmli 2x; pH 6.8), containing 10 % of 2-mercaproethanol 0.004 % bromophenol blue was modified according to a set method (2) by adding 8 M urea and more sodium dodecyl sulphate (SDS) to a final level of 10 %. All samples were diluted carefully with this modified buffer (pH 6.8) in a volumetric ratio of 1:1 and were denatured by heating in a water bath at 50 ℃ for ten minutes. All samples were centrifuged at 2000 rpm for 30 seconds and were then loaded in the polyacrylamide gel alongside the protein marker. Gel electrophoresis was performed in running buffer (pH 8.3) containing SDS (0.1 %), trizma base buffer (25 mM), glycine 192 (mM) and HCl (to adjust pH) at a fixed voltage of 120 v until all samples approached the bottom of the gel.

2.1.7.2- Bradford protein assay

The Bradford protein assay was used for the determination of silk protein concentration prior to SDS-PAGE. This technique has the ability to detect micrograms of protein in solution and is frequently applied due to ease of use and sensitivity (64). It is based on the principle of binding of Coomassie blue dye to proteins (65,66). The dye binds to the proteins in approximately two minutes and maintains colour stability in solution for up to one hour giving very reproducible results (65). The presences of cations such as sodium and potassium or carbohydrates have no or very little interference with the assay (65). The Coomassie blue dye binds to proteins readily through arginyl and lysyl residues and does not bind to free amino acids (67,68). On binding to the proteins, anionic form of the dye gives blue colour (66) and is measured using UV-Vis spectroscopy.

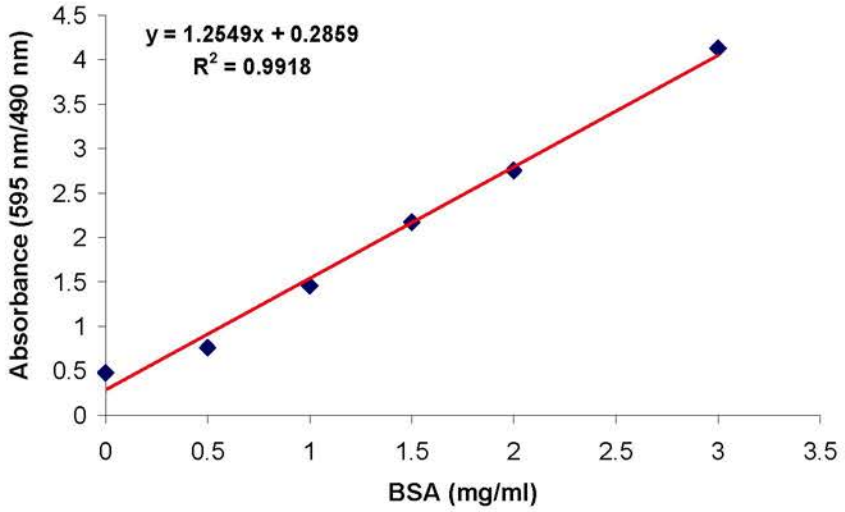

Figure 2.20: An example of calibration curve from Bradford assay using BSA standard solutions

For calibration purposes, standard solutions of bovine serum albumin (BSA) 0.5 mg/ml to 3 mg/ml were prepared. A 5 µℓ aliquot of each sample as well as BSA standards were pipetted into a 96 well plates (in triplicates), followed by addition of 250 µℓ of Bradford dye in each well. After an incubation period of 15 minutes, absorbance was measured at 590 nm and 495 nm using 96 well plate UV spectrometer (Accu reader LT-5000). A ratio of absorbance (590 nm/495 nm) increases the linearization and sensitivity of Bradford assay (64), and was therefore, used for all calculations. An example of a Bradford calibration curve is shown (Figure 2.20).

2.1.7.3- Gel staining

After electrophoresis, each gel was washed thoroughly with de-ionised distilled water to remove all residual SDS and stained. A very small amount of protein (0.1 µg) produced distinct bands using the Coomassie blue stain, while silver staining was even more sensitive and could detect as little protein as 20 ng (0.02 µg) (60). The double staining technique was used i.e. blue staining followed by more sensitive silver staining as described here. All steps were performed on a shaker.

i. Add 40 ml of Coomassie blue reagent (EZBlue) supplied by Sigma for 45 minutes
ii. Rinse gel and de-stain with de-ionised distilled water for 45 minutes

iii. Decant water and add 100 ml of fixing solution (10 % acetic acid, 50 % ethanol) and leave the gel overnight

iv. Replace fixture with 30 % ethanol solution and wait for 10 minutes

v. Water wash (200 ml) for ten minutes followed by sensitisation for ten minutes using the proteosilver sensitizer solution (100 ml of 1 %) provided in Proteosilver plus (Sigma) silver staining kit

vi. A couple of water washes (10 minutes each) and pour 100 ml of 1 % proteosilver silver solution and wait for another 10 minutes

vii. A quick wash in water (60-90 second) and pour 100 ml of diluted proteosilver developer solution (4-7 minutes), care was taken to prevent over or under developing of gels

viii. Upon appearance of bands, add 5 ml of Proteosilver stop solution in the gel tray to stop the reaction and wait for another 5 minutes

ix. Decant both developer and stop solutions and rinse gel carefully with water

x. Record the gel by scanning

2.1.8- Materials

Silk cocoons were supplied by Forest Fibres, UK and were cut by the supplier to remove silkworms. Chemicals used were sodium bicarbonate ($NaHCO_3$) 99% from Aldrich (Cat no. 34,094-4), 2-Mercaptoethanol (C_2H_6OS) 99% from Acros Organics (Cat no. 125470010) and urea (CH_4N_2O) supplied by Sigma Aldrich (Cat no. 5213-6).

Calcium chloride anhydrous ($CaCl_2$) from Fisher scientific (Cat no. C/1400/62), lithium bromide anhydrous (LiBr) from Acros organic (Cat no. 199875000) and lithium thiocyanate hydrate ($LiSCN.xH_2O$) from Aldrich (Cat no. 308374).

Cellulose dialysis cassettes supplied by Fisher Scientific (Cat no. TWT.-400-130U) and polyethylene glycol $H(OCH_2\text{-}CH_2)nOH$ supplied by Aldrich (20,240-1) were used for experiments. Formic acid (98-100 %) analytical grade (HCOOH) supplied by Fisher scientific (Cat no. F/1900/PB08) was used.

For SDS-PAGE analysis, Sodium dodecyl sulphate ($C_{12}H_{25}NaO_4S$) electrophoresis grade from Sigma (Cat no. L-3771-100G) was used for making the running buffer and modifying sample buffer, Laemmli 2x concentrate from Sigma-Aldrich (Cat no. S3401), BSA ~ 66 kDa Fluka supplied by Sigma-Aldrich (Cat no. 05476) Bradford reagent (Quick start™) from Bio-Rad (Cat no. 5000205), Pre-cast ready tris-HCl (4-15 % gradient polyacrylamide) gels from Bio-Rad (cat no. 116-1104).

HiMark pre-stained protein standard (range 30 kDa – 460 kDa) supplied by Invitrogen (Cat no. LC5699) shown in Figure 2.21-A was modified by addition of a 17 kDa myoglobin protein supplied by Sigma-Aldrich (Cat no. M5696-100MG) were used.

A

Band No.	Apparent Molecular Weight (kDa) NuPAGE® Tris-Acetate	NuPAGE® 4-12% Bis-Tris/MOPS	4% Tris-Glycine
1	460	420	500
2	268	247	279
3	238	214	251
4	171	160	164
5	117	107	121
6	71	64	--
7	55	51	--
8	41	39	--
9	31	28	--

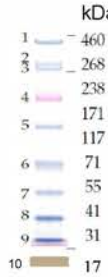

B

Figure 2.21: Protein markers used for SDS-PAGE A)- HiMark pre-stained protein standard (range 30 kDa – 460 kDa), B)- Modified by addition of 17 kDa myoglobin

For staining, Coomassie blue reagent EZBlue™ from Sigma (Cat no. G 1041) and Proteosilver™ plus silver staining kit supplied by Sigma (Cat no. PROT-SIL2) were used.

2.2- Preparation of silica nano-particles

In order to investigate the ability and effects of ceramic silica particles to interact with silk and improving mechanical properties, silica nano particles of different sizes (10-450 nm) were prepared using the modified Stöber method. In the original method (Stöber *et al;* 1968) used alcohol (methanol, ethanol, and *n*-propanol) as a solvent together with tetraalkoxysilicates. Ammonia (anhydrous 99.99%) was used as the hydrolysing agent resulting in the formation of spherical particles of *ca.* 0.05 μm to 2 μm in diameter.

It was necessary to use nano sized Stöber silica particles for this project. Different modifications (69) of the original method (70) (Table2.5) were made in an attempt to get nano sized silica particles with high degree of mono-dispersity and appropriate range of particle sizes.

2.2.1- Methods

Tetraalkoxysilane (TEOS) was hydrolysed in the presence of ammonia that also acted as a condensation catalyst and affected the average particle size formed depending upon the concentration of ammonia. For each modification, ammonia (10 M/35%) was diluted in deionised distilled water to get a range of concentrations (0.2 M to 5 M) that was used to explore their effect on silica particle size. Diluted ammonia solution (21.6 ml) from each concentration (0.2 to 5 M) was dissolved in 80 ml of ethanol and 22.3 ml/0.5 M of 98 % TEOS was dissolved in 76.6 ml of ethanol in separate vessels. Ammonia solutions of variable concentrations were mixed with TEOS solutions in 250 ml volumetric flasks with stopper (200 ml batch was prepared for each variable) and treated differently depending on the modifications (table 2.5).

Table 2.5: Different modifications used for making silica nano particles

	Stöber	**Stöber A**	**Stöber B**
TEOS/Ethanol	22.30 ml	22.30 ml	22.30 ml
Ammonia	21.6 ml (0.1M - 5M)	21.6 ml (0.1M - 5M)	21.6 ml (0.1M - 5M)
Final Volume	200 ml	200 ml	200 ml
Temperature	Room Temperature	Room Temperature	50 ^{o}C for 60 minute
Equilibrated	Un-Equilibrated	Equilibrated	Un-Equilibrated

All solutions were stirred for 15 minutes at 600 rpm using a 12 mm magnetic stirrer and kept under ambient conditions in stoppered flasks. TEOS was hydrolysed and subsequently silicic acid condensed in the presence of ethanol and ammonia forming silica particles. For Stöber and Stöber A batches, solutions were mixed and kept at room temperature while for Stöber B only; solutions were heated for one hour at 50 ° C and then kept at ambient conditions. Alcoholic ammonia and TEOS solutions for Stöber A were equilibrated by placing them in separate vessels in the dark for one week before mixing while in case of Stöber and Stöber B; solutions were un-equilibrated and mixed immediately at room temperature. Particle sizes from different solutions were analysed using DLS (2.1.3.3) and scanning electron microscopy (SEM).

The particle size was observed to increase with increasing concentration of ammonia added for any modification similar to that observed for the original method (70). The smallest particles were obtained with 0.2 M added ammonia solution in any modification (13-18 nm), while the largest average particles were obtained from 5 M added ammonia solution (Figure 2.22). These experiments had very good reproducibility with slight difference in particle sizes among different batches produced and suggested that a range of Stöber silica nano-particle can be produced by varying ammonia contents. Similar effects of ammonia concentration on particle studies were observed in previous studies (70,71).

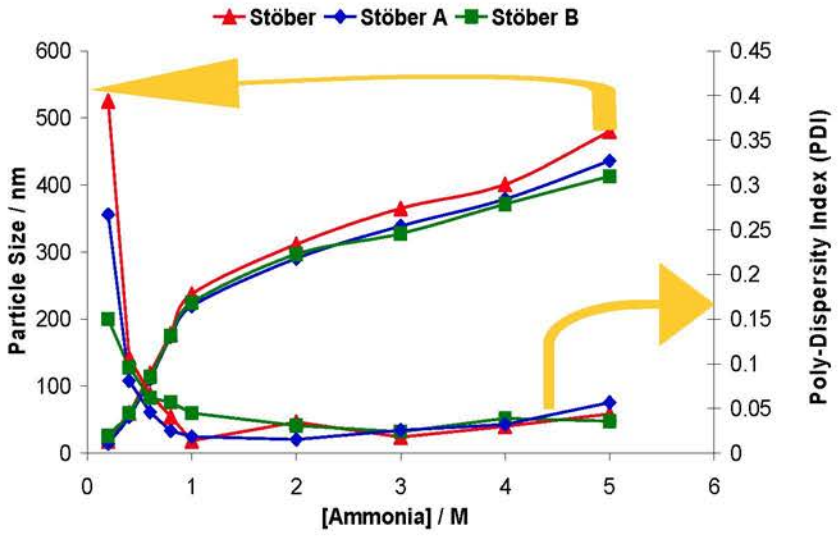

Figure 2.22: The relationship between added ammonia concentration and silica particle sizes and PDI.

PDI was observed to be higher in smaller particle samples which is thought to be due to their tendency to form aggregates due to high surface energy (71). A PDI of less than 0.1 is considered to reflect mono disperse systems (Malvern instruments\DTS5.00\FAQ), all solutions having greater than 0.5 M added ammonia showed PDI of less than 0.1 determining the uniformity of particles.

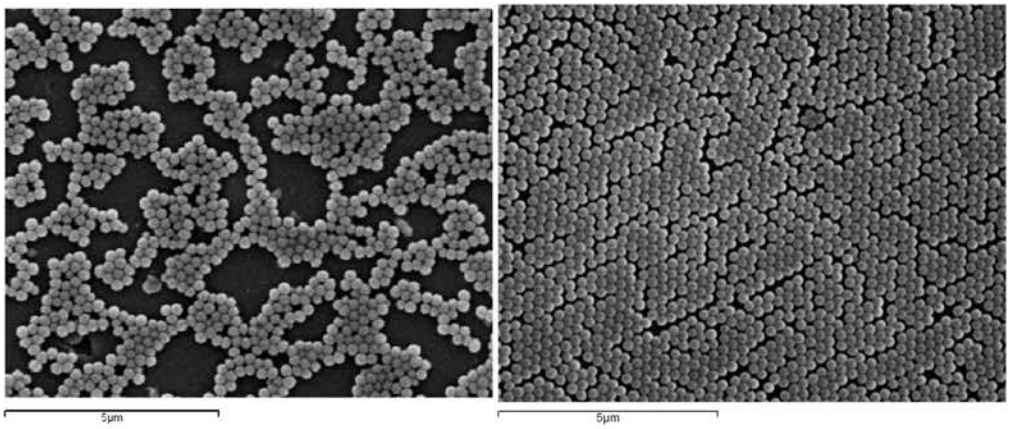

Figure 2.23: SEM images of silica particles (Stöber B/4M ammonia), average size 270 nm which is very close to the size measured by DLS (281 nm) for the same batch. (scale bar=5 µm, images taken at an accelerated voltage of 20 kV)

The Stöber B method produced the most uniform particles with lowest average PDI (Figure 2.22) and was used for all further experiment. SEM was used to check the size and morphology of silica particle and images are shown in Figure 2.23 for Stöber B/4 M ammonia.

2.2.2- Materials

Tetraethoxy silane (98 % TEOS), $[Si(OC_2H_5)_4]$ supplied by Aldrich (13,190-3) and aqueous ammonia (NH_3) from Fisher (Cat no. A/3240/PB17) were used for making all Stöber silica.

2.3- Materials fabrication

Materials were prepared using different forms of silk solutions and additions of silica using two different techniques described here.

2.3.1- Gelation route

Aqueous silk solutions can be used for making silk hydrogels and different aspects have been explored previously (31,72-74). As pH is an important parameter that affects the gelation of silk (72) as well as silica condensation (75), all experiments were performed using buffers. Gelation times of different silk solutions at different pH values were estimated by turbidity measurement using a 96 well plate reader.

2.3.1.1- Method

Silk hydrogels and composite fabrication took place using 96 well plates with changing silica and silk contents in rows or columns (Figure 2.24). The following variables were explored;

i. Silk content (0 to 32 mg)
ii. Silica source (hydrolysed TEOS or Stöber particles)
iii. Silica (Stöber) particle size (11 to 300 nm)
iv. Silica content (0 to 60 mg)
v. Buffers (Bis-tris propane/citric acid or phosphate buffer)-pH 7.0

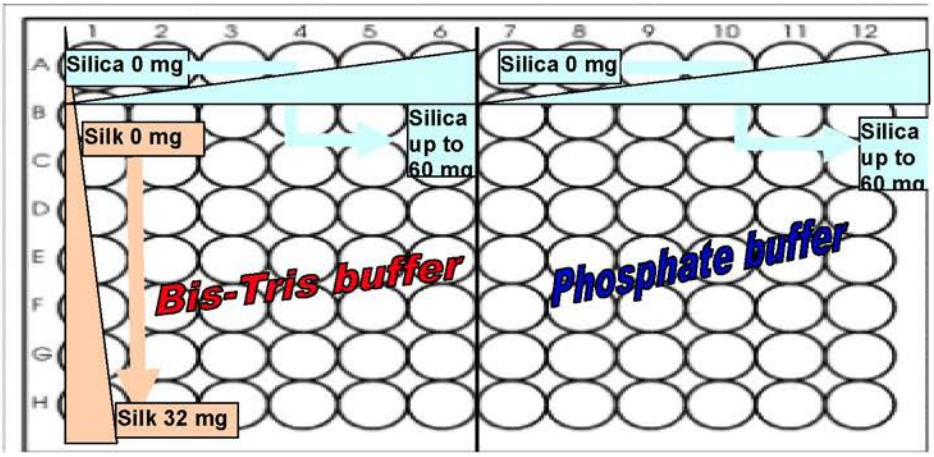

Figure 2.24: Schematic map of 96 well plate to show different variables

In order to obtain pH 7.0 bis-tris propane/citric acid (BTCA) was pippeted in one half and phosphate buffer in the other half of a plate as shown in Figure 2.24. The final concentration of buffer was maintained at 0.1 M. Aqueous silk solutions were prepared by dissolving silk (15 wt. %) in LiBr and dialysed using methods described (2.1.2.2 and 2.1.3) and concentrated up using 10 wt. % PEG in the external solution. After concentration calculation, different amounts were added in different rows (Figure 2.24). This step was followed by addition of silica in the form of hydrolysed TEOS or Stöber particles. The presence of ethanol in silica solutions helped these materials to gel in a matter of a few hours (depending on the silk and ethanol contents). Once these materials turned turbid, they were lyophilised to get solid composite materials. A detailed characterisation of these materials was performed using SEM, Fourier transform infrared spectrometry (FTIR), Thermo gravimetric analysis (TGA) and mechanical testing.

2.3.1.2- Materials

Bis-Tris propane ($C_{11}H_{26}N_2O_6$) supplied by Sigma (Cat no. B6755-100g), citric acid ($C_6H_8O_7$) anhydrous (99 %) from Acros Organics (cat no. 110450010) were used to prepared 1 M solutions and diluted to 0.1 M at the time of materials preparation. Phosphate buffer was prepared by making 1M solution at pH 7 using 5.1g of NaH_2PO_4 and 16.9g of Na_2HPO_4 in 100ml and ten times dilution was used in experiments. Hydrochloric acid (HCl) stock solutions 1M from Fisher (Cat no. J/4320/15) was used to pre-hydrolyse TEOS.

2.4-Electrospinning

Electrospinning is a technique that can be used to synthesize nanoscale fibres. This technique can be used for soluble or fusible polymers alone or polymers can be modified with additives such as particles or enzymes to get the desired properties (76). The resultant ultrafine fibres exhibit many interesting features, e.g. high surface area to mass or volume ratio, high density of pores in sub-micrometer or nano scale and vast possibilities for surface functionalization (76-79). These unique properties make electro-spun fibres an excellent candidate for a variety of biomedical applications, e.g. topical or parental drug delivery, wound dressings and scaffolding materials for tissue engineering (80). Electrospinning has been used for several biopolymers and blended biopolymers with synthetic polymers to obtain nano-fibres (76).

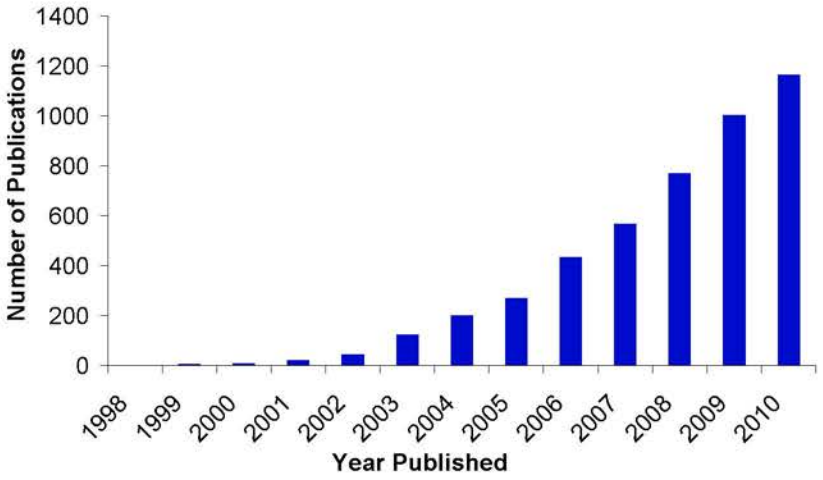

Figure 2.25: Increase in number of publications on electrospinning in recent years (Data collected from the Web of Knowledge using keyword "electrospinning")

Electrospinning has also been used for silk polymers in several studies (26,34,46,77-89) and there is a dramatic increase in the number of publications related to silk suggesting an increase in its popularity in recent years (Figure 2.25).

2.4.1- Electrospinning equipment

The electrospinning technique involves the introduction of a strong electric field between a polymer solution contained in a reservoir with a capillary tip and a metallic collection plate (90).

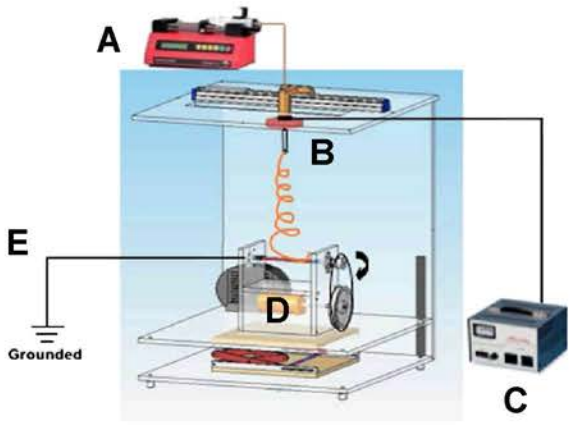

Figure 2.26: Schematic presentation of the electrospinning equipment (Zhang et al; 2009), A)- Mechanical syringe pump, B)- Metallic needle, C)- Power supply, D)- Target stage, E)- Earth cable

The process is shown schematically in Figure 2.26 (91), the polymer solution is pumped through the metallic needle (B), [55 mm long, gauge 20] at a constant flow rate using a syringe pump (A), [flow rate could be adjusted from 0.09 to 45 ml/hr]. Due to an increase in the potential voltage difference [power supply (C) can supply 0-30 kV] between the polymer solution and the collection plate (D), electrostatic forces overcome the solution surface tension to pull a jet of charged fluid that splits into nano fibres that fall towards the collection plate and solidify to become fibres. The high charge flow induces fibres separation and rapid drying. The solvent (FA) is very volatile and evaporates quickly which also help fibres solidify rapidly.

2.4.2- Factors affecting electrospinning

The morphology and properties of electro-spun fibres can be manipulated by varying a range of parameters to get fibres of the desired morphology and properties. A list of factors affecting electro-spun fibres is listed in table 2.6 (90).

Table 2.6: List of variable parameter affecting the morphology electro-spun fibres

Process Parameters	**Systemic parameters**	**Solution parameters**	**Physical parameters**
• Voltage • Flow rate • **Collection plate** ▪ Distance ▪ Angle ▪ motion	•Polymer type •Molecular weight •Polymer architecture •Solvent used	• Viscosity • Concentration • Conductivity • Dielectric constant • Surface tension • Charge of jet	• Humidity • Temperature • Air velocity

Table 2.7: Factors affecting electro-spun silk nano-fibre

Variable	**Factors**
Voltage (Kv)	24, 18,15,12,9,6
Target Distance (cm)	24, 22, 15, 7.5, 7.0
Target Angle	51°, 90°
Silk concentration (wt. %)	30, 25, 20, 15,10,5
Flow rate (ml/hour)	0.09, 0.45, 0.9, 1.8
Constant potential Gradient (kV/cm)	24/8, 21/7, 18/6, 15/5, 12/4, 9/3 (Constant=3kV/cm)

The polymer solution should have an optimal low surface tension and high enough charge density and viscosity so that collapse of the jet into droplets can be prevented before the solvent evaporates (92). These factors may be correlated and affect fibre morphology in a complex fashion. In order to understand these effects, some important parameters were explored to set up the method (table 2.7). In general, to explore one factor (variable), all other parameters and conditions were kept constant.

2.4.3- Electrospinning dope preparation

Electrospinning silk solutions were prepared in formic acid using the method described above (2.1.5 and 2.1.6). Any solution prepared was stored at ambient conditions for at least 1 hour to ensure complete solubilisation of silk and was used on the same day. For parameters analysis, only regenerated total silk (RTS) was used, however, once the method was set, all fractions and their combinations were electro-spun.

Fibre morphology was analysed using SEM and average fibre diameter was calculated by measuring 25 fibres randomly from each sample and results are discussed here. All SEM images shown here are taken at a magnification of 5000X at 20 kV.

2.4.4- Concentration and viscosity

Concentration may indirectly affect fibre morphology by changing the solution viscosity as more concentrated solutions generally give higher viscosity (Figure 2.27). Both are important parameters in producing continuous uniform fibres.

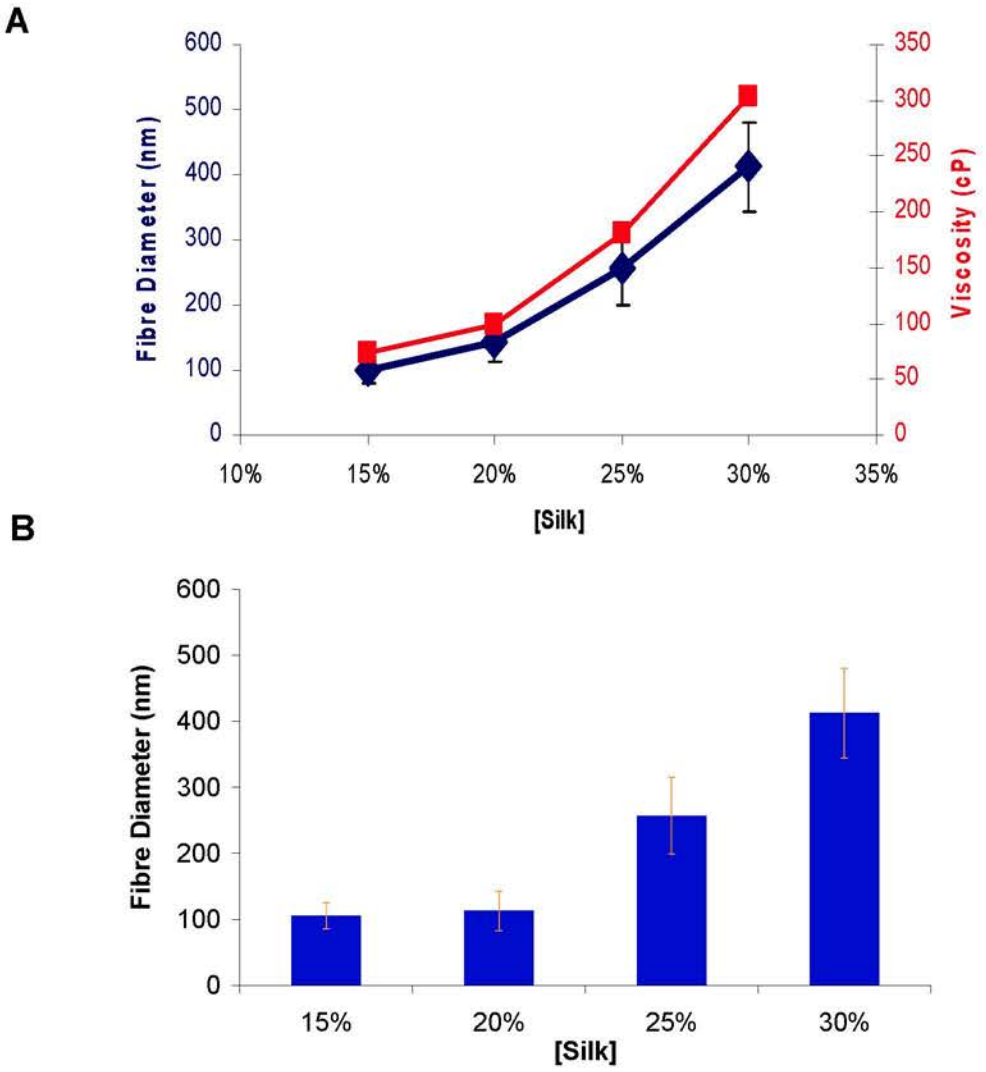

Figure 2.27: A)- Effects of concentration and viscosity on electro-spun fibre diameter, B)- Average fibre diameter at various silk concentrations

Below 20 wt.. % silk solutions, continuous and uniform fibres could not be produced under similar conditions and ended up in either droplets or mainly droplets and a few fibres (Figure 2.28).

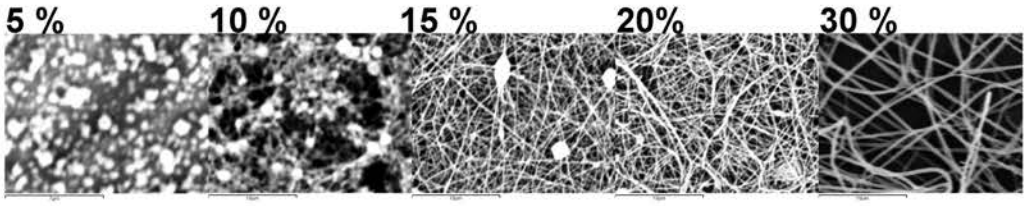

Figure 2.28: The effects of silk concentration on fibre morphology; [Fixed parameters: 24 kV, collected at 7.5 cm, flow rate 0.9 ml/hr] (scale bar=10 µm)

These results suggest that silk concentration must be 15 wt. % or more in order to get uniform continuous fibres.

2.4.5- Distance and spinning angle

Capillary tip to collection plate distance is also an important parameter observed to affect electro-spun fibre morphology (92). This distance also affects the time available for the solvent to evaporate, with a longer distance providing comparatively more time and vice versa.

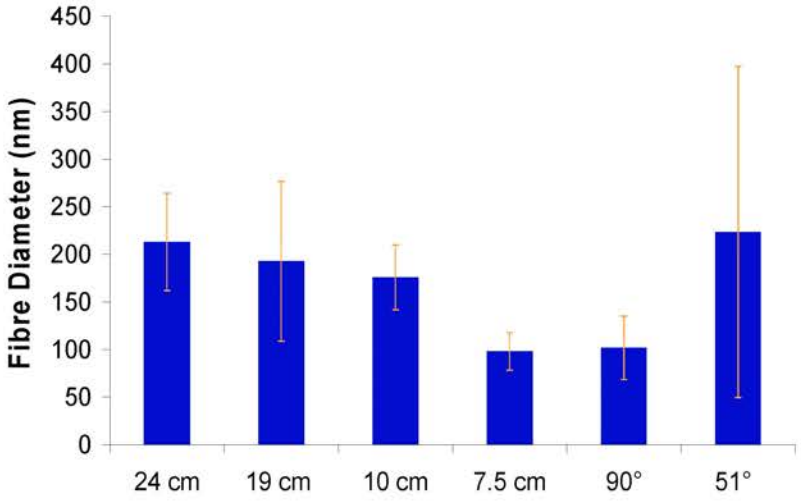

Figure 2.29: Effects of distance and angle of collection target on fibre morphology

The change of collection angle produce significantly large fibres with wider fibre size distribution (Figure 2.29), while average fibre size was observed to decrease with decreasing the collection distance

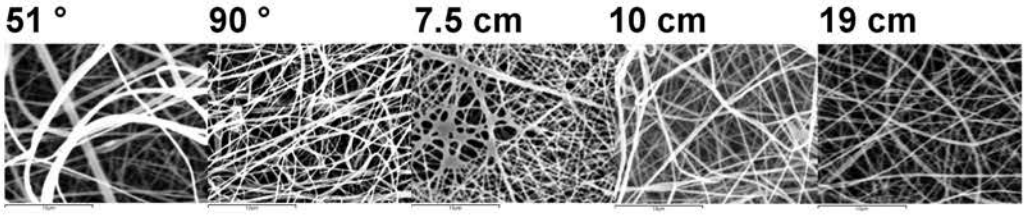

Figure 2.30: The effects of collection plate distance and angle on fibre morphology; [Fixed parameters: 20 wt. % silk, 24 kV, flow rate 0.9 ml/hr; for angle experiment distance was fixed to 7.5 cm] (scale bar=10 µm)

Concluding from these findings, all samples spun were collected at right angle at an optimum distance of 10 cm as closer than that did not provide enough time to solidify fibres (in case of 7.5 cm shown in Figure 2.30).

2.4.6- Voltage and potential gradient

Electric potential is another important parameter that can affect the final morphology of fibres (92). The effect of change in voltage may be dependent on other parameters as well; however in general electro-spun fibre diameter is decreased on increasing the electric field (45). Fibres produced at 6 kV (0.8 kV/cm) had diameters 868.94 nm ± 310.10 nm, which sharply decreased to 319.35 nm ± 148.47 nm at a voltage of 9 kV (1.2 kV/cm). Thereafter, no significant change was observed in the average fibre size up to voltage of 18 kV (2.4 kV/cm), however fibre size distribution became narrower. At the highest voltage of 24 kV (3.2 kV/cm), fibre size was significantly decreased down to 129.31 nm ± 22.29 nm showing the narrowest fibre size distribution as well (Figure 2.31-A).

The effect of voltage is strongly correlated to the collection plate distance as altering the voltage also changes the voltage/distance for a fix collection plate distance. In another set of experiments, voltage/distance was maintained at 3kV/cm by adjusting distance alongside voltage.

For all samples electro-spun silk fibres in the range of 201 nm to 220 nm diameter with a standard deviation of 42 to 62 were obtained. Surprisingly, there was no significant difference in average fibre size diameter and fibre size distribution among fibres spun at 6 kV up to 24 kV as for as distance was adjusted accordingly (Figure 2.31-B and SEM images in Figure 2.32).

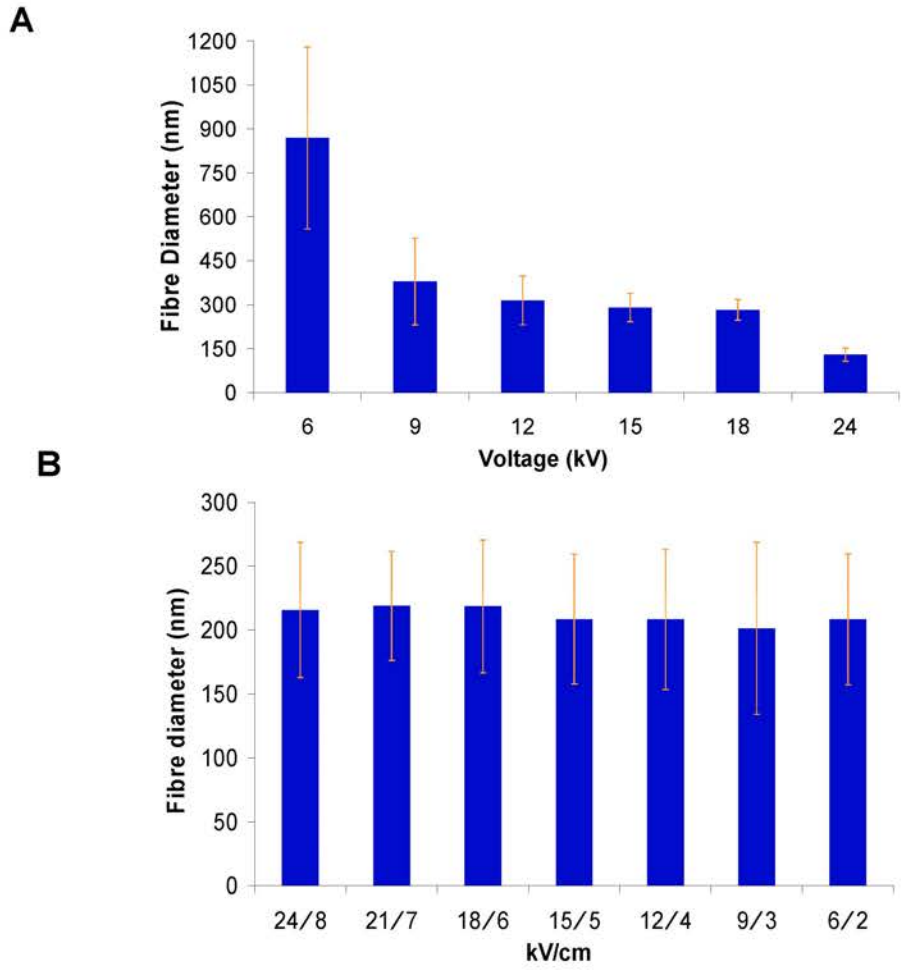

Figure2.31: The effects of voltage with different gradient potential at fixed distance of 7.5 cm (A), and constant potential gradient on fibre morphology (B)

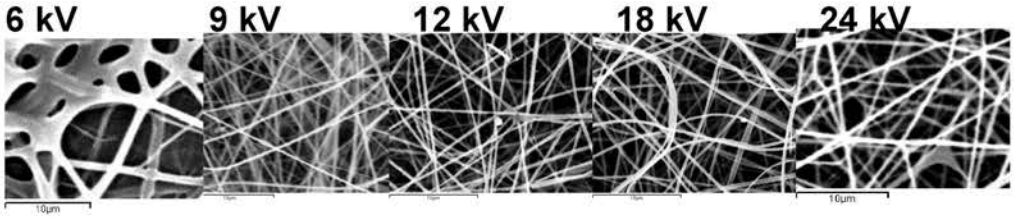

Figure 2.32: The effects of difference in voltage on fibre morphology; [Fixed parameters: 20 wt. % silk, at 7.5 cm, flow rate 0.9 ml/hr] (scale bar=10 µm)

These results suggested that potential gradient is an important parameter and must be considered while changing voltage or distance. For all further work, a constant potential gradient of 2.5 kV/cm was used.

2.4.7- Flow rate

The flow rate of the polymer solution is an important parameter as it determines the size and shape of the Taylor cone at the end of the metallic needle. The maintenance of the cone shape throughout electrospinning is necessary for a continuous polymer jet (93). The effect of flow rate was studied from 0.09 ml/hr to 1.8 ml/hr under similar electrospinning conditions [20 wt. % silk, voltage 24 kV at 7.5 cm].

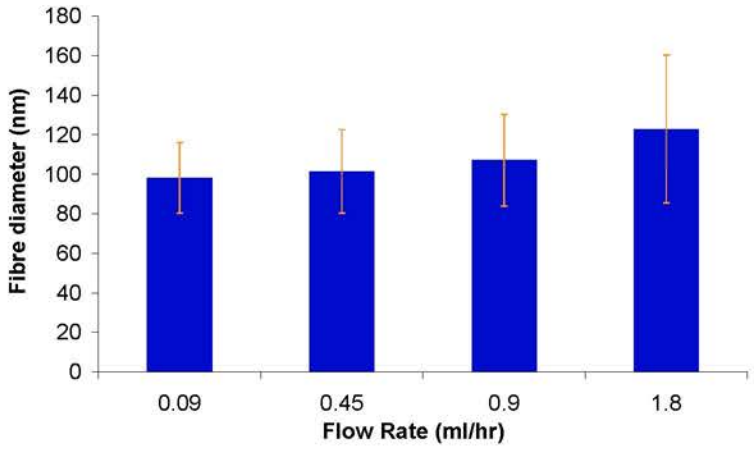

Figure 2.33: Effect of flow rate on average fibre size distribution

As a general trend, average fibre diameter slightly increased by increasing the flow rate however the difference was not significant. At a flow rate of 0.09 ml/hour, average fibre diameter was 98.17 nm ± 17.83 nm and increased to 122.85 nm ± 37.36 nm by increasing flow rate to 1.8 ml/hour (Figure 2.33). Similarly, fibre size distribution was observed to increase insignificantly with increase of flow rate. In order to have better control on fibre size distribution, a flow rate of 0.9 ml/hr was used for further experiments.

2.5- Characterization techniques

A range of characterisation techniques were used in this study.

2.5.1- Scanning electron microscopy (SEM)

Scanning electron microscopy (SEM) is mainly used for characterising surface morphology (94). SEM consists of a filament (cathode) that works on very simple principle as schematically shown in Figure 2.34. The filament produces an electron beam that passes through the lens and is used to scan the sample surface, producing secondary electrons scattered from the surface. These secondary electrons are monitored by a detector and passed to the cathode ray tube (CRT) for display. During this process X-rays are produced as well and are used for elemental analysis in modern SEM.

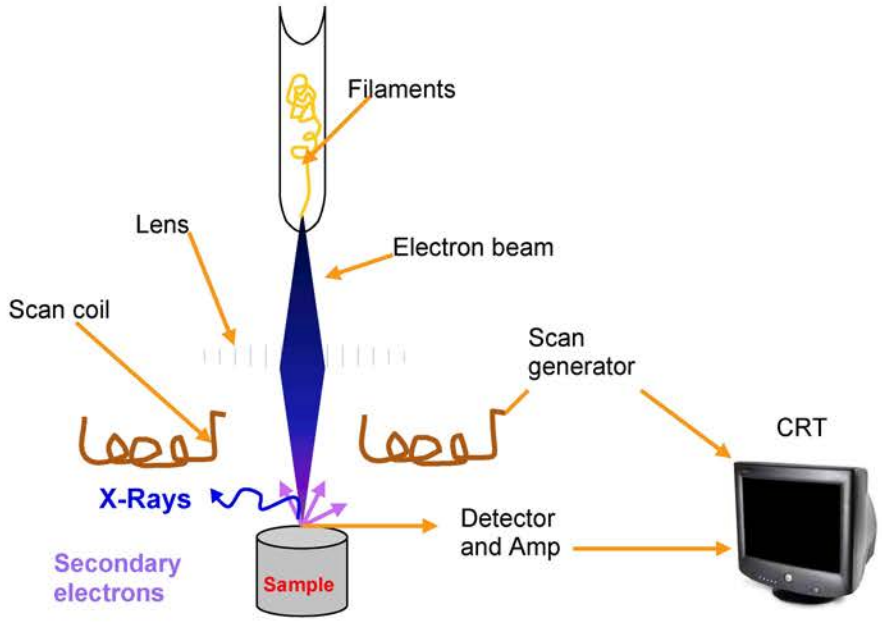

Figure 2.34: Schematic presentation of SEM principle (derived from Dawn)

The alignment of electron beam source (filament), lens, scan coil and detector is very crucial for proper functioning of SEM and to get sharp images (94). Scanning electron microscope from Jeol model JSM 840A (Figure 2.35) was used at an accelerating voltage of 20 kV.

2.5.1.1- Sample preparation for SEM

Sample material was mounted on aluminium stubs having sticky conductive tabs connecting stub and the sample material. In case of electro-spun mats, a patch of aluminium foil containing fibres was cut to stick on the stub.

Figure 2.35: Jeol scanning electron microscope model JSM-840A

For lyophilised silk or composites, material was simply sprinkled on the stub and tapped to remove any unattached fragments. All samples were gold coated with argon for two minutes using an Edwards S150B sputter coater at 1.2 kV and 4.5 mbar.

2.5.2- Fourier transform infrared spectroscopy (FTIR)

Infrared (IR) spectroscopy is a technique used to characterise materials by measuring absorbance (*A*) or transmittance (*T*) of the infrared part of the electromagnetic spectrum. The IR spectrum is usually expressed in wave numbers that are the reciprocal of wavelength and is measured in 1/centimetres (95,96).

$$\text{Wave number} = \frac{1}{\lambda} \qquad \text{(Eq 2.3)}$$

This technique works by studying the vibrational modes present in different molecules. Atoms in any molecules are found in the stage of continuous vibrational movements with respect to each other. There are different kind of vibrational movements such as stretching, bending and scissoring and may be accompanied by rotational motions (97). For infra-red spectroscopy, the vibrational mode must change the electric dipole moment during vibration (such as asymmetric vibrations) to make it infrared active and restricts its use for symmetric vibrations where change in the dipole moment is not observed (98). Infrared radiation is absorbed by molecule and combination of vibrational movements result in formation of characteristic spectra in the infrared region (97).

Table 2.8 : Characteristic absorption peaks of FTIR spectra

Nature of bond	**Absorption peak (cm^{-1})**
Symmetrical stretch of Si-O-Si (75)	800
Si-OH vibration (75)	850-950
Asymmetrical stretch of Si-O-Si (75)	1050-1150
β-turn (99,100)	1673-1691
β-sheet (99,100)	1633
α-helix (99,100)	1658
Random (99)	1647
O-H stretch in adsorbed water molecule (75)	3400-3500
O-H stretch with hydrogen bonding (75)	3650-3660
O-H stretch without hydrogen bonding (75)	3745-3750

The infrared region can be divided into three regions, near-infrared (28000-4000 cm^{-1}), mid-infrared (4000-400 cm^{-1}) and far infrared (400-10 cm^{-1}) (96). In this study, mid-infrared region was used to obtain characteristic information about samples and presence of silica and the effect of processing conditions on the secondary conformation of the silk proteins. The relevant wave numbers are given in table 2.8 suggesting mid-infrared region very important for analysis.

In modern FTIR instruments, the monochromator has been replaced by Michelson interferometer, that can work on sinusoidal transmittance pattern and records the spectrum at all wavenumbers simultaneously (95). FTIR is a characterisation technique with excellent benefits such as an ease of use, small amount of sample

material (50-200mg), time effective (as little or no sample preparation is required and can be analysed in 1-10 minutes), an ability to detect impurities (as low as 0.1-1%) and can be used for a detailed characterisation of a range of organic and inorganic materials (97).

2.5.2.1- Method for FTIR

FTIR was performed on electrospun silk mats to analyse silk conformational changes and on nanocomposites to determine in organic content. FTIR spectrometer PerkinElmer model 100 FT-IR was used. This instrument can be used both for liquid and solid sample and perform a quick measurement in the range of 7800-380cm^{-1}. All measurements were performed at resolution of 4cm^{-1} for 32 scans in the range of 4000 cm^{-1} to 400 cm^{-1}. Electrospun silk mats were analysed along with aluminium foil where was used as a blank. All spectra were interpreted using SPECTRA, OMNIC and GRAM computer software.

2.5.3- UV-Visible spectroscopy (UV-Vis)

UV-Vis spectroscopy was used to measure the absorbance of sample at a range of specific wave length (190 to 1000 nm) including UV (190 to 350) the visible light (350 to 650 nm).

Essentially, it contains a source of light, a tungsten lamp for visible light and a deuterium lamp for UV light. The light source can be controlled using a mirror as needed. In some machines, before reaching the sample, light is filtered for a specific wavelength using monochromator. The light transmitted from the sample is sensed by a detector, amplified and displayed as absorbance (*A*) or transmittance (*%T*) (95). UV-Vis is commonly used to calculate concentrations of a sample dissolved in a solvent and using solvent only as a blank and *%T* at a specific wave length can be calculated by a simple formula (95).

$$\text{Transmittance } (T) = \frac{\text{Intensity of light transmitted by sample } (I_T)}{\text{Intensity of light transmitted by Blank } (I_R)} \qquad \text{(Eq 2.4)}$$

$$\%T = \frac{(I_T)}{(I_R)} \times 100 \qquad \text{(Eq 2.5)}$$

And absorbance (*A*) can be calculated as

$$A = -\log(T) \quad \text{(Eq 2.6)}$$

Absorbance can be used for further calculation using Beer Lambert's law that can be expressed as (95,101)

$$A = \epsilon bc \quad \text{(Eq 2.7)}$$

Where

'ε' is absorptive of sample at a particular wave length

'*b*' is path length through the sample

'*c*' is concentration of sample

Hence by calculating absorbance and fixing path length, concentrations of different samples can be determined. The UV-Vis spectroscopic technique was used in a number of experiments in the PhD study including the Bradford assay for protein concentration measurements, colour changes in silk solutions and turbidity measurements in gelling silk solutions.

2.5.4- Thermogravimetric analysis (TGA)

Thermogravimetric analysis (TGA) is used to establish changes in mass of a material as a function of temperature (102). Under the influence of different temperature/heating conditions, a material can undergo a variety of changes such as structural decomposition, alteration in moisture contents, oxidation, corrosion or gas evolution. TGA is an excellent tool to analyse such changes in a variety of materials (102) including nanocomposites (103) and nanoparticles (104). Recent advancements in TGA instrumentation allow better control over heating rates providing more isolated and dynamic environment for samples (105).

Typically, TGA is composed of highly sensitive microbalance, ceramic pans (sample holders) and a programmable furnace attached to the computer. The instrument is controlled using computer software that also collect and analyse TGA data. To prevent oxidation of samples while testing, different inert gases can be used for purging.

2.5.4.1- Method

For this study, all samples were analysed using a Mettlor Toledo model TGA/SDTA 581^e. Sample pans were pre-weighed and then loaded with sample material and

placed into the furnace. The TGA was programmed for heating samples from 30 ℃ to 600 ℃ to ensure complete combustion of organic matter. The temperature was held at 30 ℃ for the first ten minutes and then te mperature increased at a constant rate of 10 ℃/minute up to 600 ℃. An oxidising env ironment was retained by air flow at 20 ml/minute throughout the analysis. All data was collected using the software.

2.5.5- Mechanical testing

For development of new materials, it is crucial that they have the strength to withstand and tolerate stresses for the intended application. It is important to test mechanically to predict material behaviour to forces. There are different methods of assessing mechanical properties (Figure 2.36) however they all work mainly on the principle of stress and strain correlation (106). As materials being tested may be of different shapes and sizes so stress can be normalised by dividing force applied by area (107). Stress is force applied per unit area,

$$\text{Stress } (б) = \frac{\text{Force (F)}}{\text{Area (A)}} \quad \text{(Eq 2.8)}$$

It is calculated in N/m^2 or MPa. (1 N/m^2=1Pa or 10^6 N/m^2=1MPa)

While strain is deformation as result of force applied

$$\text{Strain } (\epsilon) = \frac{\text{Deformation } \Delta\ell(\ell-\ell_0)}{\text{Original length } (\ell_0)} \quad \text{(Eq 2.9)}$$

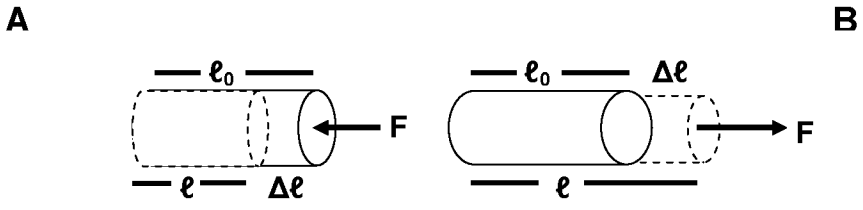

Figure 2.36: Effect of force to deform an object shown schematically, A)- Compressive stress, B)- Tensile stress. Where ℓ_0 is the original length and ℓ refer to final size and $\Delta\ell = \ell - \ell_0$

The mechanical behaviour of material is studied by stress-strain curve while increasing the stress at a constant rate. Stronger materials will need more force to produce strain and vice versa (Figure 2.37).

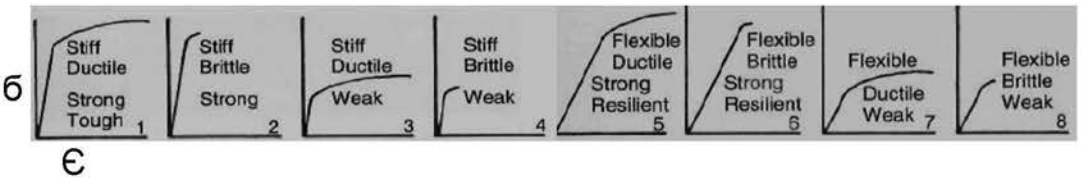

Figure 2.37: Stress-strain curves for materials having different combinations of mechanical properties. Craig et al 2002

The mechanical tester and methods used for testing materials during this study are described below.

2.5.5.1- Mechanical tester

For all mechanical testing, a Zwick/Roell mechanical tester (model Z0.5 TS) was used. This instrument was supplied with 500 N load cell (capable to perform testing at a speed of 0.001 - 2000 mm/min) and multiple attachments to perform a variety of testing procedures. The instrument can be controlled manually as well as by computer using the software *testXpert II*. The instrument works on the principle of recording stress strain curves. Force is applied to a material by a load cell at a constant rate and deformation is recorded either in mm or % strain. This data is used to plot stress strain curves and to analyse for multiple parameters for a range of mechanical properties.

2.5.5.2- Tensile testing

Tensile testing is used to find maximum stress that a material can bear while force is applied outward (stretch as shown in Figure 2.36) from axis (108).

2.5.5.3- Method development for tensile testing of Electrospun materials

Tensile properties are often measured during new material development to compare different materials and processes and results are also used to predict the behaviour of new materials upon loading. In terms of electro-spun materials, nano fibres are always collected on a metallic target and it is almost impossible to separate them from the target without damaging the fibres. The other option for tensile testing of such material is to test them together with the metallic target and calculate the strength of the electro-spun material. A method using aluminium foil strips cut exactly the size to adapt to the electro-spun apparatus and mechanical tester and has been developed and is explained below.

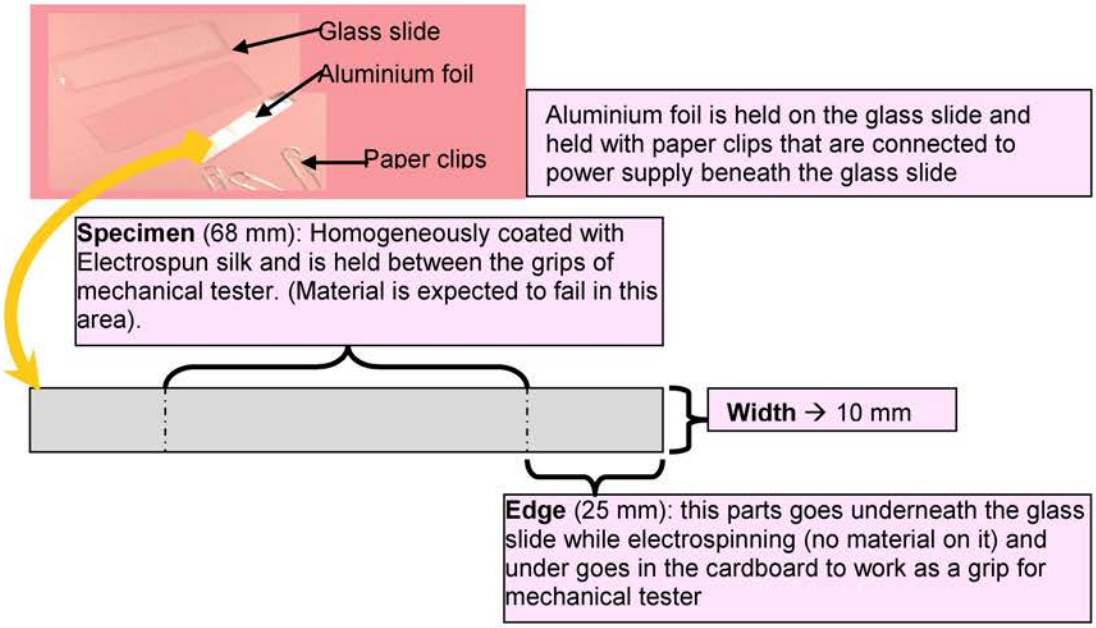

Figure 2.38: Method development for tensile testing

Briefly, aluminium strips were cut to exact size of 118 mm x 10 mm and were mounted on a glass slide using paper clips (bent at right angle) to connect to the electrospinning power supply (Figure 2.38 and 2.39). In this way, all electro-spun materials deposited on the aluminium strips gave a homogeneous coating. The part of aluminium foil beneath the glass slide did not get any fibres and was used to fix the foil inside a cardboard collar using cyanoacrylate superglue. This purpose of this attachment was to provide a solid grip for the mechanical tester to hold the sample and to prevent developing any stress concentration or tears alongside the edges while testing the material.

The Sample was held in the mechanical tester firmly and force was applied parallel to the long axis of sample at a rate of 3mm/min until the material failed.

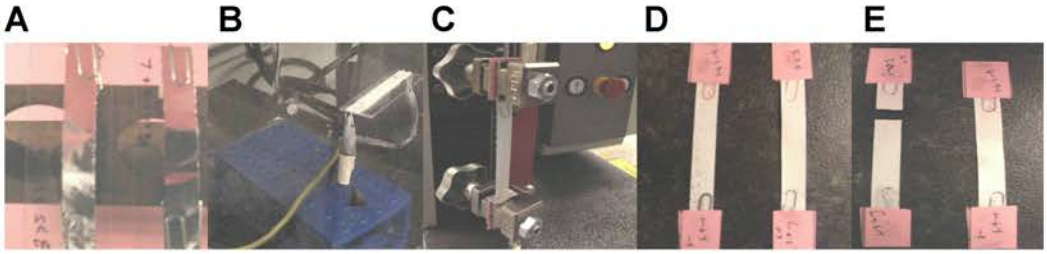

Figure 2.39: Test specimens A)- Aluminium foil as mounted on the glass slide and held with paper clips, B)- Mounted for electrospinning, power connected to paperclips, C)- electro-spun specimens glued to cardboard and ready for mechanical testing, D)- specimen placed in the mechanical tester, ready for testing, E)- Specimens after and before failure

For blank aluminium foils, all samples were tested in a series without depositing any material on them. Different stages of tensile testing are shown in Figure 2.39. All data was recorded in the testexpertII software and was exported to Microsoft excel for analysis and interpretation.

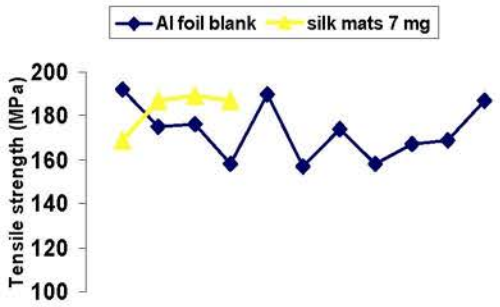

Figure 2.40: Tensile strength of identical blank aluminium foils and electro-spun mats (ca. 7 mg deposited on each specimen) compared using this method. Each data point represents multiple repeats of testing specimens

As an example, some of tensile testing results are shown in Figure 2.40 Due to the anisotropic nature of aluminium foil (substrate), blank samples showed wide variation in tensile strength whereas silk mats on foil (due to very low strength compared to aluminium foil) did not produce any different results than blank. However, this method has the potential to be used for stronger electro-spun mats.

2.5.5.4- Compression testing

Compression testing is a method used to find the maximum stress that a material can bear while force is applied inward (compress as shown in Figure 2.36) from axis (108), (compressive strength of materials).

2.5.5.5- Method for compression testing

Compression testing was used to mechanical test the nano-composites fabricated using the gelation route. Silk hydrogels and composites were fabricated using 96 well plates with changing silica and silk contents in rows or columns (Figure 2.24). All experimental is described in section 2.1.2.2 and 2.1.3.1.
Compression testing was performed on lyophilised materials inside the 96 well plate using a 4 mm diameter rod attachment on the mechanical tester compressing at a constant rate (10 mm/min). All data was collected in software *testXpert II* and exported as an excel file for interpretation.

2.6- References

(1) Hardy JG, Scheibel TR. Composite materials based on silk proteins. Progress in Polymer Science 2010 9;35(9):1093-1115.

(2) Yamada H, Nakao H, Takasu Y, Tsubouchi K. Preparation of undegraded native molecular fibroin solution from silkworm cocoons. Materials Science and Engineering: C 2001 8/15;14(1-2):41-46.

(3) Bajaj P. - Finishing of textile materials. - Journal of Applied Polymer Science - 2002;- 83(- 3):- 631-- 659.

(4) Das S. - The preparation and processing of tussah silk. - Journal of the Society of Dyers and Colourists - 1992;- 108(- 11):- 481-- 486.

(5) Hardy JG, - Scheibel TR. - Production and processing of spider silk proteins. - Journal of Polymer Science Part A: Polymer Chemistry - 2009;- 47(- 16):- 3957-- 3963.

(6) Fu C, - Shao Z, - Fritz V. Animal silks: Their structures, properties and artificial production. Chem.Commum - 2009: 6515-6529.

(7) Hardy JG, Römer LM, Scheibel TR. Polymeric materials based on silk proteins. Polymer, 2008 9/23;49(20):4309-4327.

(8) Shimura K, Kikuchi A, Ohtomo K, Katagata Y, Hyodo A. Studies on silk fibroin of bombyx mori. I. fractionation of fibroin prepared from the posterior silk gland. J Biochem 1976 October 1, 1976;80(4):693-702.

(9) Somashekarappa H, Annadurai V, Sangappa, Subramanya G, Somashekar R. Structure–property relation in varieties of acid dye processed silk fibers. Materials Letters 2002 4;53(6):415-420.

(10) Kaplan D, Adams WW, Farmer B, Viney C. Silk - Biology, structure, properties, and genetics. silk polymers 1994;544:2-16.

(11) Hakimi O, Knight DP, Vollrath F, Vadgama P. Spider and mulberry silkworm silks as compatible biomaterials. Composites Part B-Engineering 2007;38(3):324-337.

(12) Zhang Y. Applications of natural silk protein sericin in biomaterials. Biotechnol Adv 2002 5;20(2):91-100.

(13) Dewair M, Baur X, Ziegler K. Use of immunoblot technique for detection of human IgE and IgG antibodies to individual silk proteins, Journal of Allergy and Clinical Immunology 1985 10;76(4):537-542.

(14) Panilaitis B, Altman GH, Chen J, Jin H, Karageorgiou V, Kaplan DL. Macrophage responses to silk. Biomaterials 2003 8;24(18):3079-3085.

(15) Kodama K. The preparation and physico-chemical properties of sericin. Biochem J 1926 , 1926;20(6):1208-1222.

(16) Ayutsede J, Gandhi M, Sukigara S, Micklus M, Chen H, Ko F. Regeneration of Bombyx mori silk by electrospinning. Part 3: characterization of electrospun nonwoven mat. Polymer 2005 2/14;46(5):1625-1634.

(17) Geddes AJ, Graham GN, Morris HR, Lucas F, Barber M, Wolstenholme WA. Mass-spectrometric determination of the amino acid sequences in peptides isolated from protein silk fibroin of Bombyx mori.

(18) Chen X, Knight DP, Shao Z, Vollrath F. Regenerated Bombyx silk solutions studied with rheometry and FTIR. Polymer 2001 12;42(25):09969-09974.

(19) Wang H, Zhang Y, Shao H, Hu X. A study on the flow stability of regenerated silk fibroin aqueous solution. International Journal of Biological Macromolecules 2005 7;36(1-2):66-70.

(20) Jin HJ, Kaplan DL. Mechanism of silk processing in insects and spiders. Nature 2003;424(6952):1057-1061.

(21) Tamada Y. Modification of fibroin film with a chimera fibroin fragment for improvement of cell adhesion. Biomaterials Regulating Cell Function and Tissue Development 1998;530:27-32.

(22) Um IC, Kweon HY, Lee KG, Park YH. The role of formic acid in solution stability and crystallization of silk protein polymer. Int J Biol Macromol 2003 12;33(4-5):203-213.

(23) Phillips DM, Drummy LF, Conrady DG, Fox DM, Naik RR, Stone MO, et al. Dissolution and regeneration of bombyx mori silk fibroin using ionic liquids. J Am Chem Soc 2004;126(44):14350-14351.

(24) Ajisawa A. Dissolution of silk fibroin withcalciumchloride/ethanol aqeous solution. J Seric Sci Jpn 1998;67(2):91-94.

(25) Damrongrungruang T, Siritapetawee M, Kamanarong K, Limmonthon S, Rattanathongkom A, Maensiri S, Et Al. Fabrication of electrospun thai silk fibroin nanofiber and its effect on human gingival fibroblast: a preliminary study. Journal of Oral Tissue Engineering 2007;5(1):1-6.

(26) Ki CS, Kim JW, Hyun JH, Lee KH, Hattori M, Rah DK, et al. Electrospun three-dimensional silk fibroin nanofibrous scaffold. J Appl Polym Sci 2007;106:3922-3928.

(27) Min B, Lee G, Kim SH, Nam YS, Lee TS, Park WH. Electrospinning of silk fibroin nanofibers and its effect on the adhesion and spreading of normal human keratinocytes and fibroblasts in vitro. Biomaterials, 2004 0;25(7-8):1289-1297.

(28) Park WH, Jeong L, Yoo DI, Hudson S. Effect of chitosan on morphology and conformation of electrospun silk fibroin nanofibers. Polymer, 2004 9/29;45(21):7151-7157.

(29) Li W, Mauck RL, Tuan RS. Electrospun Nanofibrous Scaffolds: Production, Characterization, and Applications for Tissue Engineering and Drug Delivery. Journal of Biomedical Nanotechnology September 2005;1:259-275(17).

(30) Sukigara S, Gandhi M, Ayutsede J, Micklus M, Ko F. Regeneration of Bombyx mori silk by electrospinning—part 1: processing parameters and geometric properties. Polymer, 2003 9;44(19):5721-5727.

(31) Kim K, Jeong L, Park H, Shin S, Park W, Lee S, et al. Biological efficacy of silk fibroin nanofiber membranes for guided bone regeneration. Journal of Biotechnology, 2005 11/21;120(3):327-339.

(32) Kino R, Ikoma T, Yunoki S, Nagai N, Tanaka J, Asakura T, et al. Preparation and characterization of multilayered hydroxyapatite/silk fibroin film. Journal of Bioscience and Bioengineering, 2007 6;103(6):514-520.

(33) Fong H, Chun I, Reneker DH. Beaded nanofibers formed during electrospinning. Polymer 1999 7;40(16):4585-4592.

(34) Wang H, Shao HL, Hu XC. Structure of silk fibroin fibers made by an electrospinning process from a silk fibroin aqueous solution. J Appl Polym Sci 2006;101(2):961-968.

(35) Zainuddin, Le TT, Park Y, Chirila TV, Halley PJ, Whittaker AK. The behavior of aged regenerated Bombyx mori silk fibroin solutions studied by 1H NMR and rheology. Biomaterials 2008 11;29(32):4268-4274.

(36) Chu B. Laser light scattering : basic principles and practice. 2nd ed. Boston, Mass.: Academic; 1991.

(37) Berne BJ. Dynamic light scattering : with applications to chemistry, biology and physics. New York ; London: Wiley-Interscience; 1976.

(38) Inoue S, Tanaka K, Arisaka F, Kimura S, Ohtomo K, Mizuno S. Silk fibroin of bombyx mori is secreted, assembling a high molecular mass elementary unit consisting of H-chain, L-chain, and P25, with a 6:6:1 Molar Ratio. J Biol Chem 2000 December 15, 2000;275(51):40517-40528.

(39) Tanaka K, Inoue S, Mizuno S. Hydrophobic interaction of P25, containing Asn-linked oligosaccharide chains, with the H-L complex of silk fibroin produced by Bombyx mori. Insect Biochemistry and Molecular Biology 1999 3;29(3):269-276.

(40) Ha S, Gracz HS, Tonelli AE, Hudson SM. Structural study of irregular amino acid sequences in the heavy chain of bombyx mori silk fibroin. Biomacromolecules 2005;6(5):2563-2569.

(41) Tanaka K, Kajiyama N, Ishikura K, Waga S, Kikuchi A, Ohtomo K, et al. Determination of the site of disulphidelinkage between heavy and light chains of silk fibroin produced by Bombyx mori. Biochimica et Biophysica Acta (BBA) - Protein Structure and Molecular Enzymology 1999 6/15;1432(1):92-103.

(42) Kikuchi Y, Mori K, Suzuki S, Yamaguchi K, Mizuno S. Structure of the Bombyx mori fibroin light-chain-encoding gene: upstream sequence elements common to the light and heavy chain. Gene 1992 1/15;110(2):151-158.

(43) Um IC, Kweon H, Park YH, Hudson S. Structural characteristics and properties of the regenerated silk fibroin prepared from formic acid. International Journal of Biological Macromolecules 2001 8/20;29(2):91-97.

(44) Bini E, Knight DP, Kaplan DL. Mapping domain structures in silks from insects and spiders related to protein assembly. Journal of Molecular Biology 2004 1/2;335(1):27-40.

(45) Sukigara S, Gandhi M, Ayutsede J, Micklus M, Ko F. Regeneration of Bombyx mori silk by electrospinning. Part 2. Process optimization and empirical modeling using response surface methodology. Polymer 2004 5;45(11):3701-3708.

(46) Silva SS, Maniglio D, Motta A, Mano JF, Reis RL, Migliaresi C. Genipin-modified silk-fibroin nanometric nets. Macromol Biosci 2008 AUG 11;8(8):766-774.

(47) Lee K, Ki C, Baek D, Kang G, Ihm D, Park Y. Application of electrospun silk fibroin nanofibers as an immobilization support of enzyme. Fibers and Polymers 2005 09/09;6(3):181-185.

(48) Wenk E, Wandrey AJ, Merkle HP, Meinel L. Silk fibroin spheres as a platform for controlled drug delivery. Journal of Controlled Release 2008 11/24;132(1):26-34.

(49) Earland C, Raven Dj. A new solvent for silk. Nature 1954 09/04;174(4427):461-461.

(50) Weber K, Osborn M. The Reliability of Molecular Weight Determinations by Dodecyl Sulfate-Polyacrylamide Gel Electrophoresis. Journal of Biological Chemistry 1969 August 25;244(16):4406-4412.

(51) Rinaldi A, Gambuti A, Moine-Ledoux V, Moio L. Evaluation of the astringency of commercial tannins by means of the SDS–PAGE-based method. Food Chem 2010 10/15;122(4):951-956.

(52) Picariello G, De Martino A, Mamone G, Ferranti P, Addeo F, Faccia M, et al. Proteomic study of muscle sarcoplasmic proteins using AUT-PAGE/SDS-PAGE as two-dimensional gel electrophoresis. Journal of Chromatography B 2006 3/20;833(1):101-108.

(53) Swank MW, Kumar V, Zhao J, Wu G. A novel method of loading samples onto mini-gels for SDS-PAGE: Increased sensitivity and Western blots using sub-microgram quantities of protein. J Neurosci Methods 2006 12/15;158(2):224-233.

(54) Rouxel C, Daniel A, Jérôme M, Etienne M, Fleurence J. Species identification by SDS-PAGE of red algae used as seafood or a food ingredient. Food Chem 2001 8;74(3):349-353.

(55) Redaelli R, Morel M-, Autran J-, Pogna NE. Genetic analysis of low Mr glutenin subunits fractionated by two-dimensional electrophoresis (A-PAGE × SDS-PAGE). J Cereal Sci 1995 1;21(1):5-13.

(56) Monk BC. Electrotransfer of SDS-PAGE separated polypeptides to the DE81 blotting matrix and detection of Chlamydomonas antigens and glycoconjugates. J Immunol Methods 1987 1/26;96(1):19-28.

(57) Abraham G, Cooper PD. Anomalous behavior of certain poliovirus polypeptides during SDS-gel electrophoresis. Anal Biochem 1976 6;73(2):439-446.

(58) Shapiro AL, Viñuela E, V. Maizel J. Molecular weight estimation of polypeptide chains by electrophoresis in SDS-polyacrylamide gels. Biochem Biophys Res Commun 1967 9/7;28(5):815-820.

(59) Takasu Y, Yamada H, Tsubouchi K. Isolation of three main sericin components from the cocoon of the silkworm, Bombyx mori. Biosci Biotechnol Biochem 2002;66(12):2715-2718.

(60) Stryer L. Biochemistry. San Francisco: W. H. Freeman & Co; 1975.

(61) Banker GA, Cotman CW. Measurement of free electrophoretic mobility and retardation coefficient of protein-sodium dodecyl sulfate complexes by gel electrophoresis. Journal of Biological Chemistry 1972 September 25;247(18):5856-5861.

(62) Lehninger AL. Biochemistry : The molecular basis of cell structure and function. : Worth; 1970.

(63) Campbell MK. Biochemistry. Philadelphia: Saunders College Pub; 1991.

(64) Zor T, Selinger Z. Linearization of the bradford protein assay increases its sensitivity: theoretical and experimental studies. Anal Biochem 1996 5/1;236(2):302-308.

(65) Bradford MM. A rapid and sensitive method for the quantitation of microgram quantities of protein utilizing the principle of protein-dye binding. Anal Biochem 1976 5/7;72(1-2):248-254.

(66) Kruger NJ. The Bradford method for protein quantitation. 1996:15.

(67) Compton SJ, Jones CG. Mechanism of dye response and interference in the Bradford protein assay. Anal Biochem 1985 12;151(2):369-374.

(68) Congdon RW, Muth GW, Splittgerber AG. The Binding Interaction of Coomassie Blue with Proteins. Anal Biochem 1993 9;213(2):407-413.

(69) Enomoto N, Takata M, Kamada K, Hojo J, Fudouzi H. Novel processing for improving monodispersity of ceramic spheres and colloidal crystallinity. Science and Technology of Advanced Materials 2006 10;7(7):662-666.

(70) Stöber W, Fink A, Bohn E. Controlled growth of monodisperse silica spheres in the micron size range. Journal of Colloid and Interface Science, 1968 1;26(1):62-69.

(71) Kim JW, Kim LU, Kim CK. Size control of silica nanoparticles and their surface treatment for fabrication of dental nanocomposites. Biomacromolecules 2007 01/01;8(1):215-222.

(72) Kim U, Park J, Li C, Jin H, Valluzzi R, Kaplan DL. Structure and properties of silk hydrogels. Biomacromolecules 2004;5(3):786-792.

(73) Hou A, Chen H. Preparation and characterization of silk/silica hybrid biomaterials by sol–gel crosslinking process. Materials Science and Engineering: B 2010 3/15;167(2):124-128.

(74) Matsumoto A, Chen J, Collette AL, Kim UJ, Altman GH, Cebe P, et al. Mechanisms of silk fibroin sol-gel transitions. J Phys Chem B 2006;110(43):21630-21638.

(75) Iler RK. The chemistry of silica : solubility, polymerization, colloid and surface properties, and biochemistry. New York ; Chichester: Wiley; 1979.

(76) Greiner A, Wendorff JH. Electrospinning: A fascinating method for the preparation of ultrathin fibres. Angewandte Chemie-International Edition 2007;46(30):5670-5703.

(77) Bao Weiwei, Zhang Youzhu, Yin Guibo, Wu Jialin. The structure and property of the electrospinning silk fibroin. e-Polymers 2008 AUG 4:098.

(78) Soffer L, Wang X, Mang X, Kluge J, Dorfmann L, Kaplan DL, et al. Silk-based electrospun tubular scaffolds for tissue-engineered vascular grafts. J Biomater Sci -Polym Ed 2008;19(5):653-664.

(79) Meechaisue C, Wutticharoenmongkol P, Waraput R, Huangjing T, Ketbumrung N, Pavasant P, et al. Preparation of electrospun silk fibroin fiber mats as bone scaffolds: a preliminary study. Biomedical Materials 2007;2:181-188.

(80) Jeong L, Lee KY, Park WH. Effect of solvent on the characteristics of electrospin regenerated silk fibroin nanofibers. ASBM7: Advanced Biomaterials VII 2007;342-343:813-816.

(81) Amiraliyan N, Nouri M, Kish MH. Electrospinning of silk nanofibers. I. An investigation of nanofiber morphology and process optimization using response surface methodology. Fibers and Polymers 2009;10(2):167-176.

(82) Cao H, Chen X, Huang L, Shao Z. Electrospinning of reconstituted silk fiber from aqueous silk fibroin solution. Materials Science and Engineering: C 2009 8/31;29(7):2270-2274.

(83) Kang M, Chen P, Jin H. Preparation of multiwalled carbon nanotubes incorporated silk fibroin nanofibers by electrospinning. Current Applied Physics 2009 1;9(1, Supplement 1):S95-S97.

(84) Zhou J, Cao C, Ma X. A novel three-dimensional tubular scaffold prepared from silk fibroin by electrospinning. Int J Biol Macromol 2009 12/1;45(5):504-510.

(85) Alessandrino A, Marelli B, Arosio C, Fare S, Tanzi MC, Freddi G. Electrospun silk fibroin mats for tissue engineering. Engineering in Life Sciences 2008;8(3):219-225.

(86) Schiffman JD, Schauer CL. A review: Electrospinning of biopolymer nanofibers and their applications. Polym Rev 2008;48(2):317-352.

(87) Zhu Z, Ohgo K, Watanabe R, Takezawa T, Asakura T. Preparation and characterization of regenerated Bombyx mori silk fibroin fiber containing recombinant cell-adhesive proteins; nonwoven fiber and monofilament. J Appl Polym Sci 2008;109(5):2956-2963.

(88) Gandhi M, Yang HJ, Shor L, Ko F. Regeneration of bombyx mori silk by electrospinning: A comparative study of the biocompatibility of natural and synthetic polymers for tissue engineering applications. Journal of Biobased Materials and Bioenergy 2007;1(2):274-281.

(89) Peh RF, Suthikum V, Goh CH, Toh SL. Novel electrospun-knitted silk scaffolds for ligament tissue engineering. World Congress on Medical Physics and Biomedical Engineering 2006, Vol 14, Pts 1-6 2007;14:3287-3290.

(90) Deitzel JM, Kleinmeyer J, Harris D, Beck Tan NC. The effect of processing variables on the morphology of electrospun nanofibers and textiles. Polymer 2001 1;42(1):261-272.

(91) Zhang X, Reagan MR, Kaplan DL. Electrospun silk biomaterial scaffolds for regenerative medicine. Adv Drug Deliv Rev 2009 10/5;61(12):988-1006.

(92) Ioannis S. C. Novel nanocomposites and nanoceramics based on polymer nanofibers using electrospinning process—A review. J Mater Process Technol 2005 8/30;167(2-3):283-293.

(93) Taylor G. Electrically driven jets. Proceedings of the Royal Society of London A Mathematical and Physical Sciences 1969 December 02;313(1515):453-475.

(94) Chescoe D, Royal Microscopical Society (Great Britain). The operation of transmission and scanning electron microscopes. : Oxford University Press; 1990.

(95) Currell G. Analytical instrumentation : performance characteristics and quality. Chichester: Wiley; 2000.

(96) Ross SD. Inorganic infrared and Raman spectra. London: McGraw-Hill; 1972.

(97) Handbook of instrumental techniques for analytical chemistry. Upper Saddle River, N.J.; London: Prentice Hall PTR; Prentice-Hall International (UK); 1997.

(98) Lau WS. Infrared characterization for microelectronics. Singapore; River Edge, NJ: World Scientific; 1999.

(99) Tunc S, Maitz MF, Steiner G, Vázquez L, Pham MT, Salzer R. In situ conformational analysis of fibrinogen adsorbed on Si surfaces. Colloids and Surfaces B: Biointerfaces 2005 5/25;42(3-4):219-225.

(100) Costantino HR, Griebenow K, Mishra P, Langer R, Klibanov AM. Fourier-transform infrared spectroscopic investigation of protein stability in the lyophilized form. Biochimica et Biophysica Acta (BBA) - Protein Structure and Molecular Enzymology 1995 11/15;1253(1):69-74.

(101) Calloway D. Beer-Lambert Law. J Chem Educ 1997 07/01;74(7):744-null.

(102) Mansfield E, Kar A, Quinn TP, Hooker SA. Quartz crystal microbalances for microscale thermogravimetric analysis. Anal Chem 2010 12/15;82(24):9977-9982.

(103) Rana PK, Swain SK, Sahoo PK. Synthesis, characterization, and properties of intercalated poly(2-ethyl hexylacrylate)/silicate nanocomposites: XRD, TEM, IR, TGA, superabsorbency, pressure-sensitive adhesion, and biodegradation. J Appl Polym Sci 2004;93(3):1007-1011.

(104) Bom D, Andrews R, Jacques D, Anthony J, Chen B, Meier MS, et al. Thermogravimetric analysis of the oxidation of multiwalled carbon nanotubes: evidence for the role of defect sites in carbon nanotube chemistry. Nano Letters 2002 06/01;2(6):615-619.

(105) Serapiglia M, Cameron K, Stipanovic A, Smart L. High-resolution Thermogravimetric analysis for rapid characterization of biomass composition and selection of shrub willow varieties. Appl Biochem Biotechnol 2008;145(1):3-11.

(106) Restorative dental materials. 11th ed. St. Louis, Mo. ; London: Mosby; 2002.

(107) Biomaterials science : an introduction to materials in medicine. 2nd ed. Amsterdam ; London: Elsevier Academic Press; 2004.

(108) Phillips' science of dental materials. 11th ed. St. Louis, Mo. ; Great Britain: Saunders; 2003.

Chapter 3
BIOCHEMISTRY OF *BOMBYX MORI* SILK AND FRACTIONS

In this chapter, the structure of the *Bombyx mori* (BM) silk, isolation and biochemical confirmation of different BM silk fractions is described.

3.1- Introduction

Silks are biocompatible and biodegradable proteins (1) that are spun into fibres by silkworms and spiders at ambient conditions (2). Considering the natural sources of silk, there are many silk producing animals but most natural silk is usually obtained from silk worm *Bombyx mori* (BM) due to ease of domestication (1). BM silk is known to have unique properties required for biomedical applications, for example, biocompatibility for a range of applications, is nontoxic, non-irritant (3-5) and has excellent mechanical properties (6). Silk has an ability to perform under a wide range of conditions of humidity and temperature (7). Due to the unique properties of silk, there is an increasing interest in silk for biological applications (8) Silk has a

very long history in biomaterial applications as it has been used as a surgical suture material successfully for decades (9). More recently, silk has also been introduced into other biomaterials applications such as tissue engineering scaffolds (10-14) and drug delivery (15,16).

3.2- Structural Components of *Bombyx mori* silk

Structurally, *Bombyx mori* silk primarily consists of two protein components, sericin and fibroin (17,18) The structural components of BM silk are shown in Figure 3.1.

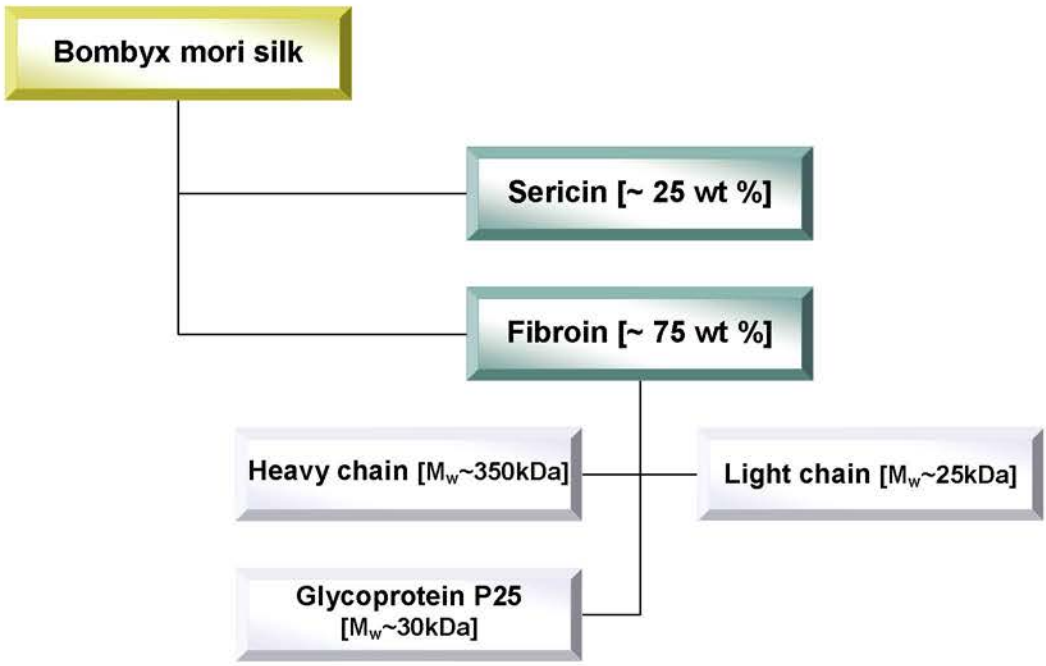

Figure 3.1: The structural components of *Bombyx mori* silk

3.2.1- Sericin

Glue like sericin is a glycoprotein of amorphous nature that accounts for approximately 20-30 wt % of BM silk (19), it has a Mw (10-300 kDa), is rich in serine and is secreted by a separate pair of glands in silk worms (20). Sericin plays a functional role, coating cocoons, adheres the twin filaments and cocoons (21) and protects silk from microbial degradation, animal digestion and environmental damages (22). It also has some surprising properties such as UV resistance, oxidation resistance and an ability to absorb and release moisture easily (20).

Sericin is composed of 18 different amino acids (20,23,24) where 80 % of them are contain serine (S), aspartic acid (D) and glycine (G) giving it good moisture absorbing properties (24). The relative composition of amino acids may vary to some extent depending on the source of silk and processing method (20,23-25) is compared in table 3.1.

Table 3.1: Proportions of different amino acids (%) in sericin (20,23-25)

Amino Acid	Zhang (20)	Wu (23)	Sothornvit (24)	Vaithanomsat (25)
Serine	28	27.3	32.74	31.99
Aspartic acid	17.97	18.80	17.64	15.74
Glycine	16.29	10.70	9.89	14.20
Glutamic acid	6.25	7.20	7.31	6.28
Arginine	3.52	4.90	6.16	4.29
Threonine	7.78	7.50	5.51	7.73
Tyrosine	2.87	4.60	4.63	3.01
Alanine	5.20	4.30	3.86	4.85
Valine	3.77	3.80	3.14	3.30
Lysine	1.21	2.10	3.05	4.17
Histidine	1.32	1.70	1.81	1.49
Leucine	1.21	1.70	1.44	0.96
Isoleucine	0.64	1.30	1.04	0.72
Phenylalanine	0.64	1.60	1.08	0.37
Proline	---	1.20	0.59	0.71
Methionine	0.79	0.50	0.11	---
Cystine	0.69	0.30	---	0.20

Sericin is soluble in water due to presence of high contents of hydrophilic amino acids (~ 70 %), with large sericin peptides being soluble in hot water while small peptides can be dissolved in cold water (20). Due to the proven role of sericin in inducing allergic and immunological reactions (26,27), it is crucial to remove all sericin from fibroin for any biological application. A variety of methods have been described in the literature to remove sericin (18,25,28,29).

3.2.2- Silk Fibroin (SF)

Silk fibroin is the structural protein of BM silk fibres and is insoluble in many solvents and water (4,17). Silk fibroin is a large protein macromolecule constructed of more than 5000 amino acids (30,31) and accounts for approximately 75 wt % of total BM silk (19). Silk fibroin comprises both a crystalline region (~ 66 %) and an amorphous

(~ 33 %) region (32). The crystalline portion of fibroin is composed of repeating units of the amino acids glycine (G), alanine (A), and serine (S), typically $[G\text{-}A\text{-}G\text{-}A\text{-}G\text{-}S]_n$ and forms a β-sheet structure in the spun fibres which is responsible for good mechanical properties (32,33). The amorphous region mainly consists of the amino acids phenylalanine (F), tyrosine (Y) having large side chains that is responsible for the hygroscopic properties of the material (34). The proportion of different amino acids in silk fibroin has been known for more than 60 years and their contribution in silk fibroin in shown in table 3.2

Table 3.2: Amino acid composition of BM silk fibroin (35)

Amino acid	**Abbreviation**	**Residue %** (35)
Glycine	G	44.7
Alanine	A	25.7
Serine	S	11.9
Tyrosine	Y	5.4
Valine	V	2.4
Aspartic acid	D	1.6
Phenylalanine	F	1.6
Glutamic acid	E	1.1
Threonine	T	1.0
Isoleucine	I	0.6
Leucine	L	0.5
Proline	P	0.5
Arginine	R	0.5
Lysine	K	0.4
Histidine	H	0.2

According to Pauling and Corey (36), the repetitions of amino acids result in β-sheet formation that assembles in an anti-parallel fashion. This type of β-sheet packing results in a polar-antiparallel pattern and is also found in crystalline poly -$[A\text{-}G]_n$ (37). The Pauling-Corey model was accepted until it was suggested by Takahashi et al; (38) that β-sheets can assemble in different ways, parallel or anti-parallel with polar or non-polar orientation of side chains, favouring antipolar-antiparallel orientation (Figure 3.2) with alanine and serine pointing up and down alternatively across a β-sheets. This type of orientation results in less regular packing of β-sheet than The Pauling-Corey model (31). More recently, it has been proposed that β-sheet in silk fibroin may be parallel instead of anti-parallel (31); all possible assembly orientations are show in Figure 3.2.

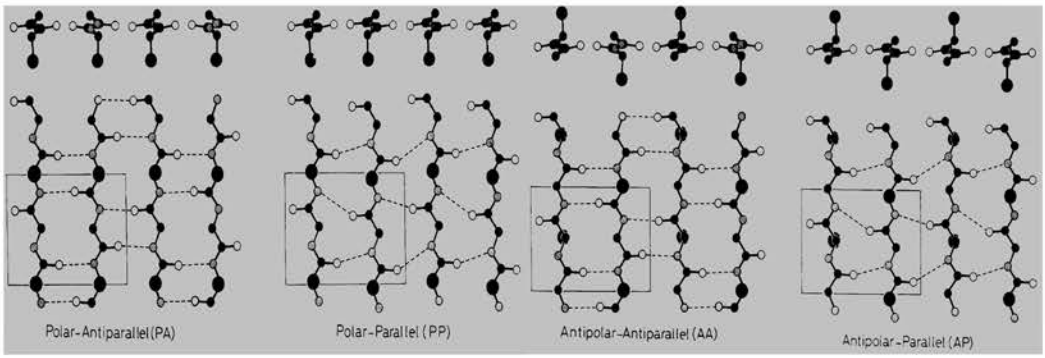

Figure 3.2: Schematic presentation of hydrogen bonding orientation and possible β-sheet models (40).

For a long time, Silk fibroin was considered a single large polypeptide; but Shimura *et al;* 1976 (39), demonstrated that silk fibroin was composed of at least two protein subunits. The BM silk fibroin components, heavy chain (H-fibroin) and light chain (L-fibroin) are attached to each other by disulphide bridges (Figure 3.3). Another component of silk fibroin is a glycoprotein P25 attached by non-covalent interactions to covalently bonded heavy and light chain complex (40,41).

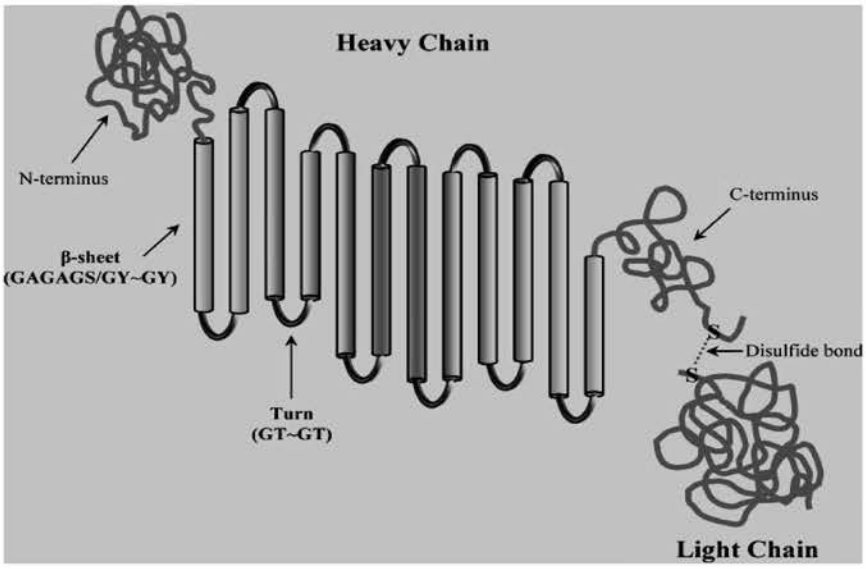

Figure 3.3: Schematic presentation of light and heavy fibroin assembly in BM silk. Redrawn from Ha et al. 2005 (48).

Quantitatively, H-fibroin, L-fibroin and P25 are present in the silk fibroin in a molar ratio of 6:6:1 respectively (40) suggesting that P25 ia attached to a set of six (H-L fibroin) dimers $[(H\text{-}L)_6.P25]$ (40). The glycoprotein P25 has Mw of ~ 30 kDa, secreted with H-fibroin (41) and considered important in maintaining the integrity of

silk fibres however its role in the formation of silk fibroin is not yet clear (40). Interestingly, in a few species of silk worms (*saturniidae* family), the L-chain and P25 are missing and silk is composed of H-chain only (42).

3.2.2.1- Heavy chain silk

The heavy chain (H-Fibroin) has a Mw ~350 kDa (43) and contributes about 46 % mole fraction of silk fibroin (40). The primary structure of H-fibroin is formed by highly repetitive sequence of GAGAGS, GAGAGY and GAGAGVGY amino acids (31,33,44), that are mainly hydrophobic (44). The secondary structure is mainly β-sheet with anti-parallel assembly (31,33) resulting in enhanced stability, crystallinity and mechanical properties in the spun fibres (45). Due to a very organised and unique conformation, H-chain has a very important structural role in BM silk (46). However, in addition to the highly organised domains there is also the presence of about eleven irregular sequences of about 31 amino acid residues however their role is not clearly understood (46).

3.2.2.2- Light chain silk

Light chain (L-Fibroin) has a Mw ~25 kDa (43) and contributes about 46 % mole fraction of silk fibroin (40). The L-fibroin shows comparatively more hydrophilic properties and is relatively elastic (40) with little or no crystallinity in its structure (30,43). Both types of fibroin are linked by a single disulfide bond between Cys-c20 of H-fibroin and Cys-172 of L-fibroin (43) and the absence of such a disulfide linkage results in reduced *in vivo* secretion of silk fibroin (47).

It is evident from the comparison in table 3.3 that heavy chain is quite similar in amino acid composition to the silk fibroin (table 3.3 above), however it is very different to the L-fibroin. The structural differences in both types affect the physical properties of these proteins that can be utilised to suit different biomedical applications. In this study, it is shown that both silk fractions can be mixed together in different proportions (described later) to adjust the final properties of such materials.

Very little has been reported on the solution studies and materials fabrication using the light and heavy silk fibroin separately. The L-fibroin separated in this study has the novel benefit that it can be manipulated for making biomaterials in its natural form.

Table:3.3: A comparison of heavy and light chain silk fibroin (30,48)			
		Heavy Chain	**Light chain**
Physical	Relative molar ratio (40)	1	1
	Crystallinity (43)	More	None
	Hydrophobicity (40)	More	Less
	M_w (49,50)	~ 350 kDa	~ 27kDa
Structural	Amino acids residues	5263 (48)	262 (30)
	Glycine	43 % (48)	9 % (30)
	Alanine	30 % (48)	14 % (30)
	Serine	12 % (48)	10 % (30)
In this study	Solubility in formic acid	Insoluble	Soluble
	Solubility in ionic solution	Soluble on heating	Soluble
	Gelation time (aqueous silk)	Rapid	Slow
	Physical appearance	Fibrous	Amorphous

As there is a significant difference in the molecular weight of both silk fractions that can be crucial to influence the material properties. Generally, higher molecular weight can result in improving the mechanical and physical properties (such as tensile strength, melt viscosity). Molecular weight of a polymer can also effect on the ability to crystallise, secondary interaction and hydrogen bonding (2). H-chain of silk fibroin having higher molecular weight (~ 350 kDa) (49,50), containing approximately 5263 amino acid residues (48). The long chain orientation of H-chain can facilitates more polymer chain entanglement, increase and viscosity and improving the mechanical properties (51). Considering the importance of molecular weight and material properties relationship, the biochemical characterisation for molecular weight of the natural *Bombyx mori* silk and its fractions is described in this chapter.

3.3- Materials and methods

Details of all materials used including protein standards and modifications (2.1.8), methods for de-gumming treatment (2.1.1), ionic silk solutions (2.1.2), dialysis methods (2.1.3), separation of silk fractions (2.1.4.1), sample preparation and method for gel electrophoresis (2.1.7.1), the Bradford assay (2.1.7.2) and gel staining methods (2.1.7.3).

3.4- Sample nomenclature

For ease of understanding and explanation, details of different samples, and their abbreviations are given in Table 3.4.

Table 3.4: The description of silk samples used in SDS-PAGE analysis

Sample	Silk type	De-gumming method	Solvent	Heat exposure (de-gumming + solvent)
A1	Total	$NaHCO_3$ – Me-SH	**$CaCl_2$ (A)**	60 minutes/100 ℃+30 minutes/85 ℃
A2	Total	$NaHCO_3$ + Me-SH	**$CaCl_2$ (A)**	60 minutes/100 ℃+30 minutes/85 ℃
A3	Total	Urea– Me-SH	**$CaCl_2$ (A)**	20 minutes/80 ℃+30 minutes/85 ℃
A4	Total	Urea +Me-SH	**$CaCl_2$ (A)**	20 minutes/80 ℃+30 minutes/85 ℃
A5	Total	$NaHCO_3$ (5 minutes)	**$CaCl_2$ (A)**	10minutes/100 ℃+30 minutes/85 ℃
B1	Total	$NaHCO_3$ – Me-SH	**Li-Br (B)**	60 minutes/100 ℃+180 minutes/65 ℃
B2	Total	$NaHCO_3$ + Me-SH	**Li-Br (B)**	60 minutes/100 ℃+180 minutes/65 ℃
B3	Total	Urea– Me-SH	**Li-Br (B)**	20 minutes/80 ℃+180 minutes/65 ℃
B4	Total	Urea +Me-SH	**Li-Br (B)**	20 minutes/80 ℃+180 minutes/65 ℃
B5	Total	$NaHCO_3$ (5 minutes)	**Li-Br (B)**	10minutes/100 ℃+180 minutes/65 ℃
C1	Total	$NaHCO_3$ – Me-SH	**LiSCN (C)**	60 minutes/100 ℃+ 0 minutes
CD1	Soluble	$NaHCO_3$ – Me-SH	**LiSCN (C)**	60 minutes/100 ℃+ 0 minutes
CUD1	Insoluble	$NaHCO_3$ – Me-SH	**LiSCN (C)**	60 minutes/100 ℃+ 0 minutes
C2	Total	$NaHCO_3$ + Me-SH	**LiSCN (C)**	60 minutes/100 ℃+ 0 minutes
CD2	Soluble	$NaHCO_3$ + Me-SH	**LiSCN (C)**	60 minutes/100 ℃+ 0 minutes
CUD2	Insoluble	$NaHCO_3$ + Me-SH	**LiSCN (C)**	60 minutes/100 ℃+ 0 minutes
C3	Total	Urea– Me-SH	**LiSCN (C)**	20 minutes/80 ℃+0 minutes
CD3	Soluble	Urea– Me-SH	**LiSCN (C)**	20 minutes/80 ℃+0 minutes
CUD3	Insoluble	Urea– Me-SH	**LiSCN (C)**	20 minutes/80 ℃+0 minutes
C4	Total	Urea +Me-SH	**LiSCN (C)**	20 minutes/80 ℃+0 minutes
CD4	Soluble	Urea +Me-SH	**LiSCN (C)**	20 minutes/80 ℃+0 minutes
CUD4	Insoluble	Urea +Me-SH	**LiSCN (C)**	20 minutes/80 ℃+0 minutes
C5	Total	$NaHCO_3$ (5 minutes)	**LiSCN (C)**	10 minutes/80 ℃+0 minutes
CD5	Soluble	$NaHCO_3$ (5 minutes)	**LiSCN (C)**	20 minutes/80 ℃+0 minutes
CUD5	Insoluble	$NaHCO_3$ (5 minutes)	**LiSCN (C)**	20 minutes/80 ℃+0 minutes
M	Ladder (17-460 kDa)			

3.5- Results and discussion

A number of studies (40,41,43) have described the functional correlation of silk components and suggested that L-fibroin and H-fibroin have different structural and physical properties that could be attractive for biomedical applications. For example, silk fractions have been used for making tissue engineering scaffolds and were compared with silk fibroin (52). The major problem in using H and L-fibroin is their separation and purification from silk cocoons without protein degradation. The processing of BM silk for any biomedical application starts with the de-gumming treatment to remove sericin. There are established methods (18,28,29), however they all involve harsh conditions of temperature and pH that degrade fibroin structure (29) and are discussed in section 3.5.2.

In vivo, silk fibroin is present in water soluble conformations and converts to a very tough, insoluble and well organised structural formation on spinning and dehydration (53,54). The exact mechanism of silk fibroin assembly in animals and how they convert water soluble protein to very tough and insoluble fibres by spinning is not well understood (54), however it appears to be an irreversible process thus making separation of fibroin fractions a challenging task. Different approaches such as column chromatography (40,52,55) and genetic engineering (56,57) have been used to separate H and L-fibroins. However the silk fibroin was being derived directly from the living silk worm by dissecting glands and involved the regeneration of silk fibroin. The study described below has provided a novel method of separating light and heavy chains from spun silk fibres that is simple to use and very cost effective. In this way, the use of natural silk components could be possible for the gelation biomaterials with less harsh processing measures. In order to confirm the success of the procedure biochemical analysis was carried on total BM silk and the separated fractions (H and L-fibroin) that has been pre-treated by a range of processing conditions as described in Table 3.4.

3.5.1- Molecular weight determination of BM silk, light and heavy fibroin

In a recent study (29), the Ajisawa method of dissolving silk was shown to cause degradation of BM silk fibroin while lithium thiocynate (LiSCN) was suggested to not cause any harm during the dissolution of BM silk and this solvent was therefore used mainly for molecular weight determination in this study. As the regenerated aqueous silk solutions of intact silk fibroin gel a lot more quickly than degraded fibroin (29). It was observed that LiSCN-silk solutions were gelled spontaneously

during dialysis indicating less damage to proteins compared to LiBr and Ajisawa reagents. The rapid gelation even at (~ 1 wt %) concentration made handling of LiSCN-silk solutions for gel electrophoresis a challenging task. To overcome this problem, LiSCN-silk solutions were dialysed against 1% SDS solutions. Due to strong denaturant nature of SDS (58) gelation times were prolonged sufficiently to allow for electrophoretic separation. However, the ingress of ions into the dialysing silk solutions resulted in imbalance of SDS content between samples and the protein standards that interfered with the gel electrophoresis process (Figure 3.4).

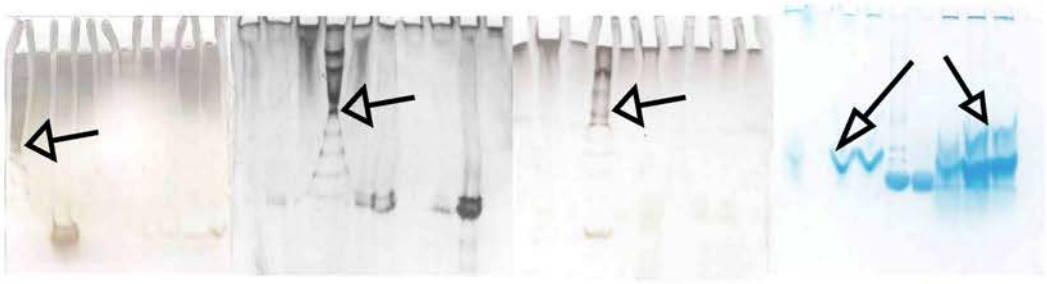

Figure 3.4: The effect of extra SDS content in silk samples as result of dialysing against 1 % SDS solutions. Defects are indicated with black arrows.

The modifications were made to the procedure with the silk fractions being stored in LiSCN and dialysed just before loading on the gels. In addition, the sample buffer was modified by addition of 8M urea, as 8M urea in the presence of SDS has been found to improve the resolutions and facilitates dissociation of protein aggregates (59-62).

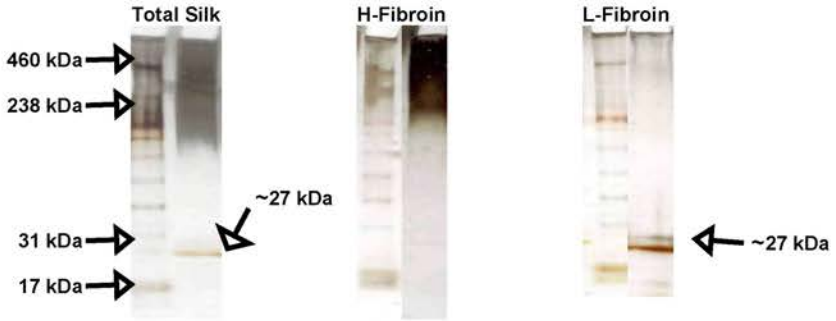

Figure 3.5: Molecular weight determination of BM silk and its fractions using SDS-PAGE analysis

In total silk fibroin (C4), a sharp band is observed at around 27 kDa (Figure 3.5) and a diffuse band (171-460 kDa) corresponding to the heavy and light chain fibroin of

total BM silk respectively. In the formic acid insoluble silk fraction (CUD4), only the top band appeared suggesting it to be from the heavy chain of BM silk. However the width (area) of band was reduced (compared to H-fibroin band in total silk), suggesting that some of the degraded silk peptides might have washed away during formic acid treatment of silk. The formic acid soluble fraction of silk (CD4), showed a complete absence of the top band (indicating that heavy chain is missing) and a produced a sharp band exactly in the light chain area of total silk (~27 kDa). These results strongly indicated that the soluble fraction is the light chain of BM silk.

In a previous study (29), sharp bands at 25 and 350 kDa representing heavy and light chain of silk fibroin were obtained using silk fibroin directly from silk worm glands. These results (Figure 3.5) suggested the the breakdown of silk fibroin (reflected in H-fibroin as well) into different size polypeptides is a result of heat treatment during processing of silk cocoons. These electrophoresis analyses were highly reproducible (for 5 repeats) and clearly demonstrated that the separated fractions are the heavy and light chain fibroin of silk.

3.5.2- Effects of de-gumming methods

In order to study the effects of different de-gumming methods (described earlier in chapter 2), silk of each type was solubilised in the LiSCN at room temperature (no heat treatment to de-gummed silk fibroin/fractions) to obtain clear silk solutions. The temperature and duration of heating used for de-gumming silk cocoons appeared to degrade fibroin into polypeptides of different sizes resulting in smear spreading in wide area of gel. Similar effects were observed in case of H-fibroin while little effect was observed on L-fibroin degradation (Figure 3.6).

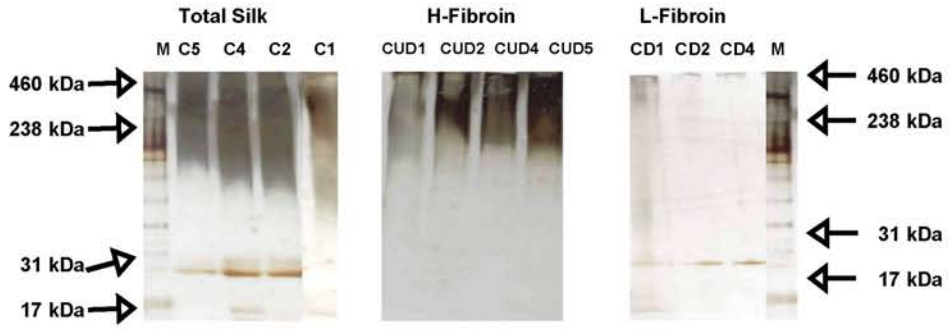

Figure 3.6: Molecular weight determination of BM silk and its fractions manipulated after different de-gumming treatments

Most protein degradation was observed in silk solutions derived from de-gumming method 1 (2 x 30 minute boiling), the band representing the heavy chain in total silk was degraded to produce a continuous smear throughout and almost merge with the light chain band (Figure 3.6, C1). There was no distinct band observed for L-fibroin. Either it was not cleaved as β-mercaptoethanol was not used in this particular de-gumming or was degraded as a result of boiling. A sharp band for L-fibroin was observed for sample C2 and C4 where β-mercaptoethanol was used and for C5 where only 10 minutes of heating was used for de-gumming corresponding to the heat treatment. These results are very similar to the results reported by Yamada et al; (29) and were used to compare the effect of de-gumming methods on silk fractions. The heavy chain performed very similar to silk fibroin (Figure 3.6), as it is structurally very similar to silk fibroin in amino acid composition (table 3.2 and 3.3). However, the width of the bands in general reduced suggesting loss of some broken polypeptides during washing of H-fibroin. Similar effects were observed in the case of L-fibroin as in CD1, a light protein smear was observed throughout suggesting broken peptides as result of heat and the light chain band in the ~ 27 kDa area was faint. In the CD4 sample, a sharper clear band for light chain was observed which could be related to the comparatively less harsh de-gumming treatment used to generate this sample.

3.5.3- Effects of ionic solutions on silk fibroin

The effect of ionic solvent on silk fibroin structure and integrity has been studied using a standard (method 4) de-gumming method (section 2.1.1). In C4 silk solution where no heating was involved and two bands for light and heavy chain were observed (Figure 3.7). The excessive break down of silk proteins were observe for samples A4 and B4 increasing the width of the protein smear on the gel.

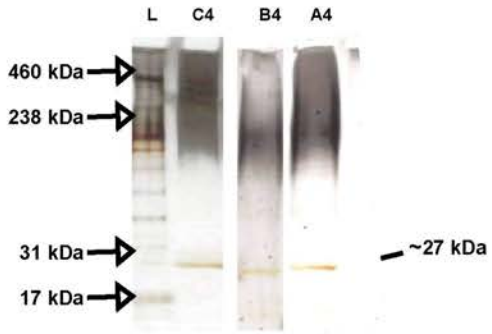

Figure 3.7: Molecular weight determination of BM silk dissolved in three different solvent systems. I)- A4 (in $CaCl_2$:EtOH:H_2O), ii)- B4 (in LiBr), iii)- C4 (in LiSCN).

It can be concluded from the discussion above that heating the silk fibroin at any stage of processing is crucial and may result in the breakdown of proteins. it also invalidated the claim (63) that de-gumming treatment does not affect silk structure. In sample C4, silk fibroin was dissolved at room temperate, however breakdown to give peptides is seen probably due to fibroin being exposed to high temperatures for de-gumming or to remove silk worms by the supplier. The sharp bands representing heavy and light fibroin were only obtained when silk fibroin directly from silk gland prior to contamination of sericin was used (29).

In a recent study (52), contrary results were reported where the authors obtained sharp bands (suggesting no protein degradation) for heavy and light fibroins using silk cocoons even after boiling for 15 minutes for de-gumming and heating at 80 ℃ to dissolve silk in Ajisawa reagent and claimed to recover intact silk proteins. In that particular study, the authors agreed that high extraction temperature degrades silk proteins specially H-fibroin, however there was no explanation given about how they prevented protein degradation and yet managed to get sharp bands even after treating silk at harsh temperatures for processing. As they started from silk cocoons (not silk fibroin from silk worm gland), so heat treatments used previously by silk worm farmers (e.g. eradication of silk worms by steam, heat drying) must theoretically result in silk protein degradation. Yamada *et al*, (29) reported slight degradation using fresh cocoons compared to native silk fibroin and this degradation increased depending on the severity and duration of heat treatment. These findings suggest that silk proteins are very sensitive and degrade slightly upon conversion of silk fibroin to fresh cocoon and may degrade further from fresh cocoons to dry cocoons. In contrast, Wadbua *et al*, (52) heated silk for de-gumming and dissolving in ionic solution and still they manage to get sharp bands for light and heavy chain silk during SDS-PAGE however no justification has been provided for their divergent results.

There are also divergent results reported regarding the use of lithium thiocynate solvent (LiSCN) with either the appearance of two distinct bands corresponding to light and heavy chain (29) or with a missing band for heavy chain in a later study by Wadbua *et al*, (52) using similar de-gumming conditions. Wadbua *et al*, considered the absence of the heavy chain band due to incomplete dissolution in a set time. However, LiSCN has been used widely (29,64,65) to dissolve silk fibroin and was also used in the study presented in this thesis. Initially, results obtained were similar to Wadbua *et al*; (absence of H-fibroin) band Figure 3.8); however this issue was resolved by a simple modification in sample buffer (section 2.1.8).

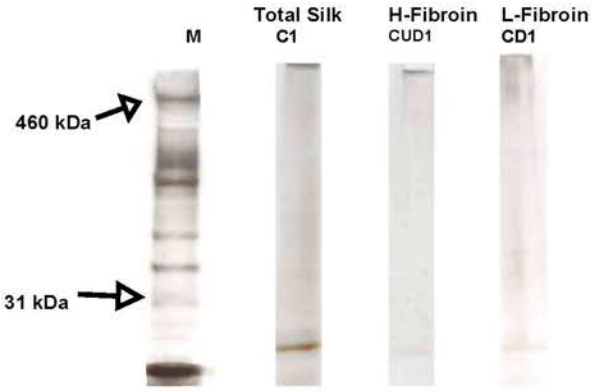

Figure 3.8: Molecular weight determination of BM silk and its fractions dissolved in LiSCN, absence of H-fibroin band while using un-modified sample buffer and its appearance when 8M urea modified buffer used (refer to Figure 3.6 for a clear appearance of H-fibroin band)

Aqueous silk solutions dialysed from LiSCN have a strong tendency to gel rapidly as a result of least damage to silk fibroin (29) and need a stronger denaturing sample buffer to prevent any folding or aggregation of protein. Modification of sample buffer by adding more SDS and 8 M urea denatures silk proteins completely and prevents any folding and expression of all silk peptides upon SDS-PAGE analysis (Figure 3.6 and 3.8). In the absence of the strong protein denaturants, silk proteins especially the H-fibroin ended in the formation of inclusion bodies thus not appearing on the gel.

3.6- Summary

This chapter has described the development of a simple, easy and straightforward method of separating well known BM silk fractions. Both fractions have different physical and structural properties from each other and silk fibroin and have been characterised for molecular weights using the SDS-PAGE analysis. It can be concluded from these experiments that the fractions separated as formic acid soluble and insoluble are light chain and heavy chain respectively and this method can be used on a large scale to derive large amounts of the different silk fractions using BM cocoons and does not involve any complex techniques or equipment. Silk fibroin is very sensitive to heat and may break down or degrade into smaller peptides. The H-fibroin that is structurally (amino acid content) very similar to silk fibroin demonstrated a similar degradation behaviour in response to heat applied during processing. Additionally, H-fibroin showed a stronger tendency to gel in aqueous solutions and needed a modified buffer to denature the protein.

There are a wide range of applications of silk fibroin in the biomedical industry however there are a very few applications of the silk fractions practically, as their separation without degradation of protein always remained a challenging task. For example, light chain separated by column chromatography and genetically modified has been used recently (56) and been found to be successful in facilitating cartilage tissue formation. The structural differences of L-fibroin (less crystallinity, amorphous region, different amino acid composition) can be beneficial for certain applications compared to silk fibroin, however further work is required to investigate these claims. Further work is required for its purification and detailed characterisation before practical applications can be developed.

With the development of this novel method of separating silk fractions, it can be hoped that there will be a sharp increase in practical applications of silk fractions in the biomedical industry. Additionally, both fractions and silk fibroin can be manipulated in different proportions to control the final properties of the silk based material more precisely. Another significant benefit is that one fraction (light chain) is soluble (up to 33 wt%) in formic acid for electrospinning and can be used to make a range of biomaterials without any need for silk regeneration, hence preventing any damage to silk protein that might be caused by regeneration procedures (i.e. chemicals, heating, freeze dry). The BM silk and separated fractions were used for making silica containing nano-composites using two different fabrication routes and are discussed in next chapters.

3.7- Referentes

(1) Numata K, Kaplan DL. Silk-based delivery systems of bioactive molecules. Adv Drug Deliv Rev 2010 12/30;62(15):1497-1508.

(2) Biomaterials science : an introduction to materials in medicine. 2nd ed. Amsterdam ; London: Elsevier Academic Press; 2004.

(3) Zuo B, Dai L, Wu Z. Analysis of structure and properties of biodegradable regenerated silk fibroin fibers. J Mater Sci 2006 06/01;41(11):3357-3361.

(4) Xu Y, Shao H, Zhang Y, Hu X. Studies on spinning and rheological behaviors of regenerated silk fibroin/N-methylmorpholine-N-oxide·H2O solutions. J Mater Sci 2005 10/07;40(20):5355-5358.

(5) Kim K, Jeong L, Park H, Shin S, Park W, Lee S, et al. Biological efficacy of silk fibroin nanofiber membranes for guided bone regeneration. Journal of Biotechnology, 2005 11/21;120(3):327-339.

(6) Gosline J, Guerette P, Ortlepp C, Savage K. The mechanical design of spider silks: from fibroin sequence to mechanical function. J Exp Biol 1999;202(23):3295-3303.

(7) Sheu H, Phyu KW, Jean Y, Chiang Y, Tso I, Wu H, et al. Lattice deformation and thermal stability of crystals in spider silk. International Journal of Biological Macromolecules 2004 10;34(5):267-273.

(8) Bogush V, Sokolova O, Davydova L, Klinov D, Sidoruk K, Esipova N, et al. A novel model system for design of biomaterials based on recombinant analogs of spider silk proteins. Journal of Neuroimmune Pharmacology 2009 03/01;4(1):17-27.

(9) Furuzono T, Ishihara K, Nakabayashi N, Tamada Y. Chemical modification of silk fibroin with 2-methacryloyloxyethyl phosphorylcholine. II. Graft-polymerization onto fabric through 2-methacryloyloxyethyl isocyanate and interaction between fabric and platelets. Biomaterials 2000 2;21(4):327-333.

(10) Gellynck K, Verdonk PCM, Van Nimmen E, Almqvist KF, Gheysens T, Schoukens G, et al. Silkworm and spider silk scaffolds for chondrocyte support. Journal of Materials Science-Materials in Medicine 2008;19(11):3399-3409.

(11) Kim HJ, Kim U, Kim HS, Li C, Wada M, Leisk GG, et al. Bone tissue engineering with premineralized silk scaffolds. Bone 2008 6;42(6):1226-1234.

(12) Peh RF, Suthikum V, Goh CH, Toh SL. Novel electrospun-knitted silk scaffolds for ligament tissue engineering. World Congress on Medical Physics and Biomedical Engineering 2006, Vol 14, Pts 1-6 2007;14:3287-3290.

(13) Nair LS, Bhattacharyya S, Laurencin CT. Development of novel tissue engineering scaffolds via electrospinning. Expert Opin Biol Ther 2004 MAY;4(5):659-668.

(14) Damrongrungruang T, Siritapetawee M, Kamanarong K, Limmonthon S, Rattanathongkom A, Maensiri S, et al. Fabrication of electrospun thai silk fibroin nanofiber and its effect on human gingival fibroblast: A preliminary study. Journal of Oral Tissue Engineering 2007;5(1):1-6.

(15) Wenk E, Wandrey AJ, Merkle HP, Meinel L. Silk fibroin spheres as a platform for controlled drug delivery. Journal of Controlled Release 2008 11/24;132(1):26-34.

(16) Li W, Mauck RL, Tuan RS. Electrospun nanofibrous scaffolds: production, characterization, and applications for tissue engineering and drug delivery. Journal of Biomedical Nanotechnology 2005;1:259-275(17).

(17) Hardy JG, Römer LM, Scheibel TR. Polymeric materials based on silk proteins. Polymer, 2008 9/23;49(20):4309-4327.

(18) Kodama K. The preparation and physico-chemical properties of sericin. Biochem J 1926 , 1926;20(6):1208-1222.

(19) Somashekarappa H, Annadurai V, Sangappa, Subramanya G, Somashekar R. Structure–property relation in varieties of acid dye processed silk fibers. Materials Letters 2002 4;53(6):415-420.

(20) Zhang Y. Applications of natural silk protein sericin in biomaterials. Biotechnol Adv 2002 5;20(2):91-100.

(21) Kaplan D, Adams WW, Farmer B, Viney C. Silk - biology, structure, properties, and genetics. Silk Polymers 1994;544:2-16.

(22) Hakimi O, Knight DP, Vollrath F, Vadgama P. Spider and mulberry silkworm silks as compatible biomaterials. Composites Part B-Engineering 2007;38(3):324-337.

(23) Wu JH. Preparation and characterization of sericin powder extracted from silk industry wastewater. Food Chem 2007;103(4):1255.

(24) Sothornvit R. Extracted sericin from silk waste for film formation. Songklanakarin Journal of Science and Technology 2010;32(1):17-22.

(25) Vaithanomsat P. Sericin separation from silk degumming wastewater. Separation and purification technology 2008;59(2):129.

(26) Dewair M, Baur X, Ziegler K. Use of immunoblot technique for detection of human IgE and IgG antibodies to individual silk proteins, Journal of Allergy and Clinical Immunology 1985 10;76(4):537-542.

(27) Panilaitis B, Altman GH, Chen J, Jin H, Karageorgiou V, Kaplan DL. Macrophage responses to silk. Biomaterials 2003 8;24(18):3079-3085.

(28) Takasu Y. Isolation of three main sericin components from the cocoon of the silkworm, Bombyx mori. Biosci Biotechnol Biochem 2002;66(12):2715.

(29) Yamada H, Nakao H, Takasu Y, Tsubouchi K. Preparation of undegraded native molecular fibroin solution from silkworm cocoons. Materials Science and Engineering: C 2001 8/15;14(1-2):41-46.

(30) Yamaguchi K, Kikuchi Y, Takagi T, Kikuchi A, Oyama F, Shimura K, et al. Primary structure of the silk fibroin light chain determined by cDNA sequencing and peptide analysis. Journal of Molecular Biology 1989 11/5;210(1):127-139.

(31) Zhou C, Confalonieri F, Jacquet M, Perasso R, Li Z, Janin J. Silk fibroin: Structural implications of a remarkable amino acid sequence. Proteins: Structure, Function, and Genetics 2001;44(2):119-122.

(32) Zhang Y, Shen W, Xiang R, Zhuge L, Gao W, Wang W. Formation of silk fibroin nanoparticles in water-miscible organic solvent and their characterization. Journal of Nanoparticle Research 2007 10/01;9(5):885-900.

(33) Mita K. Highly repetitive structure and its organization of the silk fibroin gene. J Mol Evol 1994;38(6):583.

(34) Zhang Y, Lim CT, Ramakrishna S, Huang ZM. Recent development of polymer nanofibers for biomedical and biotechnological applications. J Mater Sci Mater Med 2005;16(10):933-946.

(35) Neurath H. The proteins : chemistry, biological activity, and methods. New York: Academic Press; 1953.

(36) Marsh RE, Corey RB, Pauling L. An investigation of the structure of silk fibroin. Biochimica et Biophysica Acta 1955;16:1-34.

(37) Lotz B, Colonna Cesari F. The chemical structure and the crystalline structures of Bombyx mori silk fibroin. Biochimie 1979 4/30;61(2):205-214.

(38) Takahashi Y. Structure refinement and diffuse streak scattering of silk (Bombyx mori). Int J Biol Macromol 1999;24(2-3):127.

(39) Shimura K, Kikuchi A, Ohtomo K, Katagata Y, Hyodo A. Studies on silk fibroin of bombyx mori. i. fractionation of fibroin prepared from the posterior silk gland. J Biochem 1976;80(4):693-702.

(40) Inoue S, Tanaka K, Arisaka F, Kimura S, Ohtomo K, Mizuno S. Silk fibroin of Bombyx mori Is secreted, assembling a high molecular mass elementary unit consisting of H-chain, L-chain, and P25, with a 6:6:1 molar ratio. J Biol Chem 2000 December 15, 2000;275(51):40517-40528.

(41) Tanaka K, Inoue S, Mizuno S. Hydrophobic interaction of P25, containing Asn-linked oligosaccharide chains, with the H-L complex of silk fibroin produced by Bombyx mori. Insect Biochemistry and Molecular Biology 1999 3;29(3):269-276.

(42) Sehnal F, Zurovec M. Construction of silk fiber core in Lepidoptera. Biomacromolecules 2004 05/01;5(3):666-674.

(43) Tanaka K, Kajiyama N, Ishikura K, Waga S, Kikuchi A, Ohtomo K, et al. Determination of the site of disulfide linkage between heavy and light chains of silk fibroin produced by Bombyx mori. Biochimica et Biophysica Acta (BBA) - Protein Structure and Molecular Enzymology 1999 6/15;1432(1):92-103.

(44) Garel J. The silkworm, a model for molecular and cellular biologists. Trends Biochem Sci 1982 3;7(3):105-108.

(45) Cunniff PM, Fossey SA, Auerbach MA, Song JW. Mechanical-properties of major ampulate gland silk fibers extracted from nephila-clavipes spiders. Silk Polymers 1994;544:234-251.

(46) Ha S, Gracz HS, Tonelli AE, Hudson SM. Structural Study of Irregular Amino Acid Sequences in the Heavy Chain of Bombyx mori Silk Fibroin. Biomacromolecules 2005 09/01;6(5):2563-2569.

(47) Mori K, Tanaka K, Kikuchi Y, Waga M, Waga S, Mizuno S. Production of a chimeric fibroin light-chain polypeptide in a fibroin secretion-deficient naked pupa mutant of the silkworm Bombyx mori. J Mol Biol 1995 8/11;251(2):217-228.

(48) Wang SP, Guo TQ, Guo XY, Huang JT, Lu CD. In vivo analysis of fibroin heavy chain signal peptide of silkworm Bombyx mori using recombinant baculovirus as vector. Biochemical and Biophysical Research Communications 2006 3/24;341(4):1203-1210.

(49) Zhou CZ. Fine organization of Bombyx mori fibroin heavy chain gene. Nucleic Acids Res 2000;28(12):2413.

(50) Armato U. Method for the preparation of a non-woven silk fibroin fabrics. 2004(20040097709).

(51) Sperling LH. Introduction to physical polymer science. 2nd ed.: Wiley; 1992.

(52) Wadbua P, Promdonkoy B, Maensiri S, Siri S. Different properties of electrospun fibrous scaffolds of separated heavy-chain and light-chain fibroins of Bombyx mori. Int J Biol Macromol 2010 6/1;46(5):493-501.

(53) Bini E, Knight DP, Kaplan DL. Mapping domain structures in silks from insects and spiders related to protein assembly. Journal of Molecular Biology 2004 1/2;335(1):27-40.

(54) Foo CW, Bini E, Hensman J, Knight DP, Lewis RV, Kaplan DL. Role of pH and charge on silk protein assembly in insects and spiders. Appl Phys A 2006 02/01;82(2):223-233.

(55) Oyama F. Studies on immunological properties of fibroin heavy and light chains. The journal of biochemistry 1984;96(6):1689.

(56) Kambe Y. Effects of RGDS sequence genetically interfused in the silk fibroin light chain protein on chondrocyte adhesion and cartilage synthesis. Biomaterials 2010.

(57) Kojima K, Kuwana Y, Sezutsu H, Kobayashi I, Uchino K, Tamura T, et al. A new method for the modification of fibroin heavy chain protein in the transgenic silkworm. Biosci Biotechnol Biochem 2007;71(12):2943-2951.

(58) Takagi T, Kubo K. Sodium dodecyl sulfate-protein polypeptide complexes in 8 M urea with special reference to sodium dodecyl sulfate-polyacrylamide gel electrophoresis. Biochimica et Biophysica Acta (BBA) - Protein Structure 1979 5/23;578(1):68-75.

(59) Abraham G, Cooper PD. Anomalous behavior of certain poliovirus polypeptides during SDS-gel electrophoresis. Anal Biochem 1976 6;73(2):439-446.

(60) Swank RT. Molecular weight analysis of oligopeptides by electrophoresis in polyacrylamide gel with sodium dodecyl sulfate. Anal Biochem 1971;39(2):462.

(61) Downer NW, Robinson NC. Characterization of a seventh different subunit of beef heart cytochrome c oxidase. Similarities between the beef heart enzyme and that from other species. Biochemistry (N Y) 1976;15(13):2930-2936.

(62) Bachrach HL. Animal picornaviruses with a single major species of capsid protein. Biochem Biophys Res Commun 1973;55(1):141.

(63) Ayutsede J, Gandhi M, Sukigara S, Micklus M, Chen H, Ko F. Regeneration of Bombyx mori silk by electrospinning. Part 3: characterization of electrospun nonwoven mat. Polymer 2005 2/14;46(5):1625-1634.

(64) Bhat NV. Investigation of the structure of silk film regenerated with lithium thiocyanate solution. Journal of polymer science. Polymer Chemistry ed. 1983;21(5):1273.

(65) Tao W, Li M, Zhao C. Structure and properties of regenerated Antheraea pernyi silk fibroin in aqueous solution. International Journal of Biological Macromolecules 2007 4/10;40(5):472-478.

Chapter 4
ELECTROSPINNING FOR MATERIAL FABRICATION

In order to make silk based nano composite materials, two different fabrication methods (electrospinning and gelation) were used during this study. Both methods produced nanocomposites with entirely different morphology and mechanical properties. This chapter describes the fabrication of nano-composite materials using the electrospinning technique, effects of post treatment on conformational changes of the protein, silicification of electrospun mats and their detailed characterisation.

4.1- Introduction

Polymer nano-fibres remain an important division of nano-biomaterials due to a wide range of applications in biotechnology. The fabrication of nano-fibres has attracted a lot of research because of their very high surface area that is desirable for many biomedical applications (1). In order to fabricate nano fibres, different techniques

have been used for example, phase separation (2-4), nano-fibre seeding (5) template synthesis (6,7), self-assembly (8,9) and electrospinning (10-18). Amongst all of these techniques, electrospinning is a resourceful technique and has gained popularity in recent years (Figure 2.25) due to its crucial benefits such as ability to form continuous fibres at a nano and/or micron scale, ease of use and cost effectiveness (1). Additionally, electrospinning can be used for making polymer as well as composite fibres by blending with additives such as particles, antimicrobials or enzymes to get the desired properties (17).

4.1.1- Advantages of using electrospun nano fibres for biomedical applications

Electrospun fibres are collected in the form of porous non-woven mats in three dimensional format (19) that can provide an architecture similar to naturally occurring protein fibrils in the extracellular matrix (20,21). Nano-fibres provide high surface area to volume ratio exposing more surface area for cellular interaction (19), protein absorption and binding sites to cell receptors (22). The adsorbed proteins can alter their conformation enhancing further exposure of binding sites that is an enormous edge over micro-scale materials available for tissue regeneration (22)
Nano-fibres can facilitate packing of maximum volume fraction by controlling fibres alignment and orientation hence improving the material strength (19). The desired scaffold properties such as surface morphology, porosity and geometry can be tailored by varying different electrospinning parameters (23) and can be functionalized for certain applications, for example, bioactive agents for biomedical applications. These unique nano-structure features have made electro-spun fibres an excellent candidate for a variety of biomedical applications, e.g. topical or intravenous drug delivery, wound dressings and scaffolding materials for tissue engineering.

4.1.2- Limitations of electrospinning

In the recent years, electrospinning has become increasingly popular however still there are many shortcomings of this technique. It can produce limited three dimensional structures and cannot be used for making micro-fibres (1). The fibre morphology can be altered however not very well controlled and is further complicated by the involvement of multiple electrospinning parameters. It has low

fibre production efficiency (24) and usually takes many hours to produce a little quantity.

4.1.3- Electrospinning of silk polymers

Due to the polymeric nature of the natural silk, many researchers (10,12,13,15,16,18,25-34) have used this versatile technique for making silk based materials for biomedical applications. The procedure of electrospinning and different factors affecting the fibre's morphology has been described in section 2.4. The most crucial parameters for silk electrospinning are the viscosity of the electrospinning dope, voltage supplied, collection plate distance and nature of solvent. For example, very low viscosity solutions may result in droplet formation with or without fibres and in contrast, highly viscous solutions form thick fibres at relatively higher electric potential (35). The optimal levels and effects of some important parameters on electrospun silk mats have been studied in this project and are described in section 2.4.

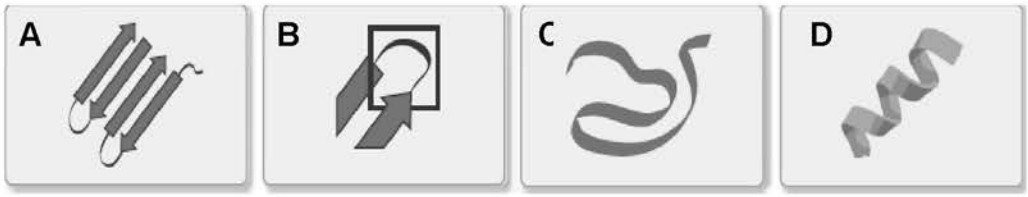

Figure 4.1: Schematic presentation of secondary silk motifs. A)- β-sheet, B)- β-turn, C)- random coil, D)- α-helix [Derived from Hardy et al; 2008]

In terms of the secondary structure of proteins, the most frequent secondary conformations are α-helix, random coil, β-turn and β-sheet shown schematically in Figure 4.1 (36).

In natural silk all four conformational types, (random coil, α-helix, β-sheet and β-turn) are present. The silk fibroin from *Bombyx mori* silk contains approximately 50 % β-sheet making it a semi-crystalline, tough and insoluble material (37) and also plays a crucial role in maintaining the mechanical properties of silk based materials (38). The relative proportion of silk secondary conformations can be changed during different stages of silk processing; with β-sheet transformation being induced using chemical or physical treatments (38-40).

Despite the fact that silk has been widely used as a biomaterial (14,28,41-44), however silk alone has a lack of osteoinductivity and there is a need to add

osteoinductive features to enable successful applications with calcified tissues (38). Silica and silica based composite materials have been proven to have osteoinductive properties (45-48) and can be used to improve the properties of silk based materials for dental applications. In this study, silk based electrospun materials have been characterised for morphology, composition, conformational variations and thermal stability.

4.2- Materials and methods

Details of all materials and method for electrospinning are described in chapter 2 (2.5). Briefly, natural *Bombyx mori* silk, heavy and light chain silk fractions were regenerated as described (2.1.5) and the dried silk was dissolved in 98-100 % formic acid at room temperature to get 20 wt. % clear solutions. The flow rate of silk solutions was adjusted at 0.9 ml/hour and was electro-spun using a potential difference of 25 kV and collected at 10 cm.

4.2.1- Silicification of electrospun mats

All electrospun mats were dipped in 30 ml of 90 % v/v ethanol for ten minutes at room temperature to induce more insoluble β-sheet conformation (12). Silicification was performed on ethanol treated silk mats as described in the literature (49). Briefly, ethanol treated silk mats were treated with 100 mM phosphate buffer at pH 7 (80 µl/mg) for 30 minutes at room temperature. Hydrolysed tetraethoxysilane (TEOS) was added (8 µl/mg) for the silicification to take place at room temperature, followed by washing with deionised distilled water to remove buffer and TEOS solutions. All silicified silk mats were left overnight in the fume hood to remove solvent. The list of all samples is given in table 4.1.

4.2.2- Sample nomenclature

For ease of understanding and explanation, details of different samples, and their abbreviations are given in Table 4.1.

Table 4.1: The description of electrospun silk samples

Sample	Stage 1	Electrospinning
T	Total silk	Silk solutions (20 wt %) were spun at room temperature using 25kV and collected on a target at 10 cm distance.
H	H-Chain	
L	L-Chain	
NL	Natural L-Chain	
H90	90% H-Chain, 10% L-Chain	
H75	75% H-Chain, 25% L-Chain	
H50	50% H-Chain, 50% L-Chain	
H25	25% H-Chain, 75% L-Chain	
	Stage 2	**Ethanol treatment (E)**
TE	Total silk	Dipping the silk electro-spun mats in 90 % v/v ethanol for 10 minutes at room temperature and dried (12)
HE	H-Chain	
LE	L-Chain	
N.LE	Natural L-Chain	
H90E	90% H-Chain, 10% L-Chain	
H75E	75% H-Chain, 25% L-Chain	
H50E	50% H-Chain, 50% L-Chain	
H25E	25% H-Chain, 75% L-Chain	
	Stage 3	**Silicification (S)**
TS	Total silk	Ethanol treated silk mats treated with 100 mM phosphate buffer (80 **µℓ/mg of silk)** for 30 minutes and adding 1 M hydrolysed TEOS (8 µℓ/mg silk) allowing 10 minutes for silica to condense and 3 water washes and air dried (49)
HS	H-Chain	
LS	L-Chain	
N.LS	Natural L-Chain	
H90S	90% H-Chain, 10% L-Chain	
H75S	75% H-Chain, 25% L-Chain	
H50S	50% H-Chain, 50% L-Chain	
H25S	25% H-Chain, 75% L-Chain	

4.2.3- Characterisation

The morphology of silk mats and the effects of ethanol and silicification treatments on the silk mats were studied using scanning electron microscopy (SEM), and elemental analysis (EDX) was used to confirm the presence or absence of silica (section 2.5.1). Thermogravimetric analysis (TGA) was used to explore the temperature related changes and infra-red spectroscopy (ATR_FTIR) for conformation changes in silk mats at different stages (section 2.5.2 and 2.5.4).

4.2.4- Curve fitting for ATR-FTIR spectra

Due to the nature of the protein backbone and its tendency to fold in complex ways, this results in the superimposition of vibrational modes corresponding to different structural motifs (β-sheet, α-helix or random coil). The de-convolution of the amide I band (1600-1700 cm^{-1}) can provide a lot more information on the structural motifs of proteins and their relative proportions (50). Peak fitting was performed using Thermo Grams suite G60 AI spectroscopy software. After baseline correction, six constrained peaks were used from 1710-1590 cm^{-1} with a maximum width of 30 cm^{-1} and drift of ± 10 cm^{-1} with 1000 iterations.

The peaks falling in the relevant areas of [β-turn (1710-1680 cm^{-1}), α-helix (1679-1660 cm^{-1}), random coil (1659-1640 cm^{-1}) and β-sheet (1639-1605cm^{-1})] were summed to calculate their relative ratios (50-52). An example of original ATR-FTIR spectra for electrospun sample and curve fitting for amide I using this method is shown in Figure 4.2.

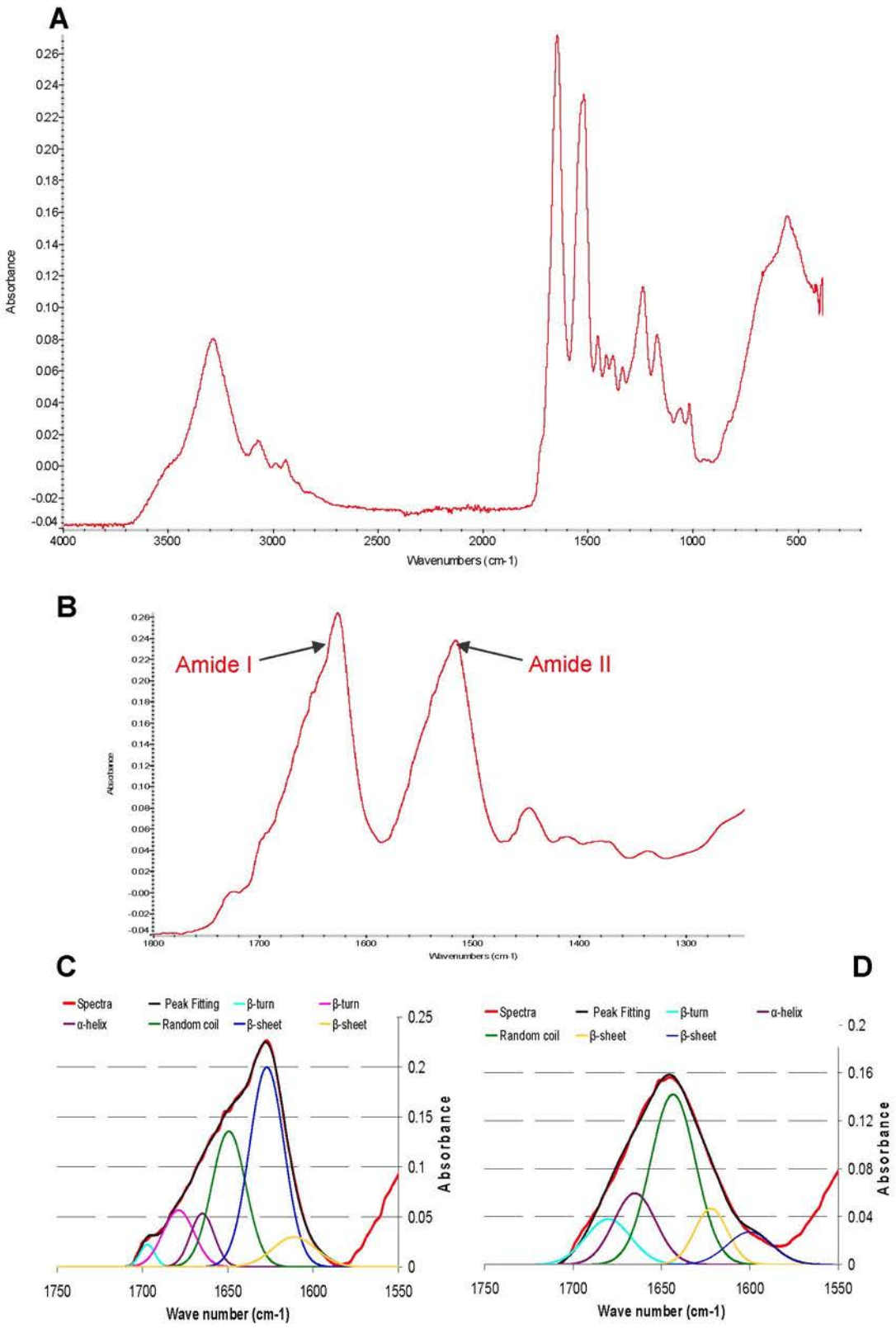

Figure 4.2: Handling of FTIR data. A)- FTIR full spectra for electrospun H-chain B)- Segmental spectra for H-chain showing amide I and II bands C)- Peak fitting of amide I for sample HSE typical of β-sheet and D)- Peak fitting for sample NL typical for random coil conformation.

4.3- Results and discussion

A number of studies (10,12-16,18,25,26,28,30,31,33,53) have been conducted on the detailed characterisation of regenerated silk electrospun materials. Natural silk fibroin is highly insoluble and has to be regenerated under damaging conditions to enable electrospinning. Similarly, very little work is available on electrospinning of silk fractions (H-chain and L-chain) and only a couple of research groups (11,54) have reported electrospinning of heavy and/or light chain recently. In this study, one component of natural *Bombyx mori* silk (L-chain) has been electrospun without need of any kind of regeneration, hence preventing it from any harsh conditions of heat and chemical treatments. Theoretically, heat treatment damages the silk proteins by breaking down peptides (as discussed in details in chapter 3) hence avoiding heat exposure should help to maintain the structural integrity of natural silk. The regenerated forms of natural silk and its fractions were also electrospun.
Furthermore, regenerated silk fractions (H-chain and L-chain) were blended in different proportions (table 4.1) to manipulate the solution properties and solid state properties of the electrospun materials. The electrospun mats from each sample were characterised immediately as spun, after treatment with ethanol to change conformation as well as after silicification on them.

4.3.1- Morphology of electrospun mats

Scanning electron microscopy is the major tool that has been used extensively to explore the surface morphology of electrospun fibres concentrating mainly on their size and shape (10,32,55-58). There are a number of factors that can affect the final morphology of electrospun fibres (2.4.2) and these were studied in preliminary experiments to adjust all parameters in order to get optimal fibre morphology (data shown in chapter 2) and average diameter and standard deviation was calculated by measuring at least 20 fibres randomly from the SEM image.
In general, the electrospun materials produced a non-woven mesh of nano fibres in the range of 80-330 nm diameter. Besides nano-fibres, bead formation was also observed in a few samples (discussed later). The most important parameter that affects the fibre morphology is the solution's viscosity (59) and can be related to fibre diameter as shown in equation 4.1 (24).

$$d \alpha \eta^2 \qquad \text{(Eq 4.1)}$$

Where d is electrospun fibre diameter and η is the solutions viscosity

The solution viscosity is directly related to the silk concentration;

$$\eta \alpha [silk] \qquad \text{(Eq 4.2)}$$

Solution viscosity and surface tension also play a crucial role in determining the optimal polymer concentration required for continuous fibre formation (55). Similarly, silk concentration may indirectly affect fibre morphology by changing the solution viscosity as more concentrated solutions generally give higher viscosity (Figure 4.3-A). Hence, the silk concentration plays a crucial role in producing uniform round fibres (60), whereas bead formation is a typical feature of low silk concentration (25). A recent study (25) demonstrated that silk concentration should be more than 7.5 wt%, 10 wt % (10) up to 12 % (60) to get bead free fibres. In order to electrospin bead free continuous fibres, concentration of all solutions was fixed to 20 wt %, however, still there was difference in the solutions viscosity (Figure 4.3-B) depending on the nature of the solution.

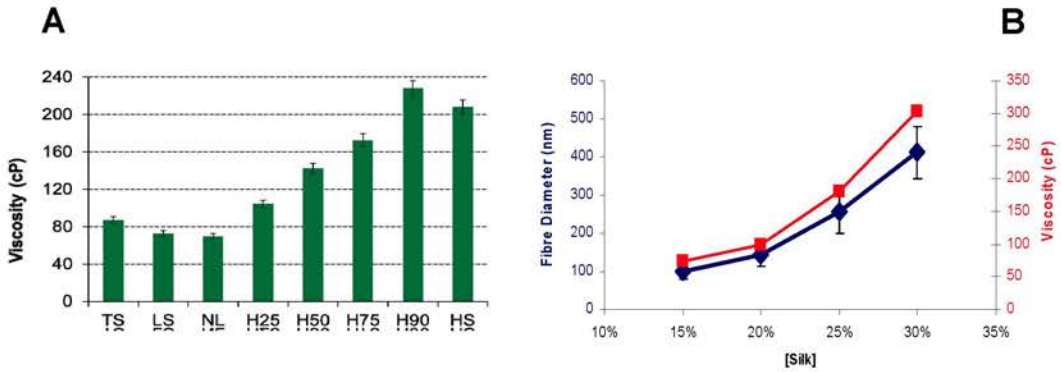

Figure 4.3: (A)- Effect of solution viscosity of various silk solutions on average fibre diameter (B)- Relationship of concentration, viscosity and their effect on electrospun fibre diameter for total silk; solution viscosities (red rectangle) of different silk solutions and fibre diameter (blue diamonds)

Electron micrographs of silk materials were compared before and after ethanol treatment and after silicification (Figure 4.4). The defective bead formation in electrospun fibres has been mentioned in many studies (61-63) and was observed for samples from natural L-chain (NL) and regenerated L-chain (L) as shown in Figure 4.4 (A1-3 and B1-3). Both silk types produces mainly beads with a few nano-fibres in the background, however these samples produced the finest fibres with an average diameter of 118.966 ± 57.39 nm for L and 123.607 ± 37.83 nm for NL (Figure 4.4-A1,2).

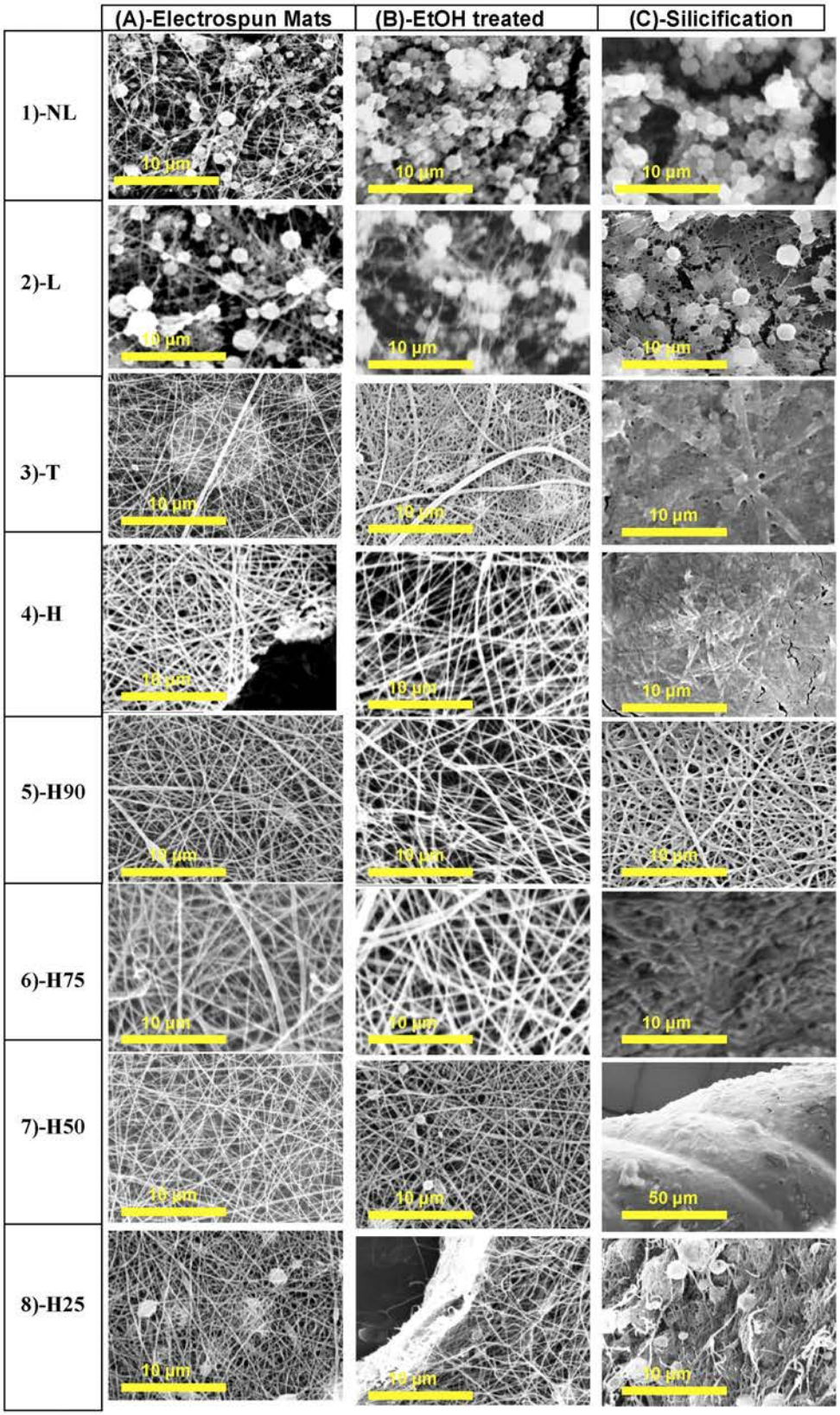

Figure 4.4: SEM images A)- Electrospun mats as spun, B)-Ethanol treated, C)-Silicified

A detailed study (61) on the bead formation described this phenomenon as related to the solution parameters mainly surface tension, viscosity, charge density and neutralisation. As all electrospinning parameters were fixed however, it was the nature of light chain that has probably comparatively less polymer chain entanglement than total silk (T) and H-chain (H) due to the structural differences and significantly lower Mw (~27 kDa). The structural differences of L-chain and H-chain have been described in the previous chapter. All these factors resulted in less viscous silk solutions (≤ 70 cP), lack of polymer chain entanglement and leading to collapse of polymer solution and defective bead formation instead of fibres.

4.3.1.1- Significance of H-chain in combination solutions

Addition of H-chain in to the regenerated L-chain solutions improved the morphology, for example, in sample H25 (75% L-chain and only 25% H-chain), showed mainly fibres with only a few beads. Surprisingly, the average fibre diameter was 123.404 ± 37.82 nm which is about the same as for NL and slightly larger than L with improved fibre size distribution. A further increase in H-chain proportion (samples H50, H75 and H90) and pure H-chain (H), resulted in continuous smooth fibres without bead formation (Figure 4.4-A.5-7). Average fibre diameter was observed to increase with increasing H-chain content, 125.532 ± 31.48 nm for H50, 157.447 ± 40.70 nm for H75 and increase up to 215.517 ± 92.45 nm for H90. The thickest fibres were observed for H-chain with an average diameter of 258.621 ± 72.13 nm.

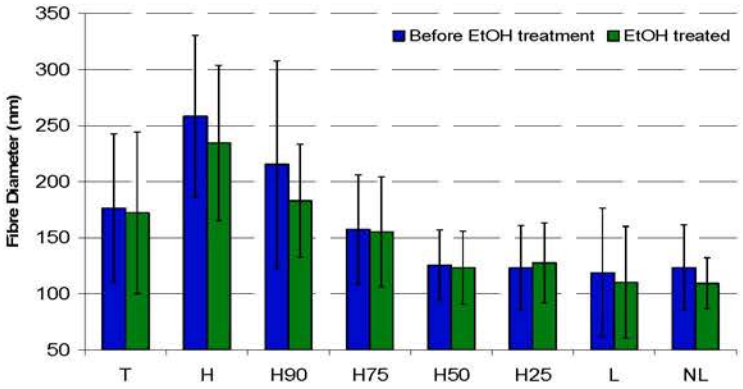

Figure 4.5: Mean fibre diameter of different electrospun silk fibres before and after ethanol post treatment.

Due to higher Mw (~350 kD) and therefore longer chain length, the addition of H-chain resulted in more polymer chain entanglement and increased the solution

viscosity, hence increasing the thickness of fibres. Average fibre diameter for total silk (T) was 176.519 ± 66.22 which corresponds with the diameter from H90 and H75 which contain by weight the equivalent proportions of H-chain and L-chain as the natural silk. These results suggested that fibre morphology of electrospun silk materials can be manipulated by adjusting the relative proportions of the two fractions.

4.3.1.2- Effects of ethanol treatment

Scanning electron micrographs of ethanol treated silk mats are presented in the middle column (B) of Figure 4.4 demonstrating no apparent changes upon ethanol treatment. However, in general all samples showed some contraction in nano-fibres by shrinking average fibre diameter to some extent (Figure 4.5). There are two main factors that have contributed to such changes firstly, the hygroscopic nature of ethanol (64) that helped to remove water and contraction on drying and secondly, the conformational changes and will be discussed later. The removal of this water promotes the formation of β-sheet structure and a subsequent contraction of the fibre diameter.

4.3.1.3- Effects of silicification

Scanning electron micrographs of silk mats after silicification are presented in the right column (C) of Figure 4 demonstrating gross changes in general morphology of fibres as a result of silica deposition. At a low magnification (1000X), they appeared as rolled flakes with no visible fibres (Figure 4.4-C7).

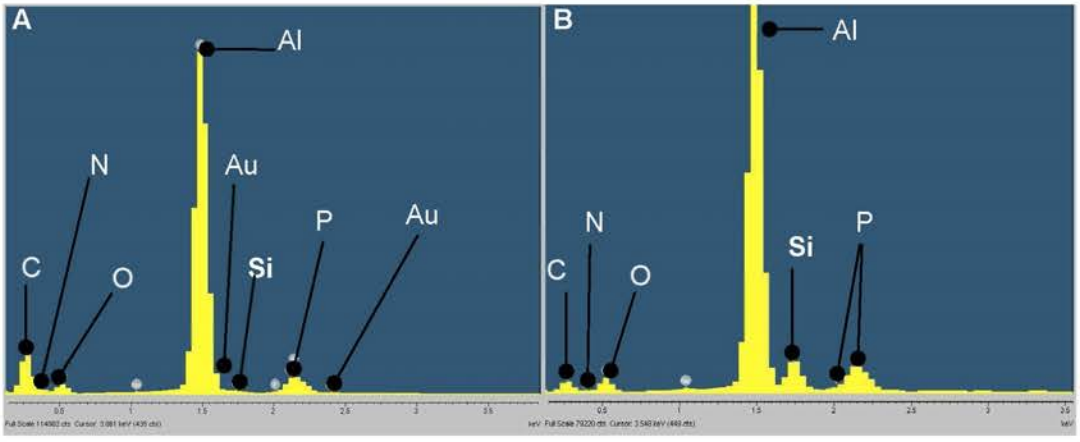

Figure 4.6: EDX spectra for electrospun sample H90. A)- As spun, B)- After silicification treatment

However at a higher magnification (5000X or more) the silk nano fibres were overlaid by silica coating and depositions around them, however fibre impressions were visible (Figure 4.4-C3-7).

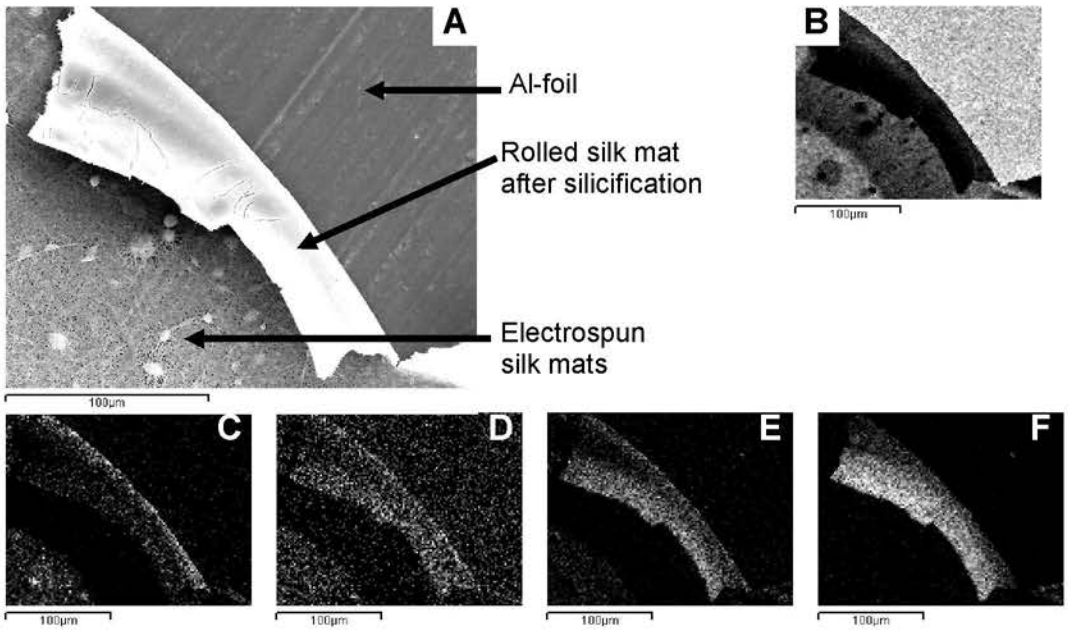

Figure 4.7: Elemental analysis of electrospun H-chain sample after silicification. A)- SEM image at 500X, B)- Map for Aluminium, C)- Map for Carbon, D)- Map for Nitrogen, E)- Map for Oxygen and F)- Map for Silicon

The morphology of silk beads (where applicable) did not appear to be affected by silicification and silica deposited mainly around nano fibres (Figure 4.4-C1-2, C8).
The presence of silica in these samples was confirmed using elemental analysis, a barely visible peak representing silicon appeared for all samples before silicification (an example spectra for H90E shown in Figure 4.6-A) suggesting a little or no silica before silicification but this become prominent for the same sample after silicification (H90S) indicating the presence of silica (Figure 4.6-B). Besides silicon and oxygen (from silica), other elements observed in the spectra were carbon, nitrogen coming mainly from silk and oxygen mainly from silica and silk. The elemental maps for sample HS in relation to SEM image (500X) are shown in Figure 4.7

4.3.2- Conformational changes in electrospun materials

The secondary conformation of silk protein is directly related to its structure and properties, with the β-sheet content particularly playing an important role in the reinforcement of mechanical properties (15) as high tensile strength is attained by

maximum β-sheet content in the final material. In contrast, the electrospun silk materials demonstrated amorphous structure mainly having non-β-sheet conformation, limiting their practical applications as a result of high water solubility and poor mechanical properties (15). However this problem can be overcome by inducing conversion of random coil and α-helix to β-sheet and increasing crystallinity (15). A variety of approaches have been used for conformational changes such as use of alcohols (12,65,66), annealing at high temperature (66), stretching (67), storage (68) UV radiation (68). Alcohols (methanol, ethanol) cause dehydration and encourage conversion of α-helix into β-sheet structure.

Infra-red spectra obtained using attenuated total reflectance (ATR) has been frequently used (26,69-72) to study silk conformations. The quantitative analysis of ATR-FTIR spectra were performed by de-convolution using peak fitting. The assigned peaks for β-turn are 1710-1680 cm^{-1}, for α-helix 1679-1660 cm^{-1}, for random coil 1659-1640 cm^{-1} and for β-sheet 1639-1605 cm^{-1} (52). The difference in the original FTIR spectra for H-chain silk mat (as spun) and after ethanol treatment is shown in Figure 4.8-A. There is clear shift of amide I peak from the area of random coil (1650 cm^{-1}) towards β-sheet areas suggesting the increase in the β-sheet contents and this was quantified by peak fitting (Figure 4.2-B). The change in the transition takes place as a result of rearrangement of hydrogen bonds and silk fibroin chains (73).

The electrospun silk mats tend to swell up when placed in ethanol providing sufficient space for the silk molecules to rearrange and change conformation (74) and they then tend to shrink slightly upon drying as seen in the SEM data. The change in conformation as a result of such chemical treatment has also been observed to affect the porosity and pore sizes of silk electrospun materials (75). A methanol treatment for 60 minutes was found to decrease the pore volume from 76.1% to 68.1% and maximum pore size was shrunk from 220 μm (as spun), to 190 μm after methanol treatment (75). All these findings strongly suggest that electrospun silk materials have a tendency to shrink under such chemical treatment and results are consistent with SEM data.

The quantitative comparison of conformational changes after ethanol treatment is shown in Figure 4.9. The conformation of electrospun silk mats appeared mainly random coil and α-helix collectively contributing about 32%-73% with comparatively less β-sheet content (20%-38%). As a result of ethanol treatment, a significant increase in the β-sheet content was observed mainly from transition of α-helix and β-turn in to β-sheet. There was relatively little effect on random coil contents and little change in its proportion was observed in each sample (Figure 4.9).

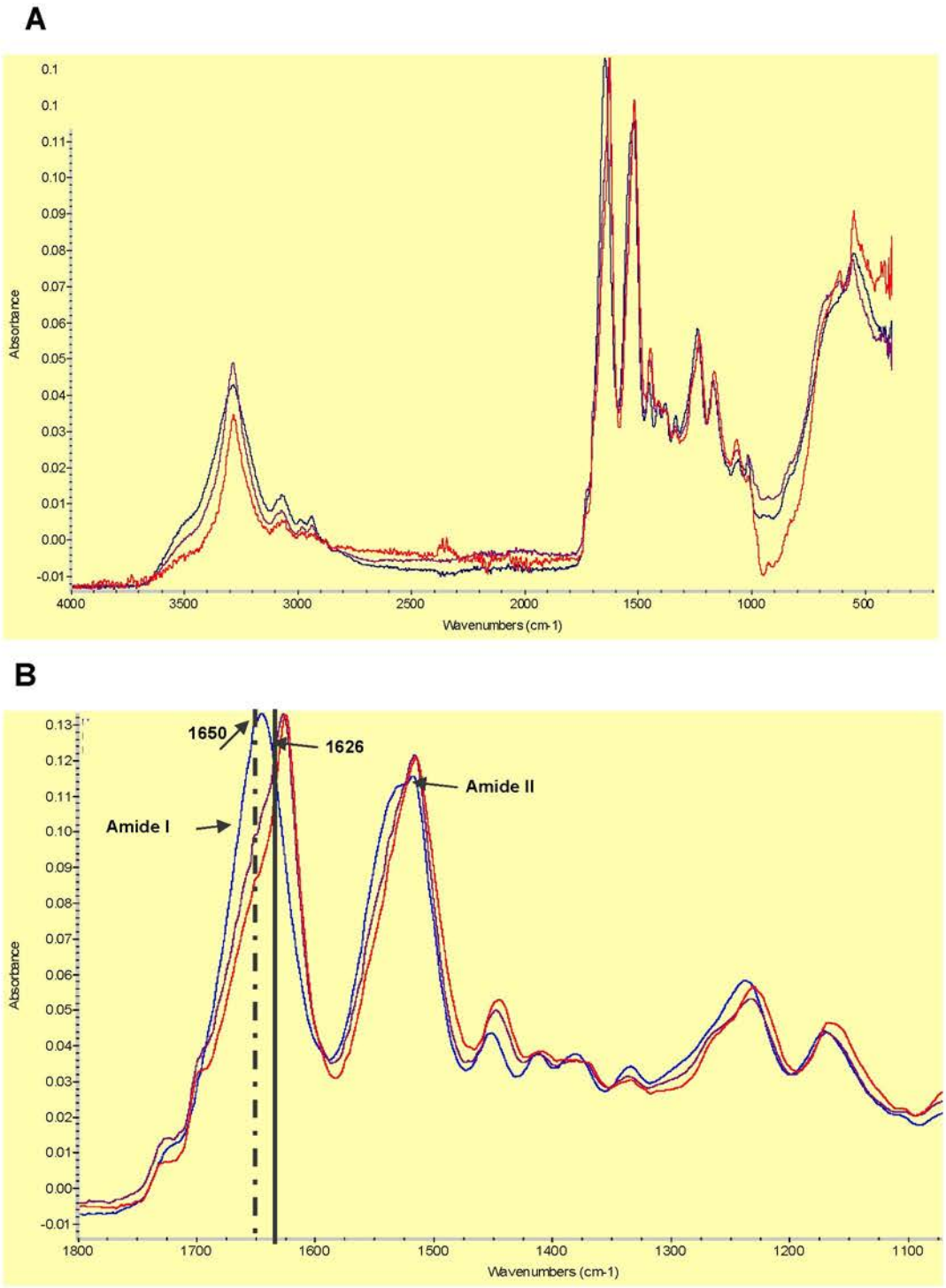

Figure 4.8: Comparison of FTIR spectrum for H-chain electrospun mat **(H)** compared for the effect of ethanol treatment **(H.E)** and silicification treatment **(H.S)**, A)- Full FTIR spectra and B)- Amide I and II regions .

All samples attained β-sheet contents in a narrow range of 40-50.7% the lowest being for sample L.E (40.00%), and highest for sample H.E (50.76 %). All combination samples (H90E, H75E, H50E, and H25E) attained (45.61-48.18%) β-

sheet content. Another important finding was that a general trend to reduce in β-turn content was observed as a result of ethanol treatment suggesting that longer β-sheet (with comparatively few β-turns) regions are more likely in the ethanol treated silk mats.

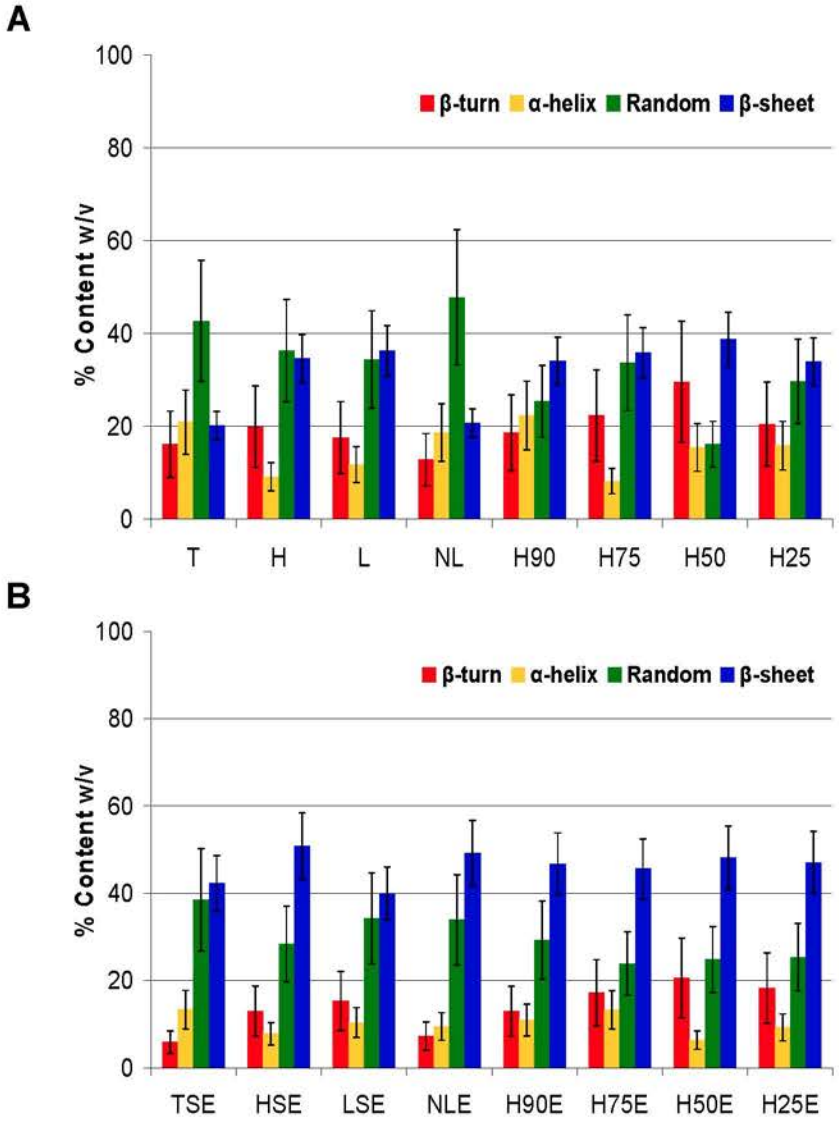

Figure 4.9: Quantitative comparison of secondary conformations in silk different mats A)- As spun, B)- After ethanol treatment

The electrospinning solvent (formic acid) is well known for producing clear stable silk solutions and more importantly β-sheet conformation in silk fibroin upon evaporation from cast materials (76,77). However it is not true for electrospun silk materials from formic acid as these have significantly lower β-sheet content than silk films cast from

formic acid solutions (Figure 4.10) hence, justification for the importance of post treatment to improve silk structure.

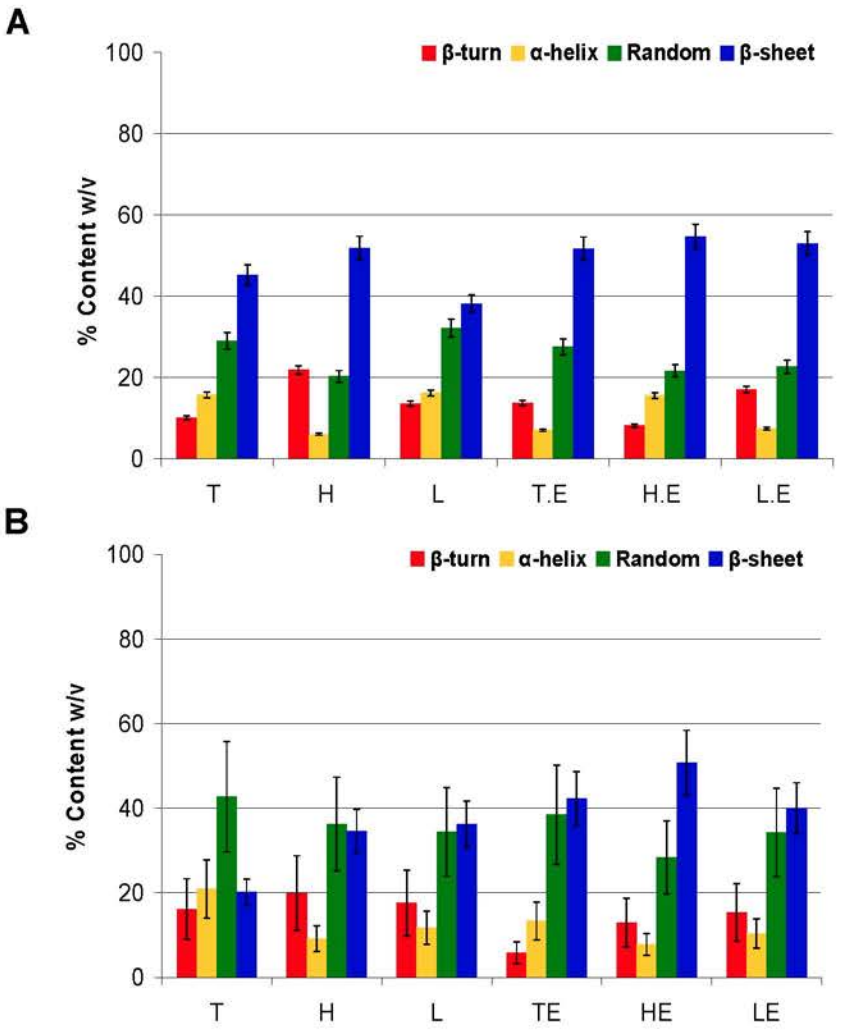

Figure 4.10: Comparison of secondary conformation and effect of ethanol treatment A)- Cast films from formic acid B)- Electrospun using formic acid

The main difference in cast films and electrospun fibres was the β-sheet content that was 45%, 51% and 38% for total, H-chain and L-chain respectively, whereas lower β-sheet contents in general for electrospun materials just 20% for total and about 36 % for L-chain and H-chain were measured. In terms of ethanol treatment, it did not make a big difference on silk cast films as a rise in β-sheet content observed was as little as 12.5%, 5 % and 26% for total, H-chain and L-chain respectively. In contrast, a

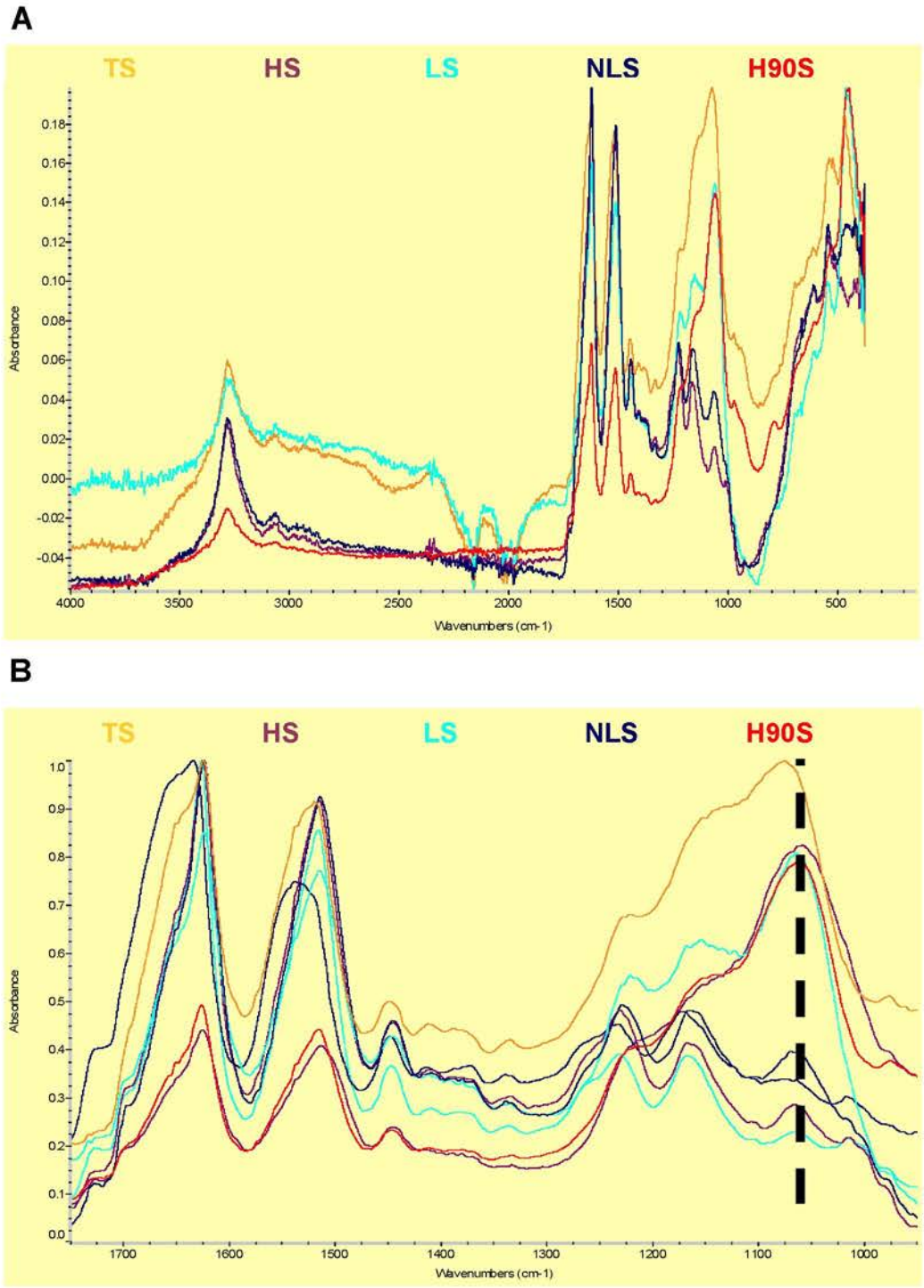

Figure 4.11: FTIR spectra for various silk samples after silicification showing an additional peak representing Si-O-Si bond, A)- Full FTIR spectra, B)- Relevant section

larger transition into β-sheet was observed in electrospun silk mats, 52 % in total silk, 32% for H-chain and 35% for L-chain (Figure 4.10-B).

The random coil in the spun mats is due to the quick evaporation of the electrospinning solvent formic acid. Silk protein molecules don't get sufficient time to rearrange their conformation and solidify immediately (15). The exaggerated effect of ethanol on electrospun mats is due to the initial high level of random coil and α-helix, the high surface area of nano structure (56,78), high porosity (≥76%) and pore volume 2.017 ml/g (75). High surface area and porosity allow easy access for the ethanol. For any format of silk materials described above, H-chain settled showed more β-sheet than any other fraction suggesting the potential for manipulating properties of silk materials and these results are consistent with gelation (discussed later) and solution properties of H-chain alone.

The FTIR spectra for silicification samples did not show any changes in the β-sheet conformation of the protein, however the presence of silica was confirmed by the appearance of an additional peak representing the asymmetrical stretch of Si-O-Si in the area 1100-1060 cm^{-1} (Figure 4.11).

The β-sheet conformation result in the formation of crystalline domains in the silk (56,79) of about 40-50 % of natural *Bombyx mori* silk (37,80) hence producing a semi-crystalline structure. Although ethanol treatment of electrospun silk material helped to increase the β-sheet content up to 45-50 % (as much as in natural silk) with the co-existence of crystalline and non-crystalline region in the spun materials (15). However, mechanical properties of regenerated silk are very poor compared to natural silk and this is the biggest hurdle in the use of regenerated silk materials for many applications (79). These results suggest that it is not only the conformational motifs that affect the properties but certain other factors such as degradation of silk proteins during processing are also involved and need further work. A range of different approaches already has been attempted to overcome this issue such as different processing techniques (81), coagulation with other different polymers (57,82-84) and reinforcement with inorganic particles (38,85,86).

4.3.3-Mechainical Testing

Considering the importance of mechanical properties as described above, tensile testing of electrospun mats was attempted using a method described in chapter 2 (2.5.5.3). Due to the anisotropic nature of aluminium foil, the results obtained were not conclusive (data shown in Figure 2.45 in chapter 2). The separation of electrospun materials from the target is the biggest challenge and different methods were attempted to separate aluminium foil such as peeling silk mats or dipping in liquid nitrogen to benefit from differences in the co-efficient of thermal expansion of

silk and metal foil. Unfortunately no method was successful at separating electrospun silk from the target.

An alternative method of mechanical testing can be the nano-scale testing of single fibres however a major problem is again the separation of single fibres and their attachment to the testing grips and no reports could be found on such testing (35). Another contributing factor in this regard is the non-woven nature of the electrospun fibre and it could be really difficult to align more than one fibre in one axis. Generally, nano-fibres have been supposed to have better mechanical presentation than micro-fibres (35). It is evident that poor mechanical properties such as low compressive strength and hardness are a huge challenge for the practical applications of regenerated silk biomaterials.

4.3.4- Thermal properties of electrospun silk materials

In order to study the thermal behaviour of electrospun mats and effects of chemical treatments, Thermogravimetric analysis (TGA) were performed. All samples were analysed along with aluminium foil and TGA curves are shown in Figure 4.12-A. Each samples was heated from 30 ° C up to 600 ° C with incremental increase in temperature 10 ° C/minutes and weight loss was calculated. The top most line in each chart represents aluminium foil (foil) where no weight loss was observed until maximum temperature was attained.

In relation to weight loss and temperature changes, generally TGA curves for silk samples demonstrated four distinct steps,

I) Initial weight loss of about 6-7 % for temperature of 0-105 ° C considered to be the evaporation of water in silk.

II) There is almost no or very little change in residual weight for up to 250 ° C mainly from bonded water suggesting the stability of silk in this range.

III) A sharp decrease in weight (approximately 65 %) from 195 ° C up to 425 °C suggesting major thermal decomposition of silk protein.

IV) Finally, complete loss of organic matter at a very slow rate between 425 °C-600 ° C suggesting complete combustion of residual carbon based material.

The TGA data for electrospun materials is very similar to the thermal analysis of *Bombyx mori* silk cocoons and silk fibres (87), where they found initial weight loss of (9% for cocoon and 8.2% for silk fibre) as result of water evaporation followed by a sharp decrease in the weight from 150 to 450℃ as a result of silk degradation.

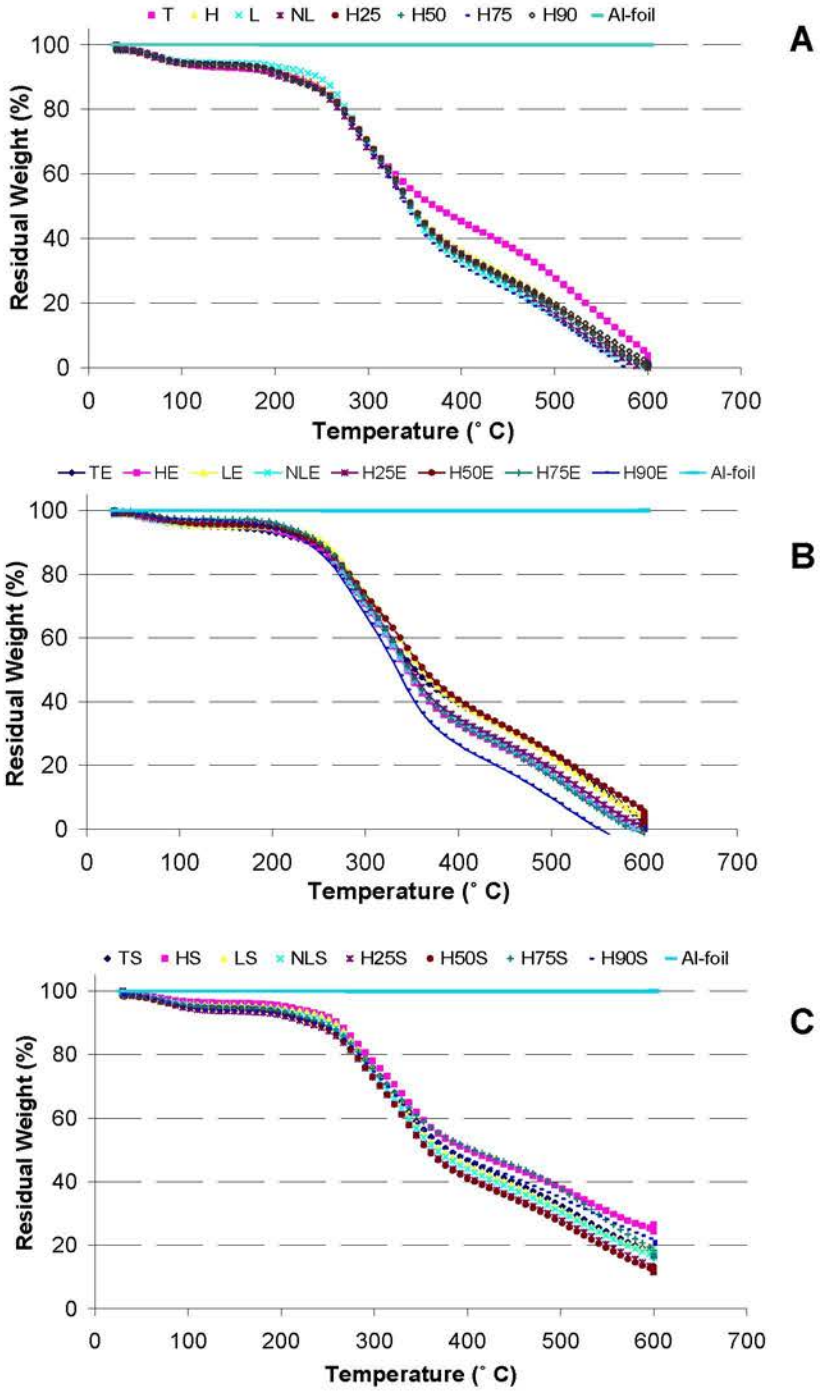

Figure 4.12: TGA curves for electrospun silk materials A)- As spun, B)- Ethanol treated, C)- Silicified

However, in this study, initial weight loss as a result of water evaporation was just 6 % and as less amount of free water is expected in the electrospun materials due to their very high surface area. These results suggested that silk is thermally stable up to 250℃ and silk based materials can be autoclaved without the loss of functional integrity (88,89) hence, fulfilling a vital requirement needed for biological applications.

The effects of ethanol treatment on thermal analysis are represented in Figure 4.12-B. There was a clear difference observed in the initial loss of water content, in contrast to the 6% weight loss due to water evaporation from as spun silk mats, only 2.5% weight loss was observed for ethanol treated samples up to 105 °C followed by a slight weight loss until 250 °C and similar p attern of weight loss was observed thereafter. This pattern is related to the hygroscopic properties of ethanol and its ability to remove water and is also consistent with fibre shrinkage found in SEM and conformational changes observed by FTIR analysis. The ethanol treatment (for 10 minutes) also increased the thermal stability of silk (up to 20℃) due to an increase in the crystallinity of silk (77). There were no significant differences observed between different ethanol treated samples. As thermal stability is also related to crystallinity and β-sheet content (77) and β-sheet conformation was increased to 45-50% for all ethanol treated samples and this was reflected in TGA analysis. Annealing of electrospun silk fibres above 280℃ ma y cause degradation and a narrow window of temperature (210℃-230℃) is recom mended for annealing to prevent degradation (90).

For silicified samples (Figure 4.12-C), these generally showed water weight loss patterns very similar to as spun silk mats (before ethanol treatment) and this is due to the fact that silk mats trapped some water during the silicification reaction involving aqueous buffer and silica precursor solutions. The presence of inorganic content did not change the pattern of silk degradation and followed exactly the same trend as observed for ethanol treated silk. The only difference was the amount of residue (12-26%) representing inorganic content. The different amounts of residual inorganic content was observed for different samples (Figure 4.12-C), the highest for H (26.12%) followed by H90 (20.56%), H75 (18.34%), total and L-chain (18-19%) and lowest amounts for H50 (13.32%) and H25 (12.22%). These results suggested that H-chain tend to retain more silica and residual weight was observed to decrease in direct relation to the decreasing proportion of H-chain in samples. In a recent study (49), where a similar method was used for the silicification using R5 based genetically engineered silk chimera films, it observed that 10% silica was left after thermal analysis. The results presented here in suggest that silica

condensation is affected by the type of polymer/silk used and H-chain, H90 and H75 electrospun mats condensed significantly more silica. This may be due to different amino acid composition of H-chain that contains more hydrophobic domains (91). The silica can be entrapped in the hydrophobic segments during the condensation process (92) hence more liking of silica for H-chain may be due to the presence of more hydrophobic amino acids and more β-sheet conformation compared to L-chain and total silk.

4.4- Summary

This chapter has described the characterisation of silk based nanocomposite materials fabricated using different silk fractions and their blends in variable proportions. H-chain alone produced higher viscosity solutions due to its unique structural features compared to L-chain. The blends of both silk fractions enabled manipulation of the final properties of the mixture and can be tailored as desired. The chemical treatment of electrospun mats with ethanol proved to be a useful technique and equally effective in increasing β-sheet contribution for all silk fractions. Ethanol treatment resulted in slight shrinkage of nano-fibres, increase in β-sheet and insolubility of silk with H-chain maintaining the most β-sheet before and after ethanol treatment.

The silicification reaction condensed silica on electrospun silk mats which was confirmed by elemental analysis, FTIR and TGA, however the amount of silica condensed was variable with the maximum entrapped by H-chain due to more hydrophobic amino acids (primary structure) and more β-sheet (secondary structure). Until now the electrospinning of silk fractions (separated using formic acid) has not been reported and no research has been performed on electrospinning of blended solutions of silk fractions. In order to improve the solution properties of natural silk, it has been blended with a variety of other polymers such as gelatine (26), cross linkers such as genipin (16), keratin (43), collagen (93), poly vinyl alcohol (84), chimeric silk proteins (94,95) and many other materials (42,96-98). However this study has opened a gateway to improve certain properties (viscosity, fibre diameter, conformation and strength) by making silk-silk composites and make materials with tuneable properties depending on the need of an application. Finally, for this first time, it has been possible to electrospun the natural silk (L-chain) successfully without the need of regenerating, hence producing silk material with better structural integrity.

These materials from natural silk (as discussed earlier) showed comparable properties to regenerated silk materials and hence hold a great potential for future applications, Further work is required for the better understanding of the structure and chemical behaviour of silk fractions and to explore the outcome of more silk-silk blends specially using natural silk mixed with regenerated silks.

4.5- References

(1) Zhang Y, Lim CT, Ramakrishna S, Huang ZM. Recent development of polymer nanofibers for biomedical and biotechnological applications. J Mater Sci Mater Med 2005;16(10):933-946.

(2) Smith LA, Ma PX. Nano-fibrous scaffolds for tissue engineering. Colloids and Surfaces B: Biointerfaces 2004 12/10;39(3):125-131.

(3) Ma PX. Synthetic nano-scale fibrous extracellular matrix. J Biomed Mater Res 1999;46(1):60.

(4) Yang F. Fabrication of nano-structured porous PLLA scaffold intended for nerve tissue engineering. Biomaterials 2004;25(10):1891.

(5) Zhang X. Synthesis of polyaniline nanofibers by nanofiber seeding. J Am Chem Soc 2004;126(14):4502.

(6) Martin CR. Template synthesis of electronically conductive polymer nanostructures. Acc Chem Res 1995;28(2):61.

(7) Lakshmi BB. Sol-gel template synthesis of semiconductor oxide micro-and nanostructures. Chemistry of materials 1997;9(11):2544.

(8) Hartgerink JD. Self-assembly and mineralization of peptide-amphiphile nanofibers. Science 2001;294(5547):1684.

(9) Niece KL. Self-assembly combining two bioactive peptide-amphiphile molecules into nanofibers by electrostatic attraction. J Am Chem Soc 2003;125(24):7146.

(10) Amiraliyan N, Nouri M, Kish MH. Electrospinning of silk nanofibers. I. An investigation of nanofiber morphology and process optimization using response surface methodology. Fibers and Polymers 2009;10(2):167-176.

(11) Wadbua P, Promdonkoy B, Maensiri S, Siri S. Different properties of electrospun fibrous scaffolds of separated heavy-chain and light-chain fibroins of Bombyx mori. Int J Biol Macromol 2010 6/1;46(5):493-501.

(12) Cao H, Chen X, Huang L, Shao Z. Electrospinning of reconstituted silk fiber from aqueous silk fibroin solution. Materials Science and Engineering: C 2009 8/31;29(7):2270-2274.

(13) Kang M, Chen P, Jin H. Preparation of multiwalled carbon nanotubes incorporated silk fibroin nanofibers by electrospinning. Current Applied Physics 2009 1;9(1, Supplement 1):S95-S97.

(14) Zhang X, Reagan MR, Kaplan DL. Electrospun silk biomaterial scaffolds for regenerative medicine. Adv Drug Deliv Rev 2009 10/5;61(12):988-1006.

(15) Zhou J, Cao C, Ma X. A novel three-dimensional tubular scaffold prepared from silk fibroin by electrospinning. Int J Biol Macromol 2009 12/1;45(5):504-510.

(16) Silva SS, Maniglio D, Motta A, Mano JF, Reis RL, Migliaresi C. Genipin-modified silk-fibroin nanometric nets. Macromol Biosci 2008 AUG 11;8(8):766-774.

(17) Greiner A, Wendorff JH. Electrospinning: A fascinating method for the preparation of ultrathin fibres. Angewandte Chemie-International Edition 2007;46(30):5670-5703.

(18) Jeong L, Lee KY, Park WH. Effect of solvent on the characteristics of electrospin regenerated silk fibroin nanofibers. ASBM7: Advanced Biomaterials VII 2007;342-343:813-816.

(19) Electrospinning for tissue regeneration. Oxford: Woodhead Publishing; 2011.

(20) Li W, Laurencin CT, Caterson EJ, Tuan RS, Ko FK. Electrospun nanofibrous structure: A novel scaffold for tissue engineering. J Biomed Mater Res 2002;60(4):613-621.

(21) Agarwal S, Wendorff JH, Greiner A. Use of electrospinning technique for biomedical applications. Polymer 2008 12/8;49(26):5603-5621.

(22) Stevens MM, George JH. Exploring and Engineering the Cell Surface Interface. Science 2005 November 18;310(5751):1135-1138.

(23) Liang D, Hsiao BS, Chu B. Functional electrospun nanofibrous scaffolds for biomedical applications. Adv Drug Deliv Rev 2007 12/10;59(14):1392-1412.

(24) He J, Liu Y, Xu L, Yu J, Sun G. BioMimic fabrication of electrospun nanofibers with high-throughput. Chaos, Solitons & Fractals 2008 8;37(3):643-651.

(25) Alessandrino A, Marelli B, Arosio C, Fare S, Tanzi MC, Freddi G. Electrospun Silk Fibroin mats for tissue engineering. Engineering in Life Sciences 2008;8(3):219-225.

(26) Bao Weiwei, Zhang Youzhu, Yin Guibo, Wu Jialin. The structure and property of the electrospinning silk fibroin. e-Polymers 2008 AUG 4:098.

(27) Schiffman JD, Schauer CL. A review: Electrospinning of biopolymer nanofibers and their applications. Polym Rev 2008;48(2):317-352.

(28) Soffer L, Wang X, Mang X, Kluge J, Dorfmann L, Kaplan DL, et al. Silk-based electrospun tubular scaffolds for tissue-engineered vascular grafts. J Biomater Sci -Polym Ed 2008;19(5):653-664.

(29) Zhu Z, Ohgo K, Watanabe R, Takezawa T, Asakura T. Preparation and characterization of regenerated Bombyx mori silk fibroin fiber containing recombinant cell-adhesive proteins; nonwoven fiber and monofilament. J Appl Polym Sci 2008 SEP 5;109(5):2956-2963.

(30) Gandhi M, Yang HJ, Shor L, Ko F. Regeneration of bombyx mori silk by electrospinning: A comparative study of the biocompatibility of natural and synthetic polymers for tissue engineering applications. Journal of Biobased Materials and Bioenergy 2007;1(2):274-281.

(31) Ki CS, Kim JW, Hyun JH, Lee KH, Hattori M, Rah DK, et al. Electrospun three-dimensional silk fibroin nanofibrous scaffold. J Appl Polym Sci 2007;106:3922-3928.

(32) Meechaisue C, Wutticharoenmongkol P, Waraput R, Huangjing T, Ketbumrung N, Pavasant P, et al. Preparation of electrospun silk fibroin fiber mats as bone scaffolds: a preliminary study. Biomedical Materials 2007;2:181-188.

(33) Peh RF, Suthikum V, Goh CH, Toh SL. Novel Electrospun-Knitted Silk Scaffolds for Ligament Tissue Engineering. World Congress on Medical Physics and Biomedical Engineering 2006, Vol 14, Pts 1-6 2007;14:3287-3290.

(34) Wang H, Shao HL, Hu XC. Structure of silk fibroin fibers made by an electrospinning process from a silk fibroin aqueous solution. J Appl Polym Sci 2006;101(2):961-968.

(35) Huang Z, Zhang Y-, Kotaki M, Ramakrishna S. A review on polymer nanofibers by electrospinning and their applications in nanocomposites. Composites Science and Technology 2003 11;63(15):2223-2253.

(36) Hardy JG, Römer LM, Scheibel TR. Polymeric materials based on silk proteins. Polymer, 2008 9/23;49(20):4309-4327.

(37) Lefèvre T, Rousseau M, Pézolet M. Protein secondary structure and orientation in silk as revealed by raman spectromicroscopy. Biophys J 2007 4/15;92(8):2885-2895.

(38) Mieszawska AJ, Fourligas N, Georgakoudi I, Ouhib NM, Belton DJ, Perry CC, et al. Osteoinductive silk–silica composite biomaterials for bone regeneration. Biomaterials 2010 12;31(34):8902-8910.

(39) Matsumoto A, Chen J, Collette AL, Kim UJ, Altman GH, Cebe P, et al. Mechanisms of silk fibroin sol-gel transitions. J Phys Chem B 2006;110(43):21630-21638.

(40) Jin HJ. Water stable silk films with reduced β-sheet content. Advanced functional materials 2005;15(8):1241.

(41) Mandal BB, Park S, Gil ES, Kaplan DL. Multilayered silk scaffolds for meniscus tissue engineering. Biomaterials 2011 1;32(2):639-651.

(42) Hu X, Lu Q, Sun L, Cebe P, Wang X, Zhang X, et al. Biomaterials from ultrasonication-induced silk fibroin and hyaluronic acid hydrogels. Biomacromolecules 2010 11/08;11(11):3178-3188.

(43) Vasconcelos A, Freddi G, Cavaco-Paulo A. Biodegradable materials based on silk fibroin and keratin. Biomacromolecules 2008;9(4):1299-1305.

(44) Horan RL, Antle K, Collette AL, Wang Y, Huang J, Moreau JE, et al. In vitro degradation of silk fibroin. Biomaterials 2005 6;26(17):3385-3393.

(45) Hench LL. The story of Bioglass®. J Mater Sci Mater Med 2006;17(11):967-978.

(46) Eglin D, Ali SAM, Perry CC. Comparative study of the in vitro apatite-forming ability of poly(epsilon-caprolactone)-silica sol-gels using three osteoconductivity tests (static, dynamic, and alternate soaking process). Journal of Biomedical Materials Research Part a 2004;69A(4):718-727.

(47) Xu HHK, Smith DT, Simon CGCG. Strong and bioactive composites containing nano-silica-fused whiskers for bone repair. Biomaterials 2004 8;25(19):4615-4626.

(48) Damen JJM, Ten Cate JM. Silica-induced precipitation of calcium phosphate in the presence of inhibitors of hydroxyapatite formation. Journal of Dental Research March 01;71(3):453-457.

(49) Foo CWP, Patwardhan SV, Belton DJ, Brandon Kitchel, Anastasiades D, Huang J, et al. Novel Nanocomposites from Spider Silk-Silica Fusion (Chimeric) Proteins. Proc Natl Acad Sci U S A 2006 Jun. 20;103(25):pp. 9428-9433.

(50) Navea S, Tauler R, Juan Ad. Application of the local regression method interval partial least-squares to the elucidation of protein secondary structure. Anal Biochem 2005 1/15;336(2):231-242.

(51) Arrondo JLR, Muga A, Castresana J, Goñi FM. Quantitative studies of the structure of proteins in solution by fourier-transform infrared spectroscopy. Prog Biophys Mol Biol 1993;59(1):23-56.

(52) Dong A, Huang P, Caughey W. Protein secondary structures in water from 2nd-derivative amide-i infrared-spectra. Biochemistry (N Y) 1990;29(13):3303-3308.

(53) Yin GB, Zhang YZ, Bao WW, Wu JL, Shi DB, Dong ZH. Study on the property of the electrospinning silk fibroin(SF). Researches and Progresses of Modern Technology on Silk, Textile and Mechanicals i 2007:381-385.

(54) Kambe Y. Effects of RGDS sequence genetically interfused in the silk fibroin light chain protein on chondrocyte adhesion and cartilage synthesis. Biomaterials 2010.

(55) Deitzel JM, Kleinmeyer J, Harris D, Beck Tan NC. The effect of processing variables on the morphology of electrospun nanofibers and textiles. Polymer 2001 1;42(1):261-272.

(56) Wang H, Zhang Y, Shao H, Hu X. Electrospun ultra-fine silk fibroin fibers from aqueous solutions. J Mater Sci 2005 10/07;40(20):5359-5363.

(57) Park WH, Jeong L, Yoo DI, Hudson S. Effect of chitosan on morphology and conformation of electrospun silk fibroin nanofibers. Polymer, 2004 9/29;45(21):7151-7157.

(58) Zarkoob S, Eby RK, Reneker DH, Hudson SD, Ertley D, Adams WW. Structure and morphology of electrospun silk nanofibers. Polymer 2004 5;45(11):3973-3977.

(59) Li W, Mauck RL, Tuan RS. Electrospun Nanofibrous Scaffolds: Production, characterization, and applications for tissue engineering and drug delivery. Journal of Biomedical Nanotechnology September 2005;1:259-275(17).

(60) Sukigara S, Gandhi M, Ayutsede J, Micklus M, Ko F. Regeneration of Bombyx mori silk by electrospinning—part 1: processing parameters and geometric properties. Polymer, 2003 9;44(19):5721-5727.

(61) Fong H, Chun I, Reneker DH. Beaded nanofibers formed during electrospinning. Polymer 1999 7;40(16):4585-4592.

(62) Shenoy SL, Bates WD, Frisch HL, Wnek GE. Role of chain entanglements on fiber formation during electrospinning of polymer solutions: good solvent, non-specific polymer–polymer interaction limit. Polymer 2005 4/25;46(10):3372-3384.

(63) Larrondo L, St. John Manley R. Electrostatic fiber spinning from polymer melts. I. Experimental observations on fiber formation and properties. Journal of Polymer Science: Polymer Physics Edition 1981;19(6):909-920.

(64) van Ewijk GA, Vroege GJ, Philipse AP. Convenient preparation methods for magnetic colloids. J Magn Magn Mater 1999 7;201(1-3):31-33.

(65) Minoura N. Physico-chemical properties of silk fibroin membrane as a biomaterial. Biomaterials 1990;11(6):430.

(66) Magoshi J, Nakamura S. Studies on physical properties and structure of silk. Glass transition and crystallization of silk fibroin. J Appl Polym Sci 1975;19(4):1013-1015.

(67) Demura M, Asakura T. Immobilization of glucose oxidase with Bombyx mori silk fibroin by only stretching treatment and its application to glucose sensor. Biotechnol Bioeng 1989;33(5):598-603.

(68) Bhat NV. Investigation of the structure of silk film regenerated with lithium thiocyanate solution. Journal of polymer science.Polymer chemistry edition 1983;21(5):1273.

(69) Chen X, Knight DP, Shao Z, Vollrath F. Regenerated Bombyx silk solutions studied with rheometry and FTIR. Polymer 2001 12;42(25):09969-09974.

(70) Chen X, Shao Z, Marinkovic NS, Miller LM, Zhou P, Chance MR. Conformation transition kinetics of regenerated Bombyx mori silk fibroin membrane monitored by time-resolved FTIR spectroscopy. Biophysical Chemistry 2001 1/31;89(1):25-34.

(71) Liu LN, Zuo BQ. Fourier transform infrared spectrometric analysis of protein secondary structures of regenerated Antheraea Pernyi silk fibroins. Researches and Progresses of Modern Technology on Silk, Textile and Mechanicals i 2007:372-376.

(72) Xue YF, He CL, Mo XM. Electrospun spider nanofibers: the influence of ethanol on the structure and properties. 2007 International Forum on Biomedical Textile Materials, Proceedings 2007:178-181.

(73) Sofia S, McCarthy MB, Gronowicz G, Kaplan DL. Functionalized silk-based biomaterials for bone formation. J Biomed Mater Res 2001;54(1):139-148.

(74) Chen X, Zhou L, Shao Z, Zhou P, Knight D, Vollrath F. Conformation transition of silk protein membranes monitored by time-resolved FT-IR spectroscopy - Conformation transition behavior of regenerated silk fibroin membranes in alcohol solution at high concentrations. hua xue xue bao 2003;61(4):625-629.

(75) Kim S, Nam Y, Lee T, Park W. Silk fibroin nanofiber. Electrospinning, properties, and structure. Polym J 2003;35(2):185-190.

(76) Um IC, Kweon HY, Lee KG, Park YH. The role of formic acid in solution stability and crystallization of silk protein polymer. Int J Biol Macromol 2003 12;33(4-5):203-213.

(77) Um IC, Kweon H, Park YH, Hudson S. Structural characteristics and properties of the regenerated silk fibroin prepared from formic acid. International Journal of Biological Macromolecules 2001 8/20;29(2):91-97.

(78) Zhang P, Yamamoto K, Aso Y, Banno Y, Sakano D, Wang Y, et al. Proteomic studies of isoforms of the p25 component of \it bombyx mori fibroin. Biosci Biotechnol Biochem 2005;69(11):2086-2093.

(79) Iridag Y, Kazanci M. Preparation and characterization of Bombyx mori silk fibroin and wool keratin. J Appl Polym Sci 2006;100(5):4260-4264.

(80) Gosline J, Guerette P, Ortlepp C, Savage K. The mechanical design of spider silks: from fibroin sequence to mechanical function. J Exp Biol 1999 December 1;202(23):3295-3303.

(81) Ha S, Tonelli AE, Hudson SM. Structural studies of bombyx mori silk fibroin during regeneration from solutions and wet fiber spinning. Biomacromolecules 2005 05/01;6(3):1722-1731.

(82) Gotoh Y. Physical properties and structure of poly (ethylene glycol)-silk fibroin conjugate films. Polymer 1997;38(2):487.

(83) Tsukada M, Freddi G, Crighton JS. Structure and compatibility of poly(vinyl alcohol)-silk fibroin (PVA/SA) blend films. Journal of Polymer Science Part B: Polymer Physics 1994;32(2):243-248.

(84) Um I, Park Y. The effect of casting solvent on the structural characteristics and miscibility of regenerated silk fibroin/Poly(vinyl alcohol) blends. Fibers and Polymers 2007 12/11;8(6):579-585.

(85) Kharlampieva E, Kozlovskaya V, Wallet B, Shevchenko VV, Naik RR, Vaia R, et al. Co-cross-linking silk matrices with silica nanostructures for robust ultrathin nanocomposites. ACS Nano 2010 12/28;4(12):7053-7063.

(86) Mieszawska AJ, Kaplan D, Perry CC. Silk/silica nanocomposites as novel biomaterials for tissue Engineering. Biophys J 2009 2;96(3, Supplement 1):635a-635a.

(87) Zhang H, Magoshi J, Becker M, Chen J Y, Matsunaga R. Thermal properties of Bombyx mori silk fibers. Journal of Applied Polymer Science 2002; 86 (8) 1817-1820.

(88) Cunniff PM, Fossey SA, Auerbach MA, Song JW. Mechanical-properties of major ampulate gland silk fibers extracted from nephila-clavipes spiders. Silk Polymers 1994;544:234-251.

(89) Magoshi J, Magoshi Y, Nakamura S, Kasai N, Kakudo M. Physical properties and structure of silk. V. Thermal behavior of silk fibroin in the random-coil conformation. Journal of Polymer Science: Polymer Physics Edition 1977;15(9):1675-1683.

(90) Zarkoob S, Reneker D, Eby R, Hudson S, Ertley D, Adams W. Structure and morphology of nano electrospun silk fibers. Abstracts of papers - American Chemical Society 1998;216:U122-U122.

(91) Ha S, Gracz HS, Tonelli AE, Hudson SM. Structural study of irregular amino acid sequences in the heavy chain of bombyx mori silk fibroin. Biomacromolecules 2005 09/01;6(5):2563-2569.

(92) Belton DJ. From biosilicification to tailored materials: Optimizing hydrophobic domains and resistance to protonation of polyamines. Proc Natl Acad Sci U S A 2008;105(16):5963.

(93) Yeo I, Oh J, Jeong L, Lee TS, Lee SJ, Park WH, et al. Collagen-based biomimetic nanofibrous scaffolds: Preparation and characterization of collagen. Biomacromolecules 2008 APR;9(4):1106-1116.

(94) Gus'kova OA, Khalatur PG, Bäuerle P, Khokhlov AR. Silk-inspired 'molecular chimeras': Atomistic simulation of nanoarchitectures based on thiophene–peptide copolymers. Chemical Physics Letters 2008 8/8;461(1-3):64-70.

(95) Mieszawska AJ, Nadkarni LD, Perry CC, Kaplan DL. Nanoscale control of silica particle formation via silk-silica fusion proteins for bone regeneration. Chemistry of Materials 2010 10/26;22(20):5780-5785.

(96) Hou A, Chen H. Preparation and characterization of silk/silica hybrid biomaterials by sol–gel crosslinking process. Materials Science and Engineering: B 2010 3/15;167(2):124-128.

(97) Xu Q, Li J, Peng Q, Wu L, Li S. Novel and simple synthesis of hollow porous silica fibers with hierarchical structure using silk as template. Materials Science and Engineering: B, 2006 2/25;127(2-3):212-217.

(98) Jin HJ, Fridrikh S, Rutledge GC, Kaplan D. Electrospinning bombyx mori silk with poly(ethylene oxide). Abstracts of Papers of the American Chemical Society 2002;224:U431-U431.

CHAPTER 5
GELATION FOR MATERIALS FABRICATION

Two different fabrication methods (electrospinning and gelation) were used to generate silk-silica nano composite materials during this study. This chapter describes the fabrication of nano-composite materials through the gelation route, conformational changes, silicification of silk hydrogels and their detailed characterisation.

5.1- Introduction

Hydrogels are three dimensional networks formed by the suspension of homopolymer or copolymer in a medium (water in the case of hydrogels) and cross linked to form an insoluble matrix (1). The formation of cross linked hydrogels structures is a complex process and may involve different kinds of interactions such as covalent or ionic chemical bonds, polymer chain entanglement, microcrystalline

formation and/or the presence of hydrogen bonding and hydrophobic effects (2). Due to structural resemblances to the biological ground matrix and excellent biocompatibility (3), hydrogels have been widely used for a variety of biological applications including scaffold materials for tissue engineering (4-22), drug delivery (15,16,23-33), as barriers to improve healing response for tissues (4,34,35), cell encapsulation (36-44) and for certain prostheses for example, contact lenses (28,45-50).

Considering the unique properties of hydrogels, extensive research has been performed on both synthetic polymers (5,9,19,35,36,51-53) as well as natural polymers such as agarose (18), alginate (40,54-58), chitosan (10,23,54,59-61), hyaluronan (14,62-67) , fibrin (68-74), collagen (22,75-77), silk (6,20,41,78-89). Silk aqueous solutions can transform in to gels (hydrogels) and the sol-gel transition process may be affected by different parameters such as silk concentration, pH, temperature and the presence of additives (90).

In a detailed study of the gelation behaviour of *Bombyx mori* (BM) silk (90), gelation was observed to accelerate by increasing silk concentration, at higher temperature, low pH (acidic pH), addition of polyethylene oxide and the presence of calcium ions, however addition of potassium ions did not affect gelation time (90). Like other hydrogels, the formation of intermolecular and intramolecular interactions including hydrophobic interactions and hydrogen bonding results in the gel transition of silk solutions (91,92). Thus rise in the temperature and silk fibroin concentration increases such interactions and hence accelerates the gelation. During gelation the secondary conformation of silk changes from more soluble random coil to more insoluble β-sheet and improves the strength of physical cross links (90).

The structural differences in the H-chain and L-chain (described earlier) is also reflected in the aqueous solutions and their gelling behaviour. Before this study, there are no reports on the gelation behaviour of formic acid separated silk fractions. In the study described below, aqueous solutions made from variable proportions of light and heavy chain and total silk were buffered at a range of pH (3-9) and were studied for their gelation behaviour. Silk and silica based nanocomposites were fabricated by adding either hydrolysed tetraethoxy silane (TEOS) or pre-condensed silica nano-particles into the aqueous silk solutions before gelation. Nanocomposite materials formed were characterised for morphology (SEM), elemental composition (EDX), protein conformational changes (FTIR), and organic/inorganic composition by thermal analysis (TGA) and mechanical properties (compression testing).

5.2- Materials and methods

Details of all materials and methods used for studying the gelation behaviour are described in chapter 2 (2.1.3 and 2.3.1). Briefly, natural *Bombyx mori* silk, heavy and light chain silk fractions were regenerated as described (2.1.5) and the regenerated aqueous silk solutions were either concentrated up by dialysing against polyethylene glycol (PEG) or were diluted by adding deionised distilled water to adjust the final silk concentration.

For the silk gelation studies, a range of different silk solutions were buffered at a range of pH using bis-tris propane/citric acid (BT) buffer in 96 well plates. The final silk concentration of all solutions was maintained (3 wt %) and turbidity (as an early sign for the onset of gelation) was measured at regular intervals for about two weeks.

In order to make silk and silica composites, either pre-condensed Stöber silica particles of different sizes (table 5.1), or hydrolysed tetraethoxysilane (TEOS) as the silica precursor was added to the aqueous silk solutions (as described in 2.3.1).

5.2.1- Sample nomenclature

For ease of understanding and explanation, details of different samples, and their naming are given in Table 5.1.

Table 5.1: The description of gelation silk samples

Sample	Stage 1	Gelation times
T	Total silk	Different silk solutions were dialysed at room temperature to get aqueous silk solutions of the same final concentration and were blended in different proportions as mentioned
H	Heavy chain silk	
L	Light chain silk	
H90	90% H-Chain, 10% L-Chain	
H75	75% H-Chain, 25% L-Chain	
H50	50% H-Chain, 50% L-Chain	
H25	25% H-Chain, 75% L-Chain	
H10	10% H-Chain, 90% L-Chain	
	Stage 2	**Silk-silica composites**
S	Total silk	Dialysed total silk solutions were buffered at pH 7 using two different buffers and were mixed with silica solution (hydrolysed TEOS or Stöber silica nanoparticles) from different sources as mentioned.
S_0	Stöber silica	
SS_1	Stöber1 (11nm) and silk	
SS_2	Stöber2 (29nm) and silk	
SS_3	Stöber3 (64nm) and silk	
SS_4	Stöber4 (159nm) and silk	
ST	Silica from TEOS and silk	
T	Silica from TEOS	
BT	Bis/tris propane & citric acid buffer	
PP	Phosphate buffer	

5.2.2- Characterisation

The gelation behaviour of different silk solutions was recorded by turbidity measurements at 595 nm using a UV-Vis spectrometer (section 2.5.3). The morphology of silk nanocomposites and the effects of silicification treatments were studied using scanning electron microscopy (SEM), and elemental composition by EDX was used to confirm the presence or absence of silica (section 2.5.1). Thermogravimetric analysis (TGA) was used to explore the organic-inorganic composition and infra-red spectroscopy (ATR-FTIR) for protein conformation changes at different stages (section 2.5.2 and 2.5.4). The peak fitting process and parameters for deconvolution of FTIR spectra have been described in the chapter 4 (4.2.4).

5.3- Results and discussion

A number of studies have been conducted on the gelation behaviour of silk and silk composites (93-97). For the gelation studies, due to high insolubility, natural silk needs to be regenerated to prepare aqueous solutions. There is little or no published work on the formic acid separated BM silk fractions (L-chain and H-chain) that are explored in this study for gelation behaviour, morphology and conformational changes.

5.3.1- Gelation times and effect of pH and ethanol

In order to fabricate silk based materials through the gelation route, it is crucial to control the gelation time in a predictable manner. In order to fabricate material using a gelation route, silk solutions should not gel spontaneously so that sufficient time can be available for processing of the silk solution well before the start of gelation. Similarly, a delay in the gelation of a silk solution can prolong the experimental procedures and can also result in undesired outcomes and make the use of the gelation route for materials fabrication impractical . In studies of the gelation behaviour of silk, it is well known that it can be controlled by parameters such as silk concentration, temperature, pH, additives (90) and sonication (41).

In this study, the gelation behaviour of regenerated solutions of silk fractions and their blends in different proportions (table 5.1) was studied at a range of pH and was also compared with total silk. As silk gelation is highly dependent on concentration, for example, under the comparable conditions, a very high silk concentration can

result in spontaneous gelation whereas concentration below 4 wt% can take many days to start gelling (91,92), hence concentration of all samples were controlled at 3 wt% for this study.

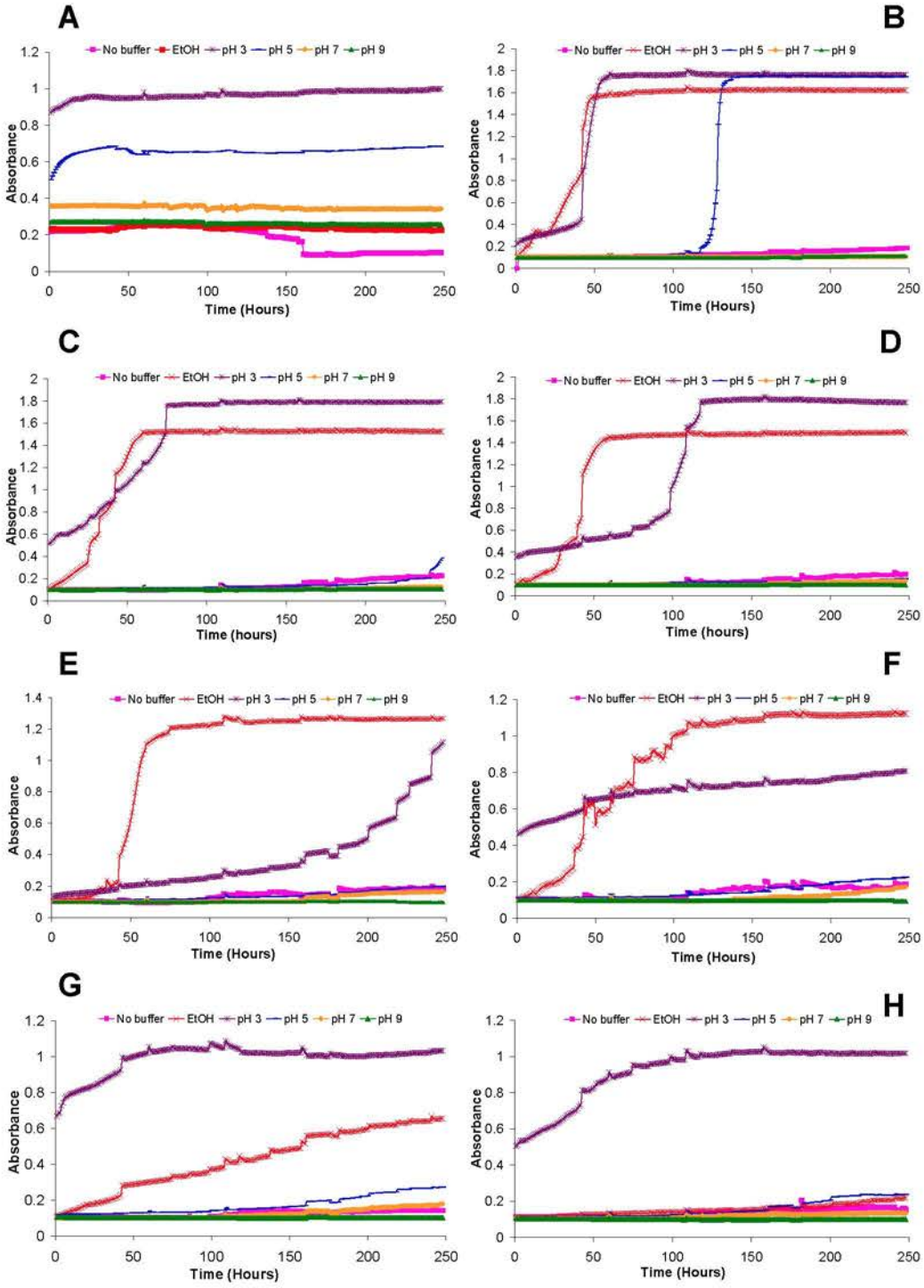

Figure: 5.1 Turbidity measurements in gelling silk solutions
A)- Total silk B)- H-chain C)- H90 D)- H75 E)- H50 F)- H25 G)- H10 H)- L-chain

In general, gelation was quicker at acidic pH for any solution, and all solutions (except total silk) were gelled within 4 days at pH 3 (Figure 5.1). The gelation behaviour of silk solutions at a range of pH is shown in table 4.2.

Table 5.2: Gelation behaviour of different silk solutions.

♦- Gelled ♦- Gelling ♦- Not gelled in 2 weeks

Sample	EtOH	pH 3	pH 5	pH 7	pH 9	No buffer
H	Day 2	Day 2	Day 5			
H90	Day 3	Day 3				
H75	Day 3	Day 4				
H50	Day 4	Day 5				
H25	Day 7	Day 5				
H10		Day 6				
L		Day 7				
T						

The H-chain and L-chain ratio was observed to influence the gelation time over a wide range of pH and took 2 days and 5 days to gel at pH 3 and 5 respectively (Figure 5.1-B). In contrast, L-chain silk solutions were not gelled under any condition except at pH 3 (Figure 5.1-H). Similarly, varying H-chain content was observed to affect the gelation behaviour on the combination silk solutions (H90, H75, H50, H25 and H10) and all gelled in 3-5 days at pH 3 (Figure 5.1-C-G). These results were compared with gelation behaviour of no buffer solutions (buffer was replaced by the same volume of deionised distilled water) and ethanol (EtOH) solutions (buffer was replaced by the same volume of 99.9 % ethanol). As un-buffered silk solutions had basic pH (7.9-8.8) no signs of gelation were observed in any "no buffer" samples. In contrast, EtOH in the samples accelerated the gelation in H-chain containing samples and resulted in gelation of these samples within 2 days (even more rapid than at pH 3). The only exceptions were samples H25 and H10 where they took longer due to presence of more proportion of L-chain (75 % and 90 % respectively) in these samples.

The transition of silk solutions to hydrogels occurs due to changes in the secondary conformation from α-helix and random coil to β-sheet that reduces the solubility of silk fibroin in water and encourages the formation of physical cross linking and gelation (91,92). The addition of a small amount of ethanol also works on the same principle i.e. by increasing the proportion of β-sheet thus accelerating the gelation process (98). The structural difference between β-sheet, random coil and β-turn are shown schematically in Figure 4.1 and the effect of ethanol treatment on the electrospun mats to enhance β-sheet contents has been discussed in detail in chapter 4.

It is crucial to mention that the diverse gelling behaviour of H-chain may be the reflection of primary and secondary structural differences in the H-chain silk. For example, the primary structure of H-fibroin is formed by the highly repetitive sequence of GAGAGS, GAGAGY and GAGAGVGY amino acids (99-101), that are mainly hydrophobic (101) and sufficient hydrophobic interactions finally result in hydrogels formation (102). In order to assess this, the secondary structure of natural silk and fractions before and after regeneration was studied using ATR-FTIR. The H-chain in the natural form showed significantly higher amount of β-sheet (76.7 %) than total silk (59.24 %) and L-chain (55.8 %) Figure 5.2-A, however, in regenerated silk solutions, H-chain showed slightly more β-sheet (5.2-B). Another difference is the significantly lower amount of β-turn in H-chain suggesting the presence of longer polymer chains that are prone to chain entanglement and hydrophobic interactions upon folding and accelerating the aggregation.

Another critical parameter related to the pH of silk solutions is the isoelectric point (p*I*). Isoelectric point (p*I*) of a polymer is the pH at which equal numbers of positively charged and negatively charged residues exist in the solutions (103). For the p*I* of a polymer, the electrostatic repulsive forces between residues are minimal due to the net balance of negative and positive charge and this accelerates the aggregation of proteins (104).

The isoelectric point for silk fibroin is 3.8-3.9 (91,92,105), hence at a pH around 3 (very close to the p*I* of silk fibroin), the interactions between silk molecules is increased by decreasing the repulsive forces giving more potential for β-sheet formation leading to hydrophobic interactions and accelerating the sol-gel transition (90).

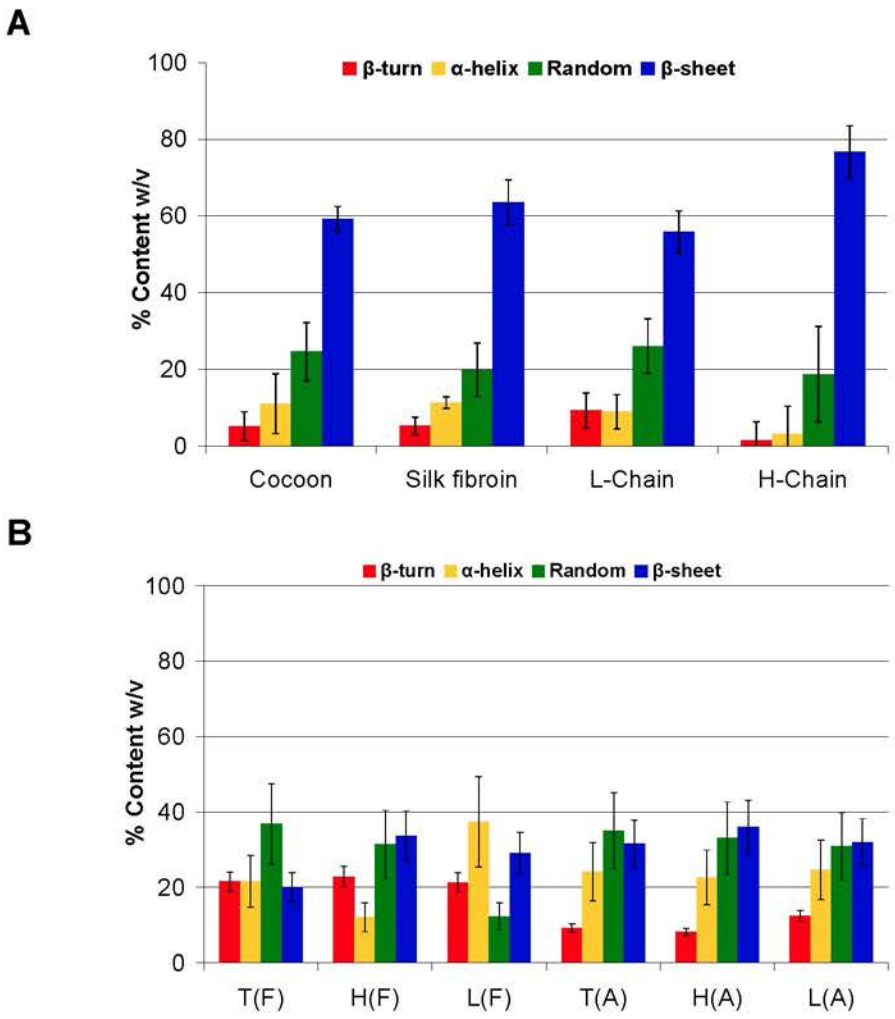

Figure 5.2: Quantitative comparison of secondary conformations in different silk materials A) - Natural silk and fractions (H-chain is having significantly more β-sheet B)- Regenerated silk solutions; Air dried (A) compared with freeze dried (F), the difference in β-sheet content is insignificant.

These results suggested that the acidic pH and addition of ethanol accelerates the formation of β-sheet structure in the silk gelation process and induces the gelation of silk solution in 2-4 days even at a very low concentration (3 wt %). As the process of silk hydrogel formation has been observed to be affected by a number of other contributing factors previously such as increasing the silk concentration (90), temperature (90), In order to control the silk gelation process, a strict monitoring of all factors affecting gelation is required in further studies to develop functional nanocomposites.

5.3.2- Morphology of silk hydrogels

Scanning electron microscopy is the major tool that has been used extensively to explore the surface morphology of silk materials (90,106-109). In general, lyophilised silk composite materials show a network and sponge like structure (Figure 5.3). In contrast to electrospun materials, no fibrous structures were observed in these materials. The SEM images of all samples prepared using BT buffer are shown in column A and B whereas samples prepared in phosphate buffer are shown in column C and D of Figure 5.3. There are no structural differences observed in the morphology of materials fabricated using the two different buffer systems.

Similarly, no correlation was observed in the morphology of materials based on different types of silica, the only exception was SS_4 where Stöber silica particles were observed embedded in to the silk matrix at a high magnification (Figure 5.3-SS_4/B and D).

5.3.3- Silicification of silk hydrogels

The presence of silica in the silk based composite materials was confirmed by FTIR and elemental analysis (EDX). The FTIR spectra produce characteristic absorption peaks for Si-O-Si bonds at 800 cm^{-1}, for Si-OH vibration at 850-950 cm^{-1} and for asymmetrical stretch of Si-O-Si bond around 1100 cm^{-1} (110). The FTIR spectrum of silk-silica composites (ST, SS_1, SS_2, SS_3, and SS_4 in the phosphate buffer) produced characteristic absorbance peaks for the symmetrical and asymmetrical stretch of Si-O-Si bonds suggesting the presence of silica (Figure 5.4).

All samples prepared using BT buffer could not be analysed using FTIR due to the interference of overlapping peaks coming from the bis-tris propane/citric acid buffer compounds (mainly carbonyl bond of citric acid with amide I band of silk); however materials from both buffers were compared by EDX elemental analysis (Figure 5.5). In Figure 5.5, EDX spectra for sample ST (A/left half), for SS_4 (B/right half) and elemental maps for carbon (C), oxygen (O), silicon (Si), sodium (Na) and phosphorous (P) are shown. In sample SS_4, alongside peaks representing C, O and N coming from silk, Si and O from silica, prominent peaks for Na and P were observed from the phosphate buffer. The spectra for the ST sample differed for Na and P peaks that appeared very small corresponding to their absence in the BT buffer. The abundance of silica was confirmed in both samples by EDX spectra as well as elemental mapping; however considerable difference in distribution of silica

in both samples was seen. For ST, where pre-hydrolysed TEOS was used as the silica precursor, the condensation of silica appears in certain areas (pointed out by red circles on the SEM image) and clearly evident in the elemental maps of Si and O. In contrast in SS_4 where pre-condensed silica particles were used, a generalised and homogeneous distribution of silica was observed (Figure 5.5).

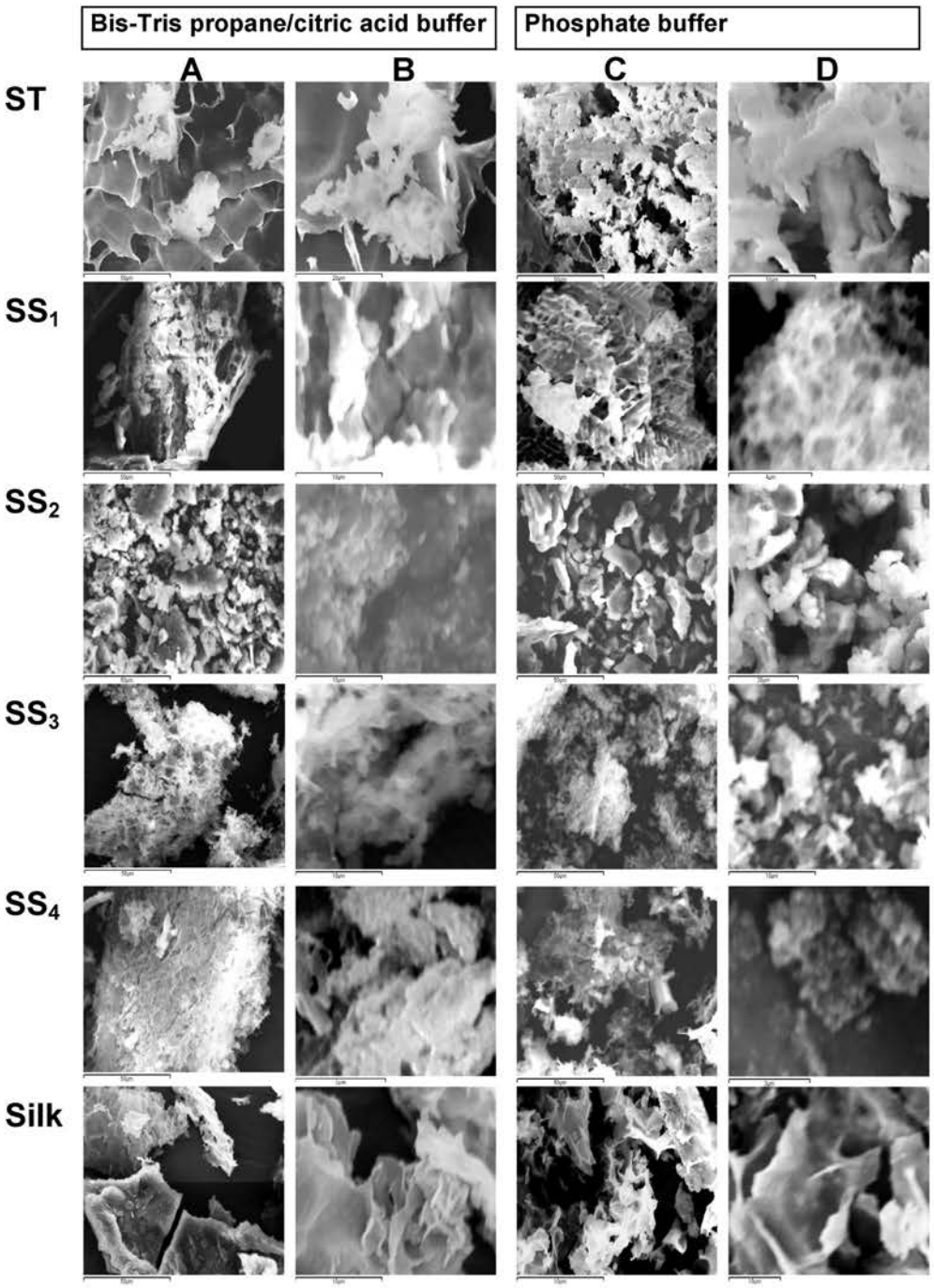

Figure 5.3: SEM image of different lyophilised silk and silk/silica composites fabricated using bis-tris propane/citric acid buffer (A and B) and phosphate buffer (C and D).

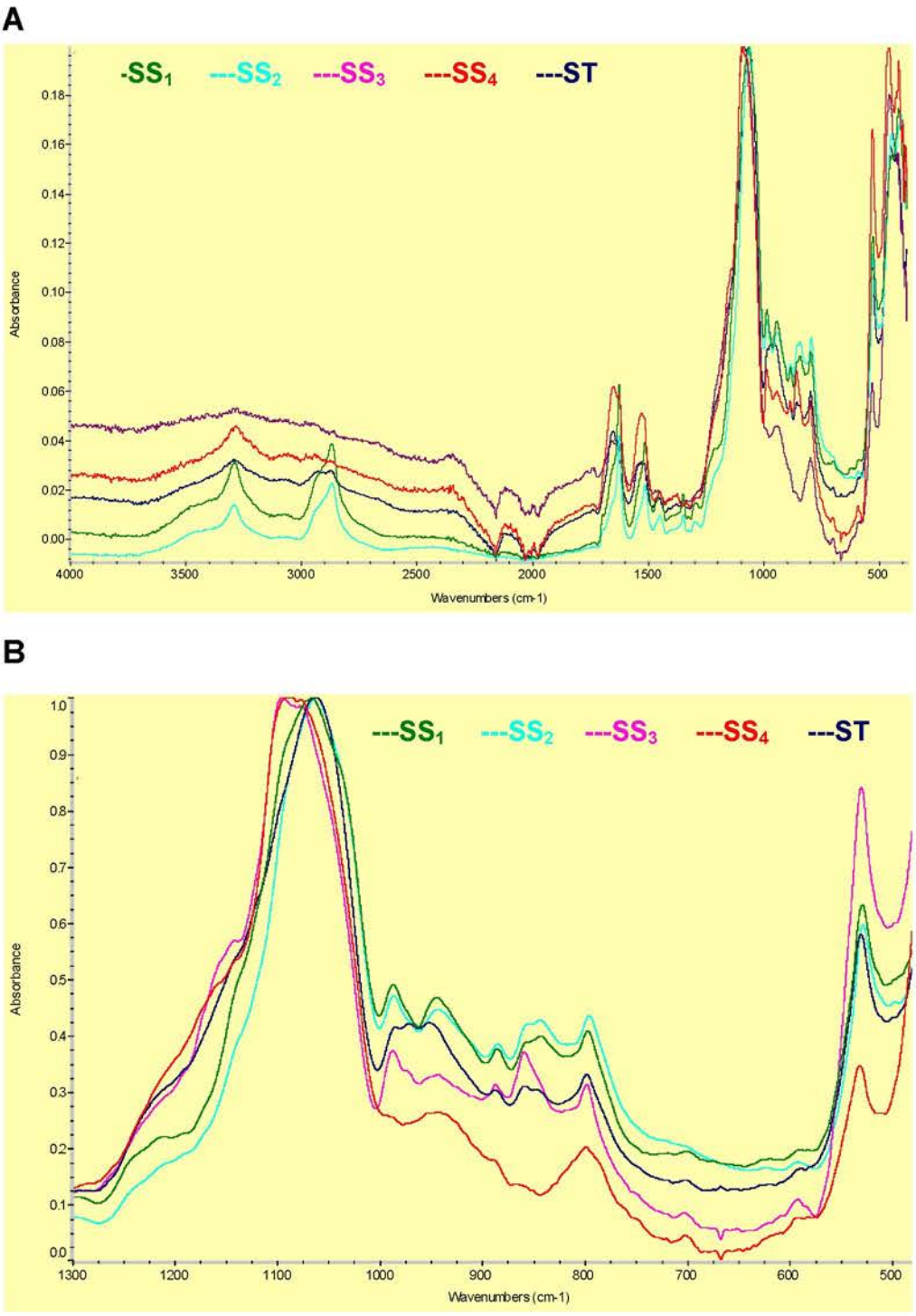

Figure 5.4: FTIR spectrum for silk and silica composites fabricated using gelation route. A)- Full spectra, B)- Relevant segment. Coloured lines representing; **___ (ST), ___ (SS_1), ___ (SS_2), ___ (SS_3), ___ (SS_4)**

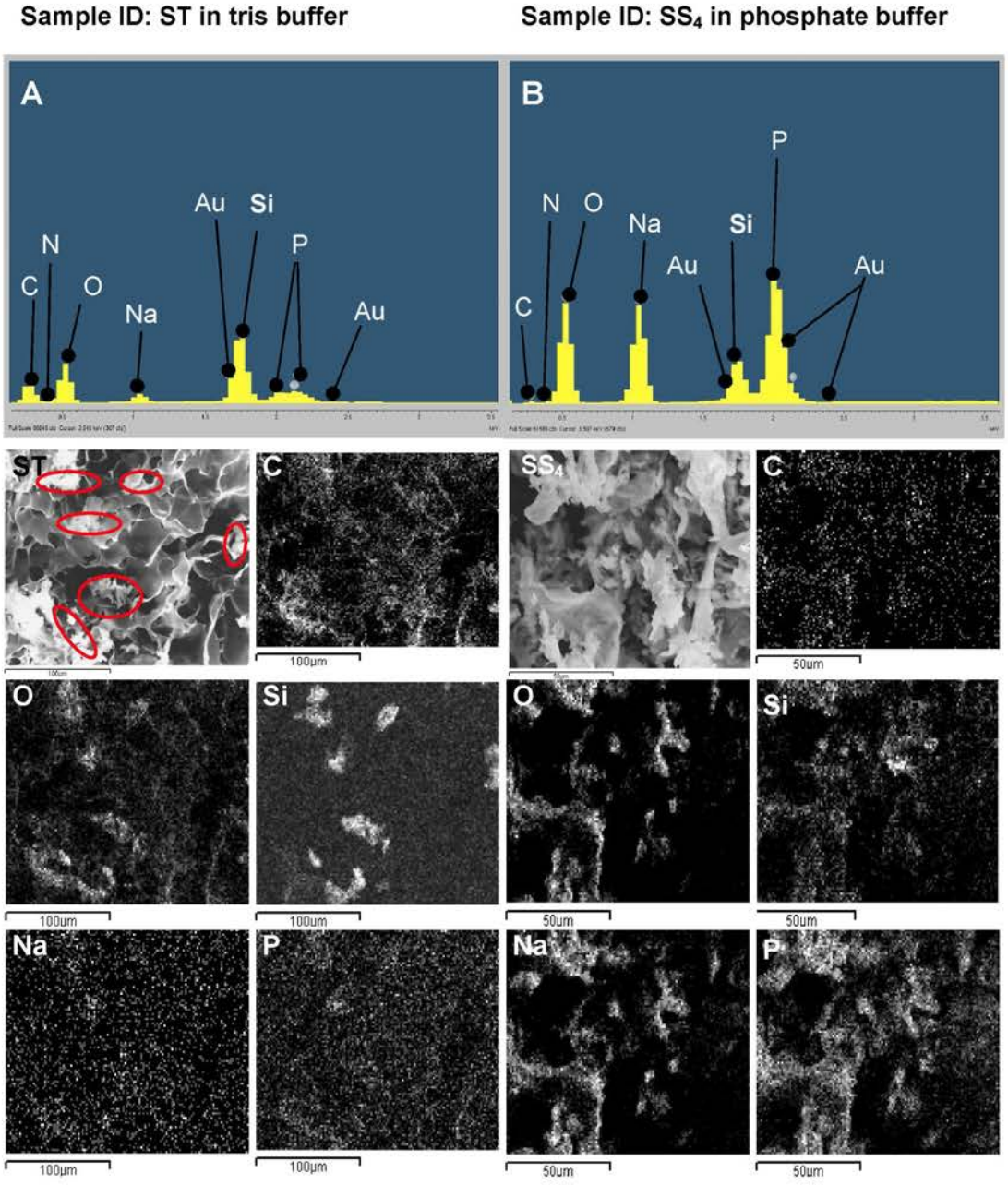

Figure 5.5: EDX spectra for A)- Sample TS in bis-tris propane/citric acid buffer and B)- Sample SS4 in phosphate buffer. Elemental maps for carbon (C), oxygen (O), silicon (Si), sodium (Na) and phosphorous (P)

The condensation of silica is a complex process and can be affected by certain parameters, such as pH and additives including presence or absence of polyamines (111). During the silica condensation process, water molecules are generated and quick removal of these water molecules can provide the driving force for the condensation (112). Similarly, due to the water repulsion ability of hydrophobic

domains present in the silk fibroin these can prevent the silica condensation around them. In contrast, Stöber silica is pre-condensed silica particles and was dispersed homogeneously in the solutions and not affected by the hydrophobicity of silk proteins.

5.3.4- Conformational analysis

The mechanical properties of silk based composite materials can be improved by enhancing β-sheet conformation (113) and has been discussed in chapter 4 (4.3.2). Infra-red spectra obtained using attenuated total reflectance (ATR) has been frequently used (114-118) to study silk conformational changes and the quantitative analysis of ATR-FTIR spectra were performed by de-convolution using a peak fitting method as described in chapter 4 (4.2.4).

The secondary conformation was studied for different silk gels dried in two different ways; air dried and lyophilised. The air dried silk gels were allowed to dry in air in the fume hood at room temperature, whereas in lyophilisation, silk gels were frozen using liquid nitrogen and dried in vacuum at -60 °C. In general, air dried silk gels produced significantly higher amounts of β-sheet compared to the corresponding freeze dried samples (Figure 5.6-A).

The β-sheet content for air dried total, H-chain and light chain silk gels were 50.6 ± 9.8 %, 57.7 ± 11.2 % and 57.4 ± 11.1 % respectively and for lyophilised gels, β-sheet content was 30.0 ± 5.9 %, 44.0 ± 8.6 % and 29.9 ± 5.8 % correspondingly. Another remarkable change was a significant drop in the random coil content suggesting that random coil mainly contributed to β-sheet conversion with alongside other conformations.

There was remarkable shrinkage in silk gels upon air drying with irregular shaped pieces being produced, whereas lyophilisation resulted in white spongy granular structures showing little overall change in size or dimensions. An X-ray diffraction study has shown that more crystallinity is produced upon air drying of silk based gels and better strength materials are also obtained (119). It can be suggested that air drying is a slow process at room temperature and silk fibroin molecules have sufficient time to move and arrange into a more organised β-sheet structure. Alongside an increase in β-sheet (upon air drying), contraction of silk gels might also have contributed to increased physical strength and crystallinity as described by Li et al (119). In contrast, during the lyophilisation process, silk gels are frozen and silk fibroin molecules cannot reorganise due to lack of molecular movements in the solid matrix.

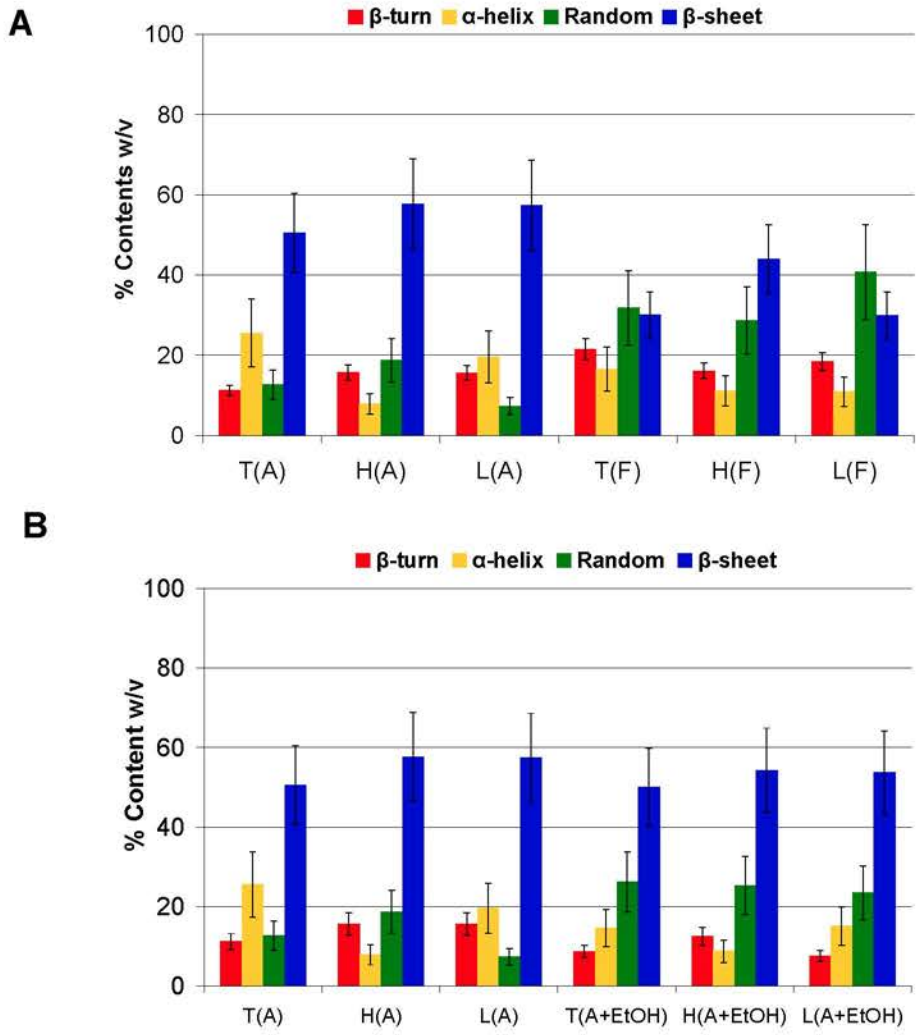

Figure 5.6: Quantitative comparison of secondary conformations in different silk gels A)- Air dried gels (A) compared with freeze dried (F), where air dried gels showed significantly higher β-sheet content than freeze dried silk gels B)- Effects of ethanol treatment on air dried silk gels, no significant differences were observed in protein conformation

As shown above (Figure 5.6-A), the β-sheet content for air dried silk gels was more than 50 % and that is more than β-sheet content (40-50 %) present in natural BM silk (120,121) and surprisingly, that high contents of β-sheet were attained without using any ethanol or annealing treatment of these gels. As ethanol treatment of electrospun mats (chapter 4), a significant increase in the β-sheet content was observed mainly from transition of coil and β-turn to β-sheet, hence air dried silk gels were also treated with ethanol in attempt to increase further the β-sheet content. In contrast to other silk materials (electrospun, films and freeze dried), ethanol treatment did not result in any increase in β-sheet contents; instead a slight decrease in β-sheet was observed (Figure 5.6-B). These results suggest that air

drying results in the highest possible β-sheet content (even more than natural silk) and this may represent the full extent of β-sheet capacity.

The ATR-FTIR spectra for silk based composite were obtained for conformational changes in the presence of silica. However, data from composite materials fabricated using BT buffer could not be analysed due to overlapping peaks of buffer and silk fibroin. The presence of silica for samples fabricated using phosphate buffer was confirmed (Figure 5.4) and data was analysed for conformational changes (Figure 5.7).

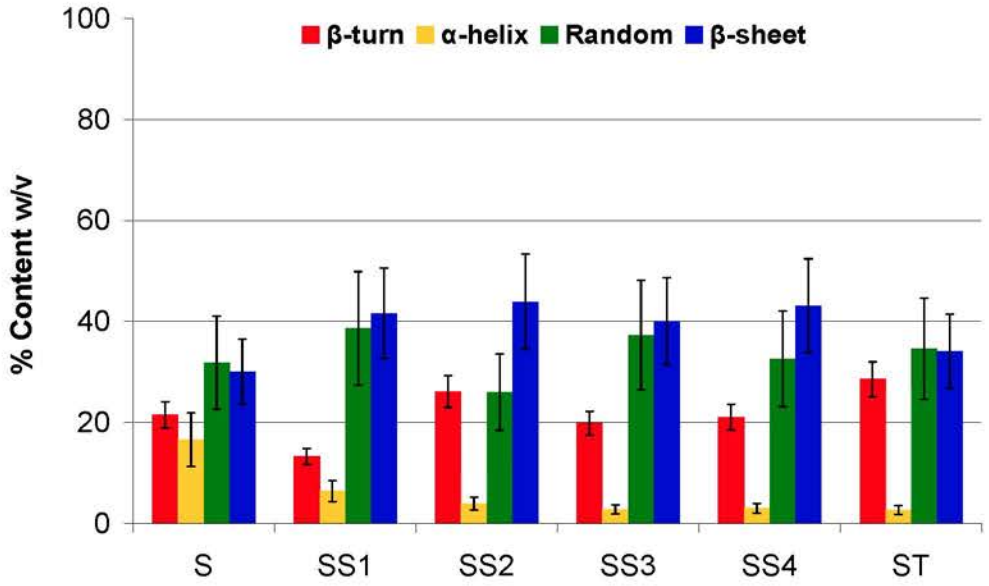

Figure 5.7: Quantitative comparison of secondary conformations in silk based composite materials.

In general, there was significantly more β-sheet content in composite materials (SS_1, SS_2, SS_3, SS_4 and ST) than silk hydrogels (S). The β-sheet content were 30.02 ± 6.15 % in silk hydrogels and increased to 40-43 ± 8.15 % for silk-Stöber silica composites (Figure 5.7) and 34.15 ± 7.0 % for silk-TEOS (ST) composites. As a result, a decrease in other conformations was observed particularly α-helix that was reduced from 16.6 ± 5.15 % in silk hydrogels to 2.6-6.4 % for silk composite materials alongside a slight decrease in β-turn. Such conformational changes to increase β-sheet content in silk composite are very likely due to the presence of high ethanol content in the hydrolysed TEOS solution and Stöber silica suspensions. Comparing the TEOS and Stöber based composites, there was slightly less β-sheet content in ST (34.15 ± 7.0 %) with a little bit of extra β-turn (Figure 5.7), suggesting

relatively smaller chain length and weak mechanical properties in ST. In comparison, the ethanol treatment of electrospun mats resulted in β-sheet content as high as 42-51 % (data shown in chapter 4) that is higher than materials produced by gelation (up to 43 %). The unique feature of electrospun materials such as surface area (higher than silk films, gels and granules) may facilitate the action of ethanol hence increasing β-sheet content.

5.3.5- Thermal analysis of silk-silica nanocomposites

The thermal behaviour of silk-silica composites was studied using Thermogravimetric analysis (TGA). The TGA curves for all samples and their relevant buffer are expressed in Figure 5.8. Similar to electrospun samples, the weight loss and temperature changes, for gelation silk samples can be demonstrated to occure in four distinct steps,

I) Initial weight loss of about 6-7 % for temperature of 0-150 ° C considered to be the evaporation of water.
II) There is almost no or very little change in residual weight for up to 190 ° C suggesting the stability of silk in this range.
III) A sharp decrease in weight from 195 ° C to around 450 °C suggesting major thermal decomposition of silk protein.
IV) Finally, complete removal of residual carbon at a very slow rate between 576 °C-700 ° C.

The TGA data for silk alone and buffered silk (S and S+buffer) is very similar to the thermal analysis of *Bombyx mori* silk cocoons and silk fibres (Figure 5.8), where others have found initial weight loss of (9% for cocoon and 8.2% for silk fibre) as result of water evaporation followed by a sharp decrease in the weight from 150 to 450℃ as a result of silk degradation (122).

In S+buffer samples, there was complete combustion with slight delay in the BT buffer due to organic nature of BT whereas residual weight of 13 % consists of sodium phosphate which remained from the phosphate buffered samples. Due to the difference in the nature of both buffers, a change in the residual weight of both buffers is clearly evident in all samples (Figure 5.8-A and B). For silk composites, 3-6 % weight loss was observed (water loss) to 250℃ suggesting these materials are stable to these temperatures and silk based materials can be autoclaved without the loss of primary structure (123,124) hence, fulfilling a vital requirement needed for

biological applications. For both buffers, SS_1 (the smallest Stöber silica particles) showed the most weight loss compared to all composite samples. Due to the unique properties of nano particles such as high surface area and high surface energy, they entrapped most organic matrix and water resulting in more weight loss. In phosphate buffer (Figure 5.8-B), there is clear trend of increasing residual weight by increasing the particle size with the most residual weight being for TEOS silica sample (ST).

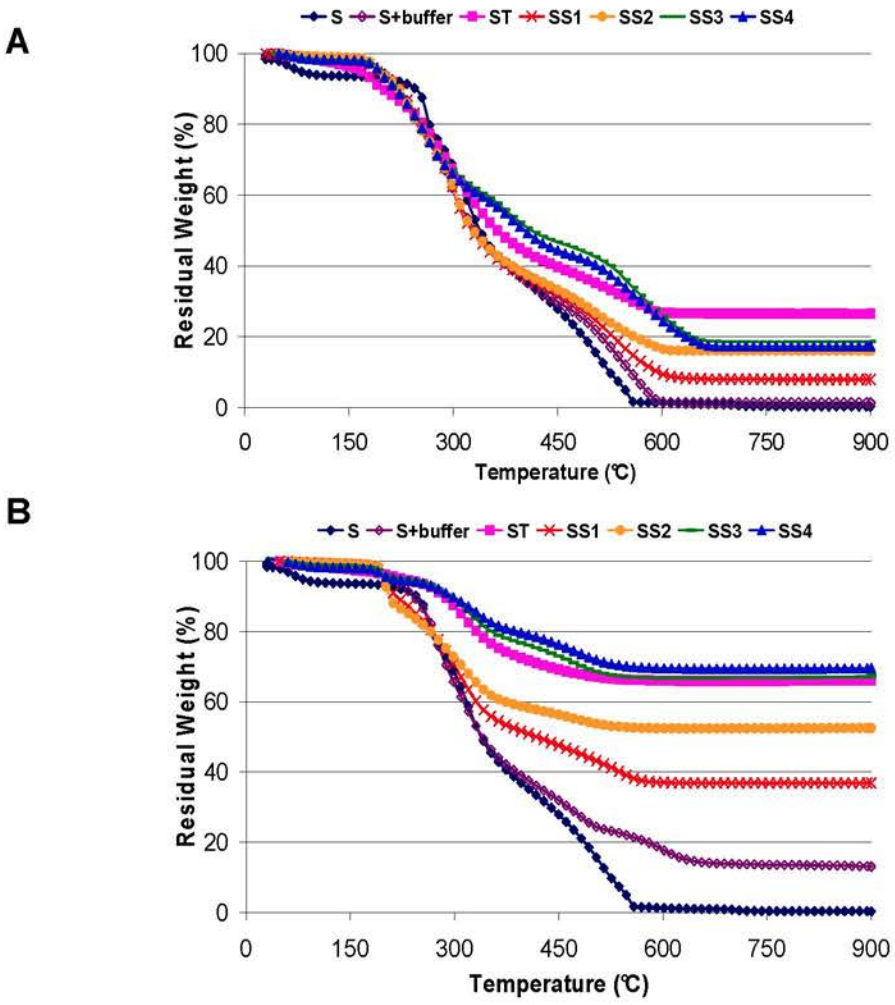

Figure 5.8: TGA curves for gelation silk composite materials A)- In bis-tris propane/citric acid buffer (BT), B)- In phosphate buffer

For samples in BT buffer (Figure 5.8-A), S and S+buffer were completely combusted suggesting no inorganic contents. In silk composite samples, the amount of residual weight representing inorganic content was 26 % for ST, and 8-17 % for silk-Stöber silica composites. For samples in phosphate buffer (Figure 5.8-B), the presence of

inorganic buffer contributed towards residual weight by increasing up to 66-69 % for ST, SS_3 and SS_4 followed by 52 % and 36 % for SS_2 and SS_1 respectively. This difference in inorganic contents is due to differences in the silica sources of TEOS and Stöber silica. Stöber silica is pre condensed silica particles and least likely to undergo any changes while mixed or suspended physically with gelling silk solutions, whereas hydrolysed TEOS condenses silica in the presence of silk fibroin and the presence of hydrophobic domains from silk specially from H-chain which can assist the silica condensation (125) and condensing silica can also be entrapped in the hydrophobic segments during the condensation process (112). This is a vital relationship of hydrophobic domains of silk fibroin that affects silica condensation from silica precursors such as TEOS as uneven condensation of TEOS silica within the sample was demonstrated by EDX, however this process was unlikely to influence pre-condensed silica as in case of Stöber particles.

5.3.6- Mechanical testing

For development of new materials, it is crucial that they have the strength to withstand and tolerate stresses for the intended application. Mechanical testing can be helpful to predict a material's behaviour to forces. For dentin tissue engineering, the scaffold material should be strong enough to support growing odontoblast process. For this purpose, nano composite materials were prepared in 96 well plates using the method described in chapter 2 (2.3.1.1) and were analysed by compression testing as described in 2.5.5.4. Briefly, different variables used are listed below.

- Silk contents (0-5 %)
- Silica contents (0-6 mg)
- Silica source (TEOS or Stöber particles) and silica particle size as well in case of Stöber silica
- Bis-tris propane and phosphate buffer at pH 7

The initial concentration of dialysed silk solution was 7.5 wt % however the final silk concentration in composite hydrogels was reduced (0-5 wt %) after addition of buffer and silica solution. The final silk concentration and their corresponding masses in the dried composite samples are presented in table 5.3.

Table 5.3: Final concentration of silk and corresponding silk weight								
[Silk] %	0	1	1.5	2	3	4	4.5	5
Silk (mg)	0	3.75	5.62	7.50	11.24	15	16.88	19.12

Silk regeneration results in loss of its excellent mechanical properties and presents a major problem in their practical applications (126). The purpose of silica addition was to manipulate the final mechanical properties of the composite materials.

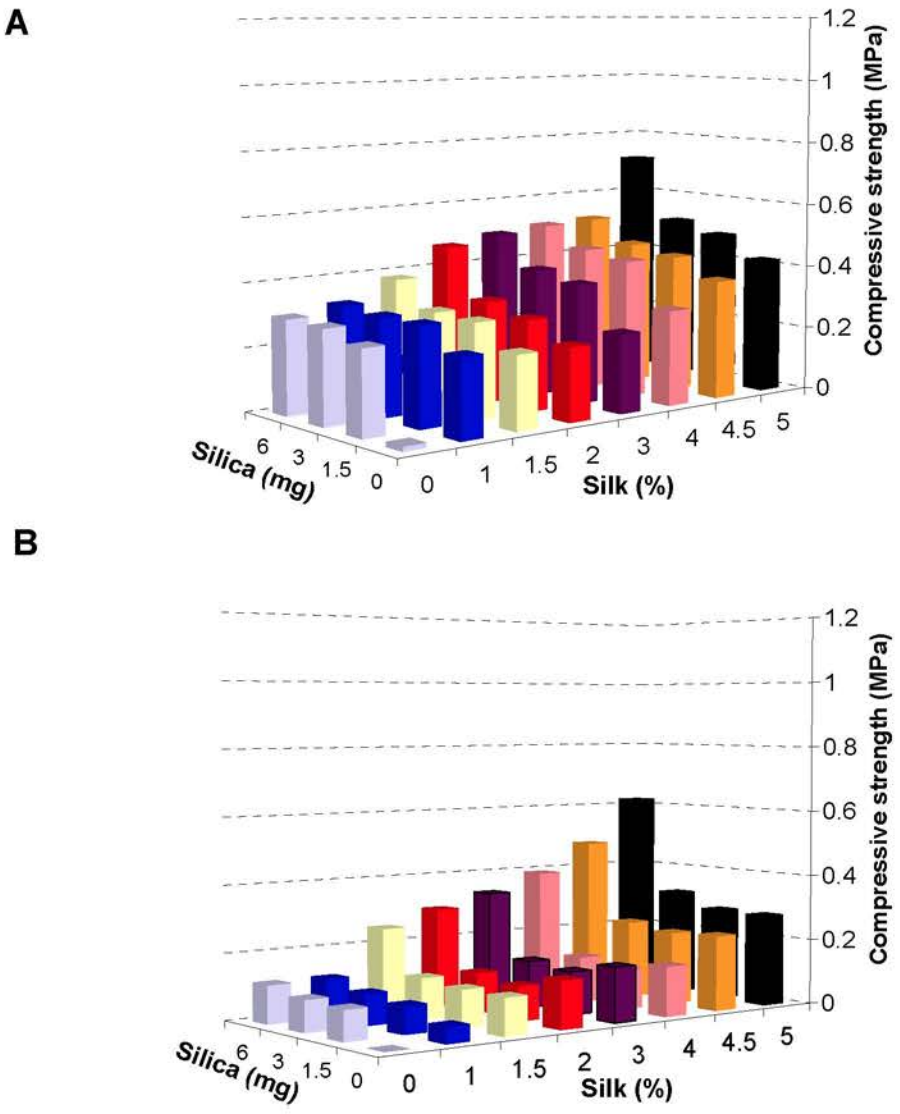

Figure 5.9: Compressive strengths of silk composites based on TEOS condensed silica; A) - In bis-tris propane citric acid buffer B) - In phosphate buffer

In general, all silk composite materials presented a very low compressive strength (Figure 5.8 and 5.9) for the range of silk concentration used, regardless of buffer.

The compressive strength of silk and TEOS condensed silica are compared in two different buffer systems (Figure 5.9). All materials had a very low strength with a compressive strength (σ_c) of 0.2 to 0.4 MPa for the highest silk samples (4-5 %) and even lower compressive strength (σ_c) for low silk concentration samples. These findings are very similar to a previous study (90) where they found very low compressive strength (σ_c) for up to 4 % silk solutions however σ_c was observed to increase more than 2.5 MPa for 16 wt % samples. The improved strength of silk materials is due to reduced pore size with increase in concentration (90). The smaller pore size can resist the stress concentration better and distribute stresses in the materials more consistently and plays a vital role in preventing the crack propagation through the material (90).

The addition of silica using hydrolysed TEOS played its role by improving the σ_c of silk composites (for all silk concentrations) to some extent (Figure 5.9). The σ_c of composites was improved further by increasing the amount of silica, with maximum σ_c of 0.6 to 0.75 MPa for sample with 5 % (19.12 mg) silk and 6 mg silica. All samples prepared using bis-tris propane/citric acid buffer (BT) generally showed clearly better σ_c than samples prepared using phosphate buffer (Figure 5.9 A and B). This difference seems to be due to the organic nature of BT buffer giving more flexibility to the final material whereas the inorganic nature of phosphate buffer made samples more brittle. These trends suggested that σ_c silk composites can be improved/increased by addition of silica and can further be improved by increasing the proportion of silica and silk.

The effects of pre-condensed Stöber silica nanoparticles on the σ_c of silk composites are described in Figure 5.10. There are similar results in terms of silk concentration and silica contents as described above for TEOS silica (Figure 5.9), i.e. σ_c was observed to improve by increasing silk and/or silica contents. In case of Stöber silica nanoparticles, different buffers did not seem to affect the strength of these materials, as Stöber silica is in the form of pre-condensed particles and distributes evenly throughout the gelling silk matrix.

However, composites with Stöber silica nanoparticles had significantly better σ_c compared to corresponding samples of TEOS silica (Figure 5.10, data shown for sample SS_3). An addition of just 3 mg improved the compressive strength of 2 % silk solutions up to 0.5 to 0.62 MPa and further increased to more than 1 MPa for 4 % silk samples and more than 1.5 MPa for 5 % silk samples. The compressive strength of TEOS silica materials remain below 0.75 MPa even upon addition of 6

mg (double the amount of Stöber silica), suggesting that Stöber silica can improve mechanical properties better that TEOS.

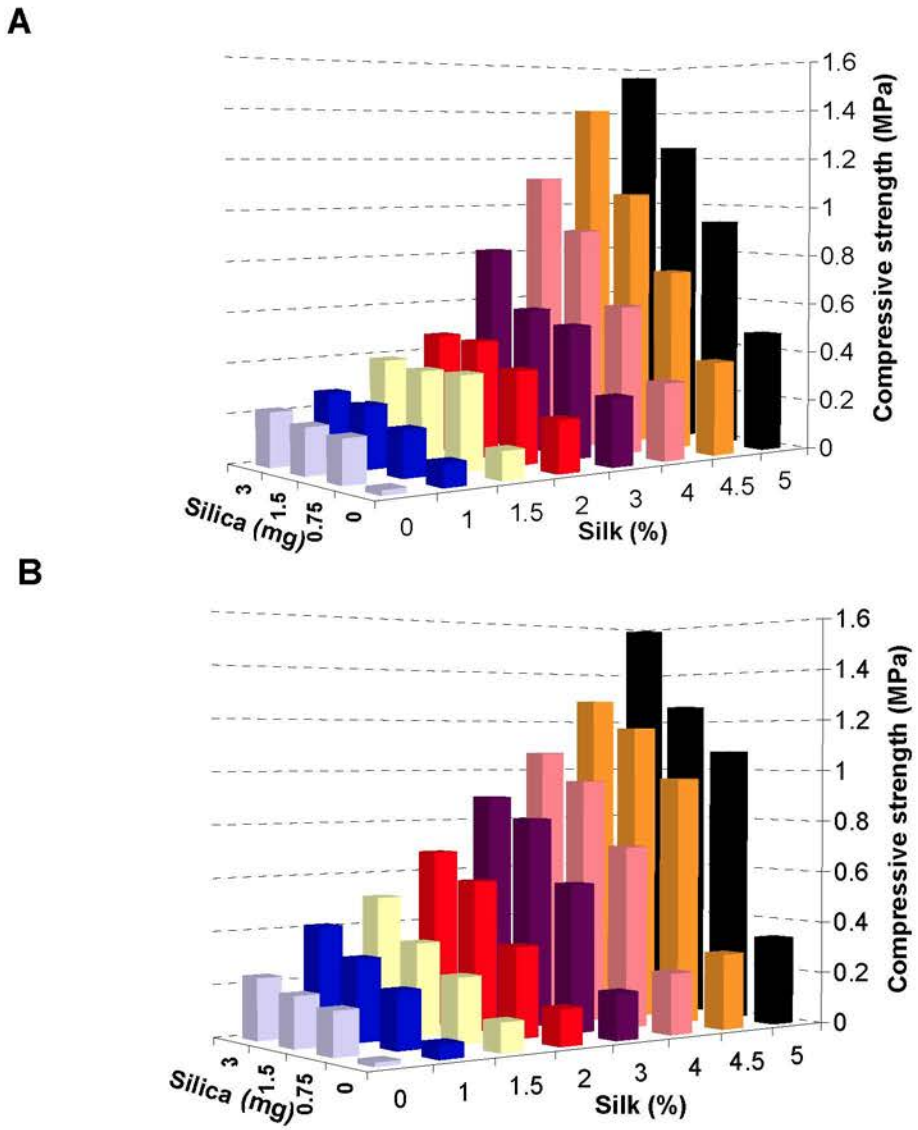

Figure 5.10: Compressive strengths of silk composites based on Stöber silica nanoparticles; A) - In bis-tris propane citric acid buffer B) - In phosphate buffer

This difference in the compressive strength may be due to the fact that Stöber silica is suspended particles that distribute uniformly in the silk matrix and absorbed applying forces better hence preventing the stress concentration and crack propagation. In contrast, TEOS silica is condensed in the silk matrix and can be influenced by the surrounding matrix such as hydrophobic domains present in the silk fibroin. Such hydrophobic domains have more affinity for silica condensation and

can assist silica condensation around them (112). The localised deposition of silica condensation was observed by EDX analysis (Figure 5.5) that can facilitate the stress concentration in the matrix around inorganic silica, crack propagation and failure of the composite materials. In addition, ethanol is produced as by product during silica condensation from hydrolysed TEOS (110) and removal of this ethanol during the drying process can further weaken the materials. All these factors contributed towards the relatively low compressive strength of composite materials from TEOS condensed silica.

It is worth mentioning another important contributing factor, the final density of the materials that was dependent on the mass of silk and silica in each sample. In order to calculate the density of each sample, the volume of a well of 96 well plate and materials density was calculated.

Volume of a well (v) = 3.14 x $(0.0033\ m)^2$ x (0.0106 m)
= 3.8 m^{-3} or 0.38 cm^{-3}

Material density = M/v ---------- (Eq 5.1)

Where 'M' is total mass of the material

The density of silk-silica composites was dependent on total mass of silk, silica and buffer in the sample and was calculated to be between 0 - 0.1 mg/ml that is very low compared to solid materials. Density of silk composite was found to be directly related to the compressive strength (Figure 5.11). The increase in density either by increasing silica content (Figure 5.11-A) or by increasing silk content (Figure 5.11-B) can increase the compressive strength in both buffers using either silica source.

The compressive strength was as low as 0.2 MPa or lower at a density of 0.031 g/ml and increased up to 1.6 MPa for denser (0.082 g/ml or more) materials. Silk has comparatively enhanced role in improving mechanical strength by increasing density. In a comparison at fixed material density of 0.082 g/ml, Figure 5.11-A, where density was increased using silica (fixed silk contents of 19.12 mg) resulted in lower compressive strength as shown in Figure 5.11-B where density was increased using silk (fixed silica content of 3mg per sample). In addition, Stöber silica containing composites have significantly higher compressive strength for a whole range of density in both buffering systems.

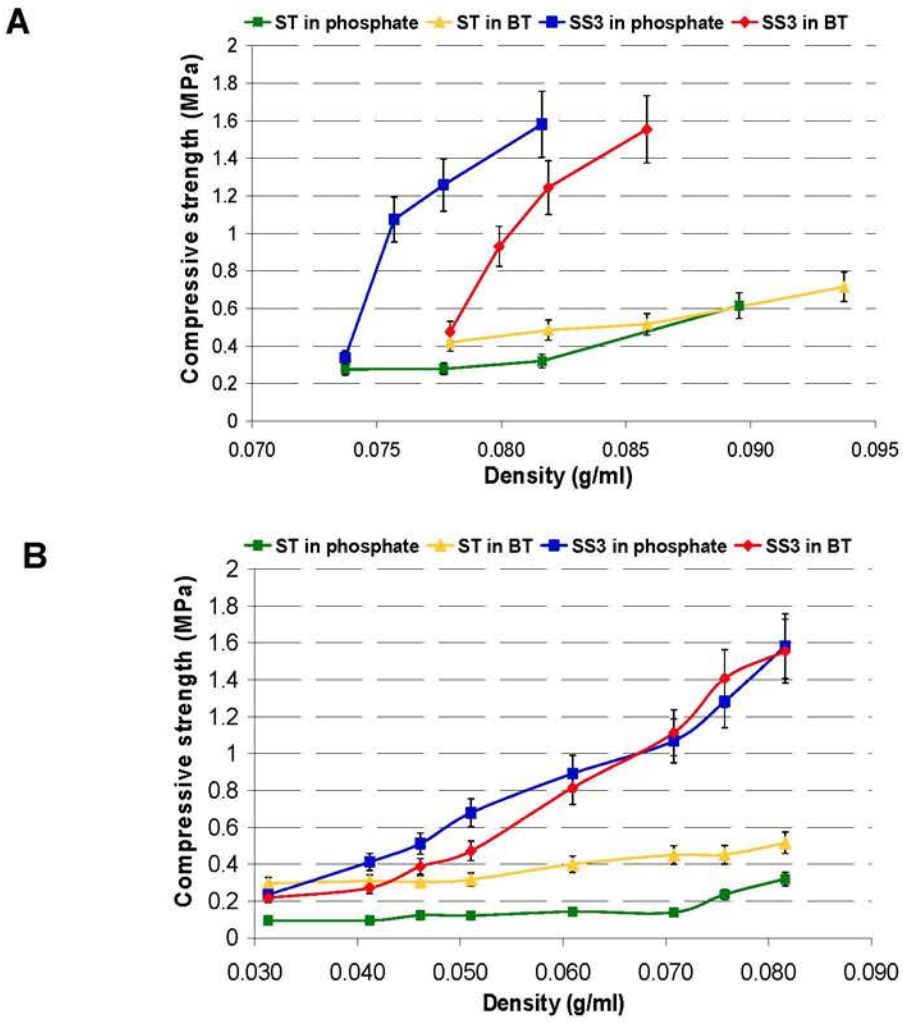

Figure 5.11: The relationship between material density and compressive strength; A) – At fixed silk content (19.12 mg), B) – At fixed silica content (3 mg).

It is evident from the discussion above that the mechanical properties of silk based composites is dependent on multiple factors such as materials density as a function of silk and silica contents, source of silica and distribution pattern. Although the size of Stöber silica particles analysed in this study (11 nm – 159 nm) did not have any significant effect on compressive strength, the Stöber silica particles (any size) produced significantly stronger composite materials compared to TEOS generated silica.

5.4- Summary

This chapter has described the characterisation of silk based nanocomposite materials fabricated using different combinations of silk and silica through the gelation route. Regenerated BM silk and its fractions were blends in variable proportions and were studied for gelation time over a range of pH. The H-chain, due to the difference in the primary and secondary structure was demonstrated to gel faster compared to other samples. The primary structure of H-fibroin is a highly repetitive sequence of mainly hydrophobic amino acids GAGAGS, GAGAGY and GAGAGVGY (99-101) and these hydrophobic interactions finally result in hydrogel formation (102). The isoelectric point (p*I*) is also a crucial factor for controlling gelation as silk fibroin solution has a tendency to gel quickly at a pH around the isoelectric point (p*I*).

Silk composite materials demonstrated a sponge like network structure and no specific morphological structural differences were observed in different samples. EDX and FTIR analysis confirmed the presence and distribution pattern of silica in composite materials. The Stöber silica particles appeared to distribute evenly in the silk matrix whereas TEOS condensed the silica in certain area derived by hydrophobic domain in of silk proteins. The mechanical properties of silk and silk composites were improved by increasing the silk concentration (contents) and increasing the material's density driven either by silk and/or silica. The Stöber silica particles were more efficient in improving mechanical properties compared to TEOS generated silica.

With the aim of improving the physical and mechanical properties of silk based composite materials, several studies have been conducted in recent years (127-135), though there are still some major obstacles in the practical application of silk composites such as fragility and poor mechanical properties (126). This study has opened a gateway to improve certain properties (gelation, secondary conformation and strength) of silk-silica composites improved and understanding of how to control the parameters to make materials with modulated final properties depending on the need of an application.

These composite materials made through the gelation route demonstrated better mechanical properties than silk hydrogels alone at a comparable concentration studied previously (90) and hence hold a great potential for future applications. Further work is required for the better understanding of the structure and gelation behaviour of silk fractions and the complex interaction of different factors affecting it. Still there is an intense need of improving the strength of these materials and can be

further extended to fabricate more dense materials by compacting more silk and/or silica and controlling morphological features such as porosity and pore size. The process of air drying for silk hydrogels produced compact materials however gross and uncontrolled shrinkage is the major concern in this process. The air dried gels also demonstrated the most β-sheet content of any sample, however further work is required to understand and control the shrinkage of such materials in a predictable manner and to improve strength potentially to drag the practical applications of silk materials even closer in future.

5.5- References

(1) Peppas NA, Huang Y, Torres-Lugo M, Ward JH, Zhang J. Physicochemical foundations and structural design of hydrogels in medicine and biology. Ann Rev Biomed Eng 2000 08/01; 2011/04;2(1):9-29.

(2) Hydrogels in medicine and pharmacy. Vol. *I*. Boca Raton, FL: CRC Press; 1986.

(3) Jhon MS, Andrade JD. Water and hydrogels. J Biomed Mater Res 1973;7(6):509-522.

(4) Thibeault SL, Klemuk SA, Chen X, Quinchia Johnson BH. In Vivo engineering of the vocal fold ecm with injectable ha hydrogels—late effects on tissue repair and biomechanics in a rabbit model. Journal of Voice 2011 3;25(2):249-253.

(5) Brandl FP, Seitz AK, Teßmar JKV, Blunk T, Göpferich AM. Enzymatically degradable poly(ethylene glycol) based hydrogels for adipose tissue engineering. Biomaterials 2010 5;31(14):3957-3966.

(6) Chao PG, Yodmuang S, Wang X, Sun L, Kaplan DL, Vunjak-Novakovic G. Silk hydrogel for cartilage tissue engineering. Journal of Biomedical Materials Research Part B: Applied Biomaterials 2010;95B(1):84-90.

(7) Jin R, Moreira Teixeira LS, Dijkstra PJ, van Blitterswijk CA, Karperien M, Feijen J. Enzymatically-crosslinked injectable hydrogels based on biomimetic dextran–hyaluronic acid conjugates for cartilage tissue engineering. Biomaterials 2010 4;31(11):3103-3113.

(8) Yue Z, Wen F, Gao S, Ang MY, Pallathadka PK, Liu L, et al. Preparation of three-dimensional interconnected macroporous cellulosic hydrogels for soft tissue engineering. Biomaterials 2010 11;31(32):8141-8152.

(9) Zhu J. Bioactive modification of poly(ethylene glycol) hydrogels for tissue engineering. Biomaterials 2010 6;31(17):4639-4656.

(10) Tan H, Chu CR, Payne KA, Marra KG. Injectable in situ forming biodegradable chitosan–hyaluronic acid based hydrogels for cartilage tissue engineering. Biomaterials 2009 5;30(13):2499-2506.

(11) Tiwari A, Grailer JJ, Pilla S, Steeber DA, Gong S. Biodegradable hydrogels based on novel photopolymerizable guar gum–methacrylate macromonomers for in situ fabrication of tissue engineering scaffolds. Acta Biomaterialia 2009 11;5(9):3441-3452.

(12) Bryant SJ, Cuy JL, Hauch KD, Ratner BD. Photo-patterning of porous hydrogels for tissue engineering. Biomaterials 2007 7;28(19):2978-2986.

(13) Khademhosseini A, Langer R. Microengineered hydrogels for tissue engineering. Biomaterials 2007 12;28(34):5087-5092.

(14) Möller S, Weisser J, Bischoff S, Schnabelrauch M. Dextran and hyaluronan methacrylate based hydrogels as matrices for soft tissue reconstruction. Biomol Eng 2007 11;24(5):496-504.

(15) Hoffman AS. Hydrogels for biomedical applications. Adv Drug Deliv Rev 2002 1/17;54(1):3-12.

(16) Nguyen KT, West JL. Photopolymerizable hydrogels for tissue engineering applications. Biomaterials 2002 11;23(22):4307-4314.

(17) Bryant SJ, Anseth KS. The effects of scaffold thickness on tissue engineered cartilage in photocrosslinked poly(ethylene oxide) hydrogels. Biomaterials 2001 3/15;22(6):619-626.

(18) Lee KY. Hydrogels for tissue engineering. Chem Rev 2001;101(7):1869.

Chapter 6
GENERAL DISCUSSION, CONCLUSIONS AND FUTURE WORK

This was an interdisciplinary research project involving studies of natural silk and silica based nanocomposites, their fabrication and characterisation aiming at an outcome for dental tissue engineering applications. This chapter describes the general discussion, conclusions and future prospects for this research project.

6.1- Discussion and conclusions

6.1.1- *Bombyx mori* silk fractions and biochemistry

In this study, natural *Bombyx mori* silk was explored to develop a new simple, convenient and practical method of separating well known components of silk fibroin; heavy chain and light chain fibroin. Silk fractions were separated as formic acid

soluble (light chain) and insoluble (heavy chain) using a simple filtration method. The novelty of this method is that it can be used on a large scale to derive large amounts of the different silk fractions from BM cocoons and does not involve any complex techniques or equipment. Silk fractions attached to each other by disulphide (covalent) bonds (1) can be isolated within a couple of hours using this method and can be simply air dried for further research.

The molecular weight of isolated silk fractions has been characterised using SDS-PAGE analysis, confirming them to be heavy and light chain components of BM silk. H-fibroin due to the presence of mainly hydrophobic domains (2) showed a stronger tendency to gel in aqueous solutions and needed a modified buffer to denature the protein for biochemical studies. Silk fibroin is very sensitive to heat and may break down or degrade into smaller peptides (3). The H-fibroin that is structurally (amino acid content) very different from light chain (1) being very similar to silk fibroin demonstrated a similar degradation behaviour in response to heat applied during processing. In certain studies (4), where excessive heat (2-12 hours at 90 °C) was used for de-gumming and dissolving in ionic solution resulted in with a silk solution which is mixture of broken down proteins of different sizes (8-200 kDa).

Silk and silk fractions are proteins and to avoid any degradation, exposure to heat at any processing stage (de-gumming and/or dissolving in ionic solutions) must be limited as much as possible. Excessive degradation of silk protein also weakens their tendency to gel (3) hence may affect the final properties of materials fabricated through the gelation route. Similarly, LiSCN-silk solutions (as very little heat treatment given) showed a strong tendency to gel due to the presence of comparatively intact fibroin. Another significant benefit of the formic acid separation is that one fraction (light chain) is soluble and stable in ionic solutions (up to 20 wt %) without heating and is also soluble in formic acid (up to 33 wt%), can be used to make a range of biomaterials without any need for silk regeneration, hence preventing any damage to silk protein that might be caused by regeneration procedures (i.e. chemicals, heating, freeze dry).

The separation of these silk fractions without degradation always remained a challenging task and limited the practical applications of them. In contrast, total silk has been used widely for a range of biomedical application. However this study has solved the dilemma of separating silk fractions and opens the gateway for active research and applications of these fractions. The structural differences of L-chain (less crystallinity, amorphous region, different amino acid composition) can be beneficial for certain applications compared to natural silk fibroin. For example, light

chain separated by column chromatography and genetically modified has been used recently (5) and been found to be successful in facilitating cartilage tissue formation. Similarly, structural features of H-chain (crystallinity, hydrophobicity) can be beneficial for certain applications where higher crystallinity or more β-sheet secondary conformation is desired.

6.1.2- Electrospun silk nanocomposites

The morphology of electrospun silk materials was studied using SEM and produced a non woven mesh of nano fibres in the range of 80-330 nm diameter depending on the silk type. The most important parameter that affects the fibre morphology is the solution's viscosity (6) which can be related to fibre diameter. A very low viscosity (80 cP or less) of silk solutions resulted in droplets or bead formation alongside nano-fibres. In order to produce continuous smooth fibres, the silk solution should be viscous enough (more than 80 cP) to overcome surface tension. At a comparable concentration, H-chain produced higher viscosity solutions due to its unique structural features compared to L-chain and total silk and produced thickest fibres (258 ± 72 nm) followed by total silk 176 ± 66 nm). However, light chain silk (both in regenerated and natural forms) produced the thinnest fibres (123 ± 37nm) alongside bead formation. This bead formation can be controlled by increasing the viscosity of the solution (7).

Very little work is available on electrospinning of silk fractions (H-chain and L-chain) and only a couple of research groups (5,8) have reported electrospinning of heavy and/or light chain recently. In the current study, one component of natural *Bombyx mori* silk (L-chain) has been electrospun without need of any kind of regeneration, hence preventing it from any harsh conditions of heat and chemical treatments, enabling one to maintain the structural integrity of natural silk. The regenerated forms of natural silk, H-chain and blends of both silk fractions were also electrospun. These blended solutions enabled manipulation of the final properties of the mixture to control the fibre formation.

The electrospun mats from each sample were characterised for secondary conformation of silk immediately as spun, after treatment with ethanol as well as after silicification of them. The treatment of electrospun mats with ethanol proved to be a useful technique and equally effective in increasing β-sheet contribution for all silk fractions. In general, ethanol treatment resulted in slight shrinkage of nano-fibres (as compared by SEM before and after ethanol treatment), increase in β-sheet

content and insolubility of silk with H-chain maintaining the most β-sheet before and after ethanol treatment.

The silicification reaction condensed silica on to the electrospun silk mats which was confirmed by elemental analysis, FTIR and TGA. The FTIR spectra confirmed the presence of silica by the appearance of an additional peak representing the asymmetrical stretch of Si-O-Si in the area 1100-1060 cm^{-1}.

The amount of silica condensed on the surface of electrospun silk mats was variable depending on the type of silk, with the maximum entrapped by H-chain possibly due to the presence of more hydrophobic amino acids (primary structure) and more β-sheet (secondary structure). The ethanol treatment (for 10 minutes) also increased the thermal stability of silk (up to 20℃) due to a n increase in β-sheet content and the crystallinity of silk (9). There were no significant differences observed between different ethanol treated samples.

In order to improve the solution properties of natural silk, it has been blended with a variety of other polymers such as gelatine (10), cross linkers such as genipin (11), keratin (12), collagen (13), poly vinyl alcohol (14), chimeric silk proteins (15-17) and many other materials (18-21). However this study has opened a gateway to improve certain properties (viscosity, fibre diameter, conformation and strength) by making silk-silk composites and make materials with tuneable properties depending on the need of an application.

6.1.3- Gelation studies

Aqueous solutions from regenerated BM silk and its fractions were blended in variable proportions and were studied for gelation time over a range of pH (pH 3- pH 9). In general, silk solutions have a tendency to gel rapidly at acidic pH and none of the silk solutions was gelled at neutral or basic pH during the period of study. In pH related control of gelation times, the isoelectric point (p*I*) is a crucial factor. The silk fibroin protein similar to other protein solutions has a tendency to gel quickly at a pH around the isoelectric point (p*I*). The isoelectric point for silk fibroin is 3.8-3.9 (22-24), hence at a pH around 3 (very close to the p*I* of silk fibroin), the interactions between silk molecules is increased by decreasing the repulsive forces and more potential for insoluble β-sheet formation leading to hydrophobic interactions and accelerating the sol-gel transition (25).

The structural differences between different silk types also affect the gelation times, H-chain due to the difference in the primary and secondary structural demonstrated to gel faster compared to other samples. The primary structure of H-fibroin is highly

repetitive sequence of mainly hydrophobic amino acids GAGAGS, GAGAGY and GAGAGVGY (2,26,27) and these hydrophobic interactions finally result in hydrogel formation quicker than other samples (28). Such performance of H-chain was also reflected in blend solution and gelation time was decrease depending on the proportion of L-chain added to each sample. Addition of ethanol also observed to enhance the gelation in H-chain containing silk samples at a range of pH. The addition of a small amount of ethanol increases the proportion of β-sheet content thus accelerating the gelation process (29).

The gelation route was used to fabricate silk-silica composites and these were characterised for morphology, composition, protein secondary conformation and mechanical properties. Silk composite materials demonstrated a sponge-like network structure and no specific structural differences were observed in different samples morphologically. The EDX and FTIR analysis confirmed the presence and distribution pattern of silica presence in composite material. In secondary conformation studies, the natural form of H-chain has the most β-sheet contents (76.7 %), significantly higher than any other format of silk. The β-sheet contents in silk materials were reduced as a result of regeneration and can be re-attained by ethanol treatment. Generally, silk hydrogels contained more β-sheet than solutions and air dried samples contained more β-sheet than freeze dried materials. Ethanol treatment resulted in more β-sheet in freeze dried silks and films. However, air dried silk hydrogels had the highest β-sheet content (more than 57 %) without ethanol treatment and no more increase was observed after ethanol treatment. However the control of the volumetric shrinkage was challenging in this process.

The mechanical properties of silk and silk composites were improved by increasing the silk concentration (contents) and increasing the material's density driven either by silk and/or silica. The Stöber silica particles came out to be more efficient in improving the mechanical properties compared to the TEOS silica. The Stöber silica particles appeared to distribute evenly in the silk matrix whereas TEOS condensed the silica in certain areas derived by hydrophobic domain in of silk proteins. This even distribution of inorganic silica particles absorb stresses better and prevent any stress concentration and crack propagation, increasing the overall strength of the material. In contrast, TEOS samples where there was uneven distribution of silica in silk matrix resulting wider zone of silk only in samples hence giving lower compression strength.

With the aim of improving the physical and mechanical properties of silk based composite materials, several studies have been conducted in recent years (16,30-38), though there are still some major obstacles in the practical application of silk

composites such as fragility and poor mechanical properties (39). The composite materials made through a gelation route in this study demonstrated better mechanical properties than silk hydrogels alone at a comparable concentration studied previously (25) and hence hold a great potential for future applications.

6.2- Future work

Extensive research has been performed on silk in the recent years, however still there are major obstacles (such as poor strength, difficulty in controlling final properties) in the biomedical applications of silk practically and more effort is needed to overcome these shortcomings.

6.2.1- *Bombyx mori* silk fractions

As a result of development of the method for separating *Bombyx mori* silk fractions (heavy and light chain) and are an open area of investigation for researchers interested in silk biochemistry, biomaterials, dental materials, tissue engineering and genetic engineering. There is a great potential for rapid increase in the biological applications of silk fractions however further work is required for its purification and detailed characterisation. Additionally, both fractions and silk fibroin can be manipulated by varying their ratios to control the final properties of the silk based material more precisely. Chemical modification and functionalization of heavy and light chain can be performed to target certain benefits in the final biomaterial.

In a recent study (16), novel nanocomposites were prepared using spider silk–R5 fusion proteins and biomimetic techniques. These fusion proteins prepared using genetic engineering techniques consisted of two components. One component of this fusion protein is the self assembling domain based on the repeat consensus of spider dragline silk, responsible for the formation of highly stable β-sheet formation and excellent mechanical properties. The second part of the fusion protein is the R5 peptide isolated from the silaffin protein of diatom (Cylindrotheca fusiformis), as a 19 amino acid unit (SSKKSGSYSGSKGSKRRIL) that has been shown to induce and regulate silica precipitation under ambient conditions (40). This fusion protein has been used in the production of nanocomposite materials containing silica particles with a narrow distribution range (0.5-2 μm). However the production of such chimeric proteins is very tough and complicated procedure. In contrast, silk can be produced easily compared to spider silk or genetic engineering and can be compared for such kind of outcome for making nanocomposites using biomimetic techniques.

6.2.2- Electrospun silk nanocomposites

Future work should be focused on the better understanding of the structure and chemical behaviour of silk fractions and to explore the outcome of more silk-silk blends specially using natural silk mixed with regenerated silks. Until now the electrospinning of silk fractions (separated using formic acid) has not been reported and no research has been performed on electrospinning of blended solutions of silk fractions. Similarly, these fractions can be blended with regenerated natural silk and their impact on the final material characterisation can be helpful in designing new biomaterials.

Mechanical properties play a vital role for developing new biomaterials and mechanical testing can provide information about how efficiently a material will perform mechanically *in vivo* for a potential application. A number of methods for the mechanical testing of electrospun silk mats have been attempted with little or no outcome. Further work is required to test electrospun materials mechanically either for non woven silk mats or for single nano-fibres. The separation of the silk mat from the target or separation and attachment of single fibre to the mechanical tester is a challenging task (41). In the recent years, many researchers have focused on three dimensional electrospinning (42-44) which may be equally beneficial for giving support to odontoblast processes for dentin tissue engineering. Additionally, three dimensional electrospun materials can be characterised easily for mechanical features such as compression or shear strength.

Spider silk and R5 chimeric proteins could not be used in this project due to insufficient quantity, however it will be interesting to compare such chimeric proteins for silica condensation with chemically modified silk fractions particularly H-chain that is rich is hydrophobic domains. In contrast, L-chain that has exhibited entirely different properties due to its unique structure such as more hydrophilic, more water uptake and rapid degradation (8) and by chemical modification of L-chain it is expected to produce different properties in nanocomposite materials.

6.2.3- Gelation studies

Further work is required for the better understanding of the structure and gelation behaviour of silk fractions and the complex interaction of different factors affecting it. Still there is an intense need to improve the strength of these materials with further extension to fabricate more dense materials, compacting more silk and/or silica and controlling morphological features such as porosity and pore size. The process of air

drying for silk hydrogels produced compact materials however gross and uncontrolled shrinkage is the major concern in this process. The air dried gels also demonstrated the most β-sheet content compared with any other sample, however further work is required to understand and control the shrinkage of these materials in a predictable manner such as supercritical drying and to improve strength potentially to drag the practical applications of silk materials even closer in future.

The mechanical properties (a big obstacle in the practical application of silk biomaterials) improved by additions of silica to total silk, however replacing total silk with H-chain or different blends can further improve the mechanical properties. In the current study, it has been proven that the density of the silk-silica nanocomposites is very important and compressive strength can be improved by fabricating more dense materials. However a density of nanocomposites in this study was very low (no more than 0.1 g/ml) so there is a need of development of a method for making denser and compact composite materials to control porosity thereby improving their strength. Although H-chain and L-chain has a wide future in biomaterials, however for practical applications, a lot of research is required for their detailed characterisation and interaction studies within the biological environment.

6.3- Final comments

This study has opened a gateway for researchers interested in silk, natural polymers, materials science, biomaterials, dental materials, genetic engineering, mineral-peptide interactions, tissue engineering, drug delivery and nano-materials to explore the silk fractions for extensive research. The information obtained in the present study is important for future investigations of silk fractions and will have potential in a wide range of applications. In order to advance the applications of silk biomaterials (either electrospun or gelled) from the research perspective to commercial stages, an extensive collaborative research involving multiple disciplines is required. It is hoped that a continuous financial investment from research funding bodies and a hard work from biomaterial scientists will open up a new range of opportunities for silk nano-materials in biomedical and biotechnical and dental applications.

6.4- References

(1) Inoue S, Tanaka K, Arisaka F, Kimura S, Ohtomo K, Mizuno S. Silk fibroin of Bombyx mori is secreted, assembling a high molecular mass elementary unit consisting of H-chain, L-chain, and p25, with a 6:6:1 molar ratio. J Biol Chem 2000 December 15, 2000;275(51):40517-40528.

(2) Garel J. The silkworm, a model for molecular and cellular biologists. Trends Biochem Sci 1982 3;7(3):105-108.

(3) Yamada H, Nakao H, Takasu Y, Tsubouchi K. Preparation of undegraded native molecular fibroin solution from silkworm cocoons. Materials Science and Engineering: C 2001 8/15;14(1-2):41-46.

(4) Zhang Y, Shen W, Xiang R, Zhuge L, Gao W, Wang W. Formation of silk fibroin nanoparticles in water-miscible organic solvent and their characterization. Journal of Nanoparticle Research 2007 10/01;9(5):885-900.

(5) Kambe Y. Effects of RGDS sequence genetically interfused in the silk fibroin light chain protein on chondrocyte adhesion and cartilage synthesis. Biomaterials 2010.

(6) Li W, Mauck RL, Tuan RS. Electrospun nanofibrous scaffolds: production, characterization, and applications for tissue engineering and drug delivery. Journal of Biomedical Nanotechnology September 2005;1:259-275(17).

(7) Fong H, Chun I, Reneker DH. Beaded nanofibers formed during electrospinning. Polymer 1999 7;40(16):4585-4592.

(8) Wadbua P, Promdonkoy B, Maensiri S, Siri S. Different properties of electrospun fibrous scaffolds of separated heavy-chain and light-chain fibroins of Bombyx mori. Int J Biol Macromol 2010 6/1;46(5):493-501.

(9) Um IC, Kweon H, Park YH, Hudson S. Structural characteristics and properties of the regenerated silk fibroin prepared from formic acid. International Journal of Biological Macromolecules 2001 8/20;29(2):91-97.

(10) Bao Weiwei, Zhang Youzhu, Yin Guibo, Wu Jialin. The structure and property of the electrospinning silk fibroin. e-Polymers 2008 AUG 4:098.

(11) Silva SS, Maniglio D, Motta A, Mano JF, Reis RL, Migliaresi C. Genipin-modified silk-fibroin nanometric nets. Macromol Biosci 2008 AUG 11;8(8):766-774.

(12) Vasconcelos A, Freddi G, Cavaco-Paulo A. Biodegradable materials based on silk fibroin and keratin. Biomacromolecules 2008;9(4):1299-1305.

(13) Yeo I, Oh J, Jeong L, Lee TS, Lee SJ, Park WH, et al. Collagen-based biomimetic nanofibrous scaffolds: Preparation and characterization of collagen. Biomacromolecules 2008 APR;9(4):1106-1116.

(14) Um I, Park Y. The effect of casting solvent on the structural characteristics and miscibility of regenerated silk fibroin/Poly(vinyl alcohol) blends. Fibers and Polymers 2007 12/11;8(6):579-585.

(15) Gus'kova OA, Khalatur PG, Bäuerle P, Khokhlov AR. Silk-inspired 'molecular chimeras': Atomistic simulation of nanoarchitectures based on thiophene–peptide copolymers. Chemical Physics Letters 2008 8/8;461(1-3):64-70.

(16) Foo CWP, Patwardhan SV, Belton DJ, Kitchel B, Anastasiades D, Huang J, et al. Novel nanocomposites from spider silk-silica fusion (chimeric) proteins. Proc Natl Acad Sci U S A 2006 JUN 20;103(25):9428-9433.

(17) Mieszawska AJ, Nadkarni LD, Perry CC, Kaplan DL. Nanoscale control of silica particle formation via silk-silica fusion proteins for bone regeneration. Chemistry of Materials 2010 10/26;22(20):5780-5785.

(18) Hou A, Chen H. Preparation and characterization of silk/silica hybrid biomaterials by sol–gel crosslinking process. Materials Science and Engineering: B 2010 3/15;167(2):124-128.

(19) Hu X, Lu Q, Sun L, Cebe P, Wang X, Zhang X, et al. Biomaterials from ultrasonication-induced silk fibroinâ^'hyaluronic acid hydrogels. Biomacromolecules 2010 11/08;11(11):3178-3188.

(20) Xu Q, Li J, Peng Q, Wu L, Li S. Novel and simple synthesis of hollow porous silica fibers with hierarchical structure using silk as template. Materials Science and Engineering: B, 2006 2/25;127(2-3):212-217.

(21) Jin HJ, Fridrikh S, Rutledge GC, Kaplan D. Electrospinning bombyx mori silk with poly(ethylene oxide). Abstracts of Papers of the American Chemical Society 2002;224:U431-U431.

(22) Ayub Z, Arai M, Hirabayashi K. Mechanism of the gelation of fibroin solution. Biosci Biotechnol Biochem 1993;57(11):1910-1912.

(23) Kang G, Nahm J, Park J, Moon J, Cho C, Yeo J. Effects of poloxamer on the gelation of silk fibroin. Macromolecular Rapid Communications 2000; 31; (21)(11):788-791.

(24) Hawley TG, Johnson TB. The isoelectric point of silk fibroin. Industrial & Engineering Chemistry 1930 03/01;22(3):297-299.

(25) Kim UJ, Park, J., Li, C, Jin H-, Valluzzi R, and Kaplan DL. Structure and properties of silk hydrogels. Biomacromolecules 2004;5:786-792.

(26) Mita K. Highly repetitive structure and its organization of the silk fibroin gene. J Mol Evol 1994;38(6):583.

(27) Zhou C, Confalonieri F, Jacquet M, Perasso R, Li Z, Janin J. Silk fibroin: Structural implications of a remarkable amino acid sequence. Proteins: Structure, Function, and Genetics 2001;44(2):119-122.

(28) Jin HJ, Kaplan DL. Mechanism of silk processing in insects and spiders. Nature 2003;424(6952):1057-1061.

(29) Cao H, Chen X, Huang L, Shao Z. Electrospinning of reconstituted silk fiber from aqueous silk fibroin solution. Materials Science and Engineering: C 2009 8/31;29(7):2270-2274.

(30) Kharlampieva E, Kozlovskaya V, Wallet B, Shevchenko VV, Naik RR, Vaia R, et al. Co-cross-linking silk matrices with silica nanostructures for robust ultrathin nanocomposites. ACS Nano 2010 12/28;4(12):7053-7063.

(31) Rajkhowa R, Gil ES, Kluge J, Numata K, Wang L, Wang X, et al. Reinforcing silk scaffolds with silk particles. Macromolecular Bioscience 2010;10(6):599-611.

(32) Kang M, Chen P, Jin H. Preparation of multiwalled carbon nanotubes incorporated silk fibroin nanofibers by electrospinning. Current Applied Physics 2009 1;9(1, Supplement 1):S95-S97.

(33) Mieszawska AJ, Kaplan D, Perry CC. Silk/silica nanocomposites as novel biomaterials for tissue engineering. Biophys J 2009 2;96(3, Supplement 1):635a-635a.

(34) Schiffman JD, Schauer CL. A review: Electrospinning of biopolymer nanofibers and their applications. Polym Rev 2008;48(2):317-352.

(35) Mandal BB, Park S, Gil ES, Kaplan DL. Multilayered silk scaffolds for meniscus tissue engineering. Biomaterials 2011 1;32(2):639-651.

(36) Hardy JG, Scheibel TR. Composite materials based on silk proteins. Progress in Polymer Science 2010 9;35(9):1093-1115.

(37) Tsioris K, Tilburey GE, Murphy AR, Domachuk P, Kaplan DL, Omenetto FG. Functionalized-silk-based active optofluidic devices. Advanced Functional Materials 2010;20(7):1083-1089.

(38) Cao B, Mao C. Oriented nucleation of hydroxylapatite crystals on spider dragline silks. Langmuir 2007;23(21):10701-10705.

(39) Iridag Y, Kazanci M. Preparation and characterization of Bombyx mori silk fibroin and wool keratin. J Appl Polym Sci 2006;100(5):4260-4264.

(40) Brott LL, Naik RR, Pikas DJ, Kirkpatrick SM, Tomlin DW, Whitlock PW, et al. Ultrafast holographic nanopatterning of biocatalytically formed silica. Nature 2001 09/20;413(6853):291.

(41) Huang Z, Zhang Y-, Kotaki M, Ramakrishna S. A review on polymer nanofibers by electrospinning and their applications in nanocomposites. Composites Science and Technology 2003 11;63(15):2223-2253.

(42) Ki CS, Kim JW, Hyun JH, Lee KH, Hattori M, Rah DK, et al. Electrospun three-dimensional silk fibroin nanofibrous scaffold. J Appl Polym Sci 2007;106:3922-3928.

(43) Wang Y, Rudym DD, Walsh A, Abrahamsen L, Kim H, Kim HS, et al. In vivo degradation of three-dimensional silk fibroin scaffolds. Biomaterials 2008 0;29(24-25):3415-3428.

(44) Zhou J, Cao C, Ma X. A novel three-dimensional tubular scaffold prepared from silk fibroin by electrospinning. Int J Biol Macromol 2009 12/1;45(5):504-510.